Towards better treatment of mycobacterial infections

Saskia E. Mudde

Towards better treatment of mycobacterial infections

Saskia Emily Mudde

ISBN: 978-94-6473-701-1

Lay-out: Douwe Oppewal
Printing: Ipskamp, Enschede

Financial support for design and printing this thesis was provided by: Paratek Pharmaceuticals, Inc., King of Prussia, Pennsylvania, USA; Selinion Medical B.V., ‘s-Hertogenbosch

Towards Better Treatment of Mycobacterial Infections

Op weg naar betere behandeling van mycobacteriële infecties

Proefschrift

ter verkrijging van de graad van doctor aan de
Erasmus Universiteit Rotterdam
op gezag van de
rector magnificus

Prof.dr.ir. A.J. Schuit

en volgens besluit van het College voor Promoties.
De openbare verdediging zal plaatsvinden op

dinsdag 11 maart 2025 om 15.30 uur

door

Saskia Emily Mudde
geboren te Breda

Erasmus University Rotterdam

Promotiecommissie:

Promotoren:	Prof.dr. A.M.C. van Rossum Dr. J.E.M. de Steenwinkel
Overige leden:	Prof.dr. B.J.A. Rijnders Dr. S.M. Arend Prof.dr. W. Bitter
Copromotor:	Dr. H.I. Bax

Contents

CHAPTER 1

Introduction and outline of the thesis

Mycobacteria encompass a diverse group of potential pathogens and can be classified into three main groups: 1) *Mycobacterium tuberculosis* complex, 2) nontuberculous mycobacteria (NTM), and 3) *Mycobacterium leprae/lepromatosis*. This thesis focusses on the first two groups. Of the multiple species belonging to the *M. tuberculosis* complex, *M. tuberculosis* is the most common causative agent of tuberculosis (TB) in humans. As opposed to *M. tuberculosis*, which is an obligate pathogen, NTM are environmental bacteria that differ greatly in their pathogenic potential.[1, 2] While *M. tuberculosis* and NTM cause distinct disease in different risk populations, they share several characteristics that contribute to both being notoriously difficult to treat. For example, they are renowned for their slow growth rate, lipid-rich and impermeable cell wall, efflux systems transporting antibiotics out of the cell, and their ability to adopt a metabolically altered, nonreplicating state in response to external stresses. All of these characteristics underlie their natural, profound ability to withstand antibiotic exposure.[3, 4] Consequently, mycobacterial disease requires prolonged treatment with multiple drugs combined that come with the risk of drug toxicity, drug-drug interactions, and the emergence of drug resistance, collectively leading to disappointing treatment success rates.[5-10] In order **to improve treatment options for mycobacterial disease**, the pool of available drugs and drug regimens should be expanded and drug (regimen) activity and efficacy needs optimization. The preclinical *in vitro* and *in vivo* studies within this thesis were conducted with that specific aim in mind.

Mycobacterium tuberculosis

It is estimated that almost a quarter of the world population is latently infected with *M. tuberculosis*,[11] which is defined by the presence of a persistent immune response to *M. tuberculosis* antigens after previous *M. tuberculosis* exposure, while clinical TB symptoms are absent.[12] Of all latently infected individuals, approximately 5-15% develop active TB at some point in their life.[13, 14] Therefore, the large number of individuals with latent TB represent a vast reservoir of potential TB cases. Active TB predominantly affects the lungs, causing symptoms like cough, fever, and weight loss, but it can affect virtually any organ in the body.

In 2022, an estimated 10.6 million people developed active TB, and 1.3 million people died from the disease, making TB the second deadliest infectious disease after COVID-19 in that year.[8] To stimulate the fight against TB, the World Health Assembly endorsed the End TB strategy in 2014, which pursues an ambitious, but highly needed 90% decline in new TB cases and a 95% drop in TB deaths in 2035 compared to the 2015 baseline. Although significant progression has been made over the years, those goals are unfortunately still far from reach, and due to COVID-19 disrupting access to TB healthcare, TB incidence and death rates are actually the highest they have been in years.[8]

The global TB epidemic is, however, not a problem of recent years. Archeological evidence of TB in humans dates back to approximately 9000 years ago,[15] and (early ancestors) of *M. tuberculosis* actually may have been coevolving with the human host for 3 million years.[16, 17] In Europe, TB particularly thrived during the industrial revolution, which was fueled by crowded housing conditions, poor hygiene and air pollution, causing an impressive 20% of all deaths in French cities between 1830 and 1900.[18] It was during this period, on March 24, 1882, that physician and microbiologist Robert Koch presented his discovery of the tubercle bacillus. In the following decennia, the TB death rate declined steeply as a consequence of isolation of people with TB in hospitals and sanatoria, urban renovation, improved social and living conditions, and better nutrition.[18, 19] However, it was not until the 1940s that the first antibiotics, which were streptomycin and para-aminosalicylic acid were identified as effective treatment for TB.[20] Clinical studies showed that combined administration of these two antibiotics not only proved to be more effective than either single drug, but also prevented emergence of streptomycin resistance.[21] These findings laid the foundation for the adage that TB should always be treated with a multiple drug combination. With the subsequent addition of isoniazid to streptomycin and para-aminosalicylic acid, treatment outcomes improved significantly with reported relapse rates as low as 5%, but this regimen was still far from ideal, requiring intramuscular administration of streptomycin and an extremely long treatment duration of 24 months.[22] Over the subsequent decades, multiple innovations, including the replacement of para-aminosalicylic acid by ethambutol (1960s), addition of rifampicin (1970s), and pyrazinamide (1980s) reduced regimen toxicity and treatment duration, ultimately leading to the implementation of the all oral standard of care as we still know it today: HRZE, which involves 2 months of isoniazid, rifampicin, pyrazinamide, and ethambutol followed by 4 months of isoniazid and rifampicin (2HRZE/4HR).[22, 23] The success of the HRZE regimen is attributable to its profound bactericidal and sterilizing activity. The bactericidal activity is believed to be driven by isoniazid in the early treatment phase and later on by rifampicin and pyrazinamide, while the sterilizing and treatment-shortening potential of the regimen are attributable to rifampicin, which is active against persistent *M. tuberculosis* populations with an altered metabolic state, and pyrazinamide. Interestingly, two months of pyrazinamide in the initial phase of treatment is sufficient to exert this sterilizing and treatment-shortening potential. Ethambutol is added in the early treatment phase to prevent selection of drug resistance, and is discontinued when susceptibility to the other drugs is confirmed, since its bactericidal activity is poor at the current tolerated dosage.[24]

While HRZE significantly reduced the required duration of drug susceptible TB treatment, thereby improving the lives of countless people, its clinical application has been accompanied by the selection of *M. tuberculosis* strains that are resistant to one or more of these drugs.[25] Resistance to the most effective first-line drugs, rifampicin and

isoniazid, significantly reduces the chances of treatment success. Until recently, the only alternatively available drug regimens were less potent, involving parental drug administration, associated with increased drug toxicity, and requiring treatment durations up to 18 months after culture conversion.[6] Fortunately, after decennia of relative scientific neglect, the field of TB drug discovery has evolved rapidly in recent years. In 2012, for the first time in 40 years, a drug with a new mechanism of action was approved for TB treatment: bedaquiline, belonging to the diarylquinoline class of drugs. Being highly active against drug resistant *M. tuberculosis* isolates, bedaquiline has revolutionized drug resistant TB treatment. Additionally, the clinical anti-TB arsenal was expanded by the approval of new anti-TB drugs pretomanid and delamanid, and drugs already approved for conditions other than TB, such as moxifloxacin and linezolid. Regimens containing these new drugs have demonstrated treatment success rates as high as 90% against drug resistant TB while **reducing treatment duration** of drug resistant TB to a mere 6-9 months in the landmark Nix-TB, ZeNix, TB-PRACTECAL, and NExT trials.[26-29] Those impressive results have led the World Health Organization to update their treatment guidelines for drug resistant TB, endorsing a 6-month regimen consisting of bedaquiline, pretomanid, linezolid, and moxifloxacin.[6] Yet, the introduction of just one new effective drug regimen will not be sufficient to realize the End TB strategy goals, and to prevent another period of scientific negligence, we must maintain momentum and **continue to identify effective drug regimens for both drug sensitive and drug resistant TB**. Insufficient tolerability, drug-drug interactions, and the emergence of *M. tuberculosis* strains resistant to the newly implemented drugs further highlight the ongoing need for TB drug development.[27, 30] In that regard, it is encouraging that the TB drug pipeline has never been more robust than it is today, including promising compounds such as next-generation diarylquinolines (e.g. TBAJ-876 and TBAJ-587), several oxazolidinones (e.g. sutezolid and delpazolid), and many more.[31] With this overwhelming availability of often similar compounds, instead of rushing forward, it might be beneficial to take a step back and **comprehensively compare** their benefits and flaws, especially for those belonging to the same class of drugs. Head-to-head comparisons of their anti-TB activity, pharmacokinetic properties, and other critical factors might facilitate strategical implementation of the various compounds, for which preclinical models play a key role.

Nontuberculous mycobacteria

Unlike *M. tuberculosis*, NTM are ubiquitous in the environment, mainly in water and soil. Infections predominantly result from exposure to such environmental NTM niches,[32] while studies on potential patient-to-patient transmission are inconclusive.[33-36] Advancements in genetic sequencing techniques have led to the identification of approximately 200 different NTM species so far,[37] which are classified as 'rapidly growing' or 'slow growing' based on the time until visible colony formation on solid media, with 7 days as the differentiating cutoff point.[38] Of all known NTM species, only a subset is isolated from

clinical samples on a regular basis. Yet, isolation of NTM species from clinical samples does not necessarily indicate NTM disease, and might actually reflect contamination or transient colonization, as the pathogenicity of those species differs considerably.[39]

In most areas of the world, including Europe, NTM disease is not notifiable. Although exact incidence numbers are therefore not tracked, there is evidence that the global prevalence of NTM disease is on the rise, especially in higher-income countries.[40, 41] Proposed reasons for the increased incidence include aging populations, better awareness among clinicians, improved diagnostic techniques, and an increase in people living with predisposing conditions.

The most common clinical manifestation of NTM is pulmonary disease and presents as fibro-cavitary disease similar to TB or as nodular-bronchiectatic disease, which are distinguished by their radiological features.[42] Fibro-cavitary disease almost exclusively occurs in patients with underlying structural lung disease such as cystic fibrosis or chronic obstructive pulmonary disease (COPD). Nodular-bronchiectatic disease typically develops in middle-aged to elderly women with a specific body morphology including a thin habitus, thoracic skeletal abnormalities, and mitral valve prolapse which has been linked to genetic changes in different gene categories.[42-45] Other clinical manifestations of NTM disease include lymphadenitis, skin, soft tissue and bone infections, healthcare-associated infections and disseminated disease.[42, 46] Lymphadenitis commonly presents as an unilateral, cervical swelling in presumptively healthy children. Skin, soft tissue, bone, and joint infections can occur as a consequence of traumatic events or surgical interventions or in the context of disseminated disease. Disseminated disease predominantly affects immunocompromised people, including people living with HIV, patients with defects in the IFN-γ/IL-12 pathway, or patients using immunosuppressive therapies (e.g. corticosteroids or TNF-α inhibitors).[42, 46]

Because of their clinical significance, *M. abscessus* and *M. avium* are the main NTM studied in this thesis.[7, 47, 48] The *M. abscessus* complex entails three different subspecies: *abscessus, bolletii*, and *massiliense*. Identification to the *M. abscessus* subspecies-level is relevant for choosing appropriate treatment based on subspecies-associated resistance mechanisms, specifically the presence of a functional erythromycin ribosomal methylase, or *erm*(41), which confers macrolide resistance and negatively impacts treatment outcome.[7, 49, 50] *M. abscessus* is one of the most challenging NTM to treat due to its intrinsic resistance to a wide range of antibacterial drugs. Current recommended antibiotics for the treatment of *M. abscessus* include a macrolide (when susceptible, preferably azithromycin), amikacin, imipenem, tigecycline, clofazimine, and linezolid. Treatment involves a combination of 3-4 of these antibiotics for at least one year after sputum conversion in case of pulmonary disease.[7] Still, treatment outcomes are poor, particularly for *M. abscessus*

subsp. *abscessus* for which treatment success rates as low as 33% have been reported.[10] The *M. avium* complex is more extensive, with *Mycobacterium avium*, *Mycobacterium intracellulare* and *Mycobacterium chimaera* being the most important members in terms of prevalence and clinical manifestations.[51] Treatment also involves long-term use of a 3-4 drug combination including a macrolide (usually azithromycin), ethambutol and either rifampicin or clofazimine. In specific cases, amikacin can be added intravenously or by inhalation.[7] *M. abscessus* complex and *M. avium* complex share multiple treatment challenges since they both require a combination of drugs for an extensive period of time, which is often accompanied by drug toxicity and drug interactions, which could compromise treatment adherence. Moreover, the pool of available (oral) antibiotics is rather limited, especially in cases of acquired drug resistance and/or drug intolerance, while, importantly, the scientific evidence supporting current treatment is scarce. Treatment of both NTM would therefore benefit from the **availability of additional effective drugs and drug combinations and a better understanding of antibiotic resistance mechanisms** that could identify strategies to counteract resistance. Contrary to the well-filled TB drug pipeline, the pipeline for NTM is only modest. Actually, since the introduction of macrolide-based treatment in the 1990s, there have not been any significant advancements in NTM treatment,[52] which is possibly due to a relative lack of dedicated research resources and international research consortia, the yet uncertain translational value of preclinical models, and the heterogeneity in NTM disease challenging the execution of clinical trials. Still, some repurposed, yet promising drug candidates are currently being evaluated for NTM infections including novel oxazolidinones, dual **β**-lactam combinations, omadacycline, and bedaquiline.[53]

Preclinical models

The field of mycobacterial drug discovery relies heavily on preclinical models to study drug activity and identify drugs and drug regimens that have the potential to improve current treatment practice, before advancing to the clinic. With that goal in mind, it is important that models are predictive of clinical outcomes. However, as models are inherently a simplification of reality, it is important to know and recognize their limitations, especially when interpreting and translating results to clinical settings.

The predictive value of various *in vitro* and *in vivo* preclinical models for TB is relatively well understood.[54-56] In TB drug development, animal models, particularly mouse models, play a key role. Mouse TB studies allow for a standardized evaluation of the relationship between drug exposure and drug response within the complex environment of a host. Given the labor-intensive and costly nature of clinical trials and the vast amount of potential drug candidates for TB, prioritization of drug regimens with the help of mouse models is highly valuable. By integrating results from various mouse studies, **mathematical modelling** can further enhance the utility of such data, thereby

allowing a comprehensive comparison of the effectiveness of different drug regimens.[57] Additionally, interpretation of mouse model data can be optimized by assessing **the impact of specific discrepancies between mice and humans**, such as **metabolism**, on drug activity, to prevent misapplication of mouse model results.[55, 58, 59]

Compared to TB, preclinical drug activity testing for NTM is still at a formative stage. The predictive value of most available models is not well-understood and models are less standardized. Also, preclinical studies typically use reference strains, but it is uncertain whether these results are generalizable to other strains or **if drug activity differs between strains**. Importantly, for NTM, a gap exists between *in vitro* drug activity testing and clinical outcome, which is illustrated by the lacking correlation between the Minimum Inhibitory Concentration, which is the foundation of drug susceptibility testing, and treatment success for most recommended antibiotics.[7] The setting of an MIC determination, in which NTM are actively replicating within a nutrient rich environment, differs significantly from the hostile environment that NTM encounter in the human body, including hypoxia, pH differences, **nutrient limitation**, or biofilm formation. As NTM are environmental bacteria, they are harnessed against hostile external influences and can adopt a **nonreplicating, metabolically altered state**, rendering them less susceptible to antibiotics.[60] It is plausible that such populations contribute to the disappointing treatment success rates and required long treatment durations. Therefore, in an effort to close the gap between *in vitro* drug activity testing and clinical outcome, it might be important to incorporate potentially relevant aspects of clinical NTM disease into the *in vitro* model arsenal. Additionally, since MIC determination is an endpoint measurement that only provides information on a drug's inhibitory activity, time-kill kinetics assays are used instead in five studies in this thesis as they not only provide information on the nature of activity (inhibitory versus killing), but also on the time- and concentration-dependency of activity.

Outline of the thesis

The overarching aim of this thesis is to identify promising treatment options for mycobacterial disease through three primary objectives:

1. To improve treatment options for TB (chapter 2)
2. To improve treatment options for NTM infections (chapter 3)
3. To improve the translational value of preclinical mycobacterial models (chapter 4)

Chapter 2 focuses on the preclinical activity of new treatment options for TB. **Chapter 2.1** assesses the treatment-shortening potential of the new treatment regimens BPaMZ and BPaL in a mouse TB model using a relapse assessment model combined with mathematical modelling. In **chapter 2.2** the preclinical body of evidence for the new

drugs delamanid and pretomanid is summarized, critically evaluating their similarities and differences.

Chapter 3 aims to improve treatment options for NTM infections with a focus on *M. abscessus* and *M. avium* using *in vitro* time-kill kinetics assays. **Chapter 3.1** investigates efflux pump upregulation in reaction to antibiotic stress in *M. abscessus* and investigates whether the putative efflux pump inhibitors thioridazine and verapamil can potentiate the activity of guideline-recommended antibiotics. Chapter 3.2 and 3.3 explore the ability of the new drug candidate omadacycline to improve NTM infections. **Chapter 3.2** evaluates the activity of omadacycline combined with guideline-recommended antibiotics against *M. abscessus*. **Chapter 3.3** explores the activity of omadacycline alone and combined with guideline-recommended antibiotics against *M. avium* and investigates whether omadacycline can prevent emergence of resistance to clarithromycin and amikacin.

Chapter 4 explores opportunities to improve the translational value of preclinical *in vitro* and *in vivo* models used in mycobacterial research. **Chapter 4.1** focuses on *in vivo*-formed metabolites with activity against *M. tuberculosis*. Using a dose-response study in a mouse TB model, the relative contribution of the TBAJ-876-M3-metabolite to the total bactericidal activity of the new TBAJ-876 compound is investigated. **Chapter 4.2** studies whether drug activity against a reference *M. abscessus* strain as assessed by time-kill kinetics assays is indicative of drug activity against clinical *M. abscessus* isolates. **Chapter 4.3** introduces an *in vitro* nutrient starvation model to induce a nonreplicating state in *M. avium* and studies uses time-kill kinetics assays to assess whether guideline-recommended and newer drug candidates are active against *M. avium* in this nonreplicating state.

In **chapter 5 and 6** the main findings of the studies included in this thesis are summarized and their implications are discussed, concluding with suggestions for future research.

References

1. Halstrom S, Price P, Thomson R. Review: Environmental mycobacteria as a cause of human infection. *Int J Mycobacteriol* 2015; **4**: 81-91.
2. van Ingen J, Bendien SA, de Lange WC et al. Clinical relevance of non-tuberculous mycobacteria isolated in the Nijmegen-Arnhem region, The Netherlands. *Thorax* 2009; **64**: 502-6.
3. Gygli SM, Borrell S, Trauner A, Gagneux S. Antimicrobial resistance in *Mycobacterium tuberculosis*: mechanistic and evolutionary perspectives. *FEMS Microbiol Rev* 2017; **41**: 354-73.
4. Nessar R, Cambau E, Reyrat JM et al. *Mycobacterium abscessus*: a new antibiotic nightmare. *J Antimicrob Chemother* 2012; **67**: 810-8.
5. World Health Organization. WHO consolidated guidelines on tuberculosis. Module 4: treatment - drug-susceptible tuberculosis treatment. Licence: CC BY-NC-SA 3.0 IGO.: World Health Organization, 2022.
6. World Health Organization. WHO consolidated guidelines on tuberculosis. Module 4: treatment - drug-resistant tuberculosis treatment, 2022 update. Licence: CC BY-NC-SA 3.0 IGO. Geneva: World Health Organization, 2022.
7. Daley CL, Iaccarino JM, Lange C et al. Treatment of Nontuberculous Mycobacterial Pulmonary Disease: An Official ATS/ERS/ESCMID/IDSA Clinical Practice Guideline. *Clin Infect Dis* 2020; **71**: e1-e36.
8. World Health Organization. Global tuberculosis report 2023. Geneva: World Health Organization, 2023.
9. Kwak N, Park J, Kim E et al. Treatment Outcomes of *Mycobacterium avium* Complex Lung Disease: A Systematic Review and Meta-analysis. *Clin Infect Dis* 2017; **65**: 1077-84.
10. Kwak N, Dalcolmo MP, Daley CL et al. *Mycobacterium abscessus* pulmonary disease: individual patient data meta-analysis. *Eur Respir J* 2019; **54**.
11. Houben RM, Dodd PJ. The Global Burden of Latent Tuberculosis Infection: A Re-estimation Using Mathematical Modelling. *PLoS Med* 2016; **13**: e1002152.
12. Mack U, Migliori GB, Sester M et al. LTBI: latent tuberculosis infection or lasting immune responses to *M. tuberculosis*? A TBNET consensus statement. *Eur Respir J* 2009; **33**: 956-73.
13. Comstock GW, Livesay VT, Woolpert SF. The prognosis of a positive tuberculin reaction in childhood and adolescence. *Am J Epidemiol* 1974; **99**: 131-8.
14. Getahun H, Matteelli A, Abubakar I et al. Management of latent *Mycobacterium tuberculosis* infection: WHO guidelines for low tuberculosis burden countries. *Eur Respir J* 2015; **46**: 1563-76.
15. Hershkovitz I, Donoghue HD, Minnikin DE et al. Detection and molecular characterization of 9,000-year-old *Mycobacterium tuberculosis* from a Neolithic settlement in the Eastern Mediterranean. *PLoS One* 2008; **3**: e3426.
16. Gutierrez MC, Brisse S, Brosch R et al. Ancient origin and gene mosaicism of the progenitor of *Mycobacterium tuberculosis*. *PLoS Pathog* 2005; **1**: e5.
17. Brosch R, Gordon SV, Marmiesse M et al. A new evolutionary scenario for the *Mycobacterium tuberculosis* complex. *Proc Natl Acad Sci U S A* 2002; **99**: 3684-9.
18. Dutour O, Colombo A, Coqueugniot H. Was the rise of TB contemporaneous with the industrial revolution? Epidemiological evolution of TB in France (17th-20th centuries) inferred from osteoarchaeological and historical archives. *Int J Paleopathol* 2021; **34**: 130-3.
19. Daniel TM. The history of tuberculosis. *Respir Med* 2006; **100**: 1862-70.

20. Weitzman D, Cayley FE, Wingfield AL. Streptomycin in the treatment of pulmonary tuberculosis. *Br J Tuberc Dis Chest* 1950; **44**: 98-104.
21. Treatment of pulmonary tuberculosis with streptomycin and para-aminosalicylic acid; a Medical Research Council investigation. *Br Med J* 1950; **2**: 1073-85.
22. Iseman MD. Tuberculosis therapy: past, present and future. *Eur Respir J Suppl* 2002; **36**: 87s-94s.
23. Murray JF, Schraufnagel DE, Hopewell PC. Treatment of Tuberculosis. A Historical Perspective. *Ann Am Thorac Soc* 2015; **12**: 1749-59.
24. Diacon AH, Donald PR. The early bactericidal activity of antituberculosis drugs. *Expert Rev Anti Infect Ther* 2014; **12**: 223-37.
25. Gandhi NR, Nunn P, Dheda K et al. Multidrug-resistant and extensively drug-resistant tuberculosis: a threat to global control of tuberculosis. *Lancet* 2010; **375**: 1830-43.
26. Nyang'wa BT, Berry C, Kazounis E et al. A 24-Week, All-Oral Regimen for Rifampin-Resistant Tuberculosis. *N Engl J Med* 2022; **387**: 2331-43.
27. Conradie F, Diacon AH, Ngubane N et al. Treatment of Highly Drug-Resistant Pulmonary Tuberculosis. *N Engl J Med* 2020; **382**: 893-902.
28. Conradie F, Bagdasaryan TR, Borisov S et al. Bedaquiline-Pretomanid-Linezolid Regimens for Drug-Resistant Tuberculosis. *N Engl J Med* 2022; **387**: 810-23.
29. Esmail A, Oelofse S, Lombard C et al. An All-Oral 6-Month Regimen for Multidrug-Resistant Tuberculosis: A Multicenter, Randomized Controlled Clinical Trial (the NExT Study). *Am J Respir Crit Care Med* 2022; **205**: 1214-27.
30. Derendinger B, Dippenaar A, de Vos M et al. Bedaquiline resistance in patients with drug-resistant tuberculosis in Cape Town, South Africa: a retrospective longitudinal cohort study. *Lancet Microbe* 2023; **4**: e972-e82.
31. Working Group on New TB Drugs. https://www.newtbdrugs.org/ (July 2024, date last accessed).
32. Honda JR, Virdi R, Chan ED. Global Environmental Nontuberculous Mycobacteria and Their Contemporaneous Man-Made and Natural Niches. *Front Microbiol* 2018; **9**: 2029.
33. Bryant JM, Grogono DM, Greaves D et al. Whole-genome sequencing to identify transmission of *Mycobacterium abscessus* between patients with cystic fibrosis: a retrospective cohort study. *Lancet* 2013; **381**: 1551-60.
34. Aitken ML, Limaye A, Pottinger P et al. Respiratory outbreak of *Mycobacterium abscessus* subspecies *massiliense* in a lung transplant and cystic fibrosis center. *Am J Respir Crit Care Med* 2012; **185**: 231-2.
35. Bange FC, Brown BA, Smaczny C et al. Lack of transmission of *Mycobacterium abscessus* among patients with cystic fibrosis attending a single clinic. *Clin Infect Dis* 2001; **32**: 1648-50.
36. Gross JE, Finklea JD, Caceres SM et al. Genomic epidemiology of *Mycobacterium abscessus* at an adult cystic fibrosis programme reveals low potential for healthcare-associated transmission. *ERJ Open Res* 2024; **10**.
37. Tortoli E. Microbiological features and clinical relevance of new species of the genus *Mycobacterium*. *Clin Microbiol Rev* 2014; **27**: 727-52.
38. Stahl DA, Urbance JW. The division between fast- and slow-growing species corresponds to natural relationships among the mycobacteria. *J Bacteriol* 1990; **172**: 116-24.
39. Zweijpfenning SMH, Ingen JV, Hoefsloot W. Geographic Distribution of Nontuberculous Mycobacteria Isolated from Clinical Specimens: A Systematic Review. *Semin Respir Crit Care Med* 2018; **39**: 336-42.
40. Prevots DR, Marras TK. Epidemiology of human pulmonary infection with nontuberculous mycobacteria: a review. *Clin Chest Med* 2015; **36**: 13-34.
41. Dahl VN, Mølhave M, Fløe A et al. Global trends of pulmonary infections with nontuberculous mycobacteria: a systematic review. *Int J Infect Dis* 2022; **125**: 120-31.

42. Griffith DE, Aksamit T, Brown-Elliott BA et al. An official ATS/IDSA statement: diagnosis, treatment, and prevention of nontuberculous mycobacterial diseases. *Am J Respir Crit Care Med* 2007; **175**: 367-416.
43. Iseman MD, Buschman DL, Ackerson LM. Pectus excavatum and scoliosis. Thoracic anomalies associated with pulmonary disease caused by *Mycobacterium avium* complex. *Am Rev Respir Dis* 1991; **144**: 914-6.
44. Prince DS, Peterson DD, Steiner RM et al. Infection with *Mycobacterium avium* complex in patients without predisposing conditions. *N Engl J Med* 1989; **321**: 863-8.
45. Szymanski EP, Leung JM, Fowler CJ et al. Pulmonary Nontuberculous Mycobacterial Infection. A Multisystem, Multigenic Disease. *Am J Respir Crit Care Med* 2015; **192**: 618-28.
46. Tortoli E. Clinical manifestations of nontuberculous mycobacteria infections. *Clin Microbiol Infect* 2009; **15**: 906-10.
47. Koh WJ, Kwon OJ, Jeon K et al. Clinical significance of nontuberculous mycobacteria isolated from respiratory specimens in Korea. *Chest* 2006; **129**: 341-8.
48. Hoefsloot W, van Ingen J, Andrejak C et al. The geographic diversity of nontuberculous mycobacteria isolated from pulmonary samples: an NTM-NET collaborative study. *Eur Respir J* 2013; **42**: 1604-13.
49. Kim HY, Kim BJ, Kook Y et al. *Mycobacterium massiliense* is differentiated from *Mycobacterium abscessus* and *Mycobacterium bolletii* by erythromycin ribosome methyltransferase gene (*erm*) and clarithromycin susceptibility patterns. *Microbiol Immunol* 2010; **54**: 347-53.
50. Nash KA, Brown-Elliott BA, Wallace RJ, Jr. A novel gene, *erm*(41), confers inducible macrolide resistance to clinical isolates of *Mycobacterium abscessus* but is absent from *Mycobacterium chelonae*. *Antimicrob Agents Chemother* 2009; **53**: 1367-76.
51. van Ingen J, Turenne CY, Tortoli E et al. A definition of the *Mycobacterium avium* complex for taxonomical and clinical purposes, a review. *Int J Syst Evol Microbiol* 2018; **68**: 3666-77.
52. Wu ML, Aziz DB, Dartois V, Dick T. NTM drug discovery: status, gaps and the way forward. *Drug Discov Today* 2018; **23**: 1502-19.
53. van der Laan R, Snabilié A, Obradovic M. Meeting the challenges of NTM-PD from the perspective of the organism and the disease process: innovations in drug development and delivery. *Respir Res* 2022; **23**: 376.
54. Bax HI, Bakker-Woudenberg I, de Vogel CP et al. The role of the time-kill kinetics assay as part of a preclinical modeling framework for assessing the activity of anti-tuberculosis drugs. *Tuberculosis (Edinb)* 2017; **105**: 80-5.
55. Ernest JP, Strydom N, Wang Q et al. Development of New Tuberculosis Drugs: Translation to Regimen Composition for Drug-Sensitive and Multidrug-Resistant Tuberculosis. *Annu Rev Pharmacol Toxicol* 2021; **61**: 495-516.
56. Berg A, Clary J, Hanna D et al. Model-Based Meta-Analysis of Relapsing Mouse Model Studies from the Critical Path to Tuberculosis Drug Regimens Initiative Database. *Antimicrob Agents Chemother* 2022; **66**: e0179321.
57. Mourik BC, Svensson RJ, de Knegt GJ et al. Improving treatment outcome assessment in a mouse tuberculosis model. *Sci Rep* 2018; **8**: 5714.
58. Driver ER, Ryan GJ, Hoff DR et al. Evaluation of a mouse model of necrotic granuloma formation using C3HeB/FeJ mice for testing of drugs against *Mycobacterium tuberculosis*. *Antimicrob Agents Chemother* 2012; **56**: 3181-95.
59. Rouan MC, Lounis N, Gevers T et al. Pharmacokinetics and pharmacodynamics of TMC207 and its N-desmethyl metabolite in a murine model of tuberculosis. *Antimicrob Agents Chemother* 2012; **56**: 1444-51.
60. Archuleta RJ, Yvonne Hoppes P, Primm TP. *Mycobacterium avium* enters a state of metabolic dormancy in response to starvation. *Tuberculosis (Edinb)* 2005; **85**: 147-58.

CHAPTER 2

Improving treatment of tuberculosis

CHAPTER 2.1

Predictive modeling to study the treatment-shortening potential of novel tuberculosis drug regimens, towards bundling of preclinical data

Saskia E. Mudde, Rami Ayoun Alsoud, Aart van der Meijden, Anna M. Upton, Manisha U. Lotlikar, Ulrika S.H. Simonsson, Hannelore I. Bax, Jurriaan E.M. de Steenwinkel

J Infect Dis. 2022 Jun; 225(11):1876-1885.

Abstract

Background

Given the persistently high global burden of tuberculosis, effective and shorter treatment options are needed. We explored the relationship between relapse and treatment length as well as interregimen differences for 2 novel antituberculosis drug regimens using a mouse model of tuberculosis infection and mathematical modeling.

Methods

Mycobacterium tuberculosis-infected mice were treated for up to 13 weeks with bedaquiline and pretomanid combined with moxifloxacin and pyrazinamide (BPaMZ) or linezolid (BPaL). Cure rates were evaluated 12 weeks after treatment completion. The standard regimen of isoniazid, rifampicin, pyrazinamide, and ethambutol (HRZE) was evaluated as a comparator.

Results

Six weeks of BPaMZ was sufficient to achieve cure in all mice. In contrast, 13 weeks of BPaL and 24 weeks of HRZE did not achieve 100% cure rates. Based on mathematical model predictions, 95% probability of cure was predicted to occur at 1.6, 4.3, and 7.9 months for BPaMZ, BPaL, and HRZE, respectively.

Conclusions

This study provides additional evidence for the treatment-shortening capacity of BPaMZ over BPaL and HRZE. To optimally use preclinical data for predicting clinical outcomes, and to overcome the limitations that hamper such extrapolation, we advocate bundling of available published preclinical data into mathematical models.

Introduction

With 10 million new cases and 1.5 million deaths in 2018, tuberculosis remains a major global problem.[1] The rise of antimicrobial resistance threatens attempts to reduce the burden of tuberculosis. Multidrug-resistant (MDR) tuberculosis requires a burdensome treatment regimen of ≥9–12 months, compromising treatment adherence.[2] Furthermore, reported treatment success rates are as low as 54%.[1] Until recently, treatment options were even more limited for extensively drug-resistant (XDR) tuberculosis.[1] Increasing attention toward the development of new therapeutic options resulted in the approval of 3 new tuberculosis compounds: bedaquiline, delamanid, and pretomanid. These compounds are being tested in combination with other new, repurposed, or established drugs to accelerate clinical implementation. Two such examples of new, all-oral regimens are bedaquiline and pretomanid combined with either moxifloxacin and pyrazinamide (BPaMZ) or linezolid (BPaL).

The superior bactericidal and sterilizing capacity of both BPaMZ and BPaL, compared with the first-line regimen, consisting of isoniazid, rifampicin, pyrazinamide, and ethambutol (HRZE), has been demonstrated in preclinical studies.[3-5] These studies indicate that BPaMZ cures *Mycobacterium tuberculosis* infection in mice in a shorter treatment duration than BPaL, which, in turn, achieves cure more quickly than HRZE. In an 8-week phase IIb clinical study, BPaMZ was shown to be safe and effective in patients with rifampicin-resistant tuberculosis.[6] The efficacy of BPaMZ in patients with drug-susceptible tuberculosis or drug-resistant tuberculosis is currently being studied in the SimpliciTB trial (ClinicalTrials registration NCT03338621). BPaL, however, was recently approved by the Food and Drug Administration and the European Medicines Agency as a 6-month regimen for XDR tuberculosis and treatment-intolerant MDR tuberculosis. BPaL was shown to improve treatment options and outcomes for this patient population, with a 90% cure rate observed in the Nix-TB trial.[7] However, exact treatment durations for BPaMZ and BPaL required to achieve desirable cure rates remain to be established through further (pre)clinical studies.

A better understanding of the relationship between treatment duration and treatment outcome is essential to guide recommendations on tuberculosis treatment duration. Because this is costly and time-consuming to assess in clinical studies, preclinical animal studies are usually conducted, and taken together with early-stage clinical trials, the results can guide the design of late-stage clinical trials.[8] However, the translational value of animal studies was critically evaluated when phase III studies investigating the integration of moxifloxacin into first line regimens failed to reproduce encouraging preclinical results.[8-13]

Mathematical modeling is one way to extract more information from animal studies, while considering the "3R" principles of replacement, reduction, and refinement.[14] Furthermore, pharmacometric modeling can significantly improve the translation of preclinical data to clinical settings.[15] We recently improved our *in vivo* experimental design, such that the data are better suited for mathematical modeling.[16] Additional treatment durations were implemented, testing fewer mice per time point. Subsequent in silico simulations enabled continuous linkage of treatment duration and probability of cure. This is an advantage over studies that investigate treatment outcome only at specific time points.

In the current work, we apply this mathematical model-based approach to evaluate treatment outcomes of BPaMZ, BPaL, and HRZE. We can thereby verify whether the strategy can be applied to other drug regimens too. Moreover, it provides insight into the relationship between treatment duration and cure rates for BPaMZ, BPaL, and HRZE, and allows for efficient comparison between the regimens. As such, results of the present study might pave the way toward bundling of available preclinical data, thereby creating even more robust models that can guide recommendations on optimal clinical tuberculosis treatment duration.

Methods

Animals, mycobacterial strain, and infection

Specified pathogen-free female BALB/c mice, aged 12–13 weeks, were obtained from Charles River. A total of 80 mice per treatment group (29 for pharmacokinetic analysis and 51 for treatment efficacy) were infected with *Mycobacterium tuberculosis* Beijing VN 2002-1585, as described elsewhere.[17] Briefly, under general anesthesia, animals were infected by intratracheal instillation of 0.96×10^5 (range, 0.88–1.10 $\times$ 10^5) colony-forming units (CFUs), followed by inhalation to ensure formation of bilateral infection. Mice were checked daily and were euthanized when humane end points were reached. The minimal inhibitory concentrations of the compounds for this *M. tuberculosis* strain were determined according to Clinical and Laboratory Standards Institutes guidelines.[18] For bedaquiline, the minimum inhibitory concentration was 0.125 mg/L, for pretomanid, 0.06 mg/L, for linezolid, 0.25 mg/L, and for moxifloxacin, 0.125 mg/L, which were considered susceptible.[19] The strain was susceptible to pyrazinamide, as tested by the BACTEC MGIT-960 system (Becton Dickinson).

Ethical approval

Experimental protocols adhered to the rules specified in the Dutch Animal Experimentation Act and were in concordance with the European Union animal directive 2010/63/EU (license nos. 117-14-04 and AVD1010020173687).

Tuberculosis drugs

Bedaquiline (supplied by TB Alliance) was formulated every 2 weeks in an acidified (pH 2) 20% (wt/vol) hydroxypropyl-β-cyclodextrin (Kleptose, Roquette) solution. Pretomanid (supplied by TB Alliance) was first suspended in 10% (w/v) hydroxypropyl-β-cyclodextrin (Kleptose, Roquette BV, Hoofddorp, The Netherlands) and stirred for 24 hours on a magnetic stirrer to form a pretomanid-hydroxypropyl-β-cyclodextrin complex. After stirring, the suspension was sonicated with a thick probe at ± 8% amplitude for 10 minutes. Next, an equal volume 20% (w/v) lecithin solution was added to reach a final concentration of 50 mg/mL. The suspension was stirred for 10 minutes on a magnetic stirrer to form a lipid bilayer around the complex. Subsequently, the suspension was sonicated at 10% amplitude for 30 minutes and was diluted in water to the desired end concentration. The suspension was stirred daily for 15 minutes before addition to the BPaL cocktail. Moxifloxacin (BOC Sciences) and pyrazinamide (Sigma-Aldrich) were dissolved together in distilled water by heating to 55°C. Linezolid (Ambinter) was suspended in a 0.5% (wt/vol) methylcellulose (Sigma-Aldrich) solution in distilled water. All formulations were stored at 4°C. Drugs were administered together in either the BPaMZ or BPaL combination in a volume of 0.2 mL, once daily by oral gavage, 5 days per week. Drug doses were as follows: bedaquiline, 25 mg/kg; pretomanid, linezolid, and moxifloxacin, 100 mg/kg each; and pyrazinamide, 150 mg/kg.

Pharmacokinetic analyses

Drug concentrations, including the *N*-desmethyl bedaquiline metabolite (M2), in mouse serum were quantified after 4 weeks of BPaMZ or BPaL treatment (steady-state drug concentrations). At 0.25, 0.5, 0.75, 1, 1.5, 2, 3, 4, 6, 8, 12, and 24 hours after drug administration 2 mice were sacrificed and blood samples were collected in 2 mL microcentrifuge tubes (Sarstedt) by orbital sinus bleeding. Samples were allowed to clot for 30 minutes at 4°C, and serum was separated by centrifugation (10.000*g* for 5 minutes). Serum was decontaminated with acetonitrile (Biosolve) at a ratio of 1:3 respectively. After vortexing and centrifugation (10.000 x *g* for 5 minutes), clear supernatant was transferred into cryotubes.

Serum samples were stored at −80°C. Serum analyte concentrations were assessed using liquid chromatography-tandem mass spectrometry (LC-MS/MS).

Standard curves and quality controls: Neat standard stock solutions for all compounds were prepared at 1.0 mg/mL in DMSO/methanol (MeOH) (1:1). To set up calibration standards and quality controls (QC), stock solutions were serially diluted in mouse serum K2 EDTA for bedaquiline, *N*-monodesmethyl bedaquiline, pretomanid, moxifloxacin, and linezolid, and in blank mouse serum containing 10% formic acid in the case of pyrazinamide. The standard curve ranged from 5 to 5.000 ng/mL. Four concentrations were used for QC, with 15 ng/mL for the low QC, 250 ng/mL for middle QC, 4.000 ng/mL for high QC, and 25.000 ng/mL for dilution QC.

Sample Extraction Procedures: Briefly, 50 µL of blank matrices, control samples, standards, and QC samples were combined with 150 µL acetonitrile (ACN), paralleling the decontamination of the study samples. For all analytes except pyrazinamide, after vortexing and centrifugation, 25 µL of supernatant from the previous step or from decontaminated study samples was combined with 200 µL ACN containing internal standard (100 ng/mL tolbutamide), except for matrix blanks where ACN without internal standard was used. The mixtures were again vortexed and centrifuged. To 25 µL of the extracted supernatant, 250 µL ACN:water 30:70 was added for analysis of bedaquiline, *N*-desmethyl bedaquiline, and pretomanid. In the case of moxifloxacin and linezolid analysis, 50 µL of the extracted supernatant was combined with 200 µL of deionized water. For the extraction procedure of pyrazinamide, after the first extraction step, 50 µL of supernatant was mixed with 50 µL ACN containing 5 ng/mL tolbutamide, or ACN without internal standard for matrix blanks. Following vortexing and centrifugation, the resulting solution was evaporated to dryness under a steady stream of nitrogen at 50°C, after which 150 µL MeOH/water (20:80) was added. All mixtures were then vortexed and centrifuged before storage at 2-8°C or further analysis by HPLC set to 4°C.

LC-MS/MS analysis: LC-MS/MS analysis of bedaquiline, M2, pretomanid, moxifloxacin, and linezolid was performed on a Shimadzu Nexera X2 liquid chromatograph with a Thermo BetaBasic-4 column (2.1 × 50 mm; 5 µm), coupled to an AB Sciex Triple Quad 5500 mass spectrometer. For pyrazinamide analysis, a Thermo Aquasil C18 column (2.1 × 50 mm; 5 µm) and AB Sciex Triple Quad 6500 mass spectrometer were used. The lower limit of quantification for all compounds was 5 ng/mL. For the mobile phase A 0.1% formic acid in water was used (with 10 mM ammonium formate in the case of moxifloxacin and linezolid) and 0.1% formic acid in ACN for the mobile phase B. Injection volumes were either 10 µL (bedaquiline, *N*-desmethyl bedaquiline, pretomanid) or 5 µL (moxifloxacin, linezolid, pyrazinamide). Quantification of the analytes was performed using multiple-reaction monitoring (MRM) of parent/product transitions in electrospray positive-ionization mode. The MRM transitions used were as follows: bedaquiline (555.2/58.1), *N*-monodesmethyl bedaquiline (541.2/480.2), pretomanid (360.2/175.1), moxifloxacin (402.3/364.2), pyrazinamide (124.1/81.1), linezolid (338.2/235.0), and tolbutamide (271/155.1). Sample

analysis was accepted if quality control sample concentrations were within 20% of the nominal concentration. Data were processed using Analyst 1.6.3 software (Sciex). The maximum drug concentrations and area under the concentration-time curve over 24 hours were determined using noncompartmental analysis in GraphPad Prism 8 software (GraphPad Software).

Treatment outcome assessment

Two weeks after infection, just before the start of treatment, 3 mice per treatment group were euthanized to determine mycobacterial load in lungs and spleen at baseline. The treatment duration ranged from 4 to 11 weeks for BPaMZ, and from 6 to 13 weeks for BPaL, based on results from other preclinical studies.[3-5] Twice weekly, treatment was stopped for 3 mice per group. To assess whether the elapsed treatment duration led to cure, mice were euthanized 12 weeks after treatment completion as described elsewhere.[17] Lungs and spleen were removed aseptically, homogenized, and serially diluted. Dilutions were cultured on 7H10 Middlebrook agar plates (BD) with activated charcoal to prevent drug carryover, and on plates without charcoal. Because *M. tuberculosis* grew better on charcoal-lacking plates, the mycobacterial load was first assessed by CFU counting on these plates. When no CFUs were detected, charcoal-containing plates were checked to determine whether this was an effect of drug carryover. The lower limit of detection is 11.5 CFUs per lung, calculated from a single colony detected in 200 µL plated from 2.3 mL of lung homogenate per mouse, and 10.5 CFUs per spleen, based on 200 µL from 2.1 mL of spleen homogenate.

Statistical analysis

CFU counts were Log_{10}-transformed before analysis. An unpaired 2-tailed *t* test was used to compare exposure to bedaquiline, M2, and pretomanid between BPaMZ and BPaL, and mean CFU counts between the treatment groups at the start of treatment. The level of statistical significance was set at $\alpha = 0.05$. Statistical analysis was performed using GraphPad Prism software, version 8 (GraphPad Software).

The experimental BPaMZ and BPaL data, together with HRZE data from a previous study with the same experimental protocol,[20] were used to build the mathematical model. All data were analyzed simultaneously to allow for evaluation of potential differences between regimens. The model building strategy was described elsewhere.[16] Observed CFU counts in the lungs at 12 weeks after treatment completion were converted to binary outcome values of cure (no CFUs detected) or failure (CFUs detected). Evaluation of different models was based on their objective function value, indicating the likelihood of a model to fit the data, scientific plausibility, parameter uncertainty, and visual predictive checks.

Model development was performed in 2 steps. First, the relation between probability of cure and treatment duration, regardless of the drug regimen, was described. The starting point was a base model which assumed there is no relation between cure rates and treatment duration. Next, different relations with respect to treatment duration were evaluated, including a linear model, an E_{max} model, and a sigmoidal E_{max} model. Among these, the model that best fitted the experimental data was taken to the second step, which evaluated whether the relation was significantly different between the 3 regimens. In a stepwise approach, various models were fitted to determine whether a given model parameter differed significantly between 1 regimen and the other 2. Only models that significantly lowered the objective function value by >3.84 points ($P < 0.05$) were further evaluated in combinations.

In the experimental setup, 3 mice were tested by treatment duration in each regimen, limiting cure rates to 0%, 33%, 67%, or 100%. To predict cure rates in the entire range between 0% and 100%, the data set was bootstrapped. Model parameters were then re-estimated using 1.000 resampled data sets from the observed data with replacement. From the resulting distribution of 1.000 parameter estimates, 95% probability of cure and 90% confidence intervals were predicted. The data were analyzed using NONMEM 7.4.3 (ICON).[21] Visual predictive checks, generated using 1.000 simulations, were produced using Xpose [22] and Perl-speaks-NONMEM (PsN) 4.10.0 software.[22] Data management and graphic analysis were performed using R 3.6.3 software.[23]

Results

Pharmacokinetics in BALB/c mice

Serum concentration-time profiles and pharmacokinetic parameters of each drug in BPaMZ and BPaL are shown in Figures 1 and 2, and Table 1. There was no significant difference in exposure to bedaquiline ($P = 0.95$), M2 ($P = 0.67$), and pretomanid ($P = 0.74$), expressed as the area under the concentration-time curve over 24 hours, between BPaMZ and BPaL. Pharmacokinetic parameters that drive treatment efficacy of the tested compounds are in line with findings of previous preclinical studies.[4, 24-30]

Pharmacodynamic analysis – *in vivo* studies

Mice tolerated both regimens well, although BPaL-treated mice were considerably more active during the first 3.5 weeks of treatment. One mouse that had received BPaL for 9 weeks required euthanasia on reaching humane end points in the 10th week after treatment completion.

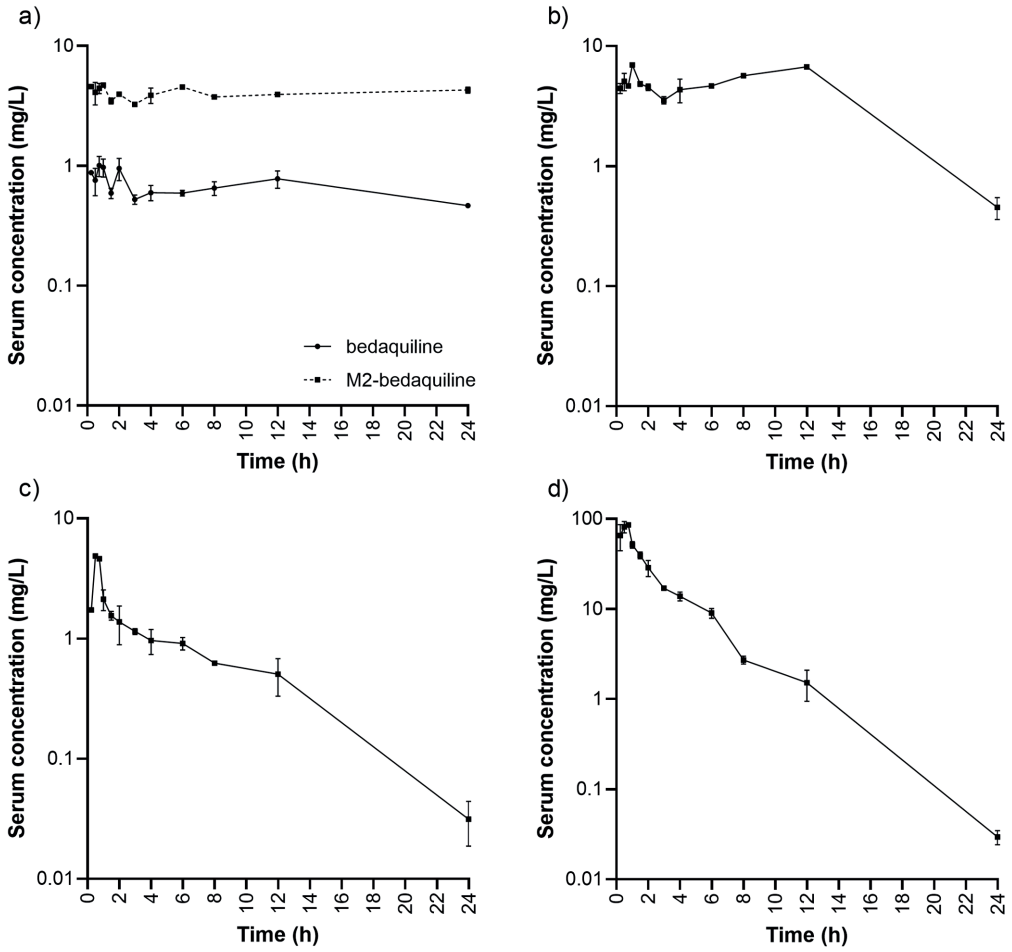

Figure 1. *Mycobacterium tuberculosis*–infected BALB/c mice (n = 2 per time point) were treated 5 times per week for 4 weeks with bedaquiline (25 mg/kg), pretomanid (100 mg/kg), moxifloxacin (100 mg/kg), and pyrazinamide (150 mg/kg). Bedaquiline and its *N*-desmethyl bedaquiline metabolite (M2) (A), pretomanid (B), moxifloxacin (C), and pyrazinamide (D) serum concentration-time profiles are plotted as means with ranges (error bars) at various time points after the last drug administration.

The mycobacterial load at 12 weeks after completion of different treatment durations is depicted in Figure 3. Starting inocula were similar in both treatment groups ($P = 0.14$). Cure was achieved in all mice receiving BPaMZ for ≥6 weeks, with all mice having culture-negative lungs after 12 weeks after treatment completion. In the BPaL group, cure rates exceeding 0% (culture-negative lungs in ≥1 of the 3 mice) were observed after 10.5, 11.0, 12.0, and 12.5 weeks of treatment. Nevertheless, the maximum treatment duration of 13 weeks did not achieve cure in all mice. Mycobacterial loads in the spleen showed similar patterns. HRZE treatment did not reach 100% cure rates. At 12 weeks after the maximum treatment duration of 24 weeks, 1 of the 3 mice had culture-positive lungs.[20]

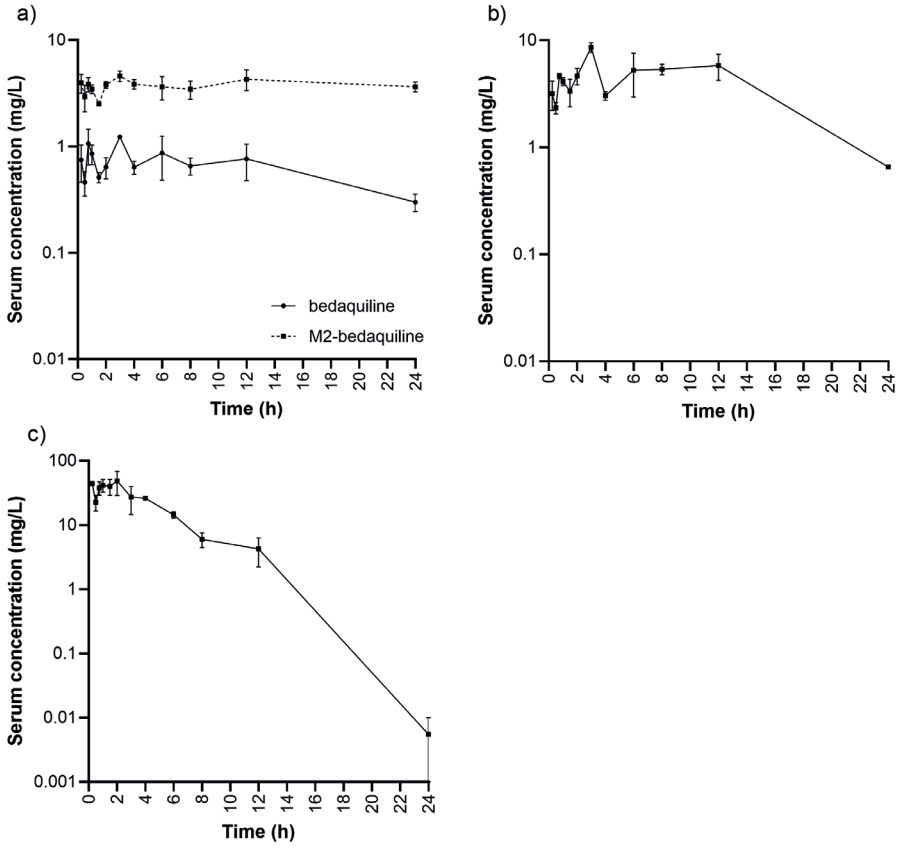

Figure 2. *Mycobacterium tuberculosis*–infected BALB/c mice (n = 2 per time point) were treated 5 times per week for 4 weeks with bedaquiline (25 mg/kg), pretomanid (100 mg/kg), and linezolid (100 mg/kg). Bedaquiline and its *N*-desmethyl bedaquiline metabolite (M2) (A), pretomanid (B), and linezolid (C) serum concentration-time profiles are plotted as means with ranges (error bars) at various time points after the last drug administration.

Table 1. Pharmacokinetic analysis serum values by treatment regimen (n = 2 per time point)

Regimen	Compound (mg/kg)	C_{max}, range, mg/L	AUC_{0-24}, mean (SEM), mg · h/L
BPaMZ	Bedaquiline (25)	0.81–1.20	15.52 (1.22)
	N-desmethyl bedaquiline	4.55–4.87	95.78 (2.34)
	Pretomanid (100)	6.89–7.03	104.20 (2.44)
	Moxifloxacin (100)	4.78–4.96	15.70 (1.67)
	Pyrazinamide (150)	89.90-81.60	186.80 (9.41)
BPaL	Bedaquiline (25)	1.20–1.26	15.32 (2.75)
	N-desmethyl bedaquiline	4.07–5.11	91.61 (9.54)
	Pretomanid (100)	7.70–9.50	99.13 (15.14)
	Linezolid (100)	28.70–68.90	240.00 (28.84)

Abbreviations: AUC_{0-24}, area under the concentration-time curve over 24 hours; BPaL, bedaquiline and pretomanid combined with linezolid; BPaMZ, bedaquiline and pretomanid combined with moxifloxacin and pyrazinamide; C_{max}, maximum serum concentration; SEM, standard error of the mean.

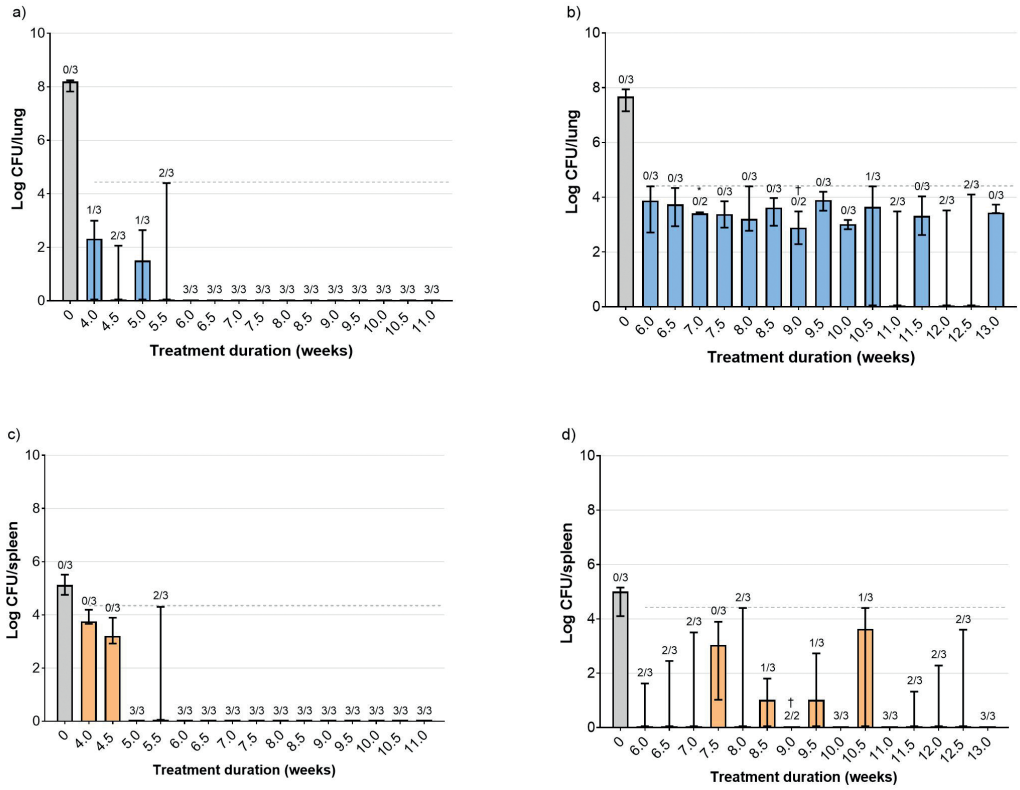

Figure 3. Mycobacterial load in lung (A, B) and spleen (C, D) expressed as medians with ranges (error bars) of colony-forming units (CFUs) at 12 weeks after different treatment durations. Mice were treated with bedaquiline and pretomanid combined with either moxifloxacin and pyrazinamide (BPaMZ) (A, C) or linezolid (BPaL) (B, D). Numbers above bars indicate the number of mice with cure relative to the total number examined. Dashed horizontal lines indicate the upper limits of detection (in CFUs). * CFU counting of 1 plate could not be performed owing to contamination. † One mouse reached humane end points and was euthanized before the planned date. Heart and lungs from this mouse were cultured, and no CFUs were recovered on the plates.

Pharmacodynamic analysis – mathematical modeling

The final model was a sigmoidal E_{max} relation regarding probability of failure ($Pr_{failure}$) and probability of cure (Pr_{cure}) in relation to treatment length and regimen, as follows:

$$Pr_{failure} = 1 - Pr_{cure} = Pr_{base} \cdot [1 - [(E_{max} \cdot Length^{\gamma})/T_{50}{}^{\gamma} + Length^{\gamma})]]$$

where E_{max} is the maximum probability of cure fixed to 1, T_{50} is the regimen-specific treatment duration at which 50% of E_{max} is achieved, Pr_{base} is the probability of failure with no treatment, and γ is the Hill factor parameter that controls the shape and steepness of the E_{max} curve. In the first step of model building, an E_{max} model was identified to best

describe the relation between probability of cure and treatment duration. A sigmoidal E_{max} model provided a significantly lower objective function value but yielded scientifically implausible estimates of E_{max} and γ. Subsequently, the impact of the regimens on the probability of cure was explored in all model parameters.

Table 2. Parameter estimates of the final mathematical model

Parameter	Final estimate	RSE, %[a]	Mean estimate (90% CI)[b]
Pr_{base}	Fixed to 1	-	Fixed to 1
E_{max}	Fixed to 1	-	Fixed to 1
T_{50}, mo			
BPaMZ	1.15	7.58	1.15 (1.01-1.30)
HRZE	5.65	6.51	5.67 (4.98-6.36)
BPaL	3.16	6.14	3.17 (2.84-3.51)
γ	9.15	18.66	10.1 (6.41-13.84)

Abbreviations: γ, Hill factor parameter; BPaL, bedaquiline and pretomanid combined with linezolid; BPaMZ, bedaquiline and pretomanid combined with moxifloxacin and pyrazinamide; CI, confidence interval; E_{max}, maximum probability of cure fixed to 1; HRZE, isoniazid, rifampicin, pyrazinamide, and ethambutol; Pr_{base}, probability of failure with no treatment; RSE, relative standard error; T_{50}, treatment duration at which 50% of E_{max} is achieved.

[a] Relative standard error on the approximate standard deviation scale as obtained from the covariance step in NONMEM.

[b] Mean estimate and 90% CIs were obtained by bootstrapping the data set, followed by reestimation with the final model (n = 1000).

[c] T_{50} differed significantly between the regimens.

The T_{50} parameter was significantly different for the 3 regimens. When the difference in T_{50} between the regimens was included in the model, a sigmoidal E_{max} relation between treatment duration and probability of cure was reevaluated and determined to best fit the data. Including a regimen-specific γ parameter gave no statistically significant difference for any of the regimens. Therefore, 1 γ parameter was deemed sufficient. Final model parameter estimates are presented in Table 2. Visual predictive checks of the final model are depicted in Figure 4. Predicted treatment durations required to achieve certain probabilities of cure are plotted in Figure 5. The model predicted that 95% probability of cure was reached after 1.6 months for BPaMZ, while this was 4.3 months for BPaL and 7.9 months for HRZE.

Discussion

In the current study, treatment with BPaMZ led to a rapid decline in mycobacterial load, and achieved cure in all mice after 6 weeks of treatment. Its treatment-shortening capacity is superior to that of BPaL and HRZE, as the mathematical model predicts that 95% probability of cure is reached after 1.6 months for BPaMZ, 4.3 months for BPaL, and 7.9 months for HRZE. The order of efficacy is consistent with other mouse tuberculosis studies, in which 1.5–2 months of BPaMZ-treatment was sufficient for cure,[3, 5] while 3 months were needed for BPaL,[4, 5] and ≥6 months for HRZE.[17]

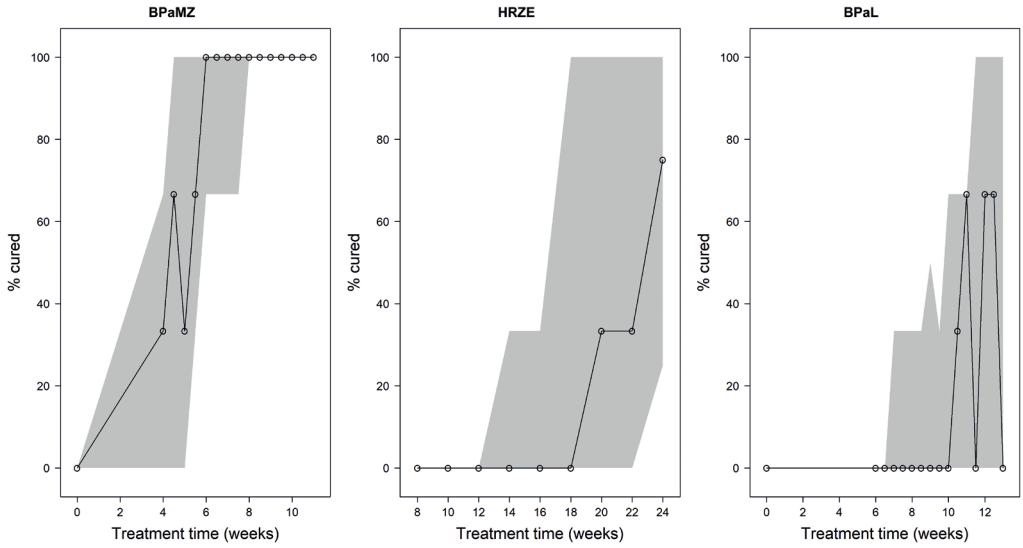

Figure 4. Visual predictive checks of the final model for each regimen, using 1000 simulations. Solid lines with open circles represent observed probabilities of cure; the shaded areas, 95% confidence intervals of the predicted cure rates. Abbreviations: BPaL, bedaquiline and pretomanid combined with linezolid; BPaMZ, bedaquiline and pretomanid combined with moxifloxacin and pyrazinamide; HRZE, isoniazid, rifampicin, pyrazinamide, and ethambutol.

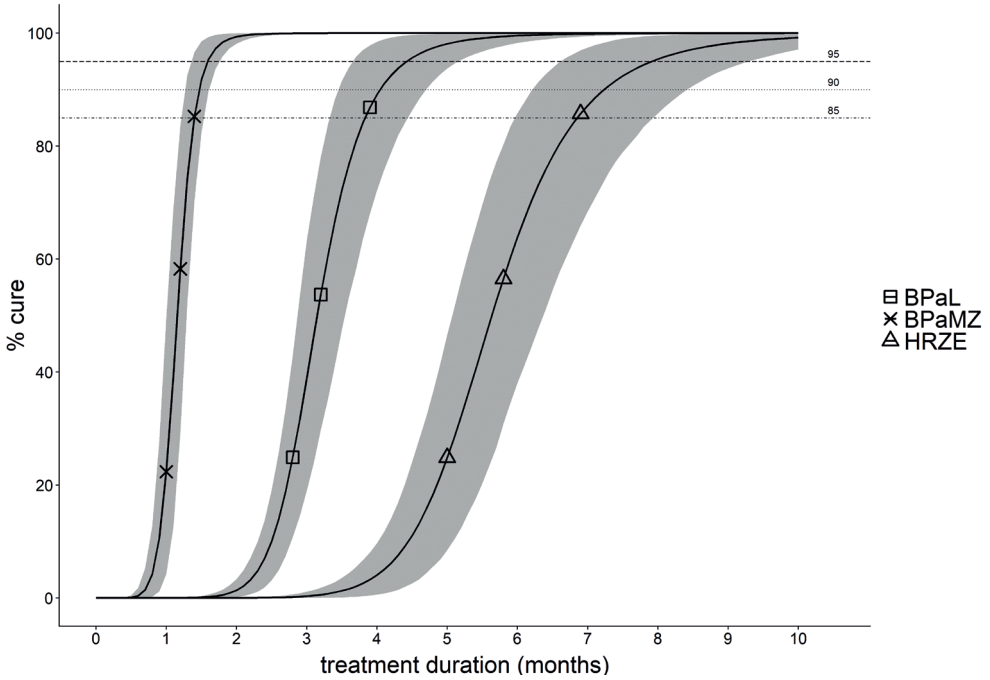

Figure 5. Model-predicted cure rates after different treatment durations for the 3 treatment regimens, using 1000 bootstraps of the original data set and with re-estimation using the final model. The lines resemble mean probabilities of cure, and gray-shaded areas, 90% confidence intervals of the predictions from the 1000 distributions of the re-estimated model parameters. Abbreviations: BPaL, bedaquiline and pretomanid combined with linezolid; BPaMZ, bedaquiline and pretomanid combined with moxifloxacin and pyrazinamide; HRZE, isoniazid, rifampicin, pyrazinamide, and ethambutol.

Compared with other mouse tuberculosis models, BPaL performance was unexpectedly low. It could be speculated that the discrepancy in BPaL efficacy is a consequence of the different *M. tuberculosis* strains used, as was previously shown for HRZE.[17, 31] We used a Beijing strain, known for its virulence and clinical relevance,[32-35] while other studies used the H37Rv strain.[4, 5] The different treatment outcomes highlight the importance of using various *M. tuberculosis* strains to assess treatment efficacy. It is noteworthy that in the context of containing regimens containing bedaquiline and pretomanid, linezolid shows differential efficacy against H37Rv versus Beijing strains, whereas moxifloxacin- and pyrazinamide-containing regimens achieve similar efficacy against both strains.[3-5] It could be that drug interactions within BPaL are more favorable in treating H37Rv than in treating Beijing strains.

This interpretation is strengthened in a finding by Bigelow et al. [36] that drug interactions within BPaL varied according to *M. tuberculosis* strain. In mice infected with HN878 (belonging to the W-Beijing family), both bedaquiline plus pretomanid and bedaquiline

plus linezolid performed better than BPaL, while against H37Rv, BPaL was the best-performing drug combination in that study. What mechanisms underlie such strain-dependent drug interactions is unclear. The reasons for the apparent superiority of BPaMZ over BPaL observed in this and other preclinical studies are not yet elucidated. *In vitro* interaction between bedaquiline and pyrazinamide is known to be synergetic,[37, 38] whereas interaction between bedaquiline and linezolid was shown to be additive,[39] indifferent,[36] or even antagonistic.[40] However, we find that exposure to bedaquiline, its M2 metabolite, and pretomanid are similar for BPaMZ and BPaL, which argues against drug-drug interactions as drivers of the rank order in treatment efficacy.

The present study confirms that the improved experimental setup and mathematical modeling, as we introduced elsewhere,[16] can shed light on the relationship between treatment duration and treatment outcome, and facilitates efficient comparison between regimens. This setup differs from conventional mouse tuberculosis studies, because treatment efficacy is assessed 12 weeks after treatment completion (sterilizing activity) but not directly after treatment completion (bactericidal activity). Moreover, sample sizes are smaller, with only 3 mice euthanized per treatment duration.[3-5, 16] Yet this design with additional treatment durations and small sample sizes still had power to evaluate treatment differences using mathematical modeling, as it was found to be sufficient to detect a 50% difference in potency between regimens and reached high precision in model parameters.[16]

In our modeling approach, we assumed that all regimens can eventually result in 100% cure (E_{max} fixed at 100%). As such, not all regimens in the mouse experiments need to reach 100% cure, as was the case for HRZE and BPaL. Especially for new regimens it can be difficult to select optimum treatment durations in the experimental design. Mathematical modeling adds value, as the probability of cure can be predicted for all regimens as long as one regimen provides information about the relationship between treatment length and almost-complete cure, together with the assumption that only T_{50} differs between the regimens. The modeling approach could also estimate Emax for regimens that never reach 100% cure. However, in this case, the experimental design would need to include data on maximal cure.

Our combined experimental-mathematical model approach provides guidance on treatment durations needed to reach certain cure rates. The Nix-TB trial, a phase III study that investigated the efficacy of BPaL in patients with MDR or XDR tuberculosis, demonstrated a 90% treatment success rate after 6 months of treatment.[7] It is tempting to speculate that shorter treatment durations might be sufficient, considering the predicted 95% probability of cure in mice at 4.3 months. However, several limitations in our model should be considered when extrapolating results to the clinical situation.

First, BALB/c mice develop cellular granulomas with minimal necrosis on tuberculosis infection,[41] whereas necrotizing, caseous lesions are a hallmark of human tuberculosis. The distinct environmental conditions in caseous lesions (eg, hypoxia, more neutral pH) influence local drug effects.[42] Bedaquiline, pretomanid, and moxifloxacin are reported to accumulate in cellular regions rather than in necrotic areas of granulomas,[25, 42, 43] while pyrazinamide and linezolid seem to diffuse equally well through these compartments.[42, 44]

This characteristic of pyrazinamide and linezolid is perhaps less clearly expressed in our mouse model, since the granulomas are mostly cellular instead of necrotizing. Hence, these diffusion patterns might imply that BPaMZ could generate more favorable results than BPaL in our model versus models with necrotic granulomas. It should be noted that although the aforementioned studies use elegant methods to approximate drug concentrations at the infection site, exposure-response relationships based on such data should be interpreted with caution.[45]

This limitation is (partly) addressed by using C3HeB/FeJ mice, in which lung disease on tuberculosis infection more closely resembles human tuberculosis.[25] As BPaMZ also seems to outperform BPaL and HRZE in C3HeB/FeJ mouse tuberculosis models,[5, 36, 46] the impact of different lung pathology on the translational value of our results is probably modest.

Second, whether a mouse tuberculosis model represents acute, subacute, or chronic infection depends on the activity of the adaptive immune system. This depends on the time window between infection and treatment initiation.[8] In acute infection models, bacilli replicate logarithmically, which is suitable for assessing a regimen's bactericidal capacity. Slowly or nonreplicating bacilli are present in chronic infection models, which are effective for determining sterilizing activity. The present model resembles subacute infection,[17] characterized by a more heterogeneous mycobacterial population.[8] Since a complex spectrum of lung lesions is present in patients with tuberculosis,[47] including data from both acute and chronic preclinical infection models could enrich the input of the mathematical model.

In conclusion, with the current study we provide additional evidence in favor of the treatment-shortening capacity of BPaMZ over BPaL, and BPaL over HRZE. To enable the optimal use of preclinical data and to overcome the limitations that hamper extrapolation of animal data to humans, we advocate bundling of available preclinical data into mathematical models. As such, the predictive value of mathematical models could be enhanced in their ability to guide decision making on treatment durations, which is needed to achieve desirable cure rates in patients with tuberculosis.

Acknowledgements

This work was supported by the TB Alliance with funding from Australia's Department of Foreign Affairs and Trade, the Bill & Melinda Gates Foundation (grant OPP1129600), Germany's Federal Ministry of Education and Research through the KfW, Irish Aid, the National Institute of Allergy and Infectious Disease, the Netherlands Ministry of Foreign Affairs, the United Kingdom Department for International Development, and the US Agency for International Development.

References

1. World Health Organization. Global tuberculosis report 2019. Geneva, Switzerland: World Health Organization, 2019.
2. World Health Organization. WHO consolidated guidelines on drug-resistant tuberculosis treatment. Geneva, Switzerland: World Health Organization, 2019.
3. Li SY, Tasneen R, Tyagi S, et al. Bactericidal and sterilizing activity of a novel regimen with bedaquiline, pretomanid, moxifloxacin, and pyrazinamide in a murine model of tuberculosis. Antimicrob Agents Chemother 2017; 61:e00913–17.
4. Tasneen R, Betoudji F, Tyagi S, et al. Contribution of oxazolidinones to the efficacy of novel regimens containing bedaquiline and pretomanid in a mouse model of tuberculosis. Antimicrob Agents Chemother 2016; 60:270–7.
5. Xu J, Li SY, Almeida DV, et al. Contribution of pretomanid to novel regimens containing bedaquiline with either linezolid or moxifloxacin and pyrazinamide in murine models of tuberculosis. Antimicrob Agents Chemother 2019; 63:e00021–19.
6. Tweed CD, Dawson R, Burger DA, et al. Bedaquiline, moxifloxacin, pretomanid, and pyrazinamide during the first 8 weeks of treatment of patients with drug-susceptible or drug-resistant pulmonary tuberculosis: a multicentre, open-label, partially randomised, phase 2b trial. Lancet Respir Med 2019; 7:1048–58.
7. Conradie F, Diacon AH, Ngubane N, et al; Nix-TB Trial Team. Treatment of highly drug-resistant pulmonary tuberculosis. N Engl J Med 2020; 382:893–902.
8. Nuermberger EL. Preclinical efficacy testing of new drug candidates. Microbiol Spectr 2017; 5:TBTB2-0034-2017.
9. Gillespie SH, Crook AM, McHugh TD, et al; REMoxTB Consortium. Four-month moxifloxacin-based regimens for drug-sensitive tuberculosis. N Engl J Med 2014; 371:1577–87.
10. Jawahar MS, Banurekha VV, Paramasivan CN, et al. Randomized clinical trial of thrice-weekly 4-month moxifloxacin or gatifloxacin containing regimens in the treatment of new sputum positive pulmonary tuberculosis patients. PLoS One 2013; 8:e67030.
11. Lanoix JP, Chaisson RE, Nuermberger EL. Shortening tuberculosis treatment with fluoroquinolones: lost in translation? Clin Infect Dis 2016; 62:484–90.
12. Nuermberger EL, Yoshimatsu T, Tyagi S, et al. Moxifloxacin-containing regimen greatly reduces time to culture conversion in murine tuberculosis. Am J Respir Crit Care Med 2004; 169:421–6.
13. Nuermberger EL, Yoshimatsu T, Tyagi S, et al. Moxifloxacin-containing regimens of reduced duration produce a stable cure in murine tuberculosis. Am J Respir Crit Care Med 2004; 170:1131–4.
14. Flecknell P. Replacement, reduction and refinement. ALTEX 2002; 19:73–8.
15. van Wijk R, Alsoud R, Lennernäs H, Simonsson U. Model informed drug discovery and development strategy for the rapid development of anti-tuberculosis drug combinations. Applied Sciences 2020; 10:2376.
16. Mourik BC, Svensson RJ, de Knegt GJ, et al. Improving treatment outcome assessment in a mouse tuberculosis model. Sci Rep 2018; 8:5714.
17. Mourik BC, de Knegt GJ, Verbon A, Mouton JW, Bax HI, de Steenwinkel JEM. Assessment of bactericidal drug activity and treatment outcome in a mouse tuberculosis model using a clinical Beijing strain. Antimicrob Agents Chemother 2017; 61:e00696–17.

18. Clinical and Laboratory Standards Institute. Susceptibility testing of Mycobacteria, Nocardia spp., and other aerobic actinomycetes. 3rd ed. CLSI standard M24. Wayne, PA: Clinical and Laboratory Standards Institute 2018;38.
19. European Committee on Antimicrobial Susceptibility Testing (EUCAST). MIC and zone diameter distributions and ECOFFs. https://mic.eucast.org/Eucast2/ Search-Controller/search.jsp?action=perform-Search&Be ginIndex=0&Micdif=mic&Num-berIndex=50&Antib=- 1&Specium=806. Accessed 29 September 2020.
20. Pieterman ED, Keutzer L, van der Meijden A, et al. Superior efficacy of a bedaquiline, delamanid and linezolid combination regimen in a mouse-TB model. J Infect Dis 2021; 224:1039–47.
21. Beal SL, Sheiner LB, Boeckmann AJ, Bauer RJ, eds. NONMEM 7.4.3 Users Guides. (1989-2018). Gaithersburg, MD, USA: ICON Development Solutions; 2018.
22. Keizer RJ, Karlsson MO, Hooker A. Modeling and simulation workbench for NONMEM: tutorial on Pirana, PsN, and Xpose. CPT Pharmacometrics Syst Pharmacol 2013; 2:e50.
23. R Core Team (2017). R: a language and environment for statistical computing. https://www.R-project.org/. Accessed 15 September 2020.
24. Grossman TH, Shoen CM, Jones SM, Jones PL, Cynamon MH, Locher CP. The efflux pump inhibitor timcodar improves the potency of antimycobacterial agents. Antimicrob Agents Chemother 2015; 59:1534–41.
25. Irwin SM, Prideaux B, Lyon ER, et al. Bedaquiline and pyrazinamide treatment responses are affected by pulmonary lesion heterogeneity in *Mycobacterium tuberculosis* infected C3HeB/FeJ mice. ACS Infect Dis 2016; 2:251–67.
26. Lakshminarayana SB, Boshoff HI, Cherian J, et al. Pharmacokinetics-pharmacodynamics analysis of bicyclic 4-nitroimidazole analogs in a murine model of tuberculosis. PLoS One 2014; 9:e105222.
27. Matsumoto M, Hashizume H, Tomishige T, et al. OPC67683, a nitro-dihydro-imidazooxazole derivative with promising action against tuberculosis *in vitro* and in mice. PLoS Med 2006; 3:e466.
28. Miyazaki E, Miyazaki M, Chen JM, Chaisson RE, Bishai WR. Moxifloxacin (BAY12-8039), a new 8-methoxyquinolone, is active in a mouse model of tuberculosis. Antimicrob Agents Chemother 1999; 43:85–9.
29. Nuermberger E, Rosenthal I, Tyagi S, et al. Combination chemotherapy with the nitroimidazopyran PA-824 and first-line drugs in a murine model of tuberculosis. Antimicrob Agents Chemother 2006; 50:2621–5.
30. Pieterman ED, Te Brake LHM, de Knegt GJ, et al. Assessment of the additional value of verapamil to a moxifloxacin and linezolid combination regimen in a murine tuberculosis model. Antimicrob Agents Chemother 2018; 62:e01354–18.
31. De Groote MA, Gruppo V, Woolhiser LK, Orme IM, Gilliland JC, Lenaerts AJ. Importance of confirming data on the *in vivo* efficacy of novel antibacterial drug regimens against various strains of *Mycobacterium tuberculosis*. Antimicrob Agents Chemother 2012; 56:731–8.
32. Ford CB, Shah RR, Maeda MK, et al. *Mycobacterium tuberculosis* mutation rate estimates from different lineages predict substantial differences in the emergence of drug-resistant tuberculosis. Nat Genet 2013; 45:784–90.
33. Karmakar M, Trauer JM, Ascher DB, Denholm JT. Hyper transmission of Beijing lineage *Mycobacterium tuberculosis*: systematic review and meta-analysis. J Infect 2019; 79:572–81.

34. Liu Q, Wang D, Martinez L, et al. *Mycobacterium tuberculosis* Beijing genotype strains and unfavourable treatment outcomes: a systematic review and meta-analysis. Clin Microbiol Infect 2020; 26:180–8.

35. Merker M, Blin C, Mona S, et al. Evolutionary history and global spread of the *Mycobacterium tuberculosis* Beijing lineage. Nat Genet 2015; 47:242–9.

36. Bigelow KM, Tasneen R, Chang YS, Dooley KE, Nuermberger EL. Preserved efficacy and reduced toxicity with intermittent linezolid dosing in combination with bedaquiline and pretomanid in a murine TB model. Antimicrob Agents Chemother 2020; 64:e01178–20.

37. Ibrahim M, Andries K, Lounis N, et al. Synergistic activity of R207910 combined with pyrazinamide against murine tuberculosis. Antimicrob Agents Chemother 2007; 51:1011–5.

38. Veziris N, Ibrahim M, Lounis N, et al. A once-weekly R207910-containing regimen exceeds activity of the standard daily regimen in murine tuberculosis. Am J Respir Crit Care Med 2009; 179:75–9.

39. de Miranda Silva C, Hajihosseini A, Myrick J, et al. Effect of Linezolid plus Bedaquiline against *Mycobacterium tuberculosis* in log phase, acid phase, and nonreplicating-persister phase in an *in vitro* assay. Antimicrob Agents Chemother 2018; 62:e00856–18.

40. Pang Y, Jing W, Lu J, et al. No *in vitro* synergistic effect of bedaquiline combined with fluoroquinolones, linezolid, and clofazimine against extensively drug-resistant tuberculosis. Diagn Microbiol Infect Dis 2019; 94:361–4.

41. Driver ER, Ryan GJ, Hoff DR, et al. Evaluation of a mouse model of necrotic granuloma formation using C3HeB/FeJ mice for testing of drugs against *Mycobacterium tuberculosis*. Antimicrob Agents Chemother 2012; 56:3181–95.

42. Prideaux B, Via LE, Zimmerman MD, et al. The association between sterilizing activity and drug distribution into tuberculosis lesions. Nat Med 2015; 21:1223–7.

43. Dartois V. The path of anti-tuberculosis drugs: from blood to lesions to mycobacterial cells. Nat Rev Microbiol 2014; 12:159–67.

44. Strydom N, Gupta SV, Fox WS, et al. Tuberculosis drugs' distribution and emergence of resistance in patient's lung lesions: a mechanistic model and tool for regimen and dose optimization. PLoS Med 2019; 16:e1002773.

45. Mouton JW, Theuretzbacher U, Craig WA, Tulkens PM, Derendorf H, Cars O. Tissue concentrations: do we ever learn? J Antimicrob Chemother 2008; 61:235–7.

46. Rosenthal IM, Tasneen R, Peloquin CA, et al. Dose-ranging comparison of rifampin and rifapentine in two pathologically distinct murine models of tuberculosis. Antimicrob Agents Chemother 2012; 56:4331–40.

47. Lenaerts A, Barry CE 3rd, Dartois V. Heterogeneity in tuberculosis pathology, microenvironments and therapeutic responses. Immunol Rev 2015; 264:288–307.

CHAPTER 2.2

Delamanid or pretomanid? A Solomonic judgement!

Saskia E. Mudde, Anna M. Upton, Anne Lenaerts,
Hannelore I. Bax, Jurriaan E.M. de Steenwinkel

J Antimicrob Chemother. 2022 Mar; 77(4):880-902.

Abstract

Given the low treatment success rates of drug-resistant tuberculosis (TB), novel TB drugs are urgently needed. The landscape of TB treatment has changed considerably over the last decade with the approval of three new compounds: bedaquiline, delamanid and pretomanid. Of these, delamanid and pretomanid belong to the same class of drugs, the nitroimidazoles. In order to close the knowledge gap on how delamanid and pretomanid compare with each other, we summarize the main findings from preclinical research on these two compounds. We discuss the compound identification, mechanism of action, drug resistance, *in vitro* activity, *in vivo* pharmacokinetic profiles, and preclinical *in vivo* activity and efficacy. Although delamanid and pretomanid share many similarities, several differences could be identified. One finding of particular interest is that certain *Mycobacterium tuberculosis* isolates have been described that are resistant to either delamanid or pretomanid, but with preserved susceptibility to the other compound. This might imply that delamanid and pretomanid could replace one another in certain regimens. Regarding bactericidal activity, based on *in vitro* and preclinical *in vivo* activity, delamanid has lower MICs and higher mycobacterial load reductions at lower drug concentrations and doses compared with pretomanid. However, when comparing *in vivo* preclinical bactericidal activity at dose levels equivalent to currently approved clinical doses based on drug exposure, this difference in activity between the two compounds fades. However, it is important to interpret these comparative results with caution knowing the variability inherent in preclinical *in vitro* and *in vivo* models.

Introduction

The approval of bedaquiline for the treatment of drug-resistant tuberculosis (TB) by the FDA in 2012 led to a revival of anti-TB drug development, as it was the first drug with a new mechanism of action to be registered for the treatment of TB in 40 years. In the years that followed, the landscape of drug-resistant TB treatment changed considerably. In 2014, another new compound, delamanid, was approved by the EMA for the treatment of MDR-TB in adults. Currently, the WHO states that delamanid is indicated for the treatment of rifampicin-resistant (RR) TB or MDR-TB in adults and children.[1] More recently, in 2019, pretomanid was the third new drug introduced to the anti-TB drug arsenal. Pretomanid was granted FDA approval, with an indication specified for treating adults with XDR-TB or drug-intolerant or non-responsive MDR-TB. It is to be combined with bedaquiline and linezolid, known as the BPaL-regimen.

The process of drug development is being accelerated by a novel approach developed by the Critical Path to TB Drug Regimens.[2] Within this approach, novel drugs are tested as a part of new multidrug regimens already in early stages of the preclinical developmental pipeline. Within such regimens, new compounds are combined with established TB compounds (e.g. pyrazinamide), other new compounds (e.g. bedaquiline and pretomanid in the BPaL regimen), or drugs that are approved for treating diseases other than TB (as was the case for linezolid). The efficacy of these new regimens is subsequently tested in clinical trials as a unit, rather than as a single drug. This is different from the traditional approach that studies the addition of a new compound to an existing regimen or the replacement of single drugs by new ones. Although the new approach enables quicker clinical implementation of novel TB drugs (illustrated by the approval of pretomanid only within the BPaL regimen), it may leave us with the question how new compounds from the same class of drugs compare with each other. In this context, it would be interesting to rank new compounds based on their efficacy, and to assess whether new drugs could be interchangeable in case of drug resistance or drug intolerance. Such questions are of particular interest for delamanid and pretomanid, since they belong to the same class of drugs. In addition, although their clinical indications differ, it is possible that future expansions of approvals would allow for treatment of individual patients with either drug, within the same regimen.

In this review, we summarize and discuss preclinical data on delamanid and pretomanid that have contributed to the implementation of these drugs in the clinic, including compound identification, mechanism of action, drug resistance, *in vitro* activity, *in vivo* pharmacokinetic profiles, and *in vivo* activity and efficacy. Their similarities and differences are discussed and remaining knowledge gaps are identified. Evaluation of clinical studies on either compound are not within the scope of this review.

Compound discovery

Delamanid and pretomanid are nitroimidazoles, a class of drugs active against a broad spectrum of microorganisms, including protozoa and anaerobic bacteria.[3] Another well-known member of the nitroimidazoles is metronidazole, for which antibacterial activity was originally discovered in 1962.[4] In the 1970s, a subclass of nitroimidazoles was identified that harbored antimycobacterial activity.[5] This property was further explored,[6] and preclinical studies demonstrated that the bicyclic 5-nitroimidazooxazole CGI-17341 was active against *Mycobacterium tuberculosis* both *in vitro* and *in vivo*.[7] Although potential mutagenicity hampered further development of this particular compound, it paved the way towards the identification of other antimycobacterial nitroimidazoles.[6, 8]

Table 1. Chemical name and structure, and mechanism of action of delamanid and pretomanid

Characteristic	Delamanid (OPC-67683)	Pretomanid (PA-824)
Developed by	Otsuka Pharmaceutical Co., Ltd.	PathoGenesis Corporation
Chemical name[a]	(2*R*)-2-methyl-6-nitro-2-[(4-{4-[4-(trifluoromethoxy)phenoxy] piperidin-1-yl} phenoxy)methyl]-2,3-dihydroimidazo[2,1-b][1,3]oxazole	(6*S*)-2-nitro-6-[[4-(trifluoromethoxy)phenyl] methoxy]-6,7-dihydro-5*H*-imidazo[2,1-b] [1,3]oxazine
Chemical structure[a]	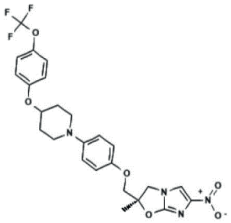	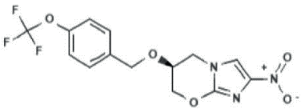
Mechanism of action	1. Inhibition of mycolic acid synthesis (methoxymycolates and ketomycolates) 2. Respiratory poisoning (reactive intermediates are yet to be identified)	1. Inhibition of mycolic acid synthesis (ketomycolates) 2. Respiratory poisoning by the release of reactive nitrogen species upon metabolic activation

[a] Information extracted from https://pubchem.ncbi.nlm.nih.gov.

Delamanid

Otsuka Pharmaceutical Co. Ltd aimed to develop an antimycobacterial compound that targets mycolic acid synthesis.[9] By random screening, three structures were identified: dihydrophenazine, urea-type and dihydroimidazooxazole derivatives. Special attention was given to the latter, given the recent positive results on the antimycobacterial activity of CGI-17341. All nitroimidazoles in the Otsuka library were screened for mutagenicity and results showed that mutagenic properties were probably related to the functional groups attached to the core structure.[9–11] In particular, derivatives containing dimethyl residues were associated with higher mutagenicity.[9] Among a series of (*R*)-form 6-nitro-

2,3-dihydroimidazo[2,1-b]oxazoles with various phenoxymethyl groups and a methyl group at the 2-position, delamanid was identified (Table 1). Its promising preclinical activity made delamanid the lead compound for further safety and efficacy studies.[9–11]

Pretomanid

In terms of the discovery of the nitroimidazoles for TB, drug discovery efforts leading to identification of pretomanid preceded those leading to delamanid. Researchers at PathoGenesis Corporation noticed the potency of CGI-17341 as well.[12] The company took an interest in nitroimidazooxazines rather than nitroimidazooxazoles, which have a six-membered ring fused to the nitroimidazole instead of a five-membered ring (Table 1). By comparing the antimycobacterial activity of a series of 328 bicyclic nitroimidazooxazines with that of CGI-17341, pretomanid was identified.[12] Pretomanid was found to be active against drug-susceptible as well as drug-resistant *M. tuberculosis* strains,[12] as was also seen for delamanid.[10] More information on optimization studies of nitroimidazooxazines that resulted in the identification of pretomanid are detailed in published patents.[13, 14]

Mechanism of action

Delamanid and pretomanid are thought to have a comparable, dual mode of action: (i) interference with mycolic acid synthesis, and (ii) respiratory poisoning.[15–17] It is noteworthy that most published research on the mechanism of action has been performed with pretomanid.

Inhibition of mycolic acid biosynthesis

Under aerobic conditions, inhibition of mycolic acid synthesis is considered to be the main mode of action of delamanid and pretomanid. Mycolic acids are a major component of the lipids forming the mycobacterial outer membrane, and are restricted to mycobacteria and related genera of the Actinobacteria phylum.[18] Mycolic acids contribute to bacterial virulence by forming a permeability barrier to drugs,[19] contributing to intracellular survival,[20] and modulating the pro-inflammatory response.[20, 21] Three classes of mycolic acids are known: α-mycolates (most abundant), methoxymycolates, and ketomycolates.[22] Delamanid inhibits synthesis of ketomycolates and methoxymycolates, but not α-mycolates,[9, 10] whereas isoniazid inhibits all three classes.[10] The exact mechanism by which delamanid blocks mycolic acid synthesis is not yet elucidated, as no mutations in delamanid-resistant organisms have been linked to cell wall synthesis.[23] Pretomanid blocks the formation of ketomycolic acid.[12] It is hypothesized that this process involves inhibition of a deazaflavin coenzyme (F_{420})-dependent enzyme that is responsible for oxidation of hydroxymycolate into ketomycolate.[24] Whether pretomanid also inhibits synthesis of the other mycolate classes is unknown.

Respiratory poisoning

Delamanid and pretomanid are prodrugs that need metabolic activation by mycobacteria to exert antimycobacterial activity (Figure 1).[10, 12, 25] In short, bio-activation of both compounds by mycobacteria depends on redox cycling of deazaflavin cofactor 420, or F_{420}. The enzyme deazaflavin-dependent nitroreductase (Ddn), which participates in the redox cycling of F_{420}, is responsible for bio-activation of both delamanid and pretomanid by the process of des-nitrification,[10, 26–28] although the compounds bind differently to Ddn.[29] Human nitroreductases were found to be unable to activate delamanid, potentially due to their use of NAD(P)H as electron donor, which has a higher redox potential compared with F_{420}.[30] Similarly, pretomanid can be metabolized, but not bio-activated, by human liver enzymes, as they do not induce des-nitrification.[31] The activation of delamanid and pretomanid being restricted to mycobacterial Ddn might (in part) explain the selective activity against mycobacteria without being genotoxic to humans.[30, 31]

Ddn-mediated metabolic activation of delamanid generates one main metabolite, desnitro-imidazooxazole, which has no antimycobacterial activity.[10] For pretomanid, Ddn reduces the imidazole ring, forming three major metabolites among which is a des-nitro form.[28] The metabolites have been described by Singh et al. [28] not to show any activity against *M. tuberculosis*. However, reduction of pretomanid releases reactive nitrogen species, such as nitric oxide (NO) which acts as an active intermediate.[16, 28] NO is thought to target cytochrome oxidases in the mycobacterial electron-transport chain,

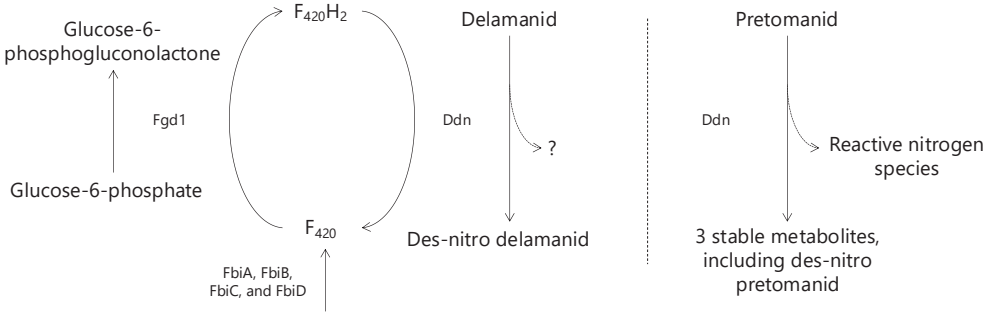

Figure 1. Schematic overview of the metabolic activation of delamanid and pretomanid by mycobacteria, adapted with permission from Liu et al.[23] and Rifat et al.[36] Delamanid and pretomanid are prodrugs that require activation by deazaflavin (F_{420})-dependent nitroreductase (Ddn). Redox cycling of deazaflavin cofactor 420, or F_{420}, is crucial in this process, which is mediated by glucose-6-phosphate dehydrogenase (Fgd1)[12,23,35,132,133] and Ddn.[10,26–28] Synthesis of F_{420} depends on FbiA, FbiB, FbiC and FbiD.[12,36–38,134] Bio-activation of delamanid by Ddn results in the formation of inactive des-nitro-imidazooxazole.[10,135] The active intermediate for delamanid has not yet been identified. Activation of pretomanid, on the other hand, generates three stable, inactive metabolites, as well as reactive nitrogen species which are responsible for respiratory poisoning by pretomanid.[26,28]

thereby hampering ATP synthesis.[16, 32] Since mycobacteria maintain their respiratory function and energy production at low levels under anaerobic conditions, they may be more vulnerable to impairment of ATP homeostasis under such circumstances.[16, 33] Transcriptional profiling of *M. tuberculosis* exposed to delamanid revealed that delamanid probably induces respiratory poisoning as well.[17] However, the active intermediate of delamanid is not yet identified. Hayashi et al. [34] recently found that mutations in type II NADH dehydrogenase (*ndh*) can give rise to delamanid resistance. The authors speculate that an NAD-delamanid adduct, instead of NO, might be responsible for its anti-mycobacterial activity. Characterizing other upregulated genes during delamanid exposure could provide additional insight into its mechanism of action.[17]

Drug resistance

Studies on drug resistance suggest that delamanid and pretomanid display no cross-resistance with other currently used TB drugs, probably due to their unique mechanism of action.[10, 12] That being said, by using a genetically modified *Mycobacterium smegmatis* strain, Hayashi et al. [34] showed that mutations in the *ndh* gene can in principle lead to resistance to isoniazid, ethambutol, and also delamanid.

Both delamanid and pretomanid have relatively high spontaneous mutation frequencies. For delamanid, the frequency of drug resistance was found to range between 1.22×10^{-5} and 6.44×10^{-6} at 16 times the MIC.[25] Spontaneous drug resistance frequencies ranging from 1.0×10^{-5} to 6.5×10^{-7} are reported for pretomanid, which are comparable to those of delamanid.[25, 27, 35] These frequencies are in line with resistance rates reported for isoniazid, but are higher than those reported for rifampicin in *M. tuberculosis*.[25] It could be that the relatively large target size for mutations (six non-essential genes, discussed below) foster these high frequencies, and the issue highlights the importance of combining these drugs with strong companion drugs during therapy.[36]

Mutations in the genes responsible for metabolic activation of delamanid and pretomanid (*fbiA, fbiB, fbiC, fbiD, fgd1*, and *ddn*) (Figure 1) have been associated with resistance to either drug in preclinical settings and in clinical isolates.[12, 25, 28, 35–47] However, additional genes might be involved in delamanid resistance, as in a recent study none of the delamanid-resistant clinical isolates harboured mutations in *fbiA/B/C*, *fgd1* or *ddn*.[48] In contrast, published findings on pretomanid-resistant clinical isolates are sparse, likely because the drug only recently earned approval for clinical use.

Table 2 summarizes the findings from several studies that have investigated both delamanid and pretomanid susceptibility of *M. tuberculosis* isolates from either preclinical

or clinical settings, together with an evaluation of gene mutations that coincided with drug resistance.[29, 36, 49] Given the similarities in the intra-bacterial metabolic pathway of delamanid and pretomanid, it is not unexpected that isolates resistant to both compounds have been identified. Out of 32 pretomanid-resistant isolates selected by Rifat et al. [36] from their mouse model of TB infection, 23 were resistant to delamanid as well (MIC >0.06 mg/L) and harbored mutations in *fbiA*, *fbiB*, *fbiC*, *fbiD*, *fgd*, and *ddn*. Lower levels of cross-resistance were reported in clinical isolates, with 2 out of 12 isolates being resistant to both compounds (delamanid MIC >16 mg/L, and pretomanid MIC 8 and >16 mg/L).[49] An E249K mutation in the *fbiA* gene (GAA→AAA) was found in one of these isolates, as well as a synonymous F320F mutation in *fgd1* (TTT→TTC). The particular *fgd1* mutation is, however, probably not responsible for drug resistance, as it was also observed in isolates susceptible to both drugs. Of particular interest are the isolates resistant to one drug only, while susceptibility to the other is preserved (Table 2). Isolates selected in a preclinical setting with various mutations in *fbiA*, *fbiB* or *fbiD* exhibited high-level resistance to pretomanid, while retaining susceptibility to delamanid with only modestly raised MICs to the critical value of 0.06 mg/L.[36] Apart from susceptibility testing, Lee et al. [29] investigated the ability of *M. tuberculosis* isolates harboring mutations in *ddn* to activate delamanid and pretomanid. Notably, of the 46 studied *ddn* mutants, two isolates were not able to activate pretomanid, but could, however, still activate delamanid. These isolates harbored an S78Y or Y133C mutation in *ddn*, both of which are naturally occurring sequence polymorphisms. This finding suggests that mutations in *ddn* such as S78Y and Y133C might cause pretomanid resistance, while maintaining susceptibility to delamanid. Molecular docking studies indicate that the dissimilarity in the ability to activate delamanid or pretomanid might be a consequence of different binding of the compounds to Ddn.[29] The authors speculate that the chemical structure of delamanid causes steric hindrance with the deazaflavin ring of F_{420} in Ddn bound to $F_{420}H_2$. As a result, delamanid binds above F_{420} in a different orientation than pretomanid. All together, these findings imply that under certain conditions delamanid and pretomanid could replace each other in case of drug resistance to one of the two drugs.

Table 2. Overview of *M. tuberculosis* isolates selected from either preclinical or clinical settings for which susceptibility to both delamanid (DLM) and pretomanid (PMD) was determined, together with an investigation of coinciding gene mutations

Author/setting of isolation	Resistance type	Resistant to[a]	MIC (mg/L)		Gene	Mutation
			DLM	PMD		
Rifat et al. (2020)[36]						
Preclinical		DLM; PMD	>16	>32	*fbiA*	Q27*
Preclinical		DLM; PMD	>16	>32	*fbiA*	D49G
Preclinical		DLM; PMD	>16	>32	*fbiA*	-G in aa 47
Preclinical		DLM; PMD	>16	>32	*fbiA*	L308P
Preclinical		DLM; PMD	>16	32	*fbiA*	Q120P
Preclinical		DLM; PMD	>16	32	*fbiA*	D286A
Preclinical		DLM; PMD	0.06-0.125	8-32	*fbiB*	L15P
Preclinical		DLM; PMD	0.125	32	*fbiB*	L173P
Preclinical		DLM; PMD	0.06-0.125	32	*fbiB*	-T in aa 684
Preclinical		DLM; PMD	>16	>32	*fbiC*	C562W
Preclinical		DLM; PMD	1	>32	*fbiC*	G194D
Preclinical		DLM; PMD	2	>32	*fbiC*	-C in aa 20
Preclinical		DLM; PMD	>16	>32	*fbiC*	K684T
Preclinical		DLM; PMD	>16	>32	*fbiC*	IS6110 ins. 85 bp upstream of *fbiC*
Preclinical		DLM; PMD	>16	>32	*fbiC*	L377P
Preclinical		DLM; PMD	>16	>32	*fbiC*	A827G
Preclinical		DLM; PMD	0.5	32	*fgd1*	K9N
Preclinical		DLM; PMD	>16	>32	*fgd1*	G191D
Preclinical		DLM; PMD	>16	≥32	*ddn*	R112W
Preclinical		DLM; PMD	>16	≥32	*ddn*	IS6110 ins. in D108
Preclinical		DLM; PMD	>16	>32	*ddn*	-G in aa 39
Preclinical		PMD	0.03	32	*fbiA*	S219G
Preclinical		PMD	0.03	16	*fbiB*	W397R
Preclinical		PMD	0.03	16-32	*fbiC*	R25G
Preclinical		PMD	0.03	16-32	*fbiC*	M776R
Preclinical		PMD	0.06	>32	*fbiD*	G147C
Preclinical		PMD	0.06	>32	*fbiD*	A132V
Preclinical		PMD	0.06	>32	*fbiD*	-ATC in aa 129
Preclinical		PMD	0.03-0.06	>32	*fbiD*	R25S
Preclinical		PMD	0.06	>32	*fbiD*	A198P
Preclinical		PMD	0.06	>32	*fbiD*	C152R
Preclinical		PMD	<0.03	>32	*fbiD*	A68E

Table 2. Continued

Author/setting of isolation	Resistance type	Resistant to[a]	MIC (mg/L)		Gene	Mutation
			DLM	PMD		
Wen et al. (2019)[49]						
Clinical	XDR	DLM; PMD	>16	8	[b]	[b]
Clinical	XDR	DLM; PMD	>16	>16	*fgd1* *fbiA*	F320F E249K
Clinical	MDR	DLM	16	0.063	*fgd1*	F320F
Clinical	MDR	DLM	>16	0.031	[b]	[b]
Clinical	MDR	DLM	0.5	0.063	*fgd1*	F320F
Clinical	MDR	DLM	>16	0.063	*fgd1*	F320F
Clinical	XDR	DLM	>16	≤0.016	*fgd1*	F320F
Clinical	XDR	PMD	≤0.016	>16	[b]	[b]
Clinical	MDR	None	≤0.016	0.13	*fgd1*	F320F
Clinical	MDR	None	≤0.016	0.25	*fgd1*	F320F
Clinical	MDR	None	≤0.016	0.5	*fgd1*	F320F
Clinical	XDR	None	≤0.016	0.25	*fgd1*	F320F
Lee et al. (2020)[29]						
Clinical		DLM; PMD	32	256	*ddn*	S78Y

Rifat et al.[36] determined the MIC by broth macrodilution assay, Wen et al.[49] by microplate Alamar blue assay (MABA) and Lee et al.[29] by resazurin assay.

[a] The clinical breakpoint for susceptibility to delamanid is ≤0.06 mg/L, as set by the EUCAST[73]; EUCAST clinical breakpoints for pretomanid are awaited. In this Table, 1 mg/L is used as the cut-off value for susceptibility to pretomanid.[70]

[b] No mutations were found in *ddn*, *fgd1*, *fbiA*, *fbiB*, or *fbiC*

In vitro activity

A single *in vitro* assay cannot cover the complexity of human TB infection comprising *M. tuberculosis* in various metabolic stages and residing in different niches. Hence, a variety of assays exists, each with a specific design and read-out. Although heterogeneity between assays hampers systematic comparison, here, we review studies reporting the following outcomes to get an impression of the *in vitro* activity of delamanid and pretomanid: standard *in vitro* susceptibility assays (MIC assays), drug activity against extracellular *M. tuberculosis* in different metabolic states, and activity against intracellular *M. tuberculosis* in macrophage assays. Although the MIC value is a measure of compound activity, it does not directly reflect *in vivo* efficacy as it is only one of many factors that drive pharmacokinetic (PK) and pharmacodynamic (PD) characteristics. In early stages of compound development, new drugs are often tested against replicating extracellular *M. tuberculosis*. These experiments are relatively easy to implement and allow for a quick

comparison of the new compound's activity with that of already established TB drugs. Regarding metabolic states, *M. tuberculosis* is thought to be present in pulmonary lesions both as replicating and nonreplicating bacteria, based on the mycobacterial growth phase.[50, 51] Evaluating drug activity against non-replicating mycobacteria is relevant, because this population is more tolerant to treatment with existing TB drugs and therefore may be responsible for the prolonged TB treatment duration needed to effect cure.[51–53] Several assays have been developed that induce a nonreplicating state in *M. tuberculosis*, including starvation, oxygen depletion, low pH, or by using specific strains such as the *M. tuberculosis* 18b strain which enters a nonreplicating state in the absence of streptomycin.[54] We chose to also include results of the first-line drugs rifampicin and isoniazid as a reference, since it is known that rifampicin is active against both replicating and nonreplicating *M. tuberculosis*,[55] while isoniazid only targets replicating bacilli.[56]

Delamanid

The MIC distribution for delamanid against clinical *M. tuberculosis* strains as reported by the EUCAST shows that MICs mostly range between ≤0.002 to 0.03 mg/L.[57] Depending on the method used, the majority of isolates have an MIC of 0.004 mg/L or 0.008 mg/L as tested by agar dilution or MGIT 960, respectively. This is in agreement with various articles reporting MICs ≤0.025 mg/L against both drug-susceptible and drug-resistant *M. tuberculosis* strains.[10, 11, 45, 48, 49, 58, 59] EUCAST sets the clinical breakpoint for strain susceptibility to delamanid at MIC ≤0.06 mg/L.[60]

Table 3 summarizes findings on the *in vitro* activity of delamanid against replicating extracellular *M. tuberculosis*. Saliu et al. [61] compared the activity of delamanid with that of rifampicin against clinical *M. tuberculosis* isolates tolerant to isoniazid, meaning that these isolates grew better than the reference H37Rv strain in the presence of 0.1 mg/L isoniazid as measured by $^{14}CO_2$ production. The authors found that against these isolates, killing rates of delamanid at 1 mg/L were comparable to those of rifampicin at 2 mg/L over 14 days of drug exposure.[61] Dalton et al. [62] showed that delamanid significantly reduced the mycobacterial numbers as measured by relative light units (RLU) after 3 days of drug exposure.

Information on *in vitro* activity of delamanid against nonreplicating bacilli is sparse (Table 4). In a study by Upton et al.,[63] the nonreplicating state was induced by oxygen depletion.[63] The authors found that delamanid at 4.4 µM was sufficient to reduce colony forming units (cfu) by 99% after 10 days of exposure. As *M. tuberculosis* can be present intracellularly in pulmonary lesions, Matsumoto et al. [10] used infected macrophages differentiated from human THP-1 monocytes to assess delamanid activity against intracellular *M. tuberculosis*. Delamanid showed strong and concentration-dependent activity, which at 0.1 mg/L was similar to that of rifampicin at 3 mg/L.

Table 3. Summary of *in vitro* activity of delamanid and pretomanid against replicating, extracellular *M. tuberculosis*

Author	*M. tuberculosis* strain	Drug treatment (dose)	Treatment duration	Read-out	Outcome
Saliu et al. (2007)[61]	Clinical INH-tolerant strains	DLM (1 mg/L)	14 days	Growth Index	Killing rates of DLM were comparable to those of RIF (2 mg/L)
Dalton et al. (2017)[62]	Bioluminescently-labelled H37Rv	DLM; PMD	3 days	RLU	DLM significantly reduced RLU. RLU levels stayed stable during PMD and RIF exposure.
Sala et al. (2010)[71]	18b, exposed to streptomycin	PMD (3 mg/L)	7 days	cfu	PMD bactericidal activity was comparable with that of INH (0.5 mg/L) and RIF (10 mg/L).
Piccaro et al. (2013)[55]	H37Rv	PMD (2 mg/L)	7 days	cfu	PMD reduced cfu counts to a comparable extent as INH (2 mg/L), but to a lesser extent than RIF (8 mg/L).

INH, isoniazid; DLM, delamanid; RIF, rifampicin; PMD, pretomanid; RLU, relative light units; cfu, colony forming units.

Only a few studies describe the *in vitro* activity of delamanid containing TB drug combinations. Matsumoto et al. [10] investigated potential synergistic activity of delamanid and first-line TB drugs against 27 clinical *M. tuberculosis* isolates by chequerboard analysis. There was no interaction observed between delamanid and rifampicin (FIC indices between >0.5 and 0.75) for the majority of isolates (88.9%). This also accounted for the interaction between delamanid and isoniazid (44.4% FIC index >0.5–0.75, 18.5% FIC index >0.75–1.0, 37% FIC index >1.0– 4.0). Also using a chequerboard assay, Chandramohan et al. [64] demonstrated either an additive or synergistic effect between delamanid and bedaquiline or moxifloxacin, depending on the *M. tuberculosis* strain being drug-susceptible, monoresistant to isoniazid or rifampicin, MDR or XDR. However, it should be pointed out that the results of chequerboard assays should be interpreted with utmost care, as it is not clear how well these artificial *in vitro* assays translate to *in vivo* results for *M. tuberculosis*.

Pretomanid

Pretomanid was only recently approved as a TB drug, and therefore, the evaluation of clinical breakpoints is currently ongoing.[65] Pretomanid activity has been assessed against drug-susceptible, MDR and XDR *M. tuberculosis* strains, with reported MICs of 0.015–1 mg/L.[12, 49, 66–69] Pending the EUCAST clinical breakpoints, the EMA proposed 1 mg/L as the critical concentration when using the MGIT system for drug susceptibility testing.[70] In addition, *M. tuberculosis* isolates with pretomanid resistance associated gene mutations have an MIC above this critical concentration.[26, 35] Based on the few studies that assessed the MIC of both delamanid and pretomanid, the reported values for delamanid (0.001–0.024 mg/L) were lower than those for pretomanid (0.012–0.200 mg/L).[10, 49, 63]

Table 4. Summary of *in vitro* activity of delamanid and pretomanid against nonreplicating, extracellular *M. tuberculosis*

Author	*M. tuberculosis* strain	Induction nonreplicating state	Drug treatment (dose)	Treatment duration	Read-out	Outcome
Upton et al. (2015)[63]	H37Rv	Oxygen depletion	DLM (4.4 µM); PMD (17.4 µM)	10 days	cfu	DLM at 4.4 µM, and PMD at 17.4 µM reduced cfu by 99%.
Lenaerts et al. (2005)[66]	H37Rv	Oxygen depletion	PMD (2, 10, 50 mg/L)	4 days	cfu	PMD showed dose-dependent bactericidal activity. At 50 mg/L, PMD activity was higher than that of INH at 50 mg/L, and was comparable to RIF at 2 mg/L, but inferior to RIF at 10 or 50 mg/L.
Hu et al. (2008)[72]	H37Rv	Starvation, oxygen depletion	PMD (0.31–20 mg/L)	4–7 days	cfu	PMD showed dose-dependent bactericidal activity. At ≤1.25 mg/L, PMD was only minimally active. Mycobacterial elimination was observed at ≥10–20 mg/L.
Sala et al. (2010)[71]	18b strain	No exposure to streptomycin	PMD (3 mg/L)	7 days	cfu	PMD activity was higher against nonreplicating than fast-replicating *M. tuberculosis*. PMD and RIF (10 mg/L) were equally active and PMD activity was superior to INH (0.5 mg/L).
Stover et al. (2000)[12]	Bioluminescently-labelled H37Rv	Oxygen depletion	PMD (10 mg/L)	7 days	RLU	PMD was active against nonreplicating mycobacteria. PMD activity (10 mg/L) was comparable to MTZ (10 mg/L), and superior to INH (10 mg/L).
Papadopoulou et al. (2007)[75]	Bioluminescently-labelled H37Rv	Oxygen depletion	PMD (6.4–12.8 mg/L)	10 days	Luminescent signal/cfu	PMD at 6.4–12.8 mg/L, and RIF at 2.5 mg/L were sufficient to kill ≥90% of *M. tuberculosis*. This activity was superior to INH (>100 mg/L).
Piccaro et al. (2013)[55]	H37Rv	Oxygen depletion	PMD (2 mg/L)	7-21 days	cfu	PMD showed time-dependent bactericidal activity, which was inferior to RIF (8 mg/L) and superior to INH (2 mg/L).
Somasundaram et al. (2013)[76]	H37Rv	Oxygen depletion	PMD (3, 12.5 mg/L)	2-21 days	cfu	PMD (12.5 mg/L) resulted in mycobacterial elimination at day 21, which was superior to RIF (1 mg/L). Bactericidal activity of PMD at 3 mg/L was comparable to RIF at 1 mg/L.
Iacobino et al. (2016)[74]	H37Rv	Starvation, oxygen depletion, low pH	PMD		cfu	PMD reduced cfu counts by ≥2 $\log_{10}$, which was similar to RIF and superior to INH.
Early et al. (2019)[73]	H37Rv	Low pH	PMD	7 days	cfu	PMD (12 µM) reduced cfu by ≥2 $\log_{10}$, similar to RIF (75 µM), whereas INH showed no activity.

DLM, delamanid; PMD, pretomanid; cfu, colony forming units; INH, isoniazid; RIF, rifampicin; MTZ, metronidazole

Pretomanid activity against replicating *M. tuberculosis* is summarized in Table 3. Sala et al. [71] demonstrated that pretomanid (3 mg/L) killed replicating *M. tuberculosis* (using the 18b strain exposed to streptomycin, which allows for the strain to replicate) to the same extent as isoniazid (0.5 mg/L) and rifampicin (10 mg/L) after 7 days of drug exposure. Using an H37Rv *M. tuberculosis* strain, Piccaro et al. [55] showed that the activity of pretomanid (2 mg/L) was comparable to that of isoniazid (2 mg/L), though it was inferior to the activity of rifampicin (8 mg/L). In a study by Dalton et al.,[62] 3 days of pretomanid exposure kept the *M. tuberculosis* load at a stable level, whereas the untreated control showed a significant increase in mycobacterial load. In comparison, the activity of delamanid in this assay was relatively higher, leading to a reduction in the mycobacterial load.

Activity of pretomanid against nonreplicating *M. tuberculosis* was more elaborately studied than for delamanid (Table 4). Its activity was shown be concentration dependent.[66, 72] In an experimental set-up using the 18b *M. tuberculosis* strain (in a nonreplicating state in the absence of streptomycin), pretomanid appeared to be more active against nonreplicating compared with replicating *M. tuberculosis*, reducing the mycobacterial load by 4.5 $\log_{10}$ cfu/mL versus 2 $\log_{10}$ cfu/mL after 7 days of drug exposure, respectively.[71] This observation matches the finding that reactive nitrogen species released upon activation of pretomanid have a greater impact on the ATP synthesis under anaerobic conditions.[16, 33] Stover et al. [12] aimed to induce a nonreplicating state in *M. tuberculosis* by microaerophilic culture conditions. In this assay, the bactericidal activity of 7 days exposure to pretomanid (10 mg/L) was comparable to that of the structurally related metronidazole (10 mg/L), and superior to that of isoniazid (10 mg/L). Lenaerts et al. [66] also observed a higher bactericidal activity of pretomanid (50 mg/L) compared to isoniazid (50 mg/L) following 4 days of drug exposure in an oxygen depletion assay. In various experimental set-ups, bactericidal activity of pretomanid against nonreplicating *M. tuberculosis* matched the activity of rifampicin.[66, 71, 73–76] Upton et al. [63] evaluated the bactericidal activity of both delamanid and pretomanid against nonreplicating *M. tuberculosis* in an oxygen depletion assay. The authors found that 17.4 µM pretomanid was sufficient to reduce cfu by 99% after 10 days of exposure, while for delamanid a concentration of 4.4 µM was sufficient to achieve this goal.[63] Published information on pretomanid activity against intracellular bacilli is rather limited. In a whole blood culture assay, Wallis et al. [77] demonstrated modest concentration-dependent bactericidal activity of pretomanid at 0–2 mg/L. In another assay, using *M. tuberculosis*-infected THP-1 cells, pretomanid at 0.1–1 mg/L led to a similar reduction in mycobacterial numbers as isoniazid at 0.3–3 mg/L. However, the intracellular activity of pretomanid was inferior to that of delamanid and rifampicin in this study.[10]

The *in vitro* activity of drug combinations was more extensively studied for pretomanid than for delamanid. Whereas delamanid combined with bedaquiline showed *in vitro* synergy,[64] additive or antagonistic effects have been reported when pretomanid was combined with bedaquiline,[77, 78] although it should be noted that different experimental designs were used in these studies, hampering comparison of the outcomes. The interaction between pretomanid and bedaquiline is of interest, since several new and promising drug regimens contain these two drugs (ClinicalTrials registration no. NCT03338621, NCT03086486, NCT02589782). An additive effect was found when pretomanid was combined with linezolid.[78] The combination of pretomanid and moxifloxacin was shown to be additive or synergistic against actively replicating or nonreplicating *M. tuberculosis*, respectively.[78–80] In this context, Drusano et al. [80] showed that the addition of bedaquiline to the combination of pretomanid and moxifloxacin achieved eradication of actively replicating *M. tuberculosis* one week sooner compared with the two-drug combination. Using a modified checkerboard assay, López-Gavín et al. [81] demonstrated that a combination of pretomanid, clofazimine, and moxifloxacin was active against drug-susceptible and MDR clinical isolates, with the activity of the drugs being additive. In a recent study using a hollow fiber infection model, the performance of the combination of pretomanid, moxifloxacin and pyrazinamide was equal to that of the standard regimen consisting of isoniazid, rifampicin and pyrazinamide (HRZ) against both replicating, nonreplicating and intracellular *M. tuberculosis*.[82] Lastly, Piccaro et al. [55] reported that when pretomanid was combined with rifampicin, moxifloxacin, and amikacin, *M. tuberculosis* was efficiently killed within 14 days in aerobic as well as hypoxic conditions, but no comparison was made with the standard regimen. Again, when interpreting these data, it is important to bear in mind the limitations regarding the translational value of these highly simplified *in vitro* drug combination assays.

Pharmacokinetics

The efficacy of a drug depends on its PD and its PK profile. By combining PK with a microbiological parameter, PK/PD indices can be determined (e.g. AUC_{0-24}/MIC or $\%T_{>MIC}$), which can be used to optimize dosing schedules.[83] Knowledge on what doses in animals reach exposures (or ideally driving PK/PD indices) that match exposures reached in humans at clinically approved doses assists in interpreting drug activity and efficacy results in animal studies and translating these to humans. Furthermore, animal studies can shed light on drug distribution, drug metabolism, and drug clearance.

Delamanid

Animal studies have shown that following oral administration of delamanid, the drug is widely distributed among various organs.[84, 85] After treating rats with a single oral dose of radioactively labelled ^{14}C-delamanid (3 mg/kg), radioactivity was detected in the lungs, central nervous system, eyeball, placenta, fetus, and breastmilk.[84] Penetration of the blood–brain barrier was confirmed by Tucker et al. [85] in a rabbit model of tuberculous meningitis. Delamanid was detected in cerebrospinal fluid, albeit at lower concentrations than in plasma. Brain tissue concentrations, on the other hand, were found to be 5-fold higher than those in plasma.[85] Results from both studies suggest that delamanid could be of value in treating extra-pulmonary TB, including TB meningitis, but further studies are required.

Delamanid is highly protein bound (>97%).[86] It is thought that plasma albumin is mainly responsible for metabolizing delamanid,[86,87] with the formation of M1 (DM-6705) as the major metabolite. Hepatic cytochrome P450 (CYP) enzymes are assumed to play a role in the subsequent degradation of M1 into another seven metabolites.[87] No interaction between delamanid and CYP isoforms was observed,[10, 88] and delamanid metabolites were found to inhibit some CYP isoforms only at considerably higher concentrations than observed in human plasma.[88] These results imply that drug–drug interactions with compounds that are metabolized by CYP enzymes, including antiretroviral drugs, are unlikely. However, this subject is being further assessed in clinical studies.[89]

Studies in mice, rats, guinea pigs, rabbits and dogs have been performed to shed light on the pharmacokinetic profile of delamanid (Table 5). The delamanid dose currently approved for clinical use is 100 mg twice a day, taken with food.[90] In a randomized, placebo-controlled, multinational clinical trial, Gler et al. [91] found an AUC of 7.925 µg·h/mL in patients treated with delamanid 100 mg twice daily for 56 days. A slightly lower AUC_{0-24} of 3.40 µg·h/mL was reported by Mallikaarjun et al. [92] in humans for delamanid at the daily dose of 200 mg. Several dosing strategies in various animal studies resulted in AUC values similar to those in humans (Table 5). In mice, 2.5, 3, and 10 mg/kg at single oral administration and 2.5 mg/kg orally administered for 4 weeks in a combination regimen with bedaquiline and linezolid led to AUC values between 3.58 and 11.55 µg·h/mL.[10, 87, 92, 93] Likewise, in rats, 3 and 10 mg/kg at single drug administration generated exposures of 7.9418 (AUC_{0-480}) and 5.68 (AUC_{0-96}) µg·h/mL, respectively.[87, 94] In guinea pigs, a single dose of delamanid at 10 mg/kg resulted in a relatively low AUC_{0-48} of 2.32 µg·h/mL, while this was 9.45 µg·h/mL for a dose of 100 mg/kg.[95] Also in rabbits and dogs delamanid exposures matching clinical exposures were shown following a single oral dose of delamanid at 5 mg/kg[85] and 10 mg/kg,[87] respectively. Using a murine chronic TB infection model, Mallikaarjun et al. [92] found that the PK/PD driver for delamanid activity was described best by the AUC_{0-24}/MIC (Pearson's correlation coefficient = 0.97), and to

a lesser extent by the $\%T_{>MIC}$ (Spearman correlation coefficient = 0.53). In that study, an AUC_{0-24}/MIC of 252 was determined to achieve 80% of the maximum activity of the drug in the mouse model. Based on the results from two human Early Bactericidal Activity studies, a mean AUC_{0-24}/MIC of 393 was established at a dose of 200 mg after 14 days of treatment.[92]

Pretomanid

Like delamanid, pretomanid is widely distributed among various organs. After a single oral administration of 40 mg/kg in rats, pretomanid was detectable in liver, heart, lung, spleen, kidney, stomach and intestine.[96] Pretomanid was shown to effectively cross the blood–brain barrier as well.[96–99] In rats, plasma concentrations were shown to be 5-fold higher than brain tissue concentrations, and 2.5-fold higher than lung tissue concentrations. However, this might be different for multiple dose administrations.[99]

In human plasma, 94% of pretomanid is protein bound.[72] Dogra et al. [31] found that after incubation of pretomanid with supernatant of human liver homogenates several minor metabolites could be identified, but not the des-nitro metabolite that is formed upon bio-activation of pretomanid by mycobacterial Ddn. Hence, while mycobacteria can activate pretomanid by des-nitrification, this process does not occur with human liver supernatant.[31] Preclinical[100, 101] and clinical[102] studies have indicated that exposure to pretomanid is altered when co-administered with several other drugs. Together, these results imply that, compared with delamanid, albumin metabolism plays a smaller role for pretomanid, and that pretomanid is at least partly metabolized in the liver.[87] However, the exact metabolic pathway of pretomanid is yet to be unraveled, and mechanisms that underlie drug–drug interactions (e.g. CYP isoenzymes and drug transporters) require further study.

Results of various animal PK studies for pretomanid are summarized in Table 6. The methods of these studies are quite heterogeneous, using different animal species (mice, rats or guinea pigs), dose levels, treatment durations, routes of administration, and treatment combinations. In humans, the currently approved dose in the clinic is 200 mg once a day to be taken with food.[70] Human clinical trials have reported AUC_{0-t} values corresponding to this dosing regimen of 28.087 µg·h/mL (single dose administration, in fasted state, monotherapy), 51.643 µg·h/mL (single dose administration, in fed state, monotherapy),[103] 30.2 µg·h/mL (7 days treatment, monotherapy), 60.487 µg·h/mL (14 days treatment, combination regimen with bedaquiline, pyrazinamide and clofazimine), 61.534 µg·h/mL (14 days treatment, combination regimen with bedaquiline and clofazimine), and 76.292 µg·h/mL (14 days treatment, combination regimen with bedaquiline and pyrazinamide).[104] As can be seen in Table 6, similar drug exposure in mice was reached after administration of a single oral dose of 25 mg/kg.[105] A single oral dose administration

Table 5. Overview of pharmacokinetic parameters of delamanid evaluated in various animal studies

Reference	Animal model	Infected	Dose (mg/kg)	Single drug or combination	Treatment duration	Route of drug administration	Sample	Methods	T_{max} (h)	$T_{1/2}$ (h)	C_{max} (mg/L)	AUC time span	AUC (µg ·h/mL)
Mallikaarjun et al. (2020)[92]	Mice, SLC:ICR	No	0.625	Single drug	Single dose	Oral gavage	Plasma	HPLC-MS/MS			0.1	0-24	1.19
	Mice, SLC:ICR	No	2.5	Single drug	Single dose	Oral gavage	Plasma	HPLC-MS/MS			0.3	0-24	3.58
	Mice, SLC:ICR	No	10	Single drug	Single dose	Oral gavage	Plasma	HPLC-MS/MS			1.01	0-24	11.55
Matsumoto et al. (2006)[10]	Mice	Yes	2.5	Single drug	Single dose	Oral	Plasma	LC-ESI-MS/MS	6	7.6	0.3	0-24	4.13
Pieterman et al. (2021)[93]	Mice, BALB/c	Yes	2.5	BDQ (25) + LZD (100)	4 weeks	Oral gavage	Plasma	LC-MS/MS	0.75		0.86-1.08	0-24	11.23
Sasahara et al. (2015)[87]	Mice, ICR	No	3	Single drug	Single dose	Oral	Plasma	LC-MS/MS	2	7.2	0.48	0-480	5.54
												0-∞	6.15
	Mice, ICR	No	30	Single drug	Single dose	Oral	Plasma	LC-MS/MS			2.31	0-24	35.84
	Mice, ICR	No	30	Single drug	13 weeks	Oral	Plasma	LC-MS/MS			2.92	0-24	36.51
Ramirez et al. (2021))[94]	Rats, Sprague Dawley	No	10	Single drug	Single dose	Oral gavage	Plasma	HPLC	3.4		0.26	0-96	5.68
Shibata et al. (2017)[84]	Rats, Sprague Dawley; males	No	3	Single drug	Single dose	Oral	Blood	Radioactivity of ^{14}C-labelled DLM	8	82.3	0.58	0-168 0-∞	19.4 22.8
	Rats, Sprague Dawley; males, fasted	No	3	Single drug	Single dose	Oral	Blood	Radioactivity of ^{14}C-labelled DLM	6.3	49.5	0.74	0-168	19.6

Table 5. Continued

Reference	Animal model	Infected	Dose (mg/kg)	Single drug or combination	Treat-ment duration	Route of drug administration	Sample	Methods	T_{max} (h)	$T_{1/2}$ (h)	C_{max} (mg/L)	AUC time span	AUC (µg ·h/mL)
	Rats, Sprague Dawley; females, non-fasted	No	3	Single drug	Single dose	Oral	Blood	Radioactivity of ^{14}C-labelled DLM	8	57.2	0.64	0-168 0-∞	20.3 22.3
	Rats, Sprague Dawley; females, fasted	No	3	Single drug	Single dose	Oral	Blood	Radioactivity of ^{14}C-labelled DLM	5	59.8	0.81	0-168	19.7
Sasahara et al. (2015)[87]	Rats, Sprague Dawley	No	3	Single drug	Single dose	Oral	Plasma	LC-MS/MS	4	5.1	0.6	0-480 0-∞	7.94 7.97
	Rats, Sprague Dawley	No	30	Single drug	Single dose	Oral	Plasma	LC-MS/MS			2.7	0-24	36.64
	Rats, Sprague Dawley	No	30	Single drug	26 weeks	Oral	Plasma	LC-MS/MS			1.8	0-24	34.24
Chen et al. (2017)[95]	Guinea pigs	No	10	Single drug	Single dose	Oral	Plasma	HPLC-ESI-MS/MS			0.21	0-48	2.32
		No	100	Single drug	Single dose	Oral	Plasma	HPLC-ESI-MS/MS			0.53	0-48	9.45
Tucker et al. (2019)[85]	Rabbits, New Zealand White	Yes	5	Single drug	Single dose	Oral gavage	Plasma	HPLC-MS/MS	12	13.9	0.26	0-24 0-48 0-∞	3.81 4.23 4.26
	Rabbits, New Zealand White	No	5	Single drug	Single dose	Oral gavage	Plasma	HPLC-MS/MS	12	14.1	0.2	0-24 0-48 0-∞	2.79 3.46 3.55

Table 5. Continued

Reference	Animal model	Infected	Dose (mg/kg)	Single drug or combination	Treat-ment duration	Route of drug administration	Sample	Methods	T_{max} (h)	$T_{1/2}$ (h)	C_{max} (mg/L)	AUC time span	AUC (µg ·h/mL)
Sasahara et al. (2015)[87]	Dogs	No	10	Single drug	Single dose	Oral	Plasma	LC-MS/MS	8	18.4	0.36	0-768	10.63
	Dogs, beagle	No	30	Single drug	Single dose	Oral	Plasma	LC-MS/MS			0.38		
	Dogs, beagle	No	30	Single drug	39 weeks	Oral	Plasma	LC-MS/MS			1.4	0-24	21.77

T_{max}, time until the highest concentration is reached; $T_{1/2}$ half-life time, time until the initial drug concentration is halved; C_{max}, highest concentration reached; DLM, delamanid.

of 54 mg/kg[106] and 4 weeks of daily oral treatment with 100 mg/kg in combination with either bedaquiline, moxifloxacin and pyrazinamide, or with bedaquiline and linezolid[107] resulted in AUC_{0-24} of 127.5, 104.2 and 99.13 µg·h/mL, respectively, which were slightly higher than the exposures reached in humans. However, at 100 mg/kg, another mouse study demonstrated higher AUC_{0-24} values ranging between 327.6 and 424.0 µg·h/mL.[108] In that study, pretomanid was either administered alone or within a combination regimen, and was given once or for 2 months.[108] None of the rat studies showed AUC values that equal human exposures.[96, 99–101] In guinea pigs, a single oral administration of 50 mg/kg, and 7 day treatment with 25 mg/kg or 50 mg/kg administered twice daily, resulted in AUC values in the range of those observed in humans at the approved clinical dose.[109]

According to Ahmad et al.,[110] pretomanid activity was best described by the free drug $\%T_{>MIC}$ ($R^2 = 0.87$), followed by free drug AUC/MIC ($R^2 = 0.60$). In the same study, simulated $\%T_{>MIC}$ values in humans at a pretomanid dose of 200 mg were predicted to be 100%, assuming an MIC of 0.03125 mg/L. Such high $\%T_{>MIC}$ values were also reported in the clinical study by Diacon et al. [104] Although pretomanid at a dose of 25 mg/kg in mice resulted in exposure (AUC) comparable to exposure in humans, this dose led to lower plasma $\%T_{>MIC}$ values than observed in clinical studies.[105] Since both $\%T_{>MIC}$ and AUC/MIC are thought to be important drivers of efficacy for pretomanid, once daily dosing with 25 to 100 mg/kg has been used in mice in attempts to model $\%T_{>MIC}$ and AUC/MIC that are similar to those observed in patients. In conclusion, determining the appropriate dosing regimen in animal models that mimics both the AUC values and $\%T_{>MIC}$ encountered in the clinic is challenging. Ongoing mouse studies are exploring a lower dose of pretomanid at 50 mg/kg or lower, administered twice a day, in order to reflect the clinical drug exposure more accurately.

Doses used for delamanid in animal models are generally lower than those for pretomanid (Tables 5 and 6), while the indicated daily dose in humans is equal for both drugs (200 mg). In humans, drug exposures corresponding to this clinical dose are lower for delamanid than for pretomanid.[92,103,104,111,112] In mice, on the other hand, drug exposures following administration of delamanid or pretomanid at 25–30 mg/kg seem to be in the same range (AUC_{0-24}: 35.84 and 50.9 µg·h/mL, respectively).[87,105] Hence, it seems reasonable that delamanid is dosed at lower levels than pretomanid in animal studies, in order to mimic exposures in humans at clinically approved doses.

In vivo activity

Animal models (mostly mouse models) are used to study the treatment response in a setting that approximates the complex environment encountered in TB-infected humans.[113] Numerous mouse TB models have been developed that differ in inoculation route and dose, incubation period, treatment duration, outcome assessment, and mouse strain.[113, 114] Treatment outcome can be evaluated immediately after treatment completion (bactericidal activity) or a few months later to determine whether mice are cured nor not, which is de fined by the absence of relapse (sterilizing activity).[113] However, most mouse strains develop cellular granulomas upon TB infection, instead of the necrotizing, caseous lesions observed in human pulmonary TB.[115] To study drug efficacy in the context of such necrotic lesions, other mouse strains (e.g. C3HeB/FeJ) or other animals (e.g. guinea pigs, rabbits or NHP) can be used.[116] In this section, studies on delamanid will be discussed first followed by pretomanid, after which the compounds will be compared. For drug combinations, only combinations that have been assessed for both delamanid and pretomanid are considered in this review.

Delamanid

An overview of results from different animal models evaluating the treatment response of delamanid is presented in Table 7 . Multiple mouse models have demonstrated bactericidal activity of delamanid at doses as low as 0.313 mg/kg (range of tested doses: 0.078 –100 mg/kg).[10, 11, 63, 93, 117–120] Dose-dependency of delamanid activity was shown in three studies.[10, 11, 120] Depending on the model, delamanid showed similar or higher bactericidal activity than rifampicin,[10, 11, 118] and activity of delamanid was shown to be equal in both immunocompromised and immunocompetent mice.[10] Two mouse studies demonstrated bactericidal activity of delamanid in animals presenting with hypoxic lesions.[95, 117] Gengenbacher et al. [117] used *Nos2*$^{-/-}$ mice that develop hypoxic lung lesions upon dermal injection with *M. tuberculosis*. In this model, lung cfu counts significantly decreased after treatment with delamanid at 1 mg/kg for 3 weeks. Using a guinea pig TB model, Chen et al. [95] showed strong bactericidal activity of delamanid (100 mg/kg) administered for 8 weeks, as no cfu could be retrieved from the lung homogenates after treatment. This activity was similar to that of the standard HRZ-regimen.[95] The potential role for delamanid in the treatment of latent TB is unknown as no preclinical studies investigating this have been published at this current time.

Table 6. Overview of pharmacokinetic parameters of pretomanid evaluated in various animal studies

Reference	Animal model	Infected	Dose (mg/kg)	Treatment combination	Treatment duration	Route of drug administration	Sample	Methods	T_{max} (h)	$T_{1/2}$ (h)	C_{max} (mg/L)	AUC time span	AUC (µg ·h/mL)
Lakshmina-rayana et al. (2014)[105]	Mice, CD-1	No	25	No		Oral	Plasma	LC-MS/MS	2	2.7	6	0-24	50.9
			10	No		Intra-venous	Plasma	LC-MS/MS		1.6			
Nuermberger et al. (2006)[108]	Mice, BALB/c	Yes	100	No	Single dose	Oral gavage	Serum	HPLC	4.7	12.8	21.4	0-24	327.6
	Mice, BALB/c	Yes	100	No	2 months	Oral gavage	Serum	HPLC	1.3	18.3	25	0-24	396.8
	Mice, BALB/c	Yes	100	RIF (10) + INH (25) + PZA (150)	Single dose	Oral gavage	Serum	HPLC	11.0	11.3	20.4	0-24	370.5
	Mice, BALB/c	Yes	100	RIF (10) + INH (25) + PZA (150)	2 months	Oral gavage	Serum	HPLC	3.3	9.7	27.7	0-24	424
Tasneen et al. (2008)[106]	Mice, BALB/c		54		Single dose	Oral	Serum				15.1	0-∞	127.5
Ahmad et al. (2011)[110]	Mice, BALB/c	No	3-1458	No	Single dose	Esophagal gavage	Serum	HPLC	4	4-6			
Mudde et al. (2022)[107]	Mice, BALB/c	Yes	100	BDQ (25) + MXF (100) + PZA (150)	4 weeks	Oral	Serum	LC-MS/MS			6.89-7.03	0-24	104.2
	Mice, BALB/c	Yes	100	BDQ (25) + LZD (100)	4 weeks	Oral	Serum	LC-MS/MS			7.7-9.5	0-24	99.13
Wang et al. (2018)[101]	Rats, Sprague Dawley	No	20	No	Single dose	Oral	Plasma	LC-MS/MS	5	5.6	3.87	0-36 0-∞	2678.74 2787.23

Table 6. Continued

Reference	Animal model	Infected	Dose (mg/kg)	Treatment combination	Treatment duration	Route of drug administration	Sample	Methods	T_{max} (h)	$T_{1/2}$ (h)	C_{max} (mg/L)	AUC time span	AUC (µg ·h/mL)
Wang et al. (2015)[96]	Rats, Sprague Dawley	No	20	No	Single dose	Oral	Plasma	LC-MS/MS	6	8.3	3.48	0-36 0-∞	3291.9 3552.7
	Rats, Sprague Dawley	No	40	No	Single dose	Oral	Plasma	LC-MS/MS	6	6.2	7.98	0-36 0-∞	5850.9 6007.9
	Rats, Sprague Dawley	No	80	No	Single dose	Oral	Plasma	LC-MS/MS	6	7.4	15.29	0-36 0-∞	12445.1 13072.1
Bratkowska et al. (2015)[99]	Rats, Sprague Dawley	No	20	No		Oral	Plasma	LC-MS/MS	6		0.63	0-∞	3.72
	Rats, Sprague Dawley	No	20	No		Intraperi-toneal	Plasma	LC-MS/MS	0.25		1.15	0-∞	3.99
Wang et al. (2014)[100]	Rats, Sprague Dawley		20	No	Single dose	Oral	Plasma	LC-MS/MS	6		3.49	0-36 0-∞	3297.50 3558.32
	Rats, Sprague Dawley		20	MXF (40) + PZA (160)	Single dose	Oral	Plasma	LC-MS/MS	4.6		6.39	0-36 0-∞	4851.29 5052.66
Sung et al. (2009)[136]	Guinea pigs	No	20	No		Intra-venous	Plasma	HPLC	0.11	1.91	9.19	0-24	26.54
	Guinea pigs	No	40	No		Oral gavage	Plasma	HPLC	4.00	2.43	4.14	0-24	25.77
	Guinea pigs	No	20	No		Insuffla-tion	Plasma	HPLC	4.33	2.83	2.01	0-24	14.80
	Guinea pigs	No	40	No		Insuffla-tion	Plasma	HPLC	3.25	4.38	3.42	0-24	32.34
	Guinea pigs	No	60	No		Insuffla-tion	Plasma	HPLC	3.60	5.91	4.58	0-32	50.96

Table 6. Continued

Reference	Animal model	Infected	Dose (mg/kg)	Treatment combination	Treatment duration	Route of drug administration	Sample	Methods	T_{max} (h)	$T_{1/2}$ (h)	C_{max} (mg/L)	AUC time span	AUC (µg ·h/mL)
Dutta et al. (2013)[109]	Guinea pigs	No	12.5	No	Single dose	Oral	Serum	HPLC	2.65	1.94	1.68	0-∞	11.19
	Guinea pigs	No	25 (BID)	No	7 days	Oral	Serum	HPLC	2.25	4.7	2.99	0-∞	42.19
	Guinea pigs	No	50	No	Single dose	Oral	Serum	HPLC	2.66	3.16	5.84	0-∞	39.79
	Guinea pigs	No	50 (BID)	No	7 days	Oral	Serum	HPLC	7	2.16	5.79	0-∞	70.95

T_{max}, time until the highest concentration is reached; $T_{1/2}$, half-life time, time until the initial drug concentration is halved; C_{max}, highest concentration reached; RIF, rifampicin; INH, isoniazid; PZA, pyrazinamide; BID, bis in die, i.e. twice a day.

Drug combination regimens containing delamanid have been studied to a lesser extent *in vivo* than combinations containing pretomanid (Table 8). Two combination regimens were studied for both compounds although not in the same experiment: (i) rifampicin and pyrazinamide together with delamanid (RDZ)[10, 95] or pretomanid (RPaZ),[106, 108] and (ii) bedaquiline and linezolid either combined with delamanid (BDL)[93] or pretomanid (BPaL).[107, 121–123] Unfortunately, no head-to-head comparisons of delamanid- or pretomanid-containing drug combinations have been published to date. The RDZ regimen (delamanid at 2.5 mg/kg) showed promising bactericidal activity in a mouse TB model, reaching culture-negativity at least 2 months faster than the standard regimen consisting of isoniazid, rifampicin, pyrazinamide and ethambutol (HRZE).[10] Similar results of the RDZ regimen (delamanid at 100 mg/kg) were found by Chen et al. [95] in a guinea pig TB model. Delamanid combined with bedaquiline and linezolid was recently evaluated by Pieterman et al. [93] Mice were infected with *M. tuberculosis* of the Beijing genotype via intratracheal instillation. Two weeks later, treatment was started with BDL (delamanid at 2.5 mg/kg) via oral gavage for 2 to 6 months. The mycobacterial load in the lungs was assessed both directly following treatment completion, and three months later to evaluate whether the infection had relapsed or not. Treatment with BDL was highly effective. Of the 15 mice treated with BDL for 4 months or longer, only 1 mouse relapsed. In the HRZE-group on the other hand, relapse rates were much higher, and after 6 months of treatment there were still bacteria in 1 out of 3 mice that could be cultured from the lungs.

Pretomanid

The *in vivo* bactericidal activity of pretomanid as a monotherapy has been evaluated in various animal studies (Table 7). In mice, pretomanid showed bactericidal activity at dose levels of 12.5–20 mg/kg or higher (range of tested doses: 1.25– 600 mg/kg).[10, 12, 66, 71, 108, 119, 120, 124, 125] In several studies, the activity of pretomanid (40–100 mg/kg) was similar to that of isoniazid (25 mg/kg)[12, 66, 124] and rifampicin (20 mg/kg).[66] The rank order in activity was slightly different in two mouse models of latent TB infection using BCG-immunized mice,[125, 126] with pretomanid (50 mg/kg) showing less activity than rifampicin (10 mg/kg), although the activity was similar to that of isoniazid (10 mg/kg). Pretomanid's promising activity in animals presenting with hypoxic pulmonary lesions was demonstrated in various animal models, including a *Nos2*$^{-/-}$ mouse model,[117] a C3HeB/ FeJ mouse model,[126] and two guinea pig models.[12, 127] The ability of pretomanid as monotherapy to cure latent TB was evaluated in one murine study using BCG-vaccinated C3HeB/FeJ mice.[126] In all mice (15/15), the infection relapsed after 4 months of treatment with only pretomanid (50 mg/kg). The same outcome was observed for isoniazid (10 mg/kg), while rifampicin (10 mg/kg) performed better with a relapse rate of 33%. Selection of resistant colonies was, however, not part of the published study.

Five studies have evaluated the bactericidal activity of both delamanid and pretomanid.[10, 63, 117, 119, 120] Again, limited information is available where both compounds are evaluated side by side in the same model, and in the same experiment. Interestingly, in all five studies, the bactericidal activity of delamanid was superior to that of pretomanid. Delamanid led to higher load reductions than pretomanid at equal dose levels,[10, 63, 119] or required lower dose levels than pretomanid to achieve a comparable load reduction.[10, 117, 120] However, comparing the bactericidal activity of the compounds in the light of drug exposure rather than dose levels adds nuance to the presumed superiority of delamanid. The clinically approved dosing regimen of delamanid (100 mg, twice a day) is reported to result in AUC values between 3.40 and 10.673 µg·h/mL.[92, 112] Higher AUC values of 28.087 to 76.292 µg·h/mL were reported for pretomanid in clinical studies (200 mg, once a day), with $\%T_{>MIC}$ (an important driver of efficacy) up to 100%.[103, 104] In mice, AUC values similar to the ones measured in patients were found for delamanid at dose levels of 2.5 to 10 mg/kg (Table 5).[10, 87, 92, 93] Although pretomanid is often dosed at 100 mg/kg in mice,[12, 63, 66, 71, 105, 106, 108, 119] in order to model the $\%T_{>MIC}$ achieved in patients, lower dose levels of pretomanid (25 to 54 mg/kg) lead to AUC values more closely reflecting AUC values reported in humans (Table 6).[105, 106] Matsumoto et al. [10] reported that in their mouse model of TB infection, delamanid at 2.5 mg/kg showed similar bactericidal activity to pretomanid at 20 mg/kg, as both dose levels reduced the mycobacterial burden in the lungs by 1.9 $\log_{10}$ cfu after 4 weeks of treatment. In line with these results, Tasneen et al. [120] observed in their mouse TB model that 8 weeks of treatment with either delamanid at 2.5 mg/kg or pretomanid at 30 mg/kg resulted in a 1.6 $\log_{10}$ reduction in lung cfu counts. Taken together, these results indicate that when the compounds are compared at dose levels equivalent to those in humans based on AUC, their bactericidal activity is quite similar.

As to the performance of pretomanid in combination with other TB drugs, the combination of pretomanid, rifampicin and pyrazinamide (RPaZ) demonstrated higher bactericidal activity than the standard HRZ regimen in two mouse TB models (Table 8).[106, 108] Relapse rates, however, did not seem to differ considerably between the two regimens.[106, 108] Pretomanid combined with bedaquiline and linezolid (BPaL) performed better than the standard regimen in various mouse TB models, in terms of bactericidal activity and relapse rates.[107, 121, 122, 128] BPaL and BDL were studied in two separate studies using the same experimental set-up, except that treatment with BDL lasted 8 to 24 weeks, while this was 6 to 13 weeks for BPaL. For both drug regimens, at least 2 to 2.5 months of treatment were needed to prevent relapse in some of the mice.[93, 107]

Table 7. Summary of treatment activity of delamanid and pretomanid as monotherapy in various animal models of tuberculosis

Author	Animal (inoculation route)	*M. tuberculosis* strain	Time until start of treatment	Drug treatment (dose, mg/kg)	Treatment duration	Route of drug administration	Drug exposure	Outcome
Gengenbacher et al. (2017)[117]	*Nos2*$^{-/-}$ mice (intradermal)	H37Rv	42 days (control) or 56 days (hypoxic lung lesions)	DLM (1); PMD (75)	70-84 days	Oral	NA	DLM and PMD were both active against nonreplicating and replicating bacilli, and had comparable bactericidal activity in hypoxic necrotic lesions.
Tasneen et al. (2015)[120]	BALB/c mice (aerosol)	H37Rv	13-14 days	DLM (3–100); PMD (10–600)	2-8 weeks	Oral	NA	DLM and PMD showed time-dependent and dose-dependent bactericidal activity. DLM was approximately 10-fold more active than PMD.
Upton et al. (2015)[63]	BALB/c mice (aerosol)	Erdman	10 days	DLM; PMD (100)	3 weeks	Oral	NA	DLM was significantly more active than PMD in this model of acute infection. DLM led to a 1 $\log_{10}$ reduction in lung cfu. PMD inhibited mycobacterial growth, but did not reduce lung cfu.
	BALB/c mice (aerosol)	Erdman	70 days	DLM; PMD (100)	3 weeks	Oral	NA	DLM was significantly more active than PMD in this model of chronic infection. DLM led to a 2 to 3 $\log_{10}$ reduction in lung cfu. PMD led to a 2 $\log_{10}$ reduction in lung cfu.
Kmentova et al. (2010)119	BALB/c mice		70 days	DLM; PMD (100)	3 weeks	Oral	NA	DLM was 10-fold more active than PMD, with 3 $\log_{10}$ versus 2 $\log_{10}$ reduction in lung cfu, respectively.
Matsumoto et al. (2006)[10]	ICR mice (intravenous)	Kurono	4 weeks	DLM (0.156-40); PMD (1.25-40)	4 weeks	Oral	$AUC_{0\text{-}24}$ = 4.13 µg·h/mL (single dose of 2.5 mg/kg DLM)	DLM led to a dose-dependent reduction in lung cfu. For PMD, RIF and INH higher doses were needed to equal the load reduction by DLM.
	BALB/c (nude) mice (intravenous)	Kurono	1 day	DLM (0.313-10)	10 days	Oral	$AUC_{0\text{-}24}$ = 4.13 µg·h/ mL (single dose of 2.5 mg/kg)	DLM led to a dose-dependent reduction in lung cfu, which was equal in immunodeficient and immunocompetent mice.

Table 7. Continued

Author	Animal (inoculation route)	*M. tuberculosis* strain	Time until start of treatment	Drug treatment (dose, mg/kg)	Treatment duration	Route of drug administration	Drug exposure	Outcome
Sasaki et al. (2006)[11]	ICR mice (intravenous)	Kurono	1 day	DLM (0.5-10)	10 days	Oral	NA	DLM led to a 2.5 log_{10} to >4.4 log_{10} reduction in lung cfu, which was superior to RIF (5 mg/kg).
	ICR mice (intravenous)	Kurono	1 day	DLM (0.078-2.5)	28 days	Oral	NA	DLM led to a dose-dependent reduction in lung cfu. DLM activity (0.313 mg/kg) was similar to RIF (5 mg/kg).
Hariguchi et al. (2020)[118]	ICR mice (intratracheal inoculation)	Kurono	4 weeks	DLM (2.5)	4 weeks	Oral	NA	DLM led to a significant 1.5 log10 reduction of lung cfu, which was similar to RIF (5 mg/kg).
Pieterman et al. (2021)[93]	BALB/c mice (intratracheal instillation)	Beijing	2 weeks	DLM (1.25, 2.5, or 5)	3 weeks	Oral	AUC_{0-24}= 11.234 µg·h/mL (4 weeks treatment, dose 2.5 mg/kg, combined with BDQ 25 mg/kg+LZD 100 mg/kg)	DLM led to a 2 log_{10} reduction in lung cfu for all tested doses.
Chen et al. (2017)[95]	Guinea pig (intratracheal inoculation)	Kurono	4 weeks	DLM (100)	4 or 8 weeks	Oral	AUC_{0-24}= 9.45 µg·h/mL (single dose of 100 mg/kg)	DLM led to a 3 log_{10} reduction in lung cfu after 4 weeks of exposure. No cfu were retrieved after 8 weeks of exposure. DLM showed bactericidal activity in hypoxic lesions.
Stover et al. (2000)[12]	BALB/c mice (intravenous)	H37Rv	4 days	PMD (25, 50, or 100)	10 days	Oral	NA	PMD led to a dose-dependent reduction in lung cfu. PMD activity (25 mg/kg) was similar to INH activity (25 mg/kg).
Tyagi et al. (2005)[124]	BALB/c mice (aerosol)	H37Rv	20 days (initial phase), 8 weeks (continuation phase)	PMD (3.125-200)	4-16 weeks	Oral	NA	PMD activity (100 mg/kg) was comparable to that of INH (25 mg/kg). PMD was active during both the initial and continuation phase of therapy.

Table 7. Continued

Author	Animal (inoculation route)	*M. tuberculosis* strain	Time until start of treatment	Drug treatment (dose, mg/kg)	Treatment duration	Route of drug administration	Drug exposure	Outcome
Lenaerts et al. (2005)[66]	C57BL/6 mice (aerosol)	Erdman	19 days	PMD (50, 100, or 300)	9 days	Oral	NA	PMD showed dose-dependent activity. PMD activity (100 mg/kg) was similar to that of RIF (20 mg/kg) and INH (25 mg/kg).
	C57BL/6 mice (aerosol)	Erdman	19 days	PMD (100)	12 weeks	Oral	NA	PMD (100 mg/kg) was as active as INH (25 mg/kg).
Lakshminarayana et al. (2014)[105]	BALB/c mice (intranasal)	H37Rv	4 weeks	PMD (25 or 100)	4 weeks	Oral	AUC_{0-24}= 50.9 µg·h/mL (dose 25 mg/kg)	At 25 mg/kg PMD led to a 1.48 log_{10} reduction in lung cfu, and to a 2.3 log_{10} reduction at 100 mg/kg.
Nuermberger et al. (2006)[108]	BALB/c mice (aerosol)	H37Rv	19 days	PMD (100)	2 months	Oral	AUC_{0-24}= 396.8 µg·h/mL (2 months treatment, dose 100 mg/kg)	PMD led to a 2 log_{10} reduction in lung cfu.
Tasneen et al. (2008)[106]	BALB/c	H37Rv	2 weeks	PMD (100)	2 months	Oral	$AUC_{0-\infty}$ =127.5 µg·h/mL (single dose of 54 mg/kg)	PMD led to a 2.7 log_{10} reduction in lung cfu, which was slightly inferior to the 3.1 log_{10} reduction by RIF (10 mg/kg).
Sala et al. (2010)[71]	BALB/c mice (intravenous)	18b without streptomycin	4 weeks	PMD (100)	8 weeks	Oral	NA	PMD led to a 1.5 log_{10} reduction in lung cfu, which was superior to INH (25 mg/kg), but inferior to RIF (10 mg/kg).
Lanoix et al. (2014)[125]	BCG-immunized BALB/c mice (aerosol)	H37Rv	6 weeks	PMD (50)	8 weeks	Oral	NA	PMD led to a 1 log_{10} reduction in lung cfu, which was similar to INH (10 mg/kg), but inferior to RIF (10 mg/kg).
	BCG-immunized C3HeB/FeJ mice (aerosol)	H37Rv	6 weeks	PMD (50)	8 weeks	Oral	NA	PMD led to a 0.75 log_{10} reduction in lung cfu, which was similar to INH (10 mg/kg), but inferior to RIF (10 mg/kg).

Table 7. Continued

Author	Animal (inoculation route)	*M. tuberculosis* strain	Time until start of treatment	Drug treatment (dose, mg/kg)	Treatment duration	Route of drug administration	Drug exposure	Outcome
Dutta et al. (2014)[126]	BCG-immunized C3HeB/FeJ mice (aerosol)	H37Rv	6 weeks	PMD (50)	1-4 months	Oral	NA	PMD led to a 2.7 $\log_{10}$ reduction in lung cfu, which was comparable to INH (10 mg/kg), but inferior to RIF (10 mg/kg). The relapse rate of PMD (assessed 3 months after completion of a 4-month treatment duration) was 100%, which was equal to INH, and higher than RIF (33%).
Stover et al. (2000)[12]	Guinea pig (aerosol)	H37Rv	4 weeks	PMD (40)	4 weeks	Oral	NA	PMD led to a 1 $\log_{10}$ reduction in lung cfu, which was comparable to INH (25 mg/kg).
Garcia-Contreras et al. (2010)[127]	Guinea pig (aerosol)	H37Rv	4 weeks	PMD (inhaled: 180 or 360 mg; oral: 40 mg/kg)	4 weeks	Inhaled or oral	NA	PMD led to a significant reduction of the mycobacterial load. Higher PMD activity was observed for oral administration versus inhaled doses.

DLM, delamanid; PMD, pretomanid; NA, not assessed; cfu, colony forming units; RIF, rifampicin; INH, isoniazid; BDQ, bedaquiline; LZD, linezolid.

Table 8. Summary of treatment efficacy of delamanid and pretomanid within various drug combination regimens in animal models of tuberculosis

Author	Animal (inoculation route)	*M. tuberculosis* strain	Incubation period until start of treatment	Drug combination (dose in mg/kg)	Treatment duration	Route of drug administration	Exposure to DLM or PMD	Outcome	
								Bactericidal activity	Relapse rates
Matsumoto et al. (2006)[10]	ICR mice (intratracheal instillation)	Kurono	28 days	2 months RIF (5) + DLM (2.5) + PZA (100) and 2 months RIF (5) + DLM (2.5)	4 months	Oral	AUC_{0-24} = 4.13 µg·h/mL (monotherapy, single dose of 2.5 mg/kg)	Faster culture-negativity (by at least 2 months) in the lungs compared to the standard regimen (HRZE).	NA
Chen et al. (2017)[95]	Guinea pigs (intratracheal instillation)	Kurono	4 weeks	RIF (25) + DLM (100) + PZA (150)	4 or 8 weeks	Oral	AUC_{0-24} = 9.45 µg·h/mL (monotherapy, single dose of 100 mg/kg)	Culture-negativity in the lungs was reached after 4 weeks of treatment versus 8 weeks for the standard regimen (HRZ).	NA
Nuermberger et al. (2006)[108]	BALB/c mice (aerosol)	H37Rv	19 days	2 months RIF (10) + PMD (100) + PZA (150) and 4 months RIF (10) + PMD (100)	6 months	Oral	AUC_{0-24}=396.8 µg·h/mL (monotherapy, 2 months treatment, dose 100 mg/kg)	Culture-negativity in the lungs was reached after 4 months of treatment versus 6 months for the standard regimen (HRZ). This difference was not statistically significant.	Relapse rates were comparable to those of the standard HRZ-regimen (2/19 versus 0/46, respectively).
Tasneen et al. (2008)[106]	BALB/c mice (aerosol)	H37Rv	2 weeks	RIF (10) + PMD (12.5/25/50/100) + PZA (150)	2, 4, 5, or 6 months	Oral	$AUC_{0-\infty}$=127.5 µg·h/mL (monotherapy, single dose of 54 mg/kg)	PMD at 50 and 100 mg/kg increased activity of RIF+PZA in a dose-dependent manner. Lung culture-negativity was reached after 2 months of treatment (PMD 100 mg/kg).	No relapse was seen after 4 months of treatment versus a relapse rate of 15% for the regimen (HRZ).

Table 8. Continued

Author	Animal (inoculation route)	*M. tuberculosis* strain	Incubation period until start of treatment	Drug combination (dose in mg/kg)	Treatment duration	Route of drug administration	Exposure to DLM or PMD	Outcome	
								Bactericidal activity	Relapse rates
Pieterman et al. (2021)[93]	BALB/c mice (intratracheal instillation)	Beijing	2 weeks	BDQ (25) + DLM (2.5) + LZD (100)	2-6 months	Oral	AUC_{0-24}= 11.234 µg·h/mL (4 weeks treatment, dose 2.5 mg/kg, BDL combination)	Culture negativity in the lungs was reached after 2 months of treatment versus 20 weeks for the standard regimen (HRZE).	No relapse was seen after treatment duration of 4 months or longer (except for 1 mouse, treated for 5 months). HRZE-treated mice still relapsed after 6 months of treatment (1/3 mice).
Tasneen et al. (2016)[128]	BALB/c mice (aerosol)	H37Rv	13-14 days	BDQ (25) + PMD (50) + LZD (100)	2-4 months	Oral	NA	Two and 3 months of treatment led to a significantly lower mycobacterial load in the lungs compared to the standard regimen (HRZ).	No relapse was seen after 3 months of treatment. Infection still relapsed in HRZ-treated mice after 4 months of treatment.
Xu et al. (2019)[123]	BALC/c mice (aerosol)	H37Rv	13 days	BDQ (25) + PMD (100) + LZD (100)	1-4 months	Oral	NA	Addition of PMD to BDQ+LZD led to a higher mycobacterial load reduction when administered for 1 and 2 months and prevented the emergence of BDQ resistance.	After 2 months of treatment with BPaL, infection relapsed in 7/15 mice. No relapse was seen after 3 months of treatment.

Table 8. Continued

Author	Animal (inoculation route)	*M. tuberculosis* strain	Incubation period until start of treatment	Drug combination (dose in mg/kg)	Treatment duration	Route of drug administration	Exposure to DLM or PMD	Outcome	
								Bactericidal activity	Relapse rates
Bigelow et al. (2020)[121]	BALB/c mice (aerosol)	H37Rv or HN878	2 weeks	BDQ (25) + PMD (50 or 100) + different LZD Dosing strategies (45 or 90)	1-3 months	Oral	NA	BDQ+PMD with different dosing strategies for LZD resulted in a higher mycobacterial load reduction compared to the standard regimen (HRZE). LZD's contribution to BDQ+PMD+LZD regimens was dependent on the *M. tuberculosis* strain.	Relapse rates were highly variable between the different LZD dosing strategies, LZD (90 mg/ kg) dosed every other day leading to the highest relapse rate (11/15 mice) and LZD (90 mg/kg) dosed daily to the lowest relapse rates (1/15 mice).
Xu et al. (2021)[122]	BALB/c mice (aerosol)	H37Rv	2 weeks	BDQ (25) + PMD (100) + LZD (100)	1 month	Oral	NA	Lung cfu were reduced by approximately 2 $\log_{10}$.	NA
Mudde et al. (2022)[107]	BALB/c mice (intratracheal instillation)	Beijing	2 weeks	BDQ (25) + PMD (100) + LZD (100)	6-13 weeks	Oral	AUC_{0-24}=104 and 99.13 µg·h/mL (4 weeks treatment, dose 100 mg/kg, BPaMZ combination or BPaL combination, respectively)	NA	Mice treated for the maximum duration of 13 weeks still showed relapse (3/3 mice).
Tasneen et al. (2021)[137]	BALB/c mice (aerosol)	HN878 (Beijing)	7 weeks	BDQ (25) + PMD (100) + LZD(100)	1 or 2 months	Oral	NA	1 month of BPaL treatment led to a 3.87 $\log_{10}$ reduction in lung cfu.	After 2 months of treatment with BPaL, infection relapsed in 7/15 mice. After 3 months of treatment with HRZE, infection relapsed in 9/15 mice.

DLM, delamanid; PMD, pretomanid; RIF, rifampicin; PZA, pyrazinamide; HRZE, isoniazid+rifampicin+pyrazinamide+ethambutol; BDQ, bedaquiline; LZD, linezolid; BDL, bedaquiline+delamanid+linezolid; BPaMZ, bedaquiline+pretomanid+moxifloxacin+pyrazinamide; BPaL, bedaquiline+pretomanid+linezolid.

Discussion

With this review, we aimed to provide an overview of preclinical data on the nitroimidazoles delamanid and pretomanid. Both compounds have contributed considerably to the change of the TB treatment landscape during the last decade, and are expected to further impact the improvement of TB treatment in the coming years. Although both compounds belong to the same drug class and share many similarities, we identified several differences between the drugs, shaping the context in which results from preclinical research on delamanid and pretomanid could inform clinical studies.

Based on what is known in the published literature, the mode of action of delamanid and pretomanid seems to differ slightly. Both compounds affect mycolic acid synthesis. Pretomanid only inhibits synthesis of ketomycolates[12] and not methoxymycolates, whereas delamanid inhibits the synthesis of both these classes.[9, 10] Although both compounds intervene in aerobic respiration, pretomanid activity generates the formation of reactive nitrogen species,[16, 28] whereas an NAD–delamanid adduct is thought to contribute to the antimycobacterial activity of delamanid.[34] Apart from the nitroimidazole ring, delamanid and pretomanid have distinct chemical structures (Table 1). However, the structural components that are thought to be involved in the antimycobacterial activity of delamanid and pretomanid are shared between the two drugs.[28, 34]

Of particular interest is the finding that certain *M. tuberculosis* isolates with preserved susceptibility to delamanid, are resistant to pretomanid (or the other way around).[29, 36, 49] Here, the different chemical structure of the compounds could play a role in terms of the binding orientation to Ddn. Lee et al. [29] demonstrated that the dual methoxy and phenoxy-methyl substituents on the C6 position of the oxazole ring cause delamanid to bind differently to Ddn than pretomanid, which contains an oxazine ring with only a single substituent at the equivalent position. As such, certain mutations in *ddn* could result in pretomanid resistance while retaining the ability to activate delamanid. The fact that drug resistance has been found in *M. tuberculosis* isolates from patients who have not been treated with delamanid or pretomanid, implies that resistance to these drugs might arise due to genetic drift.[29] Indeed, the genes associated with delamanid and pretomanid resistance are genetically diverse. Various gene mutations might result in drug resistance, while at the same time several genetic variances have been reported that were not associated with drug resistance.[39, 44, 46, 48, 68] Therefore, it is not easy to pinpoint specific mutations that indicate under what circumstances delamanid and pretomanid can replace each other in the case of drug resistance or drug intolerance. Drug susceptibility testing before and during TB treatment could be performed to overcome this problem and adapt treatment regimens accordingly.

One critical hiatus in our comparison of preclinical studies is the limited amount of available head-to-head data where both compounds are tested in the same assay or model, in the same laboratory at the same time. In order to have an accurate preclinical comparison, more one-on-one preclinical studies will have to be conducted. In addition, we acknowledge the fact that the complexity of human TB infection is not easily captured in *in vitro* assays and *in vivo* preclinical models. Therefore, the preclinical performance of compounds is an informative approximation of their effect in humans. The comparison of results between different *in vitro* assays is further complicated by the great variety in experimental design, including differences in treatment duration, metabolic state of *M. tuberculosis*, methods of inducing a nonreplicating state, and treatment dosing. Each of these variables could considerably impact the results on drug activity. This also accounts for *in vivo* TB models, with differences in animals used, inoculation dose, route of infection, incubation time, treatment dose, treatment duration, and outcome assessment. However, we also regard this plethora of assays and testing models as an advantage as every tool will provide more, and often complementary, information on both compounds under various conditions.

When comparing delamanid and pretomanid in terms of bactericidal activity *in vitro*, delamanid is more potent than pretomanid, with lower MIC values (0.001–0.024 mg/L versus 0.012–0.200 mg/L, respectively, based on head-to-head comparisons)[10, 49, 63] and delamanid effects higher mycobacterial load reductions *in vitro*, at lower drug concentrations than pretomanid (Tables 3 and 4). In various mouse models of TB infection, delamanid reduced the mycobacterial load in the lungs of mice to a greater extent than pretomanid when the drugs were administered at equal doses (Table 7),[10, 63, 119] and comparable load reductions were established when delamanid was dosed at lower levels than pretomanid.[10, 117, 120] However, it is more informative to compare the activity of delamanid and pretomanid after administration to mice at dose levels that result in drug exposures similar to those achieved at the approved clinical dose. For delamanid, this would be 2.5 to 10 mg/kg in mice, as corresponding AUC values are in the same range as AUC values reported in humans at its clinically approved dose.[10, 87, 92, 93, 112] For pretomanid, administration of 25 to 54 mg/kg in mice was reported to result in human-equivalent dose exposures, based on AUC, although 25 mg/kg was reported to result in lower % $T_{>MIC}$ lower than achieved in the clinic.[103–106] In fact, in two different mouse TB models, the activity of delamanid at 2.5 mg/kg was shown to be similar to pretomanid at 20 mg/kg and 30 mg/ kg.[10, 120] Considering that for delamanid AUC_{0-24}/MIC was found to be the main driver of activity[92] and that its activity is dose-dependent in tested concentrations up to 100 mg/kg in mice,[10, 120] one might speculate that if higher drug exposures could be safely reached in the clinic, delamanid might be expected to do better than at its currently approved clinical dose. This may also hold true for pretomanid, for which $\%T_{>MIC}$ is the

most important driving PK/PD index (and this is already >90% at the approved clinical dose), but for which AUC/MIC is also an important driver of efficacy.[104, 110]

As to delamanid-containing and pretomanid-containing regimens, no head-to-head comparisons have yet been published. In animal studies, the drug combinations where delamanid or pretomanid replaced isoniazid in the standard regimen, as well as the relatively new BPaL and BPaMZ regimens, showed higher activity and achieved cure following a shorter treatment period than the HRZE regimen. Especially for pretomanid, many other drug combinations have been assessed *in vivo*,[123, 129–131] whereas delamanid-containing TB regimens were studied to a lesser extent. Studying the substitution of pretomanid for delamanid in future studies on the efficacy of novel TB drug regimens would be worthwhile, as delamanid might be a valuable alternative to pretomanid (or vice versa) in the case of drug resistance, intolerance or significant drug–drug interactions.

References

1. World Health Organization. Consolidated Guidelines on Drug-Resistant Tuberculosis Treatment. World Health Organization, 2019.
2. Critical Path Institute. Critical Path to TB Drug Regimens. https://c-path. org/programs/cptr/.
3. Edwards DI. Nitroimidazole drugs–action and resistance mechanisms. I. Mechanisms of action. J Antimicrob Chemother 1993; 31: 9–20.
4. Shinn D. Metronidazole in acute ulcerative gingivitis. Lancet 1962; 279: 1191.
5. Cavalleri B, Ballotta R, Arioli V et al. New 5-substituted 1-alkyl-2- nitroimidazoles. J Med Chem 1973; 16: 557–60.
6. Nagarajan K, Shankar R, Rajappa S et al. Nitroimidazoles. XXI. 2,3-dihydro-6-nitroimidazo [2,1-b] oxazoles with antitubercular activity. Eur J Med Chem 1989; 24: 631–3.
7. Ashtekar DR, Costa-Perira R, Nagrajan K et al. *In vitro* and *in vivo* activities of the nitroimidazole CGI 17341 against *Mycobacterium tuberculosis*. Antimicrob Agents Chemother 1993; 37: 183–6.
8. Walsh JS, Wang R, Bagan E et al. Structural alterations that differentially affect the mutagenic and antitrichomonal activities of 5-nitroimidazoles. J Med Chem 1987; 30: 150–6.
9. Matsumoto M, Hashizume H, Tsubouchi H et al. Screening for novel antituberculosis agents that are effective against multidrug resistant tuberculosis. Curr Top Med Chem 2007; 7: 499–507.
10. Matsumoto M, Hashizume H, Tomishige T et al. OPC-67683, a nitro-dihydro-imidazooxazole derivative with promising action against tuberculosis *in vitro* and in mice. PLoS Med 2006; 3: e466.
11. Sasaki H, Haraguchi Y, Itotani M et al. Synthesis and antituberculosis activity of a novel series of optically active 6-nitro-2,3-dihydroimidazo[2,1-b]oxazoles. J Med Chem 2006; 49: 7854–60.
12. Stover CK, Warrener P, VanDevanter DR et al. A small-molecule nitroimidazopyran drug candidate for the treatment of tuberculosis. Nature 2000; 405: 962–6.
13. Baker W, Shaopei C, Keeler E. Nitroimidazole antibacterial compounds and methods of use thereof. PathoGenesis Corporation. United States Patent 1997.
14. Baker W, Shaopei C, Keeler E. Nitro-[2,1-b]imidazopyran compounds and antibacterial uses thereof. PathoGenesis Corporation. United States Patent 2000.
15. Boshoff HIM, Myers TG, Copp BR et al. The transcriptional responses of *Mycobacterium tuberculosis* to inhibitors of metabolism: novel insights into drug mechanisms of action. J Biol Chem 2004; 279: 40174–84.
16. Manjunatha U, Boshoff HI, Barry CE. The mechanism of action of PA-824: Novel insights from transcriptional profiling. Commun Integr Biol 2009; 2: 215–8.
17. Van den Bossche A, Varet H, Sury A et al. Transcriptional profiling of a laboratory and clinical *Mycobacterium tuberculosis* strain suggests respiratory poisoning upon exposure to delamanid. Tuberculosis (Edinb) 2019; 117: 18–23.
18. Embley TM, Stackebrandt E. The molecular phylogeny and systematics of the actinomycetes. Annu Rev Microbiol 1994; 48: 257–89.
19. Jarlier V, Nikaido H. Mycobacterial cell wall: structure and role in natural resistance to antibiotics. FEMS Microbiol Lett 1994; 123: 11–8.

20. Indrigo J, Hunter RL, Actor JK. Cord factor trehalose 6,6'-dimycolate (TDM) mediates trafficking events during mycobacterial infection of murine macrophages. Microbiology (Reading) 2003; 149: 2049–59.
21. Rao V, Gao F, Chen B et al. Trans-cyclopropanation of mycolic acids on trehalose dimycolate suppresses *Mycobacterium tuberculosis*-induced inflammation and virulence. J Clin Invest 2006; 116: 1660–7.
22. Batt SM, Minnikin DE, Besra GS. The thick waxy coat of mycobacteria, a protective layer against antibiotics and the host's immune system. Biochem J 2020; 477: 1983–2006.
23. Liu Y, Matsumoto M, Ishida H et al. Delamanid: from discovery to its use for pulmonary multidrug-resistant tuberculosis (MDR-TB). Tuberculosis (Edinb) 2018; 111: 20–30.
24. Purwantini E, Mukhopadhyay B. Rv0132c of *Mycobacterium tuberculosis* encodes a coenzyme F_{420}-dependent hydroxymycolic acid dehydrogenase. PLoS One 2013; 8: e81985.
25. Fujiwara M, Kawasaki M, Hariguchi N et al. Mechanisms of resistance to delamanid, a drug for *Mycobacterium tuberculosis*. Tuberculosis (Edinb) 2018; 108: 186–94.
26. Gurumurthy M, Mukherjee T, Dowd CS et al. Substrate specificity of the deazaflavin-dependent nitroreductase from *Mycobacterium tuberculosis* responsible for the bioreductive activation of bicyclic nitroimidazoles. FEBS J 2012; 279: 113–25.
27. Haver HL, Chua A, Ghode P et al. Mutations in genes for the F_{420} biosynthetic pathway and a nitroreductase enzyme are the primary resistance determinants in spontaneous *in vitro*-selected PA-824-resistant mutants of *Mycobacterium tuberculosis*. Antimicrob Agents Chemother 2015; 59: 5316–23.
28. Singh R, Manjunatha U, Boshoff HIM et al. PA-824 kills nonreplicating *Mycobacterium tuberculosis* by intracellular NO release. Science 2008; 322: 1392–5.
29. Lee BM, Harold LK, Almeida DV et al. Predicting nitroimidazole antibiotic resistance mutations in *Mycobacterium tuberculosis* with protein engineering. PLoS Pathog 2020; 16: e1008287.
30. Hanaki E, Hayashi M, Matsumoto M. Delamanid is not metabolized by *Salmonella* or human nitroreductases: a possible mechanism for the lack of mutagenicity. Regul Toxicol Pharmacol 2017; 84: 1–8.
31. Dogra M, Palmer BD, Bashiri G et al. Comparative bioactivation of the novel anti-tuberculosis agent PA-824 in mycobacteria and a subcellular fraction of human liver. Br J Pharmacol 2011; 162: 226–36.
32. Boshoff HI, Barry CE, 3rd. Tuberculosis – metabolism and respiration in the absence of growth. Nat Rev Microbiol 2005; 3: 70–80.
33. Rao SPS, Alonso S, Rand L et al. The protonmotive force is required for maintaining ATP homeostasis and viability of hypoxic, nonreplicating *Mycobacterium tuberculosis*. Proc Natl Acad Sci U S A 2008; 105: 11945–50.
34. Hayashi M, Nishiyama A, Kitamoto R et al. Adduct formation of delamanid with NAD in mycobacteria. Antimicrob Agents Chemother 2020; 64: e01755-19.
35. Manjunatha UH, Boshoff H, Dowd CS et al. Identification of a nitroimidazo-oxazine-specific protein involved in PA-824 resistance in *Mycobacterium tuberculosis*. Proc Natl Acad Sci U S A 2006; 103: 431–6.
36. Rifat D, Li SY, Ioerger T et al. Mutations in *fbiD* (*Rv2983*) as a novel determinant of resistance to pretomanid and delamanid in *Mycobacterium tuberculosis*. Antimicrob Agents Chemother 2020; 65: e01948-20.
37. Choi KP, Bair TB, Bae YM et al. Use of transposon Tn5367 mutagenesis and a nitroimidazopyran-based selection system to demonstrate a requirement for fbiA and fbiB in coenzyme $F_{(420)}$ biosynthesis by *Mycobacterium bovis* BCG. J Bacteriol 2001; 183: 7058–66.

38. Choi K-P, Kendrick N, Daniels L. Demonstration that fbiC is required by *Mycobacterium bovis* BCG for coenzyme $F_{(420)}$ and FO biosynthesis. J Bacteriol 2002; 184: 2420–8.
39. Battaglia S, Spitaleri A, Cabibbe AM et al. Characterization of genomic variants associated with resistance to bedaquiline and delamanid in naive *Mycobacterium tuberculosis* clinical strains. J Clin Microbiol 2020; 58: e01304-20.
40. Bloemberg GV, Keller PM, Stucki D et al. Acquired resistance to bedaquiline and delamanid in therapy for tuberculosis. N Engl J Med 2015; 373: 1986–8.
41. Kardan-Yamchi J, Kazemian H, Battaglia S et al. Whole genome sequencing results associated with minimum inhibitory concentrations of 14 anti-tuberculosis drugs among rifampicin-resistant isolates of *Mycobacterium tuberculosis* from iran. J Clin Med 2020; 9: 465.
42. Pang Y, Zong Z, Huo F et al. *In vitro* drug susceptibility of bedaquiline, delamanid, linezolid, clofazimine, moxifloxacin, and gatifloxacin against extensively drug-resistant tuberculosis in Beijing, China. Antimicrob Agents Chemother 2017; 61: e00900-17.
43. Polsfuss S, Hofmann-Thiel S, Merker M et al. Emergence of low-level delamanid and bedaquiline resistance during extremely drug-resistant tuberculosis treatment. Clin Infect Dis 2019; 69: 1229–31.
44. Schena E, Nedialkova L, Borroni E et al. Delamanid susceptibility testing of *Mycobacterium tuberculosis* using the resazurin microtitre assay and the BACTEC™ MGIT™ 960 system. J Antimicrob Chemother 2016; 71: 1532–9.
45. Yang JS, Kim KJ, Choi H et al. Delamanid, bedaquiline, and linezolid minimum inhibitory concentration distributions and resistance-related gene mutations in multidrug-resistant and extensively drug-resistant tuberculosis in Korea. Ann Lab Med 2018; 38: 563–8.
46. Reichmuth ML, Hömke R, Zürcher K et al. Natural polymorphisms in *Mycobacterium tuberculosis* conferring resistance to delamanid in drug-naive patients. Antimicrob Agents Chemother 2020; 64: e00513-20.
47. Yoshiyama T, Mitarai S, Takaki A et al. Multi-drug resistant tuberculosis with simultaneously acquired-drug resistance to bedaquiline and delamanid. Clin Infect Dis 2020; 73: 2329–31.
48. Wang G, Jiang G, Jing W et al. Prevalence and molecular characterizations of seven additional drug resistance among multidrug-resistant tuberculosis in China: A subsequent study of a national survey. J Infect 2021; 82: 371–7.
49. Wen S, Jing W, Zhang T et al. Comparison of *in vitro* activity of the nitroimidazoles delamanid and pretomanid against multidrug-resistant and extensively drug-resistant tuberculosis. Eur J Clin Microbiol Infect Dis 2019; 38: 1293–6.
50. Gengenbacher M, Kaufmann SH. *Mycobacterium tuberculosis*: success through dormancy. FEMS Microbiol Rev 2012; 36: 514–32.
51. Mitchison DA. The search for new sterilizing anti-tuberculosis drugs. Front Biosci 2004; 9: 1059–72.
52. Sarathy J, Dartois V, Dick T et al. Reduced drug uptake in phenotypically resistant nutrient-starved nonreplicating *Mycobacterium tuberculosis*. Antimicrob Agents Chemother 2013; 57: 1648–53.
53. Wayne LG, Hayes LG. An *in vitro* model for sequential study of shiftdown of *Mycobacterium tuberculosis* through two stages of nonreplicating persistence. Infect Immun 1996; 64: 2062–9.
54. Parish T. *In vitro* drug discovery models for *Mycobacterium tuberculosis* relevant for host infection. Expert Opin Drug Discov 2020; 15: 349–58.

55. Piccaro G, Giannoni F, Filippini P et al. Activities of drug combinations against *Mycobacterium tuberculosis* grown in aerobic and hypoxic acidic conditions. Antimicrob Agents Chemother 2013; 57: 1428–33.
56. Tudó G, Laing K, Mitchison DA et al. Examining the basis of isoniazid tolerance in nonreplicating *Mycobacterium tuberculosis* using transcriptional profiling. Future Med Chem 2010; 2: 1371–83.
57. European Committee on Antimicrobial Susceptibility Testing (EUCAST). MIC and zone diameter distributions and ECOFFs https://mic. eucast.org/Eucast2/SearchController/search.jsp?action= performSearch&BeginIndex=0&Micdif=mic&NumberIndex=50&Antib=-1&Specium=806.
58. Keller PM, Hömke R, Ritter C et al. Determination of MIC distribution and epidemiological cutoff values for bedaquiline and delamanid in *Mycobacterium tuberculosis* using the MGIT 960 system equipped with TB eXiST. Antimicrob Agents Chemother 2015; 59: 4352–5.
59. Stinson K, Kurepina N, Venter A et al. MIC of delamanid (OPC-67683) against *Mycobacterium tuberculosis* clinical isolates and a proposed critical concentration. Antimicrob Agents Chemother 2016; 60: 3316–22.
60. European Committee on Antimicrobial Susceptibility Testing (EUCAST). Breakpoint tables for interpretation of MICs and zone diameters. Version 11.0. http://www.eucast.org.
61. Saliu OY, Crismale C, Schwander SK et al. Bactericidal activity of OPC-67683 against drug-tolerant *Mycobacterium tuberculosis*. J Antimicrob Chemother 2007; 60: 994–8.
62. Dalton JP, Uy B, Okuda KS et al. Screening of anti-mycobacterial compounds in a naturally infected zebrafish larvae model. J Antimicrob Chemother 2017; 72: 421–7.
63. Upton AM, Cho S, Yang TJ et al. *In vitro* and *in vivo* activities of the nitroimidazole TBA-354 against *Mycobacterium tuberculosis*. Antimicrob Agents Chemother 2015; 59: 136–44.
64. Chandramohan Y, Padmanaban V, Bethunaickan R et al. *In vitro* interaction profiles of the new antitubercular drugs bedaquiline and delamanid with moxifloxacin against clinical *Mycobacterium tuberculosis* isolates. J Glob Antimicrob Resist 2019; 19: 348–53.
65. Agency EM. Assessment report Pretomanid FGK. Amsterdam: European Medicines Agency, 2020.
66. Lenaerts AJ, Gruppo V, Marietta KS et al. Preclinical testing of the nitroimidazopyran PA-824 for activity against *Mycobacterium tuberculosis* in a series of *in vitro* and *in vivo* models. Antimicrob Agents Chemother 2005; 49: 2294–301.
67. Khoje AD, Kulendrn A, Charnock C et al. Synthesis of non-purine analogs of 6-aryl-9-benzylpurines, and their antimycobacterial activities. Compounds modified in the imidazole ring. Bioorg Med Chem 2010; 18: 7274–82.
68. Feuerriegel S, Köser CU, Baù D et al. Impact of Fgd1 and ddn diversity in *Mycobacterium tuberculosis* complex on *in vitro* susceptibility to PA-824. Antimicrob Agents Chemother 2011; 55: 5718–22.
69. Zhang F, Li S, Wen S et al. Comparison *of in vitro* susceptibility of mycobacteria against PA-824 to identify key residues of Ddn, the deazoflavin-dependent nitroreductase from *Mycobacterium tuberculosis*. Infect Drug Resist 2020; 13: 815–22.
70. European Medicines Agency. Pretomanid FGK: EPAR – Product Information, Annex I: Summary of product characteristics. European Medicines Agency, 2020.
71. Sala C, Dhar N, Hartkoorn RC et al. Simple model for testing drugs against nonreplicating *Mycobacterium tuberculosis*. Antimicrob Agents Chemother 2010; 54: 4150–8.

72. Hu Y, Coates AR, Mitchison DA. Comparison of the sterilising activities of the nitroimidazopyran PA-824 and moxifloxacin against persisting *Mycobacterium tuberculosis*. Int J Tuberc Lung Dis 2008; 12: 69–73.

73. Early JV, Mullen S, Parish T. A rapid, low pH, nutrient stress, assay to determine the bactericidal activity of compounds against non-replicating *Mycobacterium tuberculosis*. PLoS One 2019; 14: e0222970.

74. Iacobino A, Piccaro G, Giannoni F et al. Activity of drugs against dormant *Mycobacterium tuberculosis*. Int J Mycobacteriol 2016; 5: S94–5.

75. Papadopoulou MV, Bloomer WD, McNeil MR. NLCQ-1 and NLCQ-2, two new agents with activity against dormant *Mycobacterium tuberculosis*. Int J Antimicrob Agents 2007; 29: 724–7.

76. Somasundaram S, Anand RS, Venkatesan P et al. Bactericidal activity of PA-824 against *Mycobacterium tuberculosis* under anaerobic conditions and computational analysis of its novel analogues against mutant Ddn receptor. BMC Microbiol 2013; 13: 218.

77. Wallis RS, Jakubiec W, Mitton-Fry M et al. Rapid evaluation in whole blood culture of regimens for XDR-TB containing PNU-100480 (sutezolid), TMC207, PA-824, SQ109, and pyrazinamide. PLoS One 2012; 7: e30479.

78. Drusano GL, Kim S, Almoslem M et al. The funnel: a screening technique for identifying optimal two-drug combination chemotherapy regimens. Antimicrob Agents Chemother 2021; 65: e02172-20.

79. de Miranda Silva C, Hajihosseini A, Myrick J et al. Effect of moxifloxacin plus pretomanid against *Mycobacterium tuberculosis* in log phase, acid phase, and nonreplicating-persister phase in an *in vitro* assay. Antimicrob Agents Chemother 2019; 63: e01695-18.

80. Drusano GL, Neely MN, Kim S et al. Building optimal three-drug combination chemotherapy regimens. Antimicrob Agents Chemother 2020; 64: e01610-20.

81. López-Gavín A, Tudó G, Vergara A et al. *In vitro* activity against *Mycobacterium tuberculosis* of levofloxacin, moxifloxacin and UB-8902 in combination with clofazimine and pretomanid. Int J Antimicrob Agents 2015; 46: 582–5.

82. Srivastava S, Deshpande D, Magombedze G et al. Duration of pretomanid/moxifloxacin/pyrazinamide therapy compared with standard therapy based on time-to-extinction mathematics. J Antimicrob Chemother 2020; 75: 392–9.

83. Mouton JW, Dudley MN, Cars O et al. Standardization of pharmacokinetic/pharmacodynamic (PK/PD) terminology for anti-infective drugs: an update. J Antimicrob Chemother 2005; 55: 601–7.

84. Shibata M, Shimokawa Y, Sasahara K et al. Absorption, distribution and excretion of the anti-tuberculosis drug delamanid in rats: Extensive tissue distribution suggests potential therapeutic value for extrapulmonary tuberculosis. Biopharm Drug Dispos 2017; 38: 301–12.

85. Tucker EW, Pieterse L, Zimmerman MD et al. Delamanid central nervous system pharmacokinetics in tuberculous meningitis in rabbits and humans. Antimicrob Agents Chemother 2019; 63: e00913-19.

86. Shimokawa Y, Sasahara K, Koyama N et al. Metabolic mechanism of delamanid, a new anti-tuberculosis drug, in human plasma. Drug Metab Dispos 2015; 43: 1277–83.

87. Sasahara K, Shimokawa Y, Hirao Y et al. Pharmacokinetics and metabolism of delamanid, a novel anti-tuberculosis drug, in animals and humans: importance of albumin metabolism *in vivo*. Drug Metab Dispos 2015; 43: 1267–76.

88. Shimokawa Y, Sasahara K, Yoda N et al. Delamanid does not inhibit or induce cytochrome p450 enzymes *in vitro*. Biol Pharm Bull 2014; 37: 1727–35.

89. Mallikaarjun S, Wells C, Petersen C et al. Delamanid coadministered with antiretroviral drugs or antituberculosis drugs shows no clinically relevant drug-drug interactions in healthy subjects. Antimicrob Agents Chemother 2016; 60: 5976–85.
90. European Medicines Agency. Deltyba: EPAR – Medicine overview. 2020.
91. Gler MT, Skripconoka V, Sanchez-Garavito E et al. Delamanid for multidrug-resistant pulmonary tuberculosis. N Engl J Med 2012; 366: 2151–60.
92. Mallikaarjun S, Chapagain ML, Sasaki T et al. Cumulative fraction of response for once- and twice-daily delamanid in patients with pulmonary multidrug-resistant tuberculosis. Antimicrob Agents Chemother 2020; 65: e01207-20.
93. Pieterman ED, Keutzer L, van der Meijden A et al. Superior efficacy of a bedaquiline, delamanid and linezolid combination regimen in a mouse-TB model. J Infect Dis 2021; 224: 1039–47.
94. Ramirez G, Pham AC, Clulow AJ et al. Sustained absorption of delamanid from lipid-based formulations as a path to reduced frequency of administration. Drug Deliv Transl Res 2021; 11: 1236–44.
95. Chen X, Hashizume H, Tomishige T et al. Delamanid kills dormant mycobacteria *in vitro* and in a guinea pig model of tuberculosis. Antimicrob Agents Chemother 2017; 61: e02402-16.
96. Wang L, Ma Y, Duan H et al. Pharmacokinetics and tissue distribution study of PA-824 in rats by LC-MS/MS. J Chromatogr B Analyt Technol Biomed Life Sci 2015; 1006: 194–200.
97. Shobo A, Bratkowska D, Baijnath S et al. Tissue distribution of pretomanid in rat brain via mass spectrometry imaging. Xenobiotica 2016; 46: 247–52.
98. Shobo A, Pamreddy A, Kruger HG et al. Enhanced brain penetration of pretomanid by intranasal administration of an oil-in-water nanoemulsion. Nanomedicine (Lond) 2018; 13: 997–1008.,
99. Bratkowska D, Shobo A, Singh S et al. Determination of the antitubercular drug PA-824 in rat plasma, lung and brain tissues by liquid chromatography tandem mass spectrometry: application to a pharmacokinetic study. J Chromatogr B Analyt Technol Biomed Life Sci 2015; 988: 187–94.
100. Wang L, Xu Y, Liang L et al. LC-MS/MS method for the simultaneous determination of PA-824, moxifloxacin and pyrazinamide in rat plasma and its application to pharmacokinetic study. J Pharm Biomed Anal 2014; 97: 1–8.
101. Wang L, Zhao J, Zhang R et al. Drug-drug interactions between PA-824 and darunavir based on pharmacokinetics in rats by LC-MS-MS. J Chromatogr Sci 2018; 56: 327–35.
102. Dooley KE, Luetkemeyer AF, Park J-G et al. Phase I safety, pharmacokinetics, and pharmacogenetics study of the antituberculosis drug PA-824 with concomitant lopinavir-ritonavir, efavirenz, or rifampin. Antimicrob Agents Chemother 2014; 58: 5245–52.
103. Winter H, Ginsberg A, Egizi E et al. Effect of a high-calorie, high-fat meal on the bioavailability and pharmacokinetics of PA-824 in healthy adult subjects. Antimicrob Agents Chemother 2013; 57: 5516–20.
104. Diacon AH, Dawson R, von Groote-Bidlingmaier F et al. Bactericidal activity of pyrazinamide and clofazimine alone and in combinations with pretomanid and bedaquiline. Am J Respir Crit Care Med 2015; 191: 943–53.
105. Lakshminarayana SB, Boshoff HIM, Cherian J et al. Pharmacokinetics-pharmacodynamics analysis of bicyclic 4-nitroimidazole analogs in a murine model of tuberculosis. PLoS One 2014; 9: e105222.
106. Tasneen R, Tyagi S, Williams K et al. Enhanced bactericidal activity of rifampin and/or pyrazinamide when combined with PA-824 in a murine model of tuberculosis. Antimicrob Agents Chemother 2008; 52: 3664–8.

107. Mudde SE, Alsoud RA, van der Meijden A et al. Predictive modeling to study the treatment-shortening potential of novel tuberculosis drug regimens, towards bundling of preclinical data. J Infect Dis 2022; 225(11):1876-1885.

108. Nuermberger E, Rosenthal I, Tyagi S et al. Combination chemotherapy with the nitroimidazopyran PA-824 and first-line drugs in a murine model of tuberculosis. Antimicrob Agents Chemother 2006; 50: 2621–5.

109. Dutta NK, Alsultan A, Gniadek TJ et al. Potent rifamycin-sparing regimen cures guinea pig tuberculosis as rapidly as the standard regimen. Antimicrob Agents Chemother 2013; 57: 3910–6.

110. Ahmad Z, Peloquin CA, Singh RP et al. PA-824 exhibits time-dependent activity in a murine model of tuberculosis. Antimicrob Agents Chemother 2011; 55: 239–45.

111. Ginsberg AM, Laurenzi MW, Rouse DJ et al. Safety, tolerability, and pharmacokinetics of PA-824 in healthy subjects. Antimicrob Agents Chemother 2009; 53: 3720–5.

112. Wang X, Mallikaarjun S, Gibiansky E. Population pharmacokinetic analysis of delamanid in patients with pulmonary multidrug-resistant tuberculosis. Antimicrob Agents Chemother 2020; 65: e01202-20.

113. Franzblau SG, DeGroote MA, Cho SH et al. Comprehensive analysis of methods used for the evaluation of compounds against *Mycobacterium tuberculosis*. Tuberculosis (Edinb) 2012; 92: 453–88.

114. Nuermberger EL. Preclinical efficacy testing of new drug candidates. Microbiol Spectr 2017; 5.

115. Driver ER, Ryan GJ, Hoff DR et al. Evaluation of a mouse model of necrotic granuloma formation using C3HeB/FeJ mice for testing of drugs against *Mycobacterium tuberculosis*. Antimicrob Agents Chemother 2012; 56: 3181–95.

116. Via LE, Lin PL, Ray SM et al. Tuberculous granulomas are hypoxic in guinea pigs, rabbits, and nonhuman primates. Infect Immun 2008; 76: 2333–40.

117. Gengenbacher M, Duque-Correa MA, Kaiser P et al. NOS2-deficient mice with hypoxic necrotizing lung lesions predict outcomes of tuberculosis chemotherapy in humans. Sci Rep 2017; 7: 8853.

118. Hariguchi N, Chen X, Hayashi Y et al. OPC-167832, a novel carbostyril derivative with potent antituberculosis activity as a DprE1 inhibitor. Antimicrob Agents Chemother 2020; 64: e02020-19.

119. Kmentova I, Sutherland HS, Palmer BD et al. Synthesis and structureactivity relationships of aza- and diazabiphenyl analogues of the antitubercular drug (6S)-2-nitro-6-{[4-(trifluoromethoxy)benzyl] oxy}-6,7-dihydro5H-imidazo[2,1-b][1,3] oxazine (PA-824). J Med Chem 2010; 53: 8421–39.

120. Tasneen R, Williams K, Amoabeng O et al. Contribution of the nitroimidazoles PA-824 and TBA-354 to the activity of novel regimens in murine models of tuberculosis. Antimicrob Agents Chemother 2015; 59: 129–35.

121. Bigelow KM, Tasneen R, Chang YS et al. Preserved efficacy and reduced toxicity with intermittent linezolid dosing in combination with bedaquiline and pretomanid in a murine TB model. Antimicrob Agents Chemother 2020; 64: e01178-20.

122. Xu J, Converse PJ, Upton AM et al. Comparative efficacy of the novel diarylquinoline TBAJ-587 and bedaquiline against a resistant Rv0678 mutant in a mouse model of tuberculosis. Antimicrob Agents Chemother 2021; 65: e02418-20.

123. Xu J, Li S-Y, Almeida DV et al. Contribution of pretomanid to novel regimens containing bedaquiline with either linezolid or moxifloxacin and pyrazinamide in murine models of tuberculosis. Antimicrob Agents Chemother 2019; 63: e00021-19.

124. Tyagi S, Nuermberger E, Yoshimatsu T et al. Bactericidal activity of the nitroimidazopyran PA-824 in a murine model of tuberculosis. Antimicrob Agents Chemother 2005; 49: 2289–93.

125. Lanoix J-P, Betoudji F, Nuermberger E. Novel regimens identified in mice for treatment of latent tuberculosis infection in contacts of patients with multidrug-resistant tuberculosis. Antimicrob Agents Chemother 2014; 58: 2316–21.

126. Dutta NK, Karakousis PC. PA-824 is as effective as isoniazid against latent tuberculosis infection in C3HeB/FeJ mice. Int J Antimicrob Agents 2014; 44: 564–6.

127. Garcia-Contreras L, Sung JC, Muttil P et al. Dry powder PA-824 aerosols for treatment of tuberculosis in guinea pigs. Antimicrob Agents Chemother 2010; 54: 1436–42.

128. Tasneen R, Betoudji F, Tyagi S et al. Contribution of oxazolidinones to the efficacy of novel regimens containing bedaquiline and pretomanid in a mouse model of tuberculosis. Antimicrob Agents Chemother 2016; 60: 270–7.

129. Nuermberger E, Tyagi S, Tasneen R et al. Powerful bactericidal and sterilizing activity of a regimen containing PA-824, moxifloxacin, and pyrazinamide in a murine model of tuberculosis. Antimicrob Agents Chemother 2008; 52: 1522–4.

130. Tasneen R, Li S-Y, Peloquin CA et al. Sterilizing activity of novel TMC207- and PA-824-containing regimens in a murine model of tuberculosis. Antimicrob Agents Chemother 2011; 55: 5485–92.

131. Li S-Y, Tasneen R, Tyagi S et al. Bactericidal and sterilizing activity of a novel regimen with bedaquiline, pretomanid, moxifloxacin, and pyrazinamide in a murine model of tuberculosis. Antimicrob Agents Chemother 2017; 61: e00913-17.

132. Purwantini E, Daniels L. Purification of a novel coenzyme F_{420}-dependent glucose-6-phosphate dehydrogenase from *Mycobacterium smegmatis*. J Bacteriol 1996; 178: 2861–6.

133. Purwantini E, Gillis TP, Daniels L. Presence of F_{420}-dependent glucose-6-phosphate dehydrogenase in *Mycobacterium* and *Nocardia* species, but absence from Streptomyces and Corynebacterium species and methanogenic Archaea. FEMS Microbiol Lett 1997; 146: 129–34.

134. Grinter R, Ney B, Brammananth R et al. Cellular and structural basis of synthesis of the unique intermediate dehydro-$F_{(420)}$-0 in mycobacteria. mSystems 2020; 5: e00389-20.

135. European Medicines Agency. Assessment report Deltyba, international non-proprietary name: delamanid. European Medicines Agency, 2014.

136. Sung JC, Garcia-Contreras L, Verberkmoes JL et al. Dry powder nitroimidazopyran antibiotic PA-824 aerosol for inhalation. Antimicrob Agents Chemother 2009; 53: 1338–43.

137. Tasneen R, Mortensen DS, Converse PJ et al. Dual mTORC1/mTORC2 inhibition as a host-directed therapeutic target in pathologically distinct mouse models of tuberculosis. Antimicrob Agents Chemother 2021; 65: e0025321.

CHAPTER 3

Improving treatment of nontuberculous mycobacterial infections

CHAPTER 3.1

Unraveling antibiotic resistance mechanisms in *Mycobacterium abscessus*: the potential role of efflux pumps

Saskia E. Mudde, Jodie A. Schildkraut, Nicole C. Ammerman, Corné P. de Vogel, Jurriaan E.M. de Steenwinkel, Jakko van Ingen, Hannelore I. Bax

J Glob Antimicrob Resist. 2022 Dec;31:345-352.

Abstract

Objectives

Mycobacterium abscessus is an opportunistic respiratory pathogen in patients with underlying lung disease. It is infamously known for its low treatment success rates because of its resistance to multiple classes of antibiotics. Further insight into *M. abscessus* resistance mechanisms is needed to improve treatment options. In this *in vitro* study, the role of efflux pumps in reaction to antibiotic stress is explored, as well as the ability of the putative efflux inhibitors, thioridazine and verapamil, to potentiate the activity of guideline-recommended antibiotics.

Methods

To evaluate the effects of antibiotic stress on mycobacterial efflux pumps, *M. abscessus* subspecies *abscessus* was exposed to amikacin, cefoxitin, clarithromycin, clofazimine, and tigecycline for 24 hours. Transcriptomic responses were measured by RNA sequencing to gain insight into upregulation of efflux pump encoding genes. Subsequently, in time-kill kinetics assays, the abovementioned antibiotics were combined with thioridazine and verapamil to evaluate their potentiating capacity.

Results

All five antibiotics led to a fold change of ≥2 Log_2 in expression of one or more genes encoding transporter systems. This effect was most pronounced for the ribosome-targeting antibiotics amikacin, clarithromycin, and tigecycline. Time-kill kinetics assays demonstrated synergy between amikacin, tigecycline, clofazimine, cefoxitin, and both thioridazine and verapamil.

Conclusions

Antibiotic stressors induce expression of efflux pump encoding genes in *M. abscessus*, especially antibiotics that target the ribosome. Putative efflux inhibitors thioridazine and verapamil show synergy with various guideline-recommended antibiotics, making them interesting candidates for the improvement of *M. abscessus* treatment.

Introduction

Among the nontuberculous mycobacteria (NTM), *Mycobacterium abscessus* is an important opportunistic respiratory pathogen in patients with underlying lung disease.[1] In patients with cystic fibrosis, pulmonary infection caused by *M. abscessus* can be particularly detrimental, as it is associated with accelerated progression to end stage lung disease[2] and person-to-person transmission[3] and may jeopardize successful lung transplantation.[4]

A variety of antibiotic resistance mechanisms are responsible for *M. abscessus* being infamously known as difficult to treat. This applies especially to *M. abscessus* subspecies *abscessus*, in which macrolide resistance is induced upon exposure to these drugs by the expression of the ribosome methylase-encoding erm(41) gene.[5] Apart from inducible macrolide resistance, acquired point mutations in the *rrl* gene may also abolish macrolide susceptibility.[6] Resistance to aminoglycosides by target modification and mutations in the *rrs* gene,[7] resistance to β-lactam antibiotics by the production of a class A β-lactamase,[8] and tetracycline resistance by enzymatic inactivation[9] further complicate the treatment of *M. abscessus* infections. Consequently, patients are treated for prolonged periods with multidrug therapies based on *in vitro* susceptibility testing, often accompanied by burdensome side effects. Despite intensive therapy, treatment success rates as low as 33.0% for pulmonary disease caused by *M. abscessus* subspecies *abscessus* have been reported.[10]

Apart from the abovementioned resistance mechanisms, there has been increasing evidence for the role of efflux pumps in antibiotic resistance in *M. abscessus*. Vianna et al. demonstrated that *M. abscessus* exposed to clarithromycin (CLR) showed overexpression of *MAB_1409* and *MAB_3142*, two efflux pump encoding genes.[11] In line, a recent study by Guo et al. showed an association between the upregulation of efflux pump genes *MAB_2355c, MAB_1409c*, and *MAB_1846* and CLR resistance, also in isolates without *rrl* mutations.[12] Furthermore, Richard et al. found clofazimine (CFZ)-resistant *M. abscessus* isolates harboring mutations in *MAB_2299c*, which were associated with the upregulation of an MmpS/MmpL efflux pump system and resulted in cross-resistance to bedaquiline.[13] Another study by Li et al. found mutations in *MAB_4384* encoding the repressor of the efflux pump MmpS5/MmpL5 in clinically isolated strains resistant to bedaquiline.[14] Lastly, enhanced expression of *MAB_0937c, MAB_1137c, MAB_4117c*, and *MAB_4237c*, all encoding efflux pumps and transporter systems, were shown to be upregulated upon exposure to amikacin (AMK).[15] However, the exact contribution of efflux pumps to antibiotic resistance in *M. abscessus* is not fully understood.

Increasing interest in the potential role of efflux pumps as a resistance mechanism in mycobacteria has led to the exploration of efflux inhibitors as an adjunctive therapy in

preclinical studies. The preclinical body of evidence for efflux inhibitors of both natural and synthetic origin as adjunctive therapies against mycobacteria is growing.[16] However, clinical studies evaluating efflux inhibitors have yet to be conducted. The current study concentrates on two putative efflux inhibitors: verapamil (VP) and thioridazine (TZ). Thioridazine, a phenothiazine, is originally an antipsychotic drug antagonizing dopamine receptor 2. It also has antiemetic, antihistaminic, and anticholinergic activities.[17] Although the efflux inhibitory activity of TZ has been observed in various mycobacterial species,[16] studies with TZ and *M. abscessus* are scarce. Verapamil is a calcium channel blocker used in the treatment of cardiovascular diseases[18] and has been extensively evaluated as a potentiator of antituberculosis drugs in preclinical models.[19, 20] Its capacity to inhibit drug efflux in *M. abscessus* was demonstrated by Vianna et al.[21] Therefore, we hypothesized that TZ and VP may similarly potentiate drug activity against *M. abscessus*.

Targeting drug efflux in *M. abscessus* infections could be a strategy for the development of new and more effective treatment options. For this reason, this study evaluated the effects of several guideline-recommended antibiotics on efflux pump gene expression in *M. abscessus*, as well as the ability of TZ and VP to enhance the anti-mycobacterial killing activity of these antibiotic compounds *in vitro*.

Materials and methods

Bacterial strain and culture conditions

The *M. abscessus* subsp. *abscessus* ATCC 19977 strain was used in all experiments. For the gene expression experiments (performed at Radboud University Nijmegen Medical Centre), stock vials of *M. abscessus* were stored at –70°C in trypticase soy broth containing 40% glycerol. For time-kill kinetics assays (performed at Erasmus University Medical Center Rotterdam), *M. abscessus* was cultured in Cation Adjusted Mueller Hinton broth ([CAMHB] Becton, Dickinson and Company [BD], Sparks, MD) supplemented with 10% OADC (BD) under shaking conditions at 96 rpm and 37°C. Vials with bacterial stock suspensions in CAMHB with 10% OADC were stored at –80°C until use.

Antimicrobial compounds

Amikacin (AMK), cefoxitin (FOX), clarithromycin (CLR), clofazimine (CFZ), thioridazine (TZ), and verapamil (VP) were purchased from Sigma-Aldrich (Zwijndrecht, The Netherlands). Tigecycline (TIG) was manufactured by Pfizer (Brussels, Belgium).

Drug susceptibility testing

Minimum inhibitory concentrations (MICs) were determined according to the Clinical and Laboratory Standards Institute (CLSI) guidelines (3rd edition) by broth microdilution

in CAMHB incubated at 30°C for 3 to 5 days. However, CFZ was found to precipitate in CAMHB. This issue could be resolved by diluting CFZ in CAMHB with 4% dimethyl sulfoxide (DMSO). The CLSI guidelines recommend determining the MIC of CLR after 14 days because of inducible resistance by the *erm*-gene. However, in this study, experiments with CLR did not exceed 3 days, so no induced CLR resistance was expected during this period. Therefore, the MIC of CLR was determined after 3 days of incubation.

Drug stability testing

Drug stability of AMK and FOX was evaluated by assessing antimicrobial activity over time using the standard large-plate agar diffusion assay.[22] In brief, for AMK and FOX, *Escherichia coli* ATCC 25922, susceptible to both compounds, was plated onto diagnostic sensitivity test agar (Oxoid, Hampshire, UK) or Mueller Hinton agar (BD), respectively. A standard concentration series of each drug with 2-fold increasing concentrations was prepared. Test concentrations per drug were incubated at 30°C, similar to the temperature at which the time-kill kinetics assays were performed. On days 1, 3, and 7, both the standard concentrations and a sample of the test concentrations were added onto the solid agar. The concentration of AMK and FOX in the test conditions over time was determined by comparing their inhibition zones to those of the standard concentrations, representing the remaining drug concentrations. The stability of TIG was determined similarly in a previous study, using *Micrococcus luteus*, susceptible to TIG, plated onto diagnostic sensitivity test agar.[22] For CFZ, no bacterial indicator strain is available. Therefore, a pre-incubation MIC determination with *M. abscessus* was used to determine drug stability. The MIC was determined by broth microdilution assay according to the CLSI guidelines. The CFZ concentrations were either freshly prepared or pre-incubated for 1 week at 30°C before determining the MIC. In this assay, equal MICs indicated that the compound was stable over the time course of a time-kill kinetics assay.

Gene expression

RNA sequencing was performed as described previously.[23] Bacterial inocula were grown in CAMHB with 0.05% Tween 80 until early Log-phase. Subsequently, antibiotics were added to the culture (AMK 8 mg/L, FOX 8 mg/L, CLR 4 mg/L, CFZ 1 mg/L, and TIG 0.5 mg/L), which was further incubated for 24 hours prior to RNA isolation. All conditions were completed in biological triplicate. Following lysis with bead beating, RNA isolation was performed using the Nucleospin RNA kit (Machery Nagel, Düren, Germany). Following isolation, RNA integrity was determined, rRNA was depleted, and the mRNA library was constructed and sequenced on a NextSeq 500 (Illumina, San Diego, CA). All obtained reads were mapped to the *M. abscessus* ATCC 17799 genome (NCBI reference sequence: NC_010397.1) using STAR (v2.7.0). Differential expression analysis of putative efflux transporter genes was performed in R (v3.3.3) using the DESeq2 package, and the cut-off for gene upregulation was defined as a Log_2 fold change ≥2; a *P* value (≤0.05) corrected for multiple guessing.

Time-kill kinetics assay

The concentration-dependent and time-dependent killing activity of AMK, TIG, FOX, and CFZ, alone or in combination with TZ or VP, was assessed as previously described.22 In brief, 25 mL cultures of *M. abscessus*, with a starting inoculum of ~5,5 $\times 10^5$ colony-forming units (CFU)/mL in CAMHB supplemented with 10% OADC, were exposed to AMK, FOX, TIG, or CFZ at concentrations of 1/4x or 1x the MIC with or without TZ or VP. For TZ and VP, concentrations of 1/2x or 1/8x MICs were used, as 1/2x MIC was previously shown to inhibit ethidium bromide efflux in mycobacteria.[24] Thus, the concentrations tested for each drug were as follows: AMK 4 and 16 mg/L; FOX 8 and 32 mg/L; TIG 1 and 4 mg/L; CFZ 0.125 and 0.5 mg/L; TZ 8 and 32 mg/L; and VP 128 and 512 mg/L. To prevent precipitation of CFZ in CAMHB with 10% OADC, 0.4% DMSO was added in time-kill kinetics assays with CFZ. Because CFZ at 1x MIC did not inhibit bacterial growth in the time-kill kinetic assay, MIC determination of CFZ was repeated in CAMHB supplemented with 10% OADC to better reflect the experimental conditions in the time-kill kinetics assay. As a 4-fold higher MIC of 2 mg/L was observed in the presence of 10% OADC, 4x MIC (2 mg/L) was included for CFZ. The cultures were incubated at 30 °C under shaking conditions. In a previous study, an incubation temperature of 35°C was used.[22] However, growth of *M. abscessus* at 30°C was found to be more optimal in comparison with growth at 35°C (data not shown). Also, the temperature of 30°C is in line with the CLSI (3rd edition) recommendations for MIC determinations. Based on the results of drug stability experiments, losses in drug stability were compensated for in the case of FOX and TIG by daily addition of minimal volumes (100 µL) of drug concentrations to the cultures. After 1, 3, and 7 days of drug exposure, the cultures were sampled for mycobacterial load determination (CFU/mL). Samples were centrifuged at 14.000 x *g* for 10 minutes, the supernatant was discarded, and the pellet was suspended in phosphate buffered saline. This washing procedure was performed twice to prevent drug carry-over onto the agar plates. The number of CFU per mL in the samples was determined by preparing 10-fold serial dilutions up to 10^{-7} and plating 200 µl per dilution onto Mueller Hinton agar supplemented with 10% OADC. CFU were counted after incubating the plates for 5 to 7 days at 30°C. CFU counts were Log_{10} transformed. The lower limit of detection was 0.7 Log_{10} CFU/mL. All experiments were performed in duplicate.

Synergy in the time-kill kinetics assays

Activity between antimycobacterial compounds and efflux inhibitors was considered to be synergistic when it conformed to either of the following definitions: i) a ≥100-fold (a difference of 2 Log_{10}) increase in mycobacterial killing with the 2-drug combination compared with the most active single drug, or ii) when a drug combination achieved elimination of *M. abscessus* that was not achieved by exposure to a single drug.[25] The definition of synergy was only met when at least one of these criteria was fulfilled in both (duplicate) experiments.

Results

Minimum inhibitory concentrations

The MICs established for the *M. abscessus* ATCC 19977 strain were as follows: 16 mg/L for AMK, 32 mg/L for FOX, 4 mg/L for CLR, 4 mg/L for TIG, and 0.5 mg/L for CFZ. The MIC established for TZ was 64 mg/L and that for VP was 1024 mg/L.

Drug stability

AMK was shown to be stable, but FOX showed a 33% decline daily. For TIG, an 80% decline daily was previously shown.[22] Both freshly prepared and pre-incubated CFZ concentrations demonstrated the same MIC for *M. abscessus*, indicating that CFZ was stable over the course of the time-kill kinetics assay.

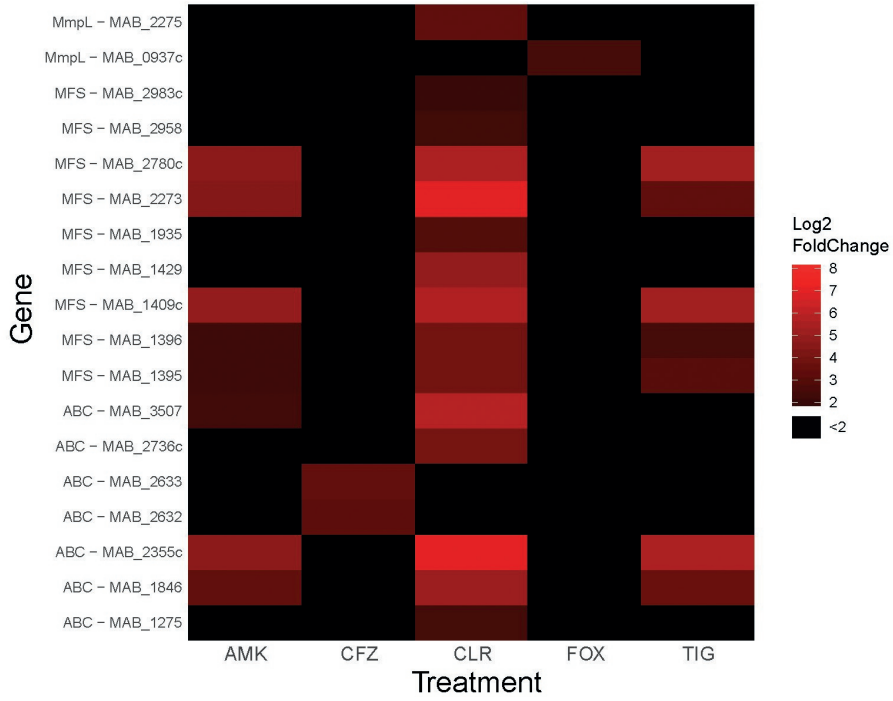

Figure 1. Differentially expressed transporter systems. Heat map illustrating transporter systems that had a fold change of ≥2 Log_2 and a *P* value of <0.05. AMK = amikacin; CFZ = clofazimine; CLR = clarithromycin; FOX = cefoxitin; TIG = tigecycline.

Gene expression

Exposure to subinhibitory concentrations of AMK, CFZ, CLR, FOX, and TIG resulted in an increased expression of a wide range of putative efflux transporter genes in *M. abscessus* (Figure 1). The largest number of upregulated efflux pump encoding genes was seen following CLR exposure (15), followed by AMK (8), and TIG (7). All genes upregulated following AMK and TIG exposure were also upregulated as a result of CLR exposure. In contrast, CFZ and FOX only induced a small set of efflux genes. CFZ induced the expression of *MAB_2632* and *MAB_2633*, encoding the CydC/CydD ABC transporter in the mycobacterial respiratory chain, while FOX induced specific expression of *MAB_0837c*, encoding a putative MmpL protein.

Time-kill kinetics assays

The time-dependent killing activities of AMK, TIG, FOX, and CFZ with or without TZ are presented in Figure 2 and Table 1, and those with or without VP are presented in Figure 3 and Table 2.

For the 1/2x MIC concentration of TZ, synergy was found with AMK at 1x MIC, TIG at 1/4x and 1x MIC, FOX at 1/4x and 1x MIC, and CFZ at 4x the MIC. When TZ at 1/2x MIC was combined with TIG at 1x MIC, no CFUs were retrieved at days 3 and 7. TZ at 1/8x MIC did not show synergy with any of the antibiotics tested. Of notice, TZ at 1/2x MIC showed substantial activity against *M. abscessus* on its own (Figure 2, Table 1).

Figure 2. Concentration-dependent and time-dependent bactericidal activity of thioridazine (TZ) at 1/8x MIC (8 mg/L) or 1/2x MIC (32 mg/L) combined with amikacin (AMK) at 1/4x MIC (4 mg/L) (A) or 1x MIC (16 mg/L) (B); tigecycline (TGC) at 1/4x MIC (1 mg/L) (C) or 1x MIC (4 mg/L) (D); cefoxitin (FOX) at 1/4x MIC (8 mg/L) (E) or 1x MIC (32 mg/L) (F); clofazimine (CFX) at 1/4x MIC (0.125 mg/L) (G); and 1x MIC (0.5 mg/L) (H) or 4x MIC (2 mg/L) (I) against *M. abscessus* subspecies *abscessus*. MIC values are based on the Clinical and Laboratory Standards Institute method. Mycobacterial cultures were exposed to the antibiotics with or without TZ for 7 days at 30°C under shaking conditions. On days 1, 3, and 7, the mycobacterial load, expressed as colony forming units (CFU), was determined by sampling the cultures and plating them onto antibiotic-free solid Mueller Hinton agar supplemented with 10% oleic acid-albumin-dextrose-catalase. The experiments were performed in duplicate. Results are expressed as the mean CFU (+/- the range). Circles indicate combinations showing synergy. The dashed horizontal line indicates the lower limit of detection of CFU.

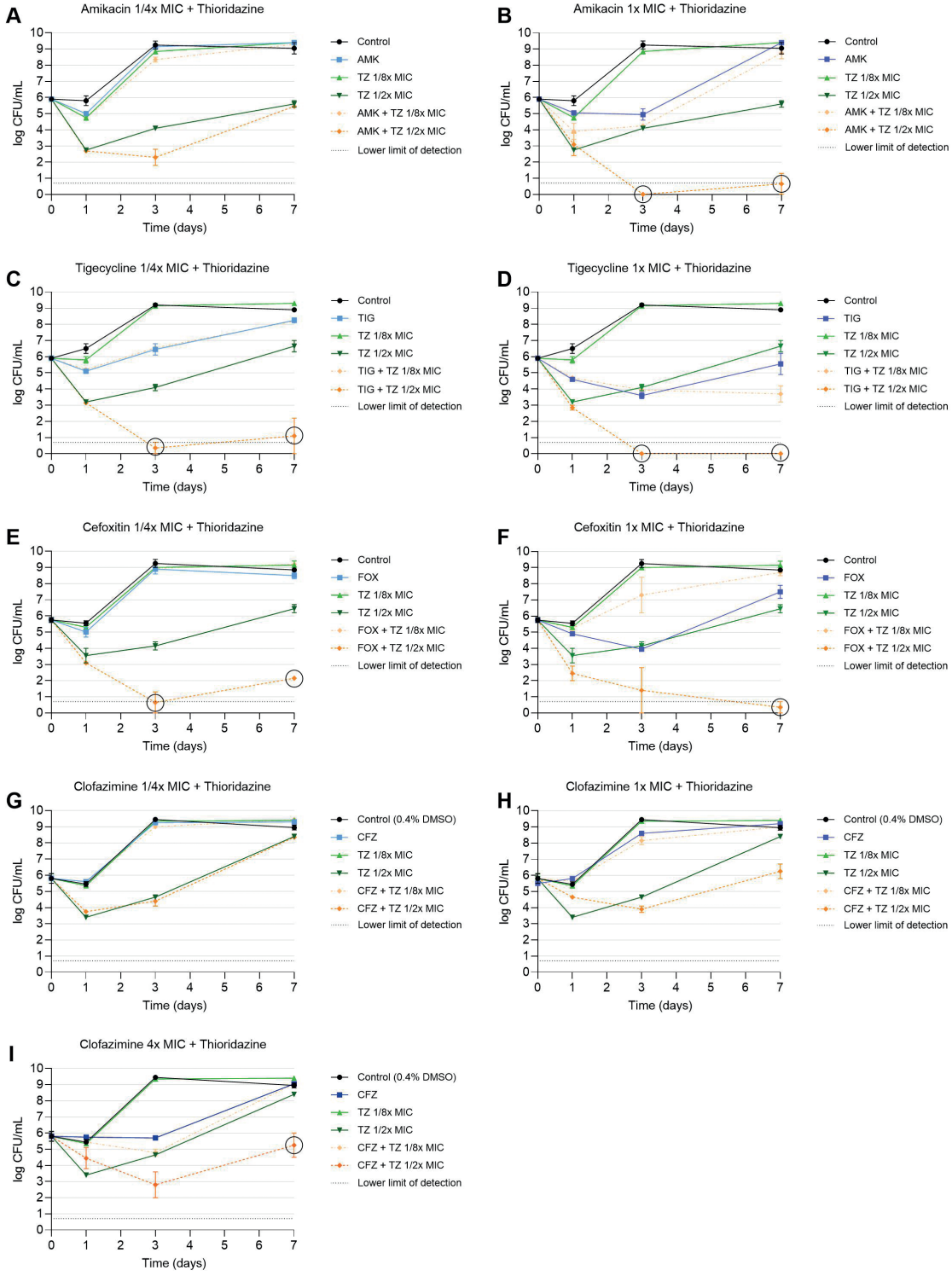
A
Amikacin 1/4x MIC + Thioridazine
log CFU/mL
Time (days)
Control
AMK
TZ 1/8x MIC
TZ 1/2x MIC
AMK + TZ 1/8x MIC
AMK + TZ 1/2x MIC
Lower limit of detection
B
Amikacin 1x MIC + Thioridazine
log CFU/mL
Time (days)
Control
AMK
TZ 1/8x MIC
TZ 1/2x MIC
AMK + TZ 1/8x MIC
AMK + TZ 1/2x MIC
Lower limit of detection
C
Tigecycline 1/4x MIC + Thioridazine
log CFU/mL
Time (days)
Control
TIG
TZ 1/8x MIC
TZ 1/2x MIC
TIG + TZ 1/8x MIC
TIG + TZ 1/2x MIC
Lower limit of detection
D
Tigecycline 1x MIC + Thioridazine
log CFU/mL
Time (days)
Control
TIG
TZ 1/8x MIC
TZ 1/2x MIC
TIG + TZ 1/8x MIC
TIG + TZ 1/2x MIC
Lower limit of detection
E
Cefoxitin 1/4x MIC + Thioridazine
log CFU/mL
Time (days)
Control
FOX
TZ 1/8x MIC
TZ 1/2x MIC
FOX + TZ 1/8x MIC
FOX + TZ 1/2x MIC
Lower limit of detection
F
Cefoxitin 1x MIC + Thioridazine
log CFU/mL
Time (days)
Control
FOX
TZ 1/8x MIC
TZ 1/2x MIC
FOX + TZ 1/8x MIC
FOX + TZ 1/2x MIC
Lower limit of detection
G
Clofazimine 1/4x MIC + Thioridazine
log CFU/mL
Time (days)
Control (0.4% DMSO)
CFZ
TZ 1/8x MIC
TZ 1/2x MIC
CFZ + TZ 1/8x MIC
CFZ + TZ 1/2x MIC
Lower limit of detection
H
Clofazimine 1x MIC + Thioridazine
log CFU/mL
Time (days)
Control (0.4% DMSO)
CFZ
TZ 1/8x MIC
TZ 1/2x MIC
CFZ + TZ 1/8x MIC
CFZ + TZ 1/2x MIC
Lower limit of detection
I
Clofazimine 4x MIC + Thioridazine
log CFU/mL
Time (days)
Control (0.4% DMSO)
CFZ
TZ 1/8x MIC
TZ 1/2x MIC
CFZ + TZ 1/8x MIC
CFZ + TZ 1/2x MIC
Lower limit of detection

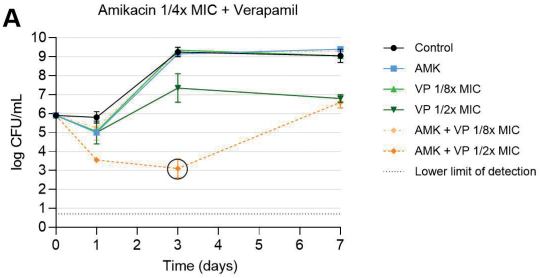
A
Amikacin 1/4x MIC + Verapamil
log CFU/mL
Time (days)
Control
AMK
VP 1/8x MIC
VP 1/2x MIC
AMK + VP 1/8x MIC
AMK + VP 1/2x MIC
Lower limit of detection

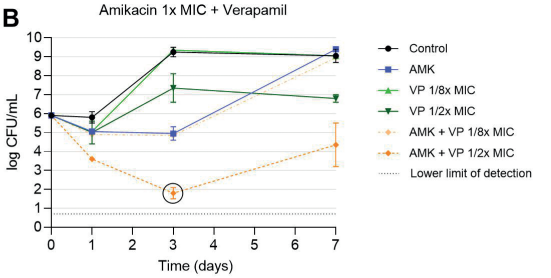
B
Amikacin 1x MIC + Verapamil
log CFU/mL
Time (days)
Control
AMK
VP 1/8x MIC
VP 1/2x MIC
AMK + VP 1/8x MIC
AMK + VP 1/2x MIC
Lower limit of detection

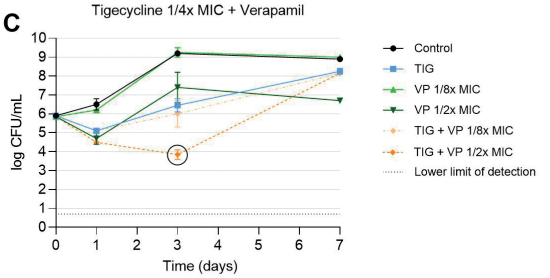
C
Tigecycline 1/4x MIC + Verapamil
log CFU/mL
Time (days)
Control
TIG
VP 1/8x MIC
VP 1/2x MIC
TIG + VP 1/8x MIC
TIG + VP 1/2x MIC
Lower limit of detection

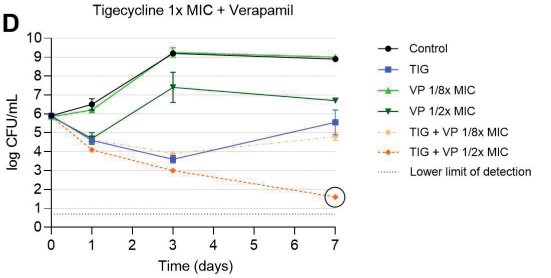
D
Tigecycline 1x MIC + Verapamil
log CFU/mL
Time (days)
Control
TIG
VP 1/8x MIC
VP 1/2x MIC
TIG + VP 1/8x MIC
TIG + VP 1/2x MIC
Lower limit of detection

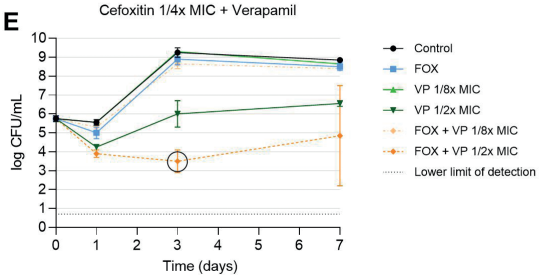
E
Cefoxitin 1/4x MIC + Verapamil
log CFU/mL
Time (days)
Control
FOX
VP 1/8x MIC
VP 1/2x MIC
FOX + VP 1/8x MIC
FOX + VP 1/2x MIC
Lower limit of detection

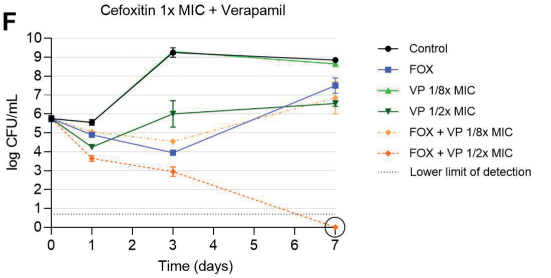
F
Cefoxitin 1x MIC + Verapamil
log CFU/mL
Time (days)
Control
FOX
VP 1/8x MIC
VP 1/2x MIC
FOX + VP 1/8x MIC
FOX + VP 1/2x MIC
Lower limit of detection

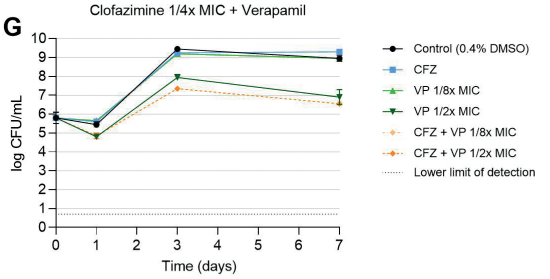
G
Clofazimine 1/4x MIC + Verapamil
log CFU/mL
Time (days)
Control (0.4% DMSO)
CFZ
VP 1/8x MIC
VP 1/2x MIC
CFZ + VP 1/8x MIC
CFZ + VP 1/2x MIC
Lower limit of detection

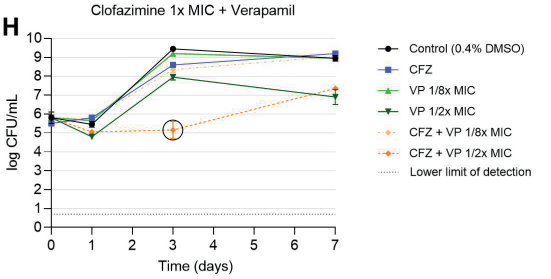
H
Clofazimine 1x MIC + Verapamil
log CFU/mL
Time (days)
Control (0.4% DMSO)
CFZ
VP 1/8x MIC
VP 1/2x MIC
CFZ + VP 1/8x MIC
CFZ + VP 1/2x MIC
Lower limit of detection

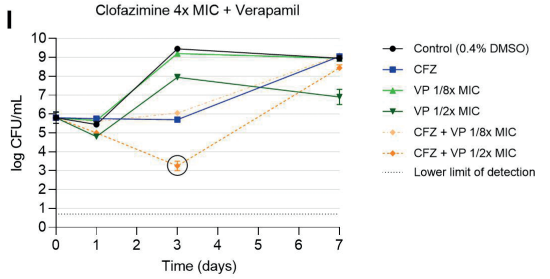
I
Clofazimine 4x MIC + Verapamil
log CFU/mL
Time (days)
Control (0.4% DMSO)
CFZ
VP 1/8x MIC
VP 1/2x MIC
CFZ + VP 1/8x MIC
CFZ + VP 1/2x MIC
Lower limit of detection

Figure 3. Concentration-dependent and time-dependent bactericidal activity of verapamil (VP) at 1/8x MIC (128 mg/L) or 1/2x MIC (512 mg/L) combined with amikacin (AMK) at 1/4x MIC (4 mg/L) (A) or 1x MIC (16 mg/L) (B); tigecycline (TGC) at 1/4x MIC (1 mg/L) (C) or 1x MIC (4 mg/L) (D); cefoxitin (FOX) at 1/4x MIC (8 mg/L) (E) or 1x MIC (32 mg/L) (F); and clofazimine (CFX) at 1/4x MIC (0.125 mg/L) (G), 1x MIC (0.5 mg/L) (H), or 4x MIC (2 mg/L) (I) against *M. abscessus* subspecies *abscessus*. MIC values are based on the Clinical and Laboratory Standards Institute method. Mycobacterial cultures were exposed to the antibiotics with or without VP for 7 days at 30°C under shaking conditions. On days 1, 3, and 7, the mycobacterial load, expressed as colony forming units (CFU), was determined by sampling the cultures and plating them onto antibiotic-free solid Mueller Hinton agar supplemented with 10% oleic acid-albumin-dextrose-catalase. The experiments were performed in duplicate. Results are expressed as the mean CFU (+/- the range). Circles indicate combinations showing synergy. The dashed horizontal line indicates the lower limit of detection of CFU.

Similar results were found for VP. Synergy was observed between VP at 1/2x MIC and AMK, and TIG and FOX at 1/4x and 1x MIC. CFZ at 1x and 4x MIC showed synergy with VP at 1/2x MIC, as well. Like TZ, the 1/8x MIC concentration of VP did not demonstrate synergy with any of the antibiotics (Figure 3, Table 2).

Table 1. Summary of interactions between amikacin (AMK), tigecycline (TIG), cefoxitin (FOX), and clofazimine (CFZ) and the efflux inhibitors thioridazine (TZ) based on the time-kill kinetics assays. Synergistic activity is indicated by '+'. MIC values are based on the CLSI method.

		Day 3		Day 7	
		1/8x MIC TZ	1/2x MIC TZ	1/8x MIC TZ	1/2x MIC TZ
AMK	1/4x MIC				
	1x MIC		+		+
TIG	1/4x MIC		+		+
	1x MIC		+		+
FOX	1/4x MIC		+		+
	1x MIC				+
CFZ	1/4x MIC				
	1x MIC				
	4x MIC				+

Table 2. Summary of interactions between amikacin (AMK), tigecycline (TIG), cefoxitin (FOX), and clofazimine (CFZ) and the efflux inhibitors verapamil (VP) based on the time-kill kinetics assays. Synergistic activity is indicated by '+'. MIC values are based on the CLSI method.

		Day 3		Day 7	
		1/8x MIC VP	1/2x MIC VP	1/8x MIC VP	1/2x MIC VP
AMK	1/4x MIC		+		
	1x MIC		+		
TIG	1/4x MIC		+		
	1x MIC				+
FOX	1/4x MIC		+		
	1x MIC				+
CFZ	1/4x MIC				
	1x MIC		+		
	4x MIC		+		

Discussion

While all five antibiotics were found to increase transcription of one or more genes encoding transporter systems, this effect was more pronounced for AMK, CLR, and TIG, as compared with CFZ and FOX. Time-kill kinetics assays showed synergistic activity between AMK, TIG, CFZ, FOX, and both TZ and VP. To our knowledge, these drug combinations have not been evaluated before against *M. abscessus in vitro*.[26]

Although the precise functions of the proteins encoded by the upregulated genes are not yet fully understood, these genes have been linked to different families of efflux pumps and other transporter systems.[12, 15, 27-29] As such, the findings in this study strengthen the growing body of evidence for efflux mediated antibiotic resistance mechanisms in *M. abscessus*.[11-13, 15]

Interestingly, compared with CFZ and FOX, gene upregulation for efflux transporters was more pronounced upon exposure to AMK, CLR, and TIG, all three being ribosome-targeting antibiotics. FOX, on the other hand, targets cell wall synthesis, and CFZ is thought to interfere with the mycobacterial respiratory chain.[23] Although one might speculate that ribosome-targeting antibiotics are more potent inducers of efflux pump systems specifically, it is good to interpret these results in a broader context of gene upregulation. In fact, it was recently shown by Schildkraut et al. that AMK, CLR, and TIG led to more extensive elevated transcriptional responses, in general, in comparison with FOX and CFZ.[23] One of the common transcriptomic responses shared by AMK, CLR, and

TIG is the upregulation of the *whiB7* regulon, a transcriptional regulator controlling genes involved in intrinsic antibiotic resistance.[23, 28] In line, in the current study, 9 of 14 efflux pump genes upregulated by exposure to AMK, CLR, and TIG are described as within the *M. abscessus whiB7* regulon.[28, 29] Induction of *whiB7* by ribosome-targeting antibiotics could perhaps explain why upregulation of efflux pump encoding genes was most explicit for AMK, CLR, and TIG. On the other hand, AMK has been considered as a weak *whiB7*-inducer[28, 29]; however, it led to substantial induction of multiple transporter genes in the current study.

Apart from a possible indirect link between efflux pumps and ribosome-targeting antibiotics via *whiB7*, there might also be a more direct link. The function of efflux pumps extends beyond efflux of antibiotics, as they contribute to cell homeostasis by secreting waste products, as well as specific substrates that assist in cell-to-cell communication, biofilm formation, and nutrient acquisition.[30] Additionally, there is increasing evidence that efflux pumps might be involved in ribosomal protection. A subfamily of ATP-binding cassette (ABC) transporters, the cytosolic ABC-F proteins, are capable of displacing antibiotics from the ribosome, thereby providing protection against ribosome targeting antibiotics.[31] More specific to *M. abscessus*, a recent study by Guo et al. found that MAB_2355c, a putative ABC transporter with homology to ABC-F proteins, is strongly induced by macrolides. Using *Escherichia coli* S30, erythromycin-inhibited ribosomal translation was reversed upon addition of purified MAB_2355c in a dose-dependent manner, suggesting a protective role towards the ribosome for this *M. abscessus* transporter.[27] Indeed, in the current study, *MAB_2355c* was strongly induced by ribosome-targeting AMK, CLR, and TIG, but not by CFZ and FOX. So far, *MAB_2355c* is the only transporter in *M. abscessus* directly linked to ribosomal protection. Additional research is needed to shed light on functions of efflux pumps beyond antibiotic efflux in *M. abscessus*.

CFZ and FOX exposure resulted only in a modest induction of efflux pump genes. FOX exposure induced specific expression of *MAB_0937c*, encoding a putative member protein of the MmpL family that is highly homologous to mmpL10 in *Mycobacterium tuberculosis*.[15, 32] MmpL10 is thought to be involved in the transport of cell wall components,[32] and may have been induced to restore the damage caused by FOX. CFZ induced expression of *MAB_2632* and *MAB_2633*, encoding the CydC/CydD ABC transporter. In *M. tuberculosis*, this transporter is thought to be essential for the function of the bd-type ubiquinol oxidoreductase.[33] This is in line with the finding that CFZ exposure induces bd-type ubiquinol oxidoreductase, which probably aids in the defense against CFZ-related oxidative stress.[23]

Based on the more extended gene upregulation upon exposure to AMK, CLR, and TIG compared with CFZ and FOX, higher levels of synergy were expected between AMK, CLR, and TIG and the putative efflux inhibitors TZ and VP. Nevertheless, equal levels of synergy with TZ and VP were observed for CFZ and FOX and for the ribosome-targeting antibiotics. Apparently, the degree of efflux pump gene expression did not correlate with the level of synergy between antibiotics and efflux inhibitors. These findings do not elucidate the precise mechanisms underlying the potentiating activity of TZ and VP but do indicate that mechanisms other than efflux inhibition might drive the synergistic interactions observed here. In fact, in the time-kill kinetics assays, TZ demonstrated considerable activity on its own. In the context of *M. tuberculosis*, TZ inhibits growth by interfering with the aerobic respiratory chain.[34] One might hypothesize that the metabolic and respiratory shifts in *M. abscessus* following exposure to commonly prescribed antibiotics[23] are hampered by TZ's effect on the respiratory chain, thus leading to non-efflux based synergistic activity. Regarding VP, Chen et al. demonstrated that VP did not increase intracellular drug concentrations in *M. tuberculosis*, contradicting its efflux inhibitory function.[35] This could be a consequence of redundancy in efflux pumps.[35] On the other hand, it has been suggested that VP inhibits drug efflux in *M. tuberculosis* more indirectly by interfering with the proton motive force, thereby affecting various transport processes in the cell.[16] It could be that such a mechanism, or yet to be identified mechanisms, also underlie the potentiating activity of VP towards antibiotics in *M. abscessus*.

A couple of limitations to this study need to be considered. First, the experiments were conducted with planktonic mycobacteria, whereas *in vivo M. abscessus* also resides intracellularly in macrophages. This is relevant, considering that VP can act on mammalian transporters, as well.[36] Whether the activity of the studied antibiotics and TZ and VP is also present against *M. abscessus* within macrophages is an important topic for further study. Secondly, experiments were only performed with a reference *M. abscessus* subspecies *abscessus* strain. Differential drug activity against the reference strain and clinical isolates of *M. abscessus* should be assessed in future experiments. Also, stability testing of TZ and VP, as well as gene expression following TZ and VP exposure, were not tested. Not having this information is a clear limitation that should be addressed in future work. Lastly, the concentrations of TZ and VP used in the time-kill kinetics assays were extremely high and not clinically feasible, considering the toxicity accompanying these drugs. In a clinical study, steady-state TZ serum concentrations ranged between 0.4 to 8.8 mg/L after a median dose of 150 mg/day,[37] which is barely equal to the concentration of 1/8x the MIC of TZ (8 mg/L). TZ at this concentration showed no (synergistic) activity in the time-kill kinetics assays. The same issue applies to VP, as serum concentrations in humans above 0.9 mg/L are considered toxic.[38] High MICs, together with the unfavorable toxicity profiles of TZ and VP, complicate the potential use of these compounds in clinical *M. abscessus* treatment. Nonetheless, the synergistic activity of TZ and VP with guideline-

recommended antibiotics shows encouraging proof-of-principle results that may inform the development of safer derivatives and targeted drug administration. For example, norverapamil has demonstrated preserved activity but has a more favorable toxicity profile.[19] Also, inhalation-based therapies with TZ and VP are currently being developed and aim to establish high local drug concentrations while reducing systemic exposure and accompanying toxicity.[39, 40]

In conclusion, induction of efflux pump encoding genes is an important response in *M. abscessus* triggered by antibiotic stressors, especially ribosome-targeting antibiotics. Putative efflux inhibitors, such as TZ and VP, show synergy with antibiotics that are currently recommended and may be promising leads for the improvement of *M. abscessus* treatment options.

References

1. Cowman S, van Ingen J, Griffith DE, Loebinger MR. Non-tuberculous mycobacterial pulmonary disease. Eur Respir J 2019;54:190 0250. doi: 10.1183/139930 03. 00250-2019
2. Qvist T, Taylor-Robinson D, Waldmann E, Olesen HV, Hansen CR, Mathiesen IH, et al. Comparing the harmful effects of nontuberculous mycobacteria and Gram negative bacteria on lung function in patients with cystic fibrosis. J Cyst Fibros 2016;15:380–5. doi: 10.1016/j.jcf.2015.09.007
3. Ruis C, Bryant JM, Bell SC, Thomson R, Davidson RM, Hasan NA, et al. Dissemination of *Mycobacterium abscessus* via global transmission networks. Nat Microbiol 2021;6:1279–88. doi: 10.1038/s41564- 021- 00963-3
4. Leard LE, Holm AM, Valapour M, Glanville AR, Attawar S, Aversa M, et al. Consensus document for the selection of lung transplant candidates: An update from the International Society for Heart and Lung Transplantation. J Heart Lung Transplant 2021;40:1349–79. doi: 10.1016/j.healun.2021.07.005
5. Nash KA, Brown-Elliott BA, Wallace RJ Jr. A novel gene, *erm(41)* , confers in-ducible macrolide resistance to clinical isolates of *Mycobacterium abscessus* but is absent from *Mycobacterium chelonae*. Antimicrob Agents Chemother 2009;53:1367–76. doi: 10.1128/AAC.01275-08
6. Wallace RJ Jr, Meier A, Brown BA, Zhang Y, Sander P, Onyi GO, et al. Genetic basis for clarithromycin resistance among isolates of *Mycobacterium chelonae* and *Mycobacterium abscessus*. Antimicrob Agents Chemother 1996;40:1676–81. doi: 10.1128/AAC.40.7.1676
7. Kim SY, Kim DH, Moon SM, Song JY, Huh HJ, Lee NY, et al. Association be-tween 16S rRNA gene mutations and susceptibility to amikacin in *Mycobacterium avium* Complex and *Mycobacterium abscessus* clinical isolates. Sci Rep 2021;11:6108. doi: 10.1038/s41598-021-85721-5
8. Soroka D, Dubée V, Soulier-Escrihuela O, Cuinet G, Hugonnet JE, Gutmann L, et al. Characterization of broad-spectrum *Mycobacterium abscessus* class A β- lactamase. J Antimicrob Chemother 2014;69:691–6. doi: 10.1093/jac/dkt410
9. Rudra P, Hurst-Hess K, Lappierre P, Ghosh P. High levels of intrinsic tetra-cycline resistance in *Mycobacterium abscessus* are conferred by a tetracycline-modifying monooxygenase. Antimicrob Agents Chemother 2018;62 e00119-18. doi: 10.1128/AAC.00119-18
10. Kwak N, Dalcolmo MP, Daley CL, Eather G, Gayoso R, Hasegawa N, et al. *Mycobacterium abscessus* pulmonary disease: individual patient data meta-analysis. Eur Respir J 2019;54:1801991. doi: 10.1183/13993003.01991-2018
11. Vianna JS, Machado D, Ramis IB, Silva FP, Bierhals DV, Abril MA, et al. The contribution of efflux pumps in *Mycobacterium abscessus* Complex resistance to clarithromycin. Antibiotics (Basel) 2019;8:153. doi: 10.3390/antibiotics8030153
12. Guo Q, Chen J, Zhang S, Zou Y, Zhang Y, Huang D, et al. Efflux pumps con-tribute to intrinsic clarithromycin resistance in clinical, *Mycobacterium abscessus* isolates. Infect Drug Resist 2020;13:447–54. doi: 10.2147/IDR.S239850
13. Richard M, Gutiérrez AV, Viljoen A, Rodriguez-Rincon D, Roquet-Baneres F, Blaise M, et al. Mutations in the MAB_2299c *tetR* regulator confer cross-resistance to clofazimine and bedaquiline in *Mycobacterium abscessus*. Antimicrob Agents Chemother 2019;63 e01316-18. doi: 10.1128/AAC.01316-18

14. Li B, Ye M, Guo Q, Zhang Z, Yang S, Ma W, et al. Determination of MIC distribution and mechanisms of decreased susceptibility to bedaquiline among clinical isolates of *Mycobacterium abscessus*. Antimicrob Agents Chemother 2018;62 e0 0175-18. doi: 10.1128/AAC.0 0175-18
15. Gorzynski M, Week T, Jaramillo T, Dzalamidze E, Danelishvili L. *Mycobacterium abscessus* genetic determinants associated with the intrinsic resistance to an-tibiotics. Microorganisms 2021;9:2527. doi: 10.3390/ microorganisms9122527
16. Remm S, Earp JC, Dick T, Dartois V, Seeger MA. Critical discussion on drug efflux in *Mycobacterium tuberculosis*. FEMS Microbiol Rev 2022;46 fuab050. doi: 10.1093/femsre/fuab050
17. National Center for Biotechnology Information. PubChem Compound Summary for CID 5452, Thioridazine. Retrieved from https://pubchem.ncbi.nlm.nih.gov/ compound/Thioridazine.
18. National Center for Biotechnology Information. PubChem Compound Summary for CID 2520, Verapamil. Retrieved from https://pubchem.ncbi.nlm.nih. gov/compound/Verapamil.
19. Adams KN, Szumowski JD, Ramakrishnan L. Verapamil, and its metabolite norverapamil, inhibit macrophage-induced, bacterial efflux pump-mediated tolerance to multiple anti-tubercular drugs. J Infect Dis 2014;210:456–66. doi: 10.1093/infdis/jiu095
20. Pieterman ED, Te Brake LHM, de Knegt GJ, van der Meijden A, Alffenaar JC, Bax HI, et al. Assessment of the additional value of verapamil to a moxifloxacin and linezolid combination regimen in a murine tuberculosis model. Antimicrob Agents Chemother 2018;62 e01354-18. doi: 10.1128/AAC.01354-18
21. Vianna JS, Ramis IB, Bierhals D, von Groll A, Ramos DF, Zanatta N, et al. Tetrahydropyridine derivative as efflux inhibitor in *Mycobacterium abscessus* . J Glob Antimicrob Resist 2019;17:296–9. doi: 10.1016/j.jgar.2018.12.020
22. Bax HI, de Vogel CP, Mouton JW, de Steenwinkel JEM. Omadacycline as a promising new agent for the treatment of infections with *Mycobacterium abscessus*. J Antimicrob Chemother 2019;74:2930–3. doi: 10.1093/jac/ dkz267
23. Schildkraut JA, Coolen JPM, Burbaud S, Sangen JJN, Kwint MP, Floto RA, et al. RNA sequencing elucidates drug-specific mechanisms of antibiotic tolerance and resistance in *Mycobacterium abscessus*. Antimicrob Agents Chemother 2022;66:e0150921. doi: 10.1128/AAC.01509-21
24. Rodrigues L, Wagner D, Viveiros M, Sampaio D, Couto I, Vavra M, et al. Thioridazine and chlorpromazine inhibition of ethidium bromide efflux in *Mycobacterium avium* and *Mycobacterium smegmatis*. J Antimicrob Chemother 2008;61:1076–82. doi: 10.1093/ jac/dkn070
25. Bax HI, Bakker-Woudenberg I, de Vogel CP, van der Meijden A, Verbon A, de Steenwinkel JEM. The role of the time-kill kinetics assay as part of a preclinical modeling framework for assessing the activity of anti-tuberculosis drugs. Tuberculosis (Edinb) 2017;105:80–5. doi: 10.1016/j.tube.2017.04.010
26. Rindi L. Efflux pump inhibitors against nontuberculous mycobacteria. Int J Mol Sci 2020;21:4191. doi: 10.3390/ijms21124191
27. Guo Q, Zhang Y, Fan J, Zhang H, Zhang Z, Li B, et al. MAB_2355c confers macrolide resistance in *Mycobacterium abscessus* by ribosome pro-tection. Antimicrob Agents Chemother 2021;65:e0033021. doi: 10.1128/ AAC. 00330-21
28. Hurst-Hess K, Rudra P, Ghosh P. *Mycobacterium abscessus whiB7* regulates a species-specific repertoire of genes to confer extreme antibiotic resistance. Antimicrob Agents Chemother 2017;61 e01347-17. doi: 10.1128/AAC.01347-17

29. Pryjma M, Burian J, Kuchinski K, Thompson CJ. Antagonism between front-line antibiotics clarithromycin and amikacin in the treatment of *Mycobacterium abscessus* infections is mediated by the *whiB7* gene. Antimicrob Agents Chemother 2017;61 e01353-17. doi: 10.1128/AAC.01353-17

30. Henderson PJF, Maher C, Elbourne LDH, Eijkelkamp BA, Paulsen IT, Hassan KA. Physiological functions of bacterial 'multidrug' efflux pumps. Chem Rev 2021;121:5417–78. doi: 10.1021/acs.chemrev.0c01226

31. Sharkey LK, Edwards TA, O'Neill AJ. ABC-F proteins mediate antibiotic resistance through ribosomal protection. mBio 2016;7:e01975. doi: 10.1128/mBio. 01975-15

32. Melly G, Purdy GE. MmpL proteins in physiology and pathogenesis of *M. tuberculosis*. Microorganisms 2019;7:70. doi: 10.3390/microorganisms7030070

33. Shi L, Sohaskey CD, Kana BD, Dawes S, North RJ, Mizrahi V, et al. Changes in energy metabolism of *Mycobacterium tuberculosis* in mouse lung and under *in vitro* conditions affecting aerobic respiration. Proc Natl Acad Sci U S A 2005;102:15629–34. doi: 10.1073/pnas.0507850102

34. Sohaskey CD. Nitrate enhances the survival of *Mycobacterium tuberculosis* during inhibition of respiration. J Bacteriol 2008;190:2981–6. doi: 10.1128/JB. 01857-07

35. Chen C, Gardete S, Jansen RS, Shetty A, Dick T, Rhee KY, et al. Verapamil targets membrane energetics in *Mycobacterium tuberculosis*. Antimicrob Agents Chemother 2018;62 e02107-17. doi: 10.1128/AAC.02107-17

36. Xu J, Tasneen R, Peloquin CA, Almeida DV, Li SY, Barnes-Boyle K, et al. Verapamil increases the bioavailability and efficacy of bedaquiline but not clofazimine in a murine model of tuberculosis. Antimicrob Agents Chemother 2018;62 e01692-17. doi: 10.1128/AAC.01692-17

37. Thanacoody HK. Thioridazine: resurrection as an antimicrobial agent? Br J Clin Pharmacol 2007;64:566–74. doi: 10.1111/j.1365-2125.2007.03021.x

38. Mandigers L, Bollen PD, Bijlstra PJ, Brands E. Severe verapamil intoxication despite correct use of low-dose verapamil. Drug Metab Pers Ther 2016;31:55–8. doi: 10.1515/dmpt-2015-0041

39. Bozorgmehr R, Edalatifard M, Safavi E, Rahimi B, Ghorbani F, Abtahi H, et al. Therapeutic effects of nebulized verapamil on chronic obstructive pulmonary disease: a randomized and double-blind clinical trial. Clin Respir J 2020;14:370–81. doi: 10.1111/crj.13142

40. Parumasivam T, Chan JG, Pang A, Quan DH, Triccas JA, Britton WJ, et al. *In vitro* evaluation of novel inhalable dry powders consisting of thioridazine and rifapentine for rapid tuberculosis treatment. Eur J Pharm Biopharm 2016;107:205–14. doi: 10.1016/j.ejpb.2016.07.014

CHAPTER 3.2

Omadacycline enhances the *in vitro* activity of clofazimine against *Mycobacterium abscessus*

Saskia E. Mudde, Henriëtte M. Meliefste, Nicole C. Ammerman, Jurriaan E.M. de Steenwinkel, Hannelore I. Bax

Int J Tuberc Lung Dis. 2024 Nov; 28(11):554-556

Abstract

Objectives

New treatment options for the opportunistic pathogen *Mycobacterium abscessus* are urgently needed, as current treatment success rates are shockingly low. In this *in vitro* study, the ability of omadacycline to potentiate activity of guideline-recommended antibiotics in the treatment of *M. abscessus* infections was assessed.

Methods

Concentration- and time-dependent antimycobacterial activity of omadacycline combined with cefoxitin, amikacin, imipenem, and clofazimine was assessed in time-kill kinetics assays.

Results

Omadacycline plus cefoxitin, amikacin, or imipenem did not demonstrate synergistic activity, with the activity of the drug combination being similar to the most active individual drug. Activity of clofazimine, however, was enhanced by omadacycline, resulting in strong killing capacity.

Conclusions

The combination of omadacycline and clofazimine showed strong *in vitro* killing activity against *M. abscessus*. This combination is particularly interesting as both compounds can be administered orally. Its potential to improve current *M. abscessus* treatment options warrants further investigation.

Introducing new drugs such as omadacycline for the treatment of *Mycobacterium abscessus* infections is important, given the disappointingly low success rates of current treatment.[1] To effectively inform clinical study design, preclinical understanding of drug activity and identification of promising drug combinations are needed. Activity of omadacycline-containing drug combinations was previously assessed using checkerboard assays[2, 3] and an *M. abscessus* lung infection mouse model.[4, 5] However, since minimum inhibitory concentration (MIC)-based assays insufficiently correlate with clinical outcomes for nontuberculous mycobacteria, and the translational value of *M. abscessus* mouse models is yet unclear, multiple preclinical approaches should be integrated to identify which drugs omadacycline should be combined with to achieve maximum potential. In this study, time-kill kinetics assays (TKK) were used to assess the activity of omadacycline combined with guideline-recommended antibiotics cefoxitin, amikacin, imipenem, and clofazimine.

Experiments were performed with *M. abscessus* subsp. *abscessus* ATCC 19977. MICs of omadacycline, cefoxitin, amikacin, imipenem, and clofazimine were 2, 32, 16, 16, and 0.5 mg/L, respectively, as determined by broth microdilution in cation-adjusted Mueller Hinton broth (CAMHB) according to the CLSI guidelines (M24, 3rd edition).

Stability of omadacycline and imipenem in CAMHB was assessed using the standard agar diffusion assay.[6, 7] Omadacycline showed a daily decline of 20%, aligning with previous findings.[6] For imipenem, a daily decline of 40% was measured. Cefoxitin previously showed a daily decline of 33%, while amikacin and clofazimine were stable for at least 7 days.[7]

TKKs were used to assess time- and concentration-dependent activity of omadacycline-containing drug combinations. *M. abscessus* cultures in CAMHB (2.5 mL) were exposed to omadacycline, with or without cefoxitin, amikacin, imipenem, or clofazimine at 1x or 4x MIC for 7 days at 30°C. Drug instability was compensated by daily addition of supplemental drug (50 µl total volume). Cultures were sampled on days 1, 3, and 7. Ten-fold dilutions were plated onto Mueller Hinton agar with 10% oleic acid, albumin, dextrose, and catalase (OADC). Colonies were counted after 5-7 days. Synergy was assessed according to previously detailed criteria.[7] Figure 1 shows TKK results of omadacycline at 1x or 4x MIC combined with cefoxitin, amikacin, imipenem, or clofazimine at 1x MIC. Overall, the activity of omadacycline combined with cefoxitin, amikacin, or imipenem was similar to single-drug activity. Clofazimine activity, however, was enhanced by omadacycline in a concentration-dependent manner. Simultaneous exposure to both drugs at 1x MIC consistently showed higher activity on day 7 compared to single drug activity, meeting the synergy criteria in 1 out of 4 replicates. For omadacycline 4x MIC, drug activity was further enhanced, with 3 out of 4 replicates clearly meeting the synergy definition and eliminating all culturable *M. abscessus*. Results of cefoxitin, amikacin, imipenem, and clofazimine at 4x MIC were comparable to 1x MIC as shown in figure 2.

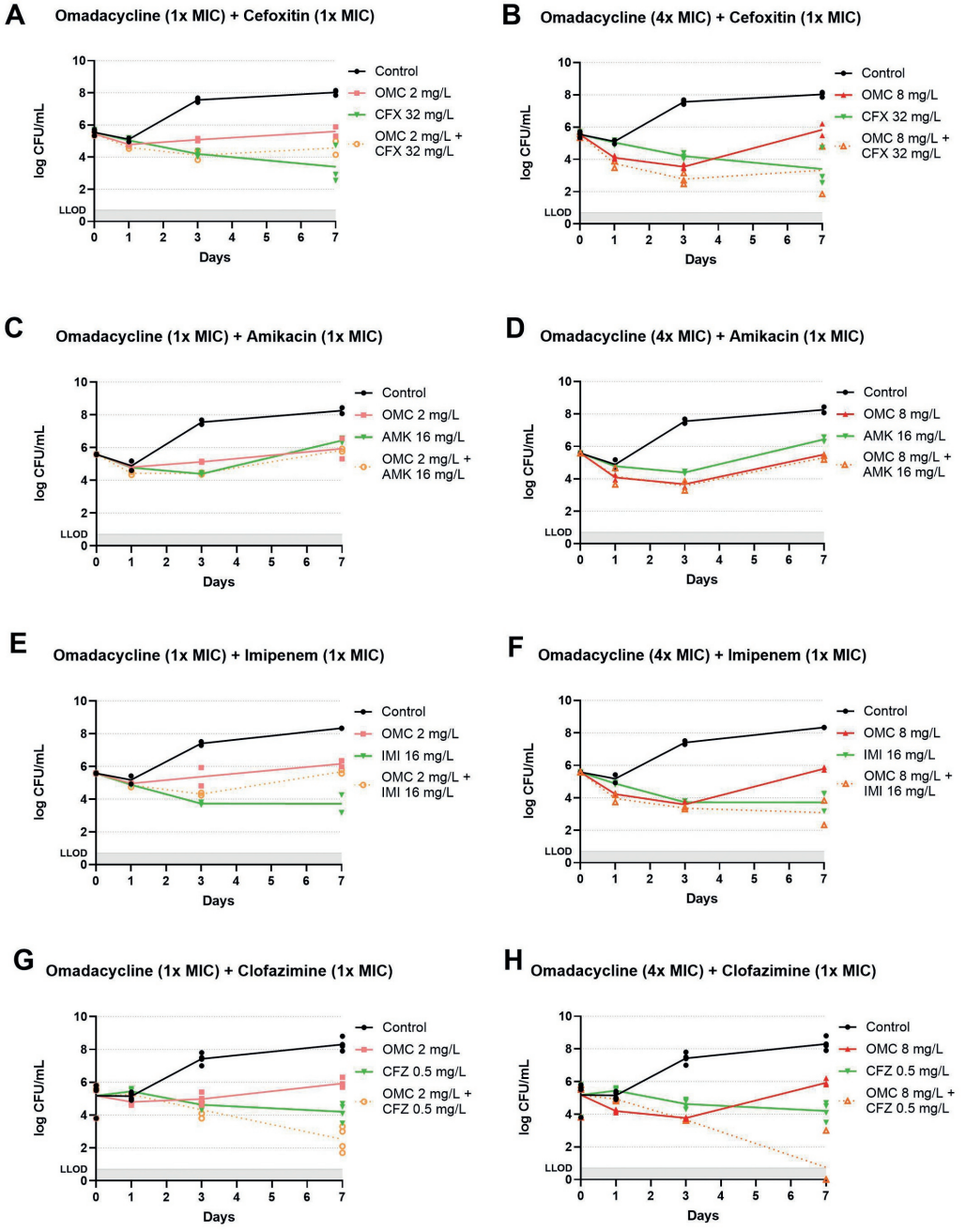

Figure 1. Time-kill kinetics assays showing the speed and magnitude of bactericidal activity of omadacycline at either 1x MIC (left), or 4x MIC (right) combined with cefoxitin (CFX, A-B), amikacin (AMK, C-D), imipenem (IMI, E-F), or clofazimine (CFZ, G-H) at 1x MIC against *M. abscessus* subspecies *abscessus* ATCC 19977. The mycobacterial load on day 0, 1, 3, and 7 from different replicates are plotted individually with the lines representing the mean Log_{10} CFU/mL.

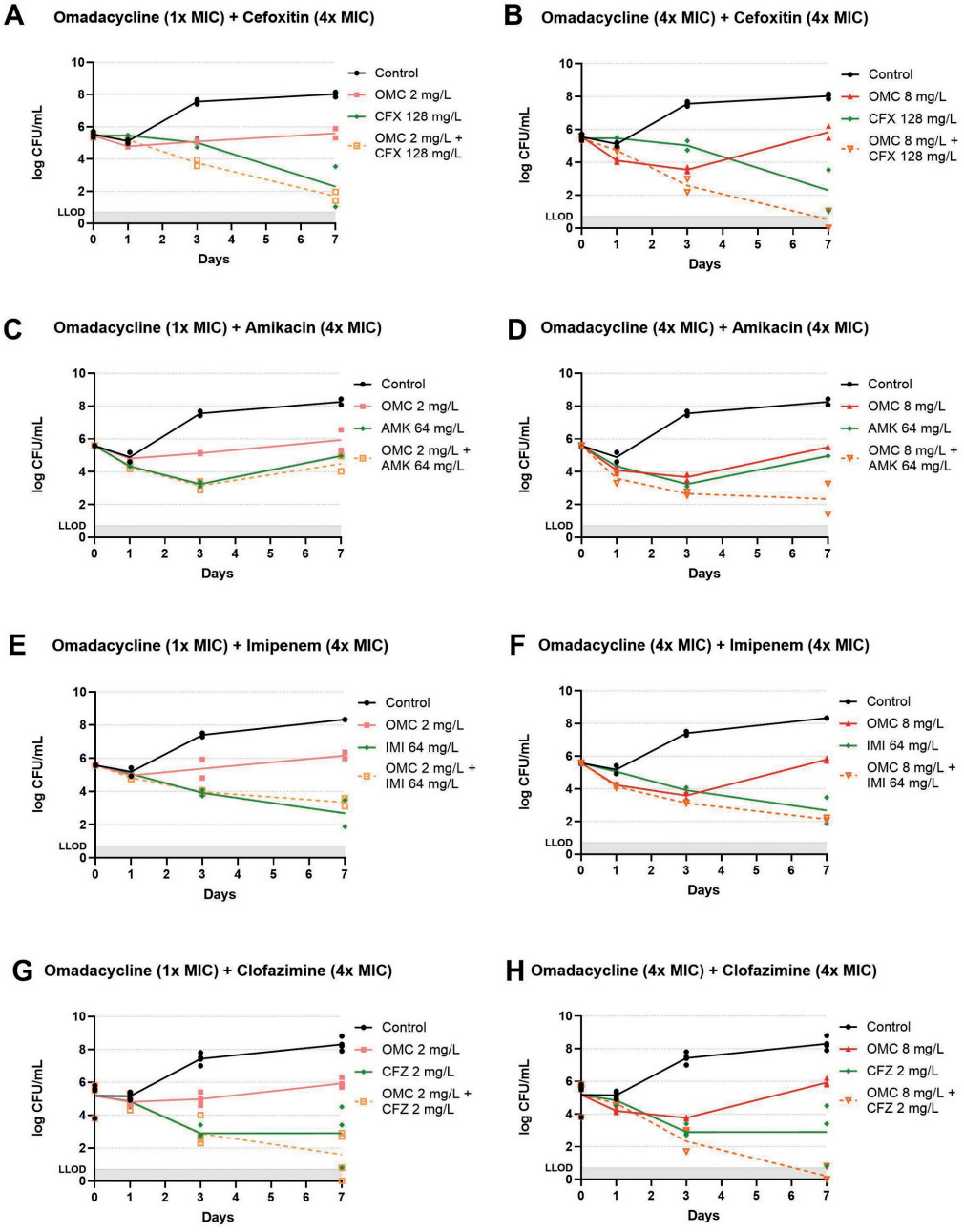

Figure 2. Time-kill kinetics assays showing the speed and magnitude of bactericidal activity of omadacycline at either 1x MIC (left), or 4x MIC (right) combined with cefoxitin (CFX, A-B), amikacin (AMK, C-D), imipenem (IMI, E-F), or clofazimine (CFZ, G-H) at 4x MIC against *M. abscessus* subspecies *abscessus* ATCC 19977. The mycobacterial load on day 0, 1, 3, and 7 from different replicates are plotted individually with the lines representing the mean Log_{10} CFU/mL.

This study extends prior *in vitro* work on omadacycline-containing drug combinations.[2, 3] Using checkerboard assays, Fujiwara et al. observed synergistic activity between omadacycline and clofazimine in 25% of clinical isolates tested.[2] Nicklas et al. reported checkerboard-based synergy between omadacycline and clofazimine for 1 out of 11 *M. abscessus* isolates.[3] These findings do not directly align with the synergy between omadacycline and clofazimine found here. However, compared to checkerboard assays, TKKs are of additive value as synergistic activity can be assessed over time, allowing to detect synergy that could be missed in checkerboard assays.

Two recent studies assessed the early bactericidal activity of omadacycline within dual or triple antibiotic regimens using an *M. abscessus* lung infection mouse model.[4, 5] In the dual antibiotic regimen study, omadacycline plus linezolid, cefoxitin, imipenem, biapenem, or rifabutin exhibited varying degrees of faster or enhanced bactericidal activity compared to individual drug activity.[4] These effects did not seem to be sustainable as they were observed in the first two weeks of treatment only, prompting some consideration on their clinical significance.[4] The triple antibiotic regimen study evaluated early bactericidal activity of omadacycline plus imipenem and amikacin, imipenem and linezolid, and clofazimine and linezolid.[5] Although addition of clofazimine to omadacycline plus linezolid did not enhance bactericidal activity, the three-drug combination produced a slight, gradual decrease in lung colony forming units (CFU) counts.[5] Overall, the enhanced and strong activity of the omadacycline-clofazimine combination as seen in this *in vitro* study was not observed in the mouse studies. Yet, several factors should be considered when comparing preclinical *in vitro* and *in vivo* findings. First, synergistic activity might be concentration-dependent as shown in the present study. In the mouse studies, omadacycline was dosed subcutaneously at 15 mg/kg, which previously resulted in peak plasma concentrations about four times lower than the omadacycline concentration that demonstrated synergy with clofazimine here.[3] Information on plasma concentrations of the companion drugs was not reported, and, importantly, it is unclear how co-administration of dexamethasone may have altered drug concentrations, complicating the comparison of *in vitro* concentrations to drug exposures in the mouse studies.[4, 5] Furthermore, establishing a reproducible mouse model of *M. abscessus* infection is challenging for multiple reasons, including the murine immune system clearing the infection, various *M. abscessus* genotypes and morphotypes, infection routes, and the choice between an acute or more chronic infection, all with immense potential impact on the results.[5, 8] Lastly, the translational value of early bactericidal activity is debatable, at least in the context of *M. tuberculosis* mouse models.[9] The findings of this study do not align with the mouse model data, but since the translational value of preclinical *in vivo M. abscessus* infection models is yet to be established, the *in vitro* synergy between omadacycline and clofazimine found here is not to be disregarded. Future clinical data will shed light on how these preclinical data translate into the clinic.

The omadacycline-clofazimine combination would be of particular interest to improve current clinical treatment, especially in the continuation phase, since for both drugs oral formulations are available. Human peak plasma concentrations after oral omadacycline dosing approximate the MIC for *M. abscessus*.[10] Although plasma concentrations equaling 4x MIC might not be achievable, omadacycline levels in alveolar cells following intravenous administration exceeded plasma concentrations, being consistently above 10 mg/L,[11] indicating that concentrations showing synergy here might be attainable at the site of infection. Also, 1x MIC of clofazimine is within the range reported for plasma clofazimine concentrations after oral dosing.[12]

In conclusion, although the results are preliminary due to the exploratory nature of the assay, the omadacycline-clofazimine combination showed promise and warrants further investigation. Since there is currently no universally accepted 'gold standard pipeline' for preclinical drug activity testing against nontuberculous mycobacteria, we advocate the integration of results obtained by various preclinical models, both *in vitro* and *in vivo*, to inform future clinical studies effectively, for example by predictive modelling.

Acknowledgements

Omadacycline was provided by Paratek Pharmaceuticals, Inc., in powder form. We would like to thank Dr. van Ingen (Radboudumc Nijmegen) for providing the *M. abscessus* subsp. *abscessus* ATCC 19977 strain (CIP104536, Collection of Institute Pasteur, Paris, France).

References

1. Daley CL, Iaccarino JM, Lange C, Cambau E, Wallace RJ, Jr., Andrejak C, et al. Treatment of Nontuberculous Mycobacterial Pulmonary Disease: An Official ATS/ERS/ESCMID/IDSA Clinical Practice Guideline. Clin Infect Dis. 2020;71(4):e1-e36.
2. Fujiwara K, Aono A, Asami T, Morimoto K, Kamada K, Morishige Y, et al. *In Vitro* Synergistic Effects of Omadacycline with Other Antimicrobial Agents against *Mycobacterium abscessus*. Antimicrob Agents Chemother. 2023;67(6):e0157922.
3. Nicklas DA, Maggioncalda EC, Story-Roller E, Eichelman B, Tabor C, Serio AW, et al. Potency of Omadacycline against *Mycobacteroides abscessus* Clinical Isolates *In Vitro* and in a Mouse Model of Pulmonary Infection. Antimicrob Agents Chemother. 2022;66(1):e0170421.
4. Rimal B, Nicklas DA, Panthi CM, Lippincott CK, Belz DC, Ignatius EH, et al. Efficacy of Omadacycline-Containing Regimen in a Mouse Model of Pulmonary *Mycobacteroides abscessus* Disease. mSphere. 2023;8(2):e0066522.
5. Rimal B, Panthi CM, Xie Y, Belz DC, Ignatius EH, Lippincott CK, et al. Efficacies of three drug regimens containing omadacycline to treat *Mycobacteroides abscessus* disease. Tuberculosis (Edinb). 2024;146:102482.
6. Bax HI, de Vogel CP, Mouton JW, de Steenwinkel JEM. Omadacycline as a promising new agent for the treatment of infections with *Mycobacterium abscessus*. J Antimicrob Chemother. 2019;74(10):2930-3.
7. Mudde SE, Schildkraut JA, Ammerman NC, de Vogel CP, de Steenwinkel JEM, van Ingen J, et al. Unraveling antibiotic resistance mechanisms in *Mycobacterium abscessus*: the potential role of efflux pumps. J Glob Antimicrob Resist. 2022;31:345-52.
8. Nicola F, Cirillo DM, Lorè NI. Preclinical murine models to study lung infection with *Mycobacterium abscessus* complex. Tuberculosis (Edinb). 2023;138:102301.
9. Andries K, Gevers T, Lounis N. Bactericidal potencies of new regimens are not predictive of their sterilizing potencies in a murine model of tuberculosis. Antimicrob Agents Chemother. 2010;54(11):4540-4.
10. Bundrant LA, Tzanis E, Garrity-Ryan L, Bai S, Chitra S, Manley A, et al. Safety and Pharmacokinetics of the Aminomethylcycline Antibiotic Omadacycline Administered to Healthy Subjects in Oral Multiple-Dose Regimens. Antimicrob Agents Chemother. 2018;62(2).
11. Gotfried MH, Horn K, Garrity-Ryan L, Villano S, Tzanis E, Chitra S, et al. Comparison of Omadacycline and Tigecycline Pharmacokinetics in the Plasma, Epithelial Lining Fluid, and Alveolar Cells of Healthy Adult Subjects. Antimicrob Agents Chemother. 2017;61(9).
12. Abdelwahab MT, Wasserman S, Brust JCM, Gandhi NR, Meintjes G, Everitt D, et al. Clofazimine pharmacokinetics in patients with TB: dosing implications. J Antimicrob Chemother. 2020;75(11):3269-77.

CHAPTER 4

Improving the translational value of preclinical mycobacterial models

CHAPTER 4.1

Relative contributions of the novel diarylquinoline TBAJ-876 and its active metabolite to the bactericidal activity in a murine model of tuberculosis

Saskia E. Mudde, Nicole C. Ammerman,
Marian T. ten Kate, Nader Fotouhi, Manisha U. Lotlikar,
Hannelore I. Bax, Jurriaan E.M. de Steenwinkel

J Infect Dis. 2024 Dec 16;230(6):e1366-e1374.

Abstract

Background

TBAJ-876 is a next-generation diarylquinoline. *In vivo*, diarylquinoline metabolites are formed with activity against *Mycobacterium tuberculosis*. Species-specific differences in parent drug-to-metabolite ratios might impact the translational value of animal model-based predictions. This study investigates the contribution of TBAJ-876 and its major active metabolite, TBAJ-876-M3 (M3), to the total bactericidal activity in a mouse tuberculosis model.

Methods

In vitro activity of TBAJ-876 and M3 was investigated and compared to bedaquiline. Subsequently, a dose-response study was conducted in *M. tuberculosis*-infected BALB/c mice treated with TBAJ-876 (1.6/6.3/25 mg/kg) or M3 (3.1/12.5/50 mg/kg). Colony-forming units in the lungs and TBAJ-876 and M3 plasma concentrations were determined. M3's contribution to TBAJ876's bactericidal activity was estimated based on M3 exposure following TBAJ-876 treatment and corresponding M3 activity observed in M3-treated animals.

Results

TBAJ-876 and M3 demonstrated profound bactericidal activity. Lungs of mice treated for 4 weeks with 50 mg/kg M3 were culture negative. Following TBAJ-876 treatment, M3 exposures were 2.2 to 3.6-fold higher than for TBAJ-876. TBAJ-876 activity was substantially attributable to M3, given its high exposure and potent activity.

Conclusion

These findings emphasize the need to consider metabolites and their potentially distinct exposure and activity profiles compared to parent drugs to enhance the translational value of mouse model-driven predictions.

Introduction

Tuberculosis remains a major global health challenge,[1] and the ongoing need to improve tuberculosis treatment outcomes has led to an expansion of the tuberculosis drug development pipeline. This resulted in the introduction of bedaquiline, a diarylquinoline that acts by inhibiting ATP synthase, which transformed the approach to treating drug-resistant tuberculosis. Multiple clinical trials demonstrated treatment success rates of approximately 90% when bedaquiline-based regimens were administered to drug-resistant tuberculosis patients.[2-5] This led to the World Health Organization endorsement of a 6-month treatment regimen including bedaquiline, pretomanid, and linezolid (BPaL), with or without moxifloxacin, for the treatment of drug-resistant tuberculosis.[6]

While proven to be an effective drug, bedaquiline comes with limitations. Its affinity for cardiac potassium hERG channels can lead to QTc interval prolongation, with the risk of cardiac arrhythmias.[7-10] Bedaquiline is highly lipophilic, contributing to drug accumulation and a long half-life, which may lead to prolonged drug exposure after treatment cessation.[8, 9] There are concerns that lingering low plasma concentrations might lead to resistance development, putting the usability of bedaquiline-containing regimens at risk.[11–13] To overcome these limitations, next-generation diarylquinolines are being developed, including TBAJ-876. TBAJ-876 has become a promising drug candidate, as it has demonstrated more potent *in vitro* activity against *Mycobacterium tuberculosis*, as well as lower lipophilicity, a shorter half-life in mice, and a potential lower risk for cardiac events due to reduced hERG channel affinity compared to bedaquiline.[9, 14] Importantly, TBAJ-876 retains activity and is more potent than bedaquiline against *M. tuberculosis* with *Rv0678* mutations, the primary cause of bedaquiline resistance in clinical isolates.[15]

Hence, interest has been growing in the preclinical activity of TBAJ-876 within various combination regimens,[15, 16] and the compound recently entered the clinical trial phase. Currently, the results of 2 phase 1 clinical trials are awaited (NCT04493671 and NCT05526911), and a phase 2 trial is planned in which TBAJ-876 will replace bedaquiline within the BPaL regimen in the treatment of drug-sensitive tuberculosis (NCT06058299).

Preclinical studies play a crucial role in evaluating the activity of new drug candidates, providing valuable input for subsequent clinical trials design. For example, pharmacodynamic and pharmacokinetic mouse studies are used to estimate a drug's antituberculosis potency and contribute to adequate dose selection to achieve desirable effects in humans.[17] In this regard, diarylquinolines are of special interest because, *in vivo*, metabolites are formed that are also active against *M. tuberculosis*.[9, 18] Rouan et al demonstrated that for bedaquiline both the parent drug and its main M2

metabolite contributed significantly to the total bedaquiline activity observed in a tuberculosis mouse model.[18] However, in humans, it is anticipated that the metabolite's contribution is considerably less than in mice, due to lower exposures to the metabolite and the metabolite being less active against *M. tuberculosis* than the parent drug.[18, 19] Like bedaquiline, TBAJ-876 is metabolized *in vivo*, with TBAJ-876-M3 (M3) as the main metabolite, formed by *N*-demethylation.[9, 16] Taking into account metabolite activity and differences in parent-to-metabolite exposure ratios between mice and humans could improve animal model-based predictions on drug activity and drug exposure in humans.

The objective of this study was to determine the contribution of M3 to the overall bactericidal activity of TBAJ-876. First, the differential activity of TBAJ-876 and the M3 metabolite against actively replicating and nonreplicating *M. tuberculosis* was assessed *in vitro*. Subsequently, the *in vivo* bactericidal activity and pharmacokinetic properties of TBAJ-876 and M3 were determined in a mouse tuberculosis model. By integrating these findings, the contribution of the M3 metabolite to the overall bactericidal activity of TBAJ-876 in a mouse tuberculosis model was estimated.

Methods

Bacterial strains

In vitro experiments were performed with the *M. tuberculosis* H37Rv reference strain and/or the clinical *M. tuberculosis* Beijing VN 2002-1585 strain.[20] In the *in vivo* studies, *M. tuberculosis* Beijing VN 2002-1585 was used. Strains were grown in Middlebrook 7H9 broth (Becton, Dickinson, and Company [BD]) with 10% oleic acid, albumin, dextrose, catalase (OADC; BD) under shaking conditions at 37°C. Bacterial stock suspensions were stored at −80°C.

In vitro activity testing

Bedaquiline, TBAJ-876, and M3 were supplied by the TB Alliance. *In vitro* experiments were performed in duplicate. Bedaquiline was used as comparator. TBAJ-876 and M3 stock solutions were prepared in dimethyl sulfoxide. Bedaquiline was dissolved in acidified 20% hydroxypropyl-β-cyclodextrin (Kleptose; Roquette), followed by pH adjustment to 2.5 using 1 N sodium hydroxide. Minimum inhibitory concentrations (MICs) of TBAJ-876 (tested range, 0.063–0.001 mg/L), M3 (tested range, 0.002–0.125 mg/L), and bedaquiline (tested range, 0.008–0.5 mg/L) against *M. tuberculosis* H37Rv and Beijing VN 2002-1585 were determined by agar proportion based on the Clinical and Laboratory Standards Institute guidelines (M24, third edition).[21]

A checkerboard assay was conducted with *M. tuberculosis* Beijing VN 2002-1585 to assess potential interaction between TBAJ-876 and M3. Two-fold increasing concentrations of TBAJ-876 (0.0001–0.016 mg/L) and M3 (0.001–0.064 mg/L) in 7H9 with 10% OADC in the columns and rows of a 96-well plate, respectively, were inoculated with mycobacterial suspensions (5×10^5 colony forming units [CFU]/mL). The MICs of TBAJ-876 and M3 alone and in combination were visually read after 10 days of incubation at 35°C with 5% CO_2. The fractional inhibitory concentration (FIC) was calculated as the MIC of TBAJ-876 and M3 in combination divided by the MIC of TBAJ-876 and M3 alone. The FIC index was calculated as the FIC of TBAJ-876 plus the FIC of M3. An FIC index of ≤0.5 indicates synergy, >4.0 antagonism, and 0.5–4.0 no interaction.[22]

Time- and concentration-dependent activity of TBAJ-876 and M3 against actively replicating or nonreplicating *M. tuberculosis* H37Rv was determined as previously described.[23] Mycobacterial cultures were exposed to 4-fold increasing concentrations of TBAJ-876 (0.00025–0.063 mg/L), M3 (0.001– 0.25 mg/L), and bedaquiline (0.004–1 mg/L). On days 1, 2, 3, and 6 culture samples were plated onto 7H10 agar plates to determine CFU/mL. A similar set-up was used to determine TBAJ-876 and M3 activity against nonreplicating mycobacteria. A nutrient starvation model was used to induce a nonreplicating state. Log-phase cultures were centrifuged for 20 minutes at 3000 x *g* and mycobacterial pellets were suspended in phosphate-buffered saline (PBS) with 0.05% tyloxapol. After a 6-week adaptation period at 37°C under shaking conditions, TBAJ-876 and M3 activity were tested as described above. The duplicate experiment was extended to 21 days.

Ethical approval animal studies

The studies involving animals (mice) were approved by the Erasmus MC Animal Welfare Body. All study protocols adhered to the rules specified in the Dutch Animal Experimentation Act and were in concordance with the European Union animal directive 2010/63/EU (license No. AVD1010020173687).

Animals, infection, and treatment

Specified pathogen-free female BALB/c mice, aged 11–12 weeks at time of infection were obtained from Charles River. This study was performed with female mice only, as they can be housed together, whereas this is not preferable for male mice. Since mice are social animals, individual housing would lead to increased stress levels. Considering the length of these experiments, the additional stress of individual housing is deemed disproportionate to the potential added scientific value. Furthermore, although sex could potentially influence drug exposure after treatment, this study focuses on the relation between drug exposure and drug activity, which is generally not influenced by sex.

The mice were divided into 2 treatment groups: 48 animals per group treated with either TBAJ-876 or M3. Infection with *M. tuberculosis* Beijing VN 2002-1585 was as previously described.[24] Under general anesthesia, 1.06×10^5 (range, $1.04–1.08 \times 10^5$) CFUs were instilled intratracheally. The animals' welfare was scored daily and the mice were euthanized in cases where humane end points (decreased response to stimuli, hunched posture, unkempt and dirty coat, respiratory distress) were reached.

TBAJ-876 and M3 were formulated weekly in 20% (wt/vol) hydroxypropyl-β-cyclodextrin (Kleptose; Roquette) acidified with 1.5% 1 N hydrogen chloride. After shaking overnight, the pH was raised to 2.0 by 1N sodium hydroxide. Formulations were stored at 6°C. The desired dose in mg/kg was based on an average mouse body weight of 22 g.

Treatment was started 2 weeks after infection. In the TBAJ-876 group, animals were treated with 25, 6.3, or 1.6 mg/kg. In the M3 group, animals were treated with 50, 12.5, or 3.1 mg/kg. Higher doses were chosen for M3 considering the virulent character of the Beijing *M. tuberculosis* strain that was used for infection and the MIC of M3 being higher than that of TBAJ-876. TBAJ-876 and M3 were administered once daily via oral gavage (volume, 0.2 mL) for 5 days per week. Animal studies were performed in 2 separate experiments: one focusing on bactericidal activity and pharmacokinetics of TBAJ-876, the other on M3. Untreated animals were not included in this study for ethical reasons considering the virulent character of the *M. tuberculosis* strain, resulting in death within 2–3 weeks after infection without adequate treatment.[25]

Mycobacterial load assessment

Three animals were euthanized just before treatment initiation to determine the *M. tuberculosis* CFU/lung at baseline. Lungs were aseptically removed, homogenized in 2 mL PBS in M-tubes using the GentleMACS Octo Dissociator (Miltenyi Biotec), 10-fold serially diluted in PBS, and plated onto 7H10 agar. After 1, 2, or 3 weeks of treatment, 3 animals per treatment dose were euthanized to determine the CFU/lung as described above. To prevent drug carry-over, treatment was stopped 72 hours before euthanasia and lung homogenates were plated onto 7H10 agar containing activated charcoal (0.4%) and 10% OADC. Per 10-fold dilution, 200 µL of the solution was plated, giving a lower limit of detection of 11.5 CFU in the lungs, based on a total lung homogenate volume of 2.3 mL. The bactericidal activity was defined as the decrease in the CFU/lung compared to start of treatment.

Pharmacokinetic analyses

TBAJ-876 and M3 plasma concentrations were determined after 4 weeks of treatment, at steady-state. Blood was collected by orbital sinus bleeding in ethylenediaminetetraacetic acid-containing microcentrifuge tubes, directly followed by euthanasia, at 1.5, 6, 24,

and 96 hours (n=2 mice per time point) after the last dose administration. Tubes were centrifuged (10.000 x *g*, 5 minutes) to obtain plasma. Acetonitrile was added in a plasma to acetonitrile ratio of 1:3, centrifuged (10.000*g*, 5 minutes), and clear supernatant was collected in cryotubes and frozen at −80°C. Per sample, 50 µL was plated onto 7H10 agar to confirm decontamination. Plasma samples were shipped on dry ice to Alliance Pharma (now Resolian, Malvern, Pennsylvania, USA) for analysis via liquid chromatography-tandem mass spectrometry.

Neat stock solutions for TBAJ-876 and M3 were prepared in DMSO at 1 mg/mL. A standard curve ranging from 1 ng/mL to 1.000 ng/mL was prepared in mouse plasma (BioIVT). For quality control, 3 concentrations were tested: 3, 50, and 800 ng/mL. The calculated concentrations were deemed acceptable if the accuracy of the quality control samples was ±20% of the nominal concentrations. The lower limit of quantification in plasma was 4 ng/mL. The blank matrix, standards, and quality control samples were prepared in a 1:3 ACN ratio to parallel the study samples. For these samples and the study samples, 10 µl was transferred to clean tubes on wet ice, followed by addition of 50 µl acetonitrile (ACN) per tube. As internal standard, 100 µl of 100 ng/mL of TBAJ-876-d6 with 0.1% formic acid in ACN was added to all tubes. The samples were thoroughly vortexed, followed by centrifugation at 20.000*g* for 3 minutes at room temperature. For each sample, 50 µl of the supernatant was transferred to a clean Axygen 96-well collection plate containing 150 µl of 0.1% formic acid in ACN:water (20:80). The plate was vortexed and centrifuged at 1.670 x *g* for 5 minutes at room temperature. The mixtures were either stored at 2-8°C or directly analysed by HPLC set at 4°C. For the plasma concentration analysis an Agilent 1290 Infinity II high-performance liquid chromatography system with Acquity BEH C18 column at room temperature (2.1 x 50 mm, 1.7 µm) and an Agilent 6495C MS/MS system were used. Liquid chromatography was performed with ammonium acetate 10 mM and 0.1% formic acid in water for mobile phase A, and 0.1% formic acid in ACN for phase B. The injection volume was 5 µl with a flow of 0.60 mL/min. Following electrospray ionization, analytes were quantified by multiple-reaction monitoring (MRM), using the following MRM transitions (m/z): TBAJ-876 (657.1/239.1); TBAJ-876-M3 (643.2/568.2); TBAJ-876-d6 (663.0/245.1). Data were processed using MassHunter Data Acquisition software, version 10.1.

Data analysis

CFU counts were Log_{10} transformed. The area under the plasma concentration-time curve ($AUC_{0\text{-}96}$) was calculated by using the trapezoid rule. A nonlinear regression dose-response inhibition model was used to investigate the relationship between CFU/lung and M3 exposure following 4 weeks of treatment with TBAJ-876 or M3. Analyses were performed using Graphpad Prism 9.5.0 software (GraphPad Software).

Results

In vitro studies: MIC, checkerboard, and time-kill kinetics assays

The aim of the *in vitro* assays was to determine the differential activity of TBAJ-876 and M3 against *M. tuberculosis*, with bedaquiline as comparator, including different bacterial metabolic states because mycobacteria can alter their metabolic activity upon external stresses encountered *in vivo*. MICs of TBAJ-876, M3, and bedaquiline against *M. tuberculosis* H37Rv and Beijing VN 2002-1585 are shown in Table 1. For all compounds, MICs for Beijing VN 2002-1585 were slightly lower than for H37Rv. MICs were 4-fold lower for TBAJ-876 than M3. The MIC of TBAJ-876 was 8 to 32-fold lower than that of bedaquiline. The checkerboard assay demonstrated a FIC index range of 0.51–2.25, indicating a lack of interaction between TBAJ-876 and M3 against Beijing VN2002-1585. Against actively replicating *M. tuberculosis*, time- and concentration-dependent activity of TBAJ-876 and M3 was similar, whereas bedaquiline required higher concentrations to achieve equivalent activity (Figure 1). Substantially reduced and delayed killing activity was observed against nonreplicating *M. tuberculosis* for TBAJ-876, M3, and bedaquiline (Figure 2). Only the highest concentration (16x MIC) of TBAJ-876 and M3 exhibited activity, with 3 weeks of exposure leading to a decrease of approximately 1.6 Log_{10} CFU/mL compared to the no drug control.

Table 1. Minimum inhibitory concentrations of TBAJ-876, M3, and bedaquiline against *M. tuberculosis* H37Rv and *M. tuberculosis* Beijing VN2002-1585

Strain	Minimum inhibitory concentration (mg/L)		
	TBAJ-876	M3	Bedaquiline
M. tuberculosis H37Rv	0.008-0.016	0.031-0.063	0.125
M. tuberculosis Beijing VN2002-1585	0.004	0.016	0.063-0.125

In vivo bactericidal activity and pharmacokinetics

TBAJ-876 was well tolerated by the mice at the tested doses. However, the animals treated with 50 mg/kg M3 continued to lose weight throughout the experiment while the tuberculosis infection was adequately controlled, indicating possible adverse effects of the metabolite administration. Both TBAJ-876 and M3 were bactericidal in a dose- and time-dependent manner (Figure 3). After 4 weeks of treatment with TBAJ-876, the median CFU count in the lungs declined from 7.7 Log_{10} CFU at treatment initiation to 4.3, 1.7 (1/5 animal was culture negative), and 1.1 Log_{10} (2/5 culture negative) in animals treated with 1.6, 6.3, or 25 mg/kg, respectively. The median CFU count in the lungs of animals treated for 4 weeks with M3 declined from 7.9 Log_{10} CFU to 3.7 (0/5 culture negative), 1.8 (1/5 culture-negative), and 0 Log_{10} CFU (4/4 culture negative) when dosed at 3.1, 12.5, or 50 mg/kg, respectively.

Table 2. *M. tuberculosis* CFU in the lungs in relation to compound exposure

Dose, mg/kg	Median Log_{10} CFU/lung at start of treatment	Median Log_{10} CFU/lung after 4 wk of treatment	TBAJ-876 AUC_{0-96}, mg·h/L	M3 AUC_{0-96}, mg·h/L
TBAJ-876				
1.6	7.7	4.3	1.9	4.3
6.3	7.7	1.7	6.8	18.4
25	7.7	1.1	29.9	108.8
M3				
3.1	7.9	3.7	-	22.1
12.5	7.9	1.8	-	33.1
50	7.9	0.0	-	209.9

Abbreviations: AUC_{0-96}, area under the concentration-time curve over 96 hours; CFU, colony-forming unit.

Steady-state plasma concentration-time profiles of TBAJ-876 and M3 after 4 weeks of TBAJ-876 treatment were dose-dependent (Figure 4A). Following TBAJ-876 treatment, exposure (AUC_{0-96} mg·h/L) to M3 was 2.2 to 3.6-fold higher than exposure to TBAJ-876 (Table 2). In M3-treated animals, dose-dependent plasma concentration-time profiles were also observed, although the dose of 12.5 mg/kg resulted in relatively low M3 plasma concentrations and exposure (Figure 4B and Table 2).

Figure 5 shows the lung CFU count relative to the exposure to M3 after treatment with either TBAJ-876 or M3. By comparing lung CFU counts at a specific level of M3 exposure following TBAJ-876 treatment to lung CFU counts at the same level of M3 exposure following M3 treatment, the relative contribution of M3 to the overall activity observed after TBAJ-876 treatment can be estimated. The underlying principle is that TBAJ-876 treatment leads to both TBAJ-876 and M3 exposure, which both determine the overall bactericidal activity, assuming no interactions between TBAJ-876 and M3 (as indicated by the checkerboard assay results). The levels of M3 exposure measured after TBAJ-876 treatment were associated with pronounced bactericidal activity in animals treated with M3 directly. For example, TBAJ-876 treatment at 6.3 mg/kg led to an M3 AUC_{0-96} of 18.4 mg·h/L and resulted in a CFU decline of 7.7 to 1.7 Log_{10}. M3 dosing at 3.1 mg/kg produced similar M3 exposures (22.1 mg·h/L), and lowered the lung CFU counts from 7.9 to 3.7 Log_{10} (Table 2 and Figure 5). This indicates that, within this mouse tuberculosis model, the M3 metabolite contributes substantially to the overall bactericidal activity observed after TBAJ-876 treatment.

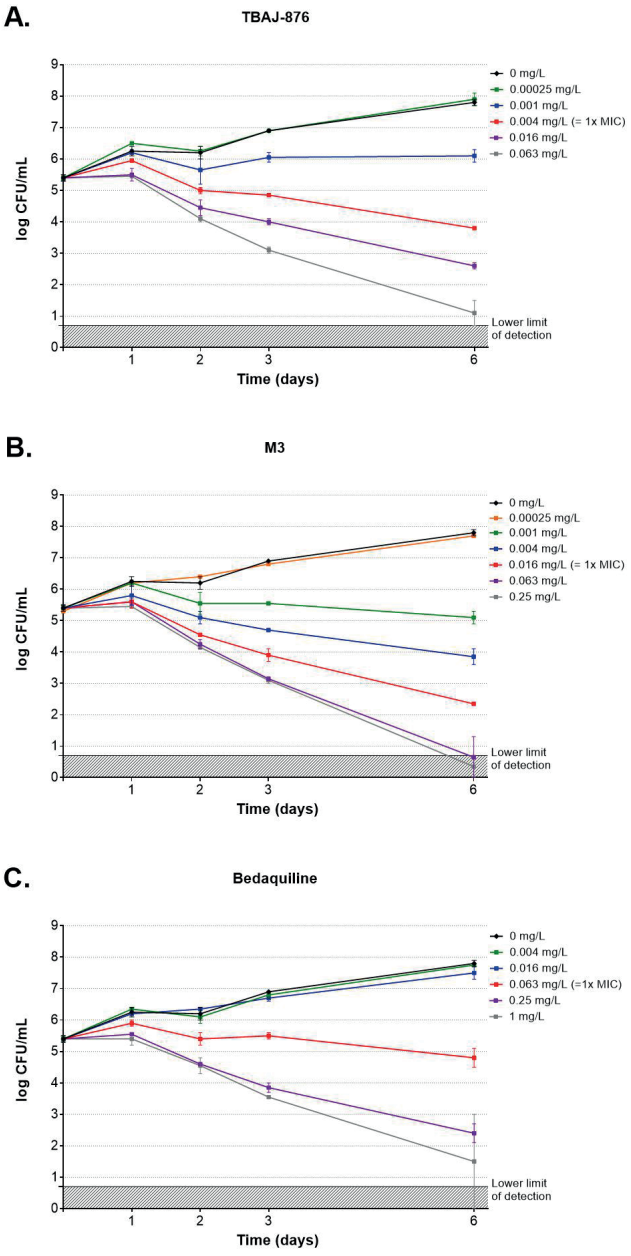

Figure 1. Time- and concentration-dependent activity of TBAJ-876 (A), M3 (B), and bedaquiline (C) against actively replicating *M. tuberculosis* Beijing VN2002-1585. Mycobacterial cultures were exposed to 4-fold increasing concentrations. The experiment was performed in duplicate, and results are presented as mean Log_{10} CFU/mL (± range). Abbreviations: CFU, colony-forming unit; MIC, minimum inhibitory concentration.

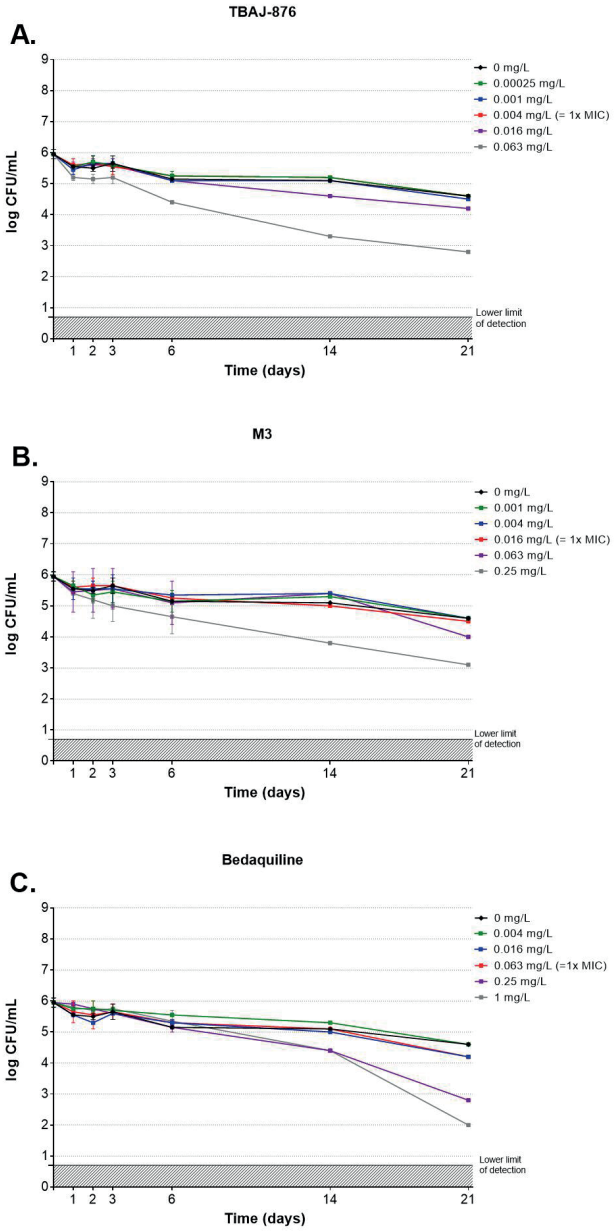

Figure 2. Time- and concentration dependent activity of TBAJ-876, M3, and bedaquiline against non-replicating *M. tuberculosis* Beijing VN2002-1585. The non-replicating state was induced by nutrient starvation. Cultures were exposed to four-fold increasing concentrations. The experiment was performed in duplicate, except for sampling days 14 and 21. Results are presented as mean Log_{10} CFU/mL (± range). Abbreviations: CFU, colony-forming unit; MIC, minimum inhibitory concentration.

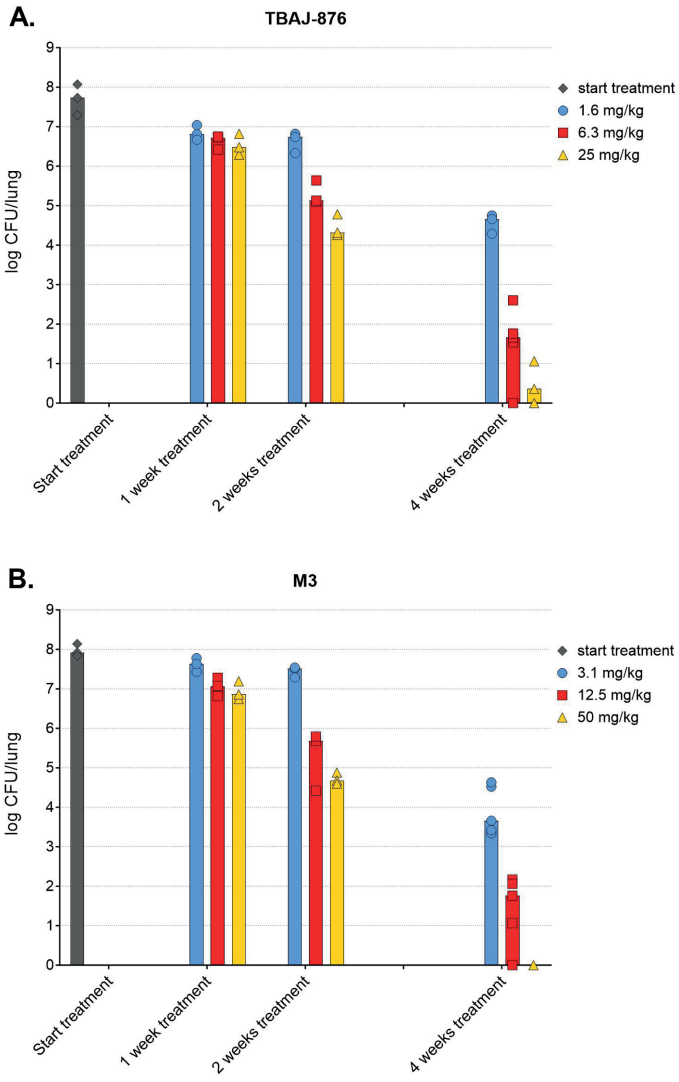

Figure 3. *In vivo* bactericidal activity of TBAJ-876 (A) and M3 (B) against *M. tuberculosis* Beijing VN2002-1585. The mycobacterial load is expressed as Log_{10} colony-forming units (CFU) in the lungs after 0, 1, 2, or 4 weeks of treatment. TBAJ-876 was dosed at 1.6, 6.3, or 25 mg/kg. M3 was dosed at 3.1, 12.5, or 50 mg/kg. Three animals were included per dose and treatment duration. Two extra animals were added to the groups that were treated for 4 weeks (n=5 per dose), which were animals included in the study for plasma concentration measurement at 96 hours after the last dose administration. One animal in the M3 experiment reached humane end points due to complications of the intratracheal *M. tuberculosis* instillation resulting in n=4 in the 50 mg/kg 4 weeks' treatment group.

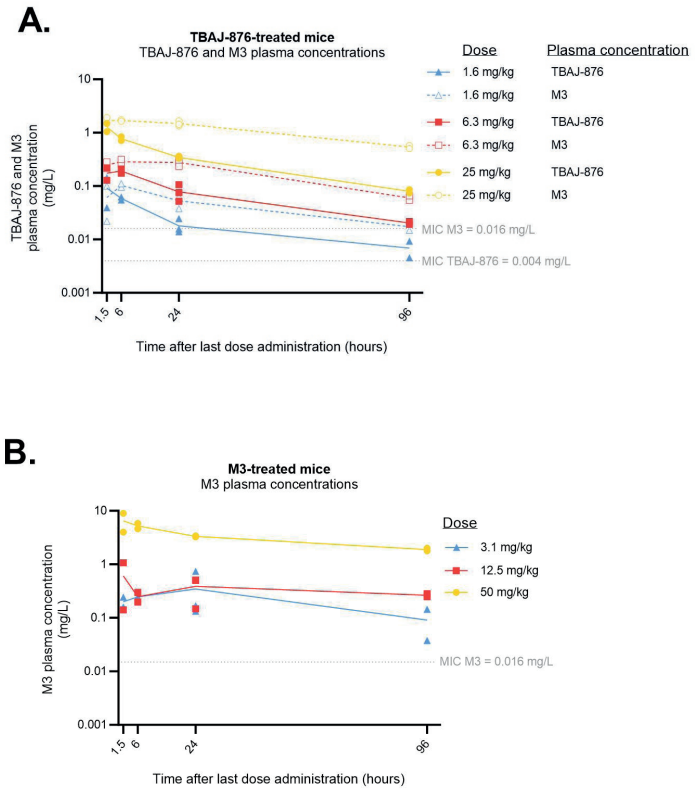

Figure 4. *In vivo* plasma concentrations of TBAJ-876 and M3 in animals infected with *M. tuberculosis* Beijing VN2002-1585 and treated with TBAJ-876 dosed at 1.6, 6.3, or 25 mg/kg (A) or M3 dosed at 3.1, 12.5, or 50 mg/kg (B) for 4 weeks. Each plasma concentration measurement is plotted individually. Two animals were included per time point. To all 24-hour groups, except for M3 50 mg/kg, 1 extra animal was included, which were spare animals included in case of drop-outs. In TBAJ-876–treated animals, plasma concentrations of both TBAJ-876 (solid lines) and M3 (dashed lines) were determined. In M3-treated animals, plasma concentrations of M3 were measured. The horizontal dotted lines represent the minimum inhibitory concentration (MIC) of TBAJ-876 and M3.

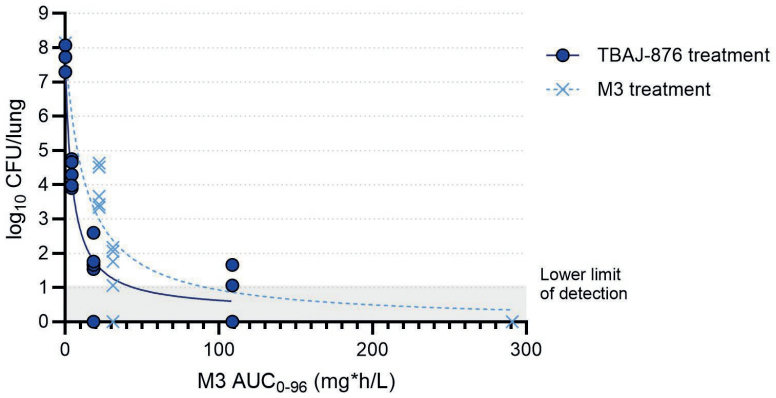

Figure 5. *M. tuberculosis* colony-forming units (CFU) in the lungs in relation to M3 exposure, defined as area under the plasma concentration time-curve from 0 to 96 hours (AUC_{0-96}). Lung CFU count was plotted against exposure to M3 after treatment with TBAJ-876 (circles) or M3 (crosses). The lines represent the relationship between lung CFU count and exposure to M3 after TBAJ-876 treatment (solid line), or M3 treatment (dashed line), based on a nonlinear regression dose-response inhibition model. The lung CFU count at x = 0 aligns with the lung CFU count at the start of treatment, as no untreated animals were included in this study.

Discussion

This study investigated the relative contribution of the main TBAJ-876 metabolite, M3, to the overall activity of TBAJ-876. So far, TBAJ-876 activity has been evaluated in several preclinical studies.[9, 15, 16, 26] However, this is the first study to assess its activity while considering the pharmacokinetics and direct bactericidal activity of the M3 metabolite. Furthermore, previous studies were conducted with *M. tuberculosis* H37Rv, whereas this study used a clinical strain of the Beijing genotype, known for its virulent properties.[24, 27, 28]

A recent mouse study investigated the pharmacokinetic properties of TBAJ-876 and M3 in uninfected mice after 1 or 7 days of TBAJ-876 treatment at 3.1 or 6.3 mg/kg.[16] Similar to our findings, the authors reported that M3 plasma concentrations were higher than TBAJ-876 following TBAJ876 treatment, the AUC of M3 being 2.4 to 4.1-fold higher than that of TBAJ-876.

Another study by Almeida et al. evaluated the bactericidal activity of TBAJ-876 dosed at 3.1, 6.3, or 12.5 mg/kg against *M. tuberculosis* H37Rv in a comparable mouse tuberculosis model.[15] Four weeks of treatment lowered lung CFU counts from 7.6 Log_{10} at the start of treatment to 4.4, 3.2, and 2.4 Log_{10} CFU for the 3 different doses, respectively. Our study confirms the profound bactericidal activity of TBAJ-876. In fact, TBAJ-876 activity was

more pronounced here. This might be attributable to differences in experimental design, including the strain used for infection. Almeida et al used the H37Rv strain, whereas we used a Beijing strain.[15] While subtle (2 to 4-fold difference), the MIC discrepancies observed between the 2 strains could hint at a possibility of higher TBAJ-876 activity against Beijing strains compared to H37Rv. Consistent with other studies,[9, 15, 29] TBAJ-876 seems more potent than bedaquiline, both dose based and exposure based.[15, 29]

Mouse tuberculosis models are an important part of the drug development pipeline. They provide insight into the *in vivo* antituberculosis activity of drug candidates within the complex system of an infected host, and enable prioritization of drug candidates and drug combinations before advancing to human clinical studies. Additionally, mouse studies can provide data for translating and predicting the dosage necessary to achieve desired treatment outcomes in humans. However, in such studies, the potential antituberculosis activity of *in vivo* formed metabolites is often not considered. Acknowledging the significance of metabolite activity and variations in metabolism between mice and humans can provide insight into whether drug activity in mice might be underestimated or overestimated compared to humans, and, as such, can enhance the accuracy of animal model-based predictions (both direct or via predictive models using preclinical data) regarding drug activity and drug exposure in humans.[17, 30]

For TBAJ-876 and M3, the parent-to-metabolite ratio in humans is not yet reported, but results are pending (NCT04493671 and NCT05526911). In direct opposition to observations in mice, where exposures to bedaquiline's main metabolite, *N*-desmethyl bedaquiline, are 2.6 to 3.3-fold higher than the parent drug, in humans, the metabolite exposure is 4 to 5-fold lower compared to the parent drug,[18, 19] suggesting a comparable scenario for TBAJ-876. As such, it is relevant to study M3's contribution to the total TBAJ-876 activity by investigating the individual activity of both compounds and the parent-to-metabolite ratio, aiming to increase the predictive value of preclinical models.

Species-specific differences in parent-to-metabolite ratios are especially relevant when metabolites are formed with distinct activity patterns against *M. tuberculosis* compared to the parent drug. Assessing the individual activity of TBAJ-876 and M3 in a mouse tuberculosis model following TBAJ-876 treatment poses a hurdle due to the concomitant formation of M3. Two approaches were used to overcome this challenge: using *in vitro* studies to compare TBAJ-876 and M3 activity and direct administration of the M3 metabolite to the animals in the mouse tuberculosis model. Evaluation of *in vitro* activity against nonreplicating *M. tuberculosis* was included because mycobacteria can alter their metabolic level in response to diverse stresses encountered within the microenvironment of tuberculosis lesions, including limited nutrient availability.[31] When parent drug and metabolite demonstrate distinct activity patterns against *M.*

tuberculosis in different metabolic state, acknowledging species-specific parent-to-metabolite ratios might be of particular importance considering differential pathology in mice versus humans.[30, 32] Regarding the MIC, a 4-fold difference was observed between TBAJ-876 and M3, comparable to the MIC difference between bedaquiline and its M2 metabolite.[18] However, the time- and concentration-dependent activity against actively replicating and nonreplicating *M. tuberculosis* was similar for TBAJ-876 and M3. *In vivo*, M3 bactericidal activity was potent, with the highest concentration rendering the lungs of all mice culture negative after only 4 weeks of treatment. Given the 2.2 to 3.6-fold higher exposure to M3 than to TBAJ-876 following treatment with TBAJ-876, combined with the profound bactericidal activity of M3, the total activity seen upon TBAJ-876 treatment seemed to be substantially attributable to M3 in our mouse model.

This study focused on variation in bactericidal activity between parent and metabolite and their relative contribution to the overall activity. In the context of (active) metabolite formation, additional factors apart from variation in bactericidal activity could be important when extrapolating findings from mouse models to humans. For example, studying whether parent and metabolite are equipotent in penetrating different regions of tuberculosis pulmonary lesions or whether they differ in activity against intracellular bacilli can be relevant,[30, 33] especially because BALB/c mice develop cellular granulomas,[32] whereas human tuberculosis granulomas are often necrotizing and caseous in nature. Even more importantly, in light of species-specific parent-to-metabolite ratios, differences in toxicity profiles of parent and metabolite could impact the association between safety of a drug in animal studies and what is expected in clinical practice.[34]

Although this study design allows for an estimation of role of the main metabolite within the total drug activity based on *in vitro* data and *in vivo* early bactericidal activity, the modest scale and exploratory nature of this study should be considered. The pharmacokinetics of TBAJ-876 and M3 relies on a limited dataset, containing 4 time points after the last dose administration with up to 3 animals per time point. However, because plasma concentration-time profiles of TBAJ-876 and M3 are reported as relatively static,[16] the restricted number of time points is unlikely to have considerably impacted the estimation of compound exposure based on $AUC_{0\text{-}96}$. However, exposure to M3 following M3 treatment at 12.5 mg/kg was not proportional with the lower and higher doses tested, and additional sampling time points or larger group sizes could have provided a more comprehensive understanding of whether the observed M3 exposure was underestimated.

In conclusion, TBAJ-876 and M3 demonstrated profound activity against *M. tuberculosis* both *in vitro* and in the mouse tuberculosis model. Notably, the *in vivo* activity of TBAJ-876 treatment appeared to depend largely on M3, given its relatively high exposure compared to the parent compound, together with its potent activity. Based on the similar potency of TBAJ-876 and M3, clinical activity of TBAJ-876 can be anticipated regardless of the parent-to-metabolite ratio, provided that exposures required for activity can be reached safely in humans. While potential species-specific differences in parent-to-metabolite ratios for TBAJ-876 and M3 may not limit extrapolation of mouse models results to humans, we advocate taking metabolites and their potentially distinct activity profiles into account to enhance the accuracy of mouse model-derived predictions on treatment efficacy in humans.

Acknowledgements

This work was supported by the TB Alliance with support from Australia's Department of Foreign Affairs and Trade, the UK Foreign, Commonwealth & Development Office, Bill and Melinda Gates Foundation (OPP1129600), and German Federal Ministry of Education and Research.

References

1. World Health Organization. Global tuberculosis report 2023. Geneva: World Health Organization, 2023.
2. Nyang'wa BT, Berry C, Kazounis E, et al. A 24-week, all-oral regimen for rifampin-resistant tuberculosis. N Engl J Med 2022; 387:2331–43.
3. Conradie F, Diacon AH, Ngubane N, et al. Treatment of highly drug-resistant pulmonary tuberculosis. N Engl J Med 2020; 382:893–902.
4. Conradie F, Bagdasaryan TR, Borisov S, et al. Bedaquilinepretomanid-linezolid regimens for drug-resistant tuberculosis. N Engl J Med 2022; 387:810–23.
5. Goodall RL, Meredith SK, Nunn AJ, et al. Evaluation of two short standardised regimens for the treatment of rifampicin-resistant tuberculosis (STREAM stage 2): an open-label, multicentre, randomised, non-inferiority trial. Lancet 2022; 400:1858–68.
6. World Health Organization. WHO consolidated guidelines on tuberculosis. Module 4: treatment—drug-resistant tuberculosis treatment, 2022 update. Geneva: World Health Organization, 2022.
7. Dooley KE, Rosenkranz SL, Conradie F, et al. QT effects of bedaquiline, delamanid, or both in patients with rifampicinresistant tuberculosis: a phase 2, open-label, randomised, controlled trial. Lancet Infect Dis 2021; 21:975–83.
8. Guillemont J, Meyer C, Poncelet A, Bourdrez X, Andries K. Diarylquinolines, synthesis pathways and quantitative structure-activity relationship studies leading to the discovery of TMC207. Future Med Chem 2011; 3:1345–60.
9. Choi PJ, Conole D, Sutherland HS, et al. Synthetic studies to help elucidate the metabolism of the preclinical candidate TBAJ-876-A less toxic and more potent analogue of bedaquiline. Molecules 2020; 26:25.
10 Al-Khatib SM, Stevenson WG, Ackerman MJ, et al. 2017 AHA/ACC/HRS guideline for management of patients with ventricular arrhythmias and the prevention of sudden cardiac death: executive summary: a report of the American College of Cardiology/ American Heart Association task force on Clinical Practice Guidelines and the Heart Rhythm Society. Heart Rhythm 2018; 15:e190–252.
11. Andries K, Villellas C, Coeck N, et al. Acquired resistance of *Mycobacterium tuberculosis* to bedaquiline. PLoS One 2014; 9:e102135.
12. Derendinger B, Dippenaar A, de Vos M, et al. Bedaquiline resistance in patients with drug-resistant tuberculosis in Cape Town, South Africa: a retrospective longitudinal cohort study. Lancet Microbe 2023; 4:e972–82.
13. Mallick JS, Nair P, Abbew ET, Van Deun A, Decroo T. Acquired bedaquiline resistance during the treatment of drug-resistant tuberculosis: a systematic review. JAC Antimicrob Resist 2022; 4:dlac029.
14. Sutherland HS, Tong AST, Choi PJ, et al. Variations in the C-unit of bedaquiline provides analogues with improved biology and pharmacology. Bioorg Med Chem 2020; 28:115213.
15. Almeida D, Converse PJ, Li SY, Upton AM, Fotouhi N, Nuermberger EL. Comparative efficacy of the novel diarylquinoline TBAJ-876 and bedaquiline against a resistant Rv0678 mutant in a mouse model of tuberculosis. Antimicrob Agents Chemother 2021; 65:e0141221.
16. Li SY, Converse PJ, Betoudji F, et al. Next-generation diarylquinolines improve sterilizing activity of regimens with pretomanid and the novel oxazolidinone TBI-223 in a mouse tuberculosis model. Antimicrob Agents Chemother 2023; 67:e0003523.

17. Ernest JP, Strydom N, Wang Q, et al. Development of new tuberculosis drugs: translation to regimen composition for drug-sensitive and multidrug-resistant tuberculosis. Annu Rev Pharmacol Toxicol 2021; 61:495–516.
18. Rouan MC, Lounis N, Gevers T, et al. Pharmacokinetics and pharmacodynamics of TMC207 and its N-desmethyl metabolite in a murine model of tuberculosis. Antimicrob Agents Chemother 2012; 56:1444–51.
19. van Heeswijk RP, Dannemann B, Hoetelmans RM. Bedaquiline: a review of human pharmacokinetics and drugdrug interactions. J Antimicrob Chemother 2014; 69:2310–8.
20. de Steenwinkel JE, ten Kate MT, de Knegt GJ, et al. Drug susceptibility of *Mycobacterium tuberculosis* Beijing genotype and association with MDR TB. Emerg Infect Dis 2012; 18:660–3.
21. Clinical and Laboratory Standards Institute (CLSI). Susceptibility testing of mycobacteria, Nocardia spp., and other aerobic Actinomycetes. 3rd ed. CLSI standard M24. Wayne, PA: CLSI, 2018.
22. Odds FC. Synergy, antagonism, and what the chequerboard puts between them. J Antimicrob Chemother 2003; 52:1.
23. Bax HI, Bakker-Woudenberg IAJM, de Vogel CP, van der Meijden A, Verbon A, de Steenwinkel JEM. The role of the time-kill kinetics assay as part of a preclinical modeling framework for assessing the activity of anti-tuberculosis drugs. Tuberculosis (Edinb) 2017; 105:80–5.
24. Mourik BC, de Knegt GJ, Verbon A, Mouton JW, Bax HI, de Steenwinkel JEM. Assessment of bactericidal drug activity and treatment outcome in a mouse tuberculosis model using a clinical Beijing strain. Antimicrob Agents Chemother 2017; 61:e00696-17.
25. de Steenwinkel JE, ten Kate MT, de Knegt GJ, et al. Consequences of noncompliance for therapy efficacy and emergence of resistance in murine tuberculosis caused by the Beijing genotype of *Mycobacterium tuberculosis*. Antimicrob Agents Chemother 2012; 56:4937–44.
26. Ragunathan P, Shuyi Ng P, Singh S, et al. GaMF1.39's antibiotic efficacy and its enhanced antitubercular activity in combination with clofazimine, telacebec, ND-011992, or TBAJ-876. Microbiol Spectr 2023; 11:e0228223.
27. Liu Q, Wang D, Martinez L, et al. *Mycobacterium tuberculosis* Beijing genotype strains and unfavourable treatment outcomes: a systematic review and meta-analysis. Clin Microbiol Infect 2020; 26:180–8.
28. Karmakar M, Trauer JM, Ascher DB, Denholm JT. Hyper transmission of Beijing lineage *Mycobacterium tuberculosis*: systematic review and meta-analysis. J Infect 2019; 79:572–81.
29. Pieterman ED, Keutzer L, van der Meijden A, et al. Superior efficacy of a bedaquiline, delamanid, and linezolid combination regimen in a mouse tuberculosis model. J Infect Dis 2021; 224:1039–47.
30. Mehta K, Guo T, van der Graaf PH, van Hasselt JGC. Predictions of bedaquiline and pretomanid target attainment in lung lesions of tuberculosis patients using translational minimal physiologically based pharmacokinetic modeling. Clin Pharmacokinet 2023; 62: 519–32.
31. Iacobino A, Piccaro G, Giannoni F, Mustazzolu A, Fattorini L. Fighting tuberculosis by drugs targeting nonreplicating *Mycobacterium tuberculosis* bacilli. Int J Mycobacteriol 2017; 6:213–21.
32. Driver ER, Ryan GJ, Hoff DR, et al. Evaluation of a mouse model of necrotic granuloma formation using C3HeB/FeJ mice for testing of drugs against *Mycobacterium tuberculosis*. Antimicrob Agents Chemother 2012; 56:3181–95.

33. Irwin SM, Prideaux B, Lyon ER, et al. Bedaquiline and pyrazinamide treatment responses are affected by pulmonary lesion heterogeneity in *Mycobacterium tuberculosis* infected C3HeB/FeJ mice. ACS Infect Dis 2016; 2: 251–67.

34. van Beek SW, Tanneau L, Meintjes G, et al. Model-Predicted impact of ECG monitoring strategies during bedaquiline treatment. Open Forum Infect Dis 2022; 9:ofac372.

CHAPTER 4.2

Mycobacterium abscessus strain variability in preclinical drug development, does it really matter?

Saskia E. Mudde, Henriëtte M. Meliefste,
Nicole C. Ammerman, Jurriaan E.M. de Steenwinkel,
Hannelore I. Bax

J Antimicrob Chemother. 2024 Dec;79(12):3169-3173.

Abstract

Background

New treatment options for *Mycobacterium abscessus* infections are urgently needed. Since a correlation between minimum inhibitory concentrations (MIC) and clinical outcomes is not clearly established, potency of novel drugs needs to be evaluated using additional *in vitro* drug activity assays. Preclinical drug activity assays generally use the *M. abscessus* type strain ATCC 19977. However, *M. abscessus* complex entails a genetically and morphologically diverse group, and it is questionable whether drug activity observed against ATCC 19977 is representative for drug activity against clinical *M. abscessus* isolates.

Objective

To assess whether the relationship between MIC and the quantitative antimycobacterial activity of amikacin, imipenem, and clofazimine differs between the ATCC 19977 strain and clinical *M. abscessus* isolates.

Methods

Experiments were performed with *M. abscessus* ATCC 19977 and a subset of six clinical isolates covering the three *M. abscessus* subspecies and the smooth and rough morphotype. Cultures were exposed to the drugs at four-fold increasing, MIC-standardized concentrations, and the mycobacterial load was assessed over time.

Results

Concentration- and time-dependent activity of amikacin, imipenem, and clofazimine against the six clinical isolates was similar. Only slight variations in drug activity were observed between ATCC 19977 and clinical isolates.

Conclusion

Time- and concentration dependent drug activity against the ATCC 19977 strain seems indicative for *in vitro* drug behavior against MABC clinical isolates. Including one clinical smooth morphotype isolate alongside ATCC 19977 seems appropriate for reliable interpretation of this particular *in vitro* drug activity assay as part of the *M. abscessus* preclinical drug development pipeline.

Introduction

Mycobacterium abscessus complex (MABC) comprises a group of rapidly growing non-tuberculous mycobacteria, notorious for their ability to cause detrimental lung infections, especially in patients with underlying lung disease.[1, 2] MABC's intrinsic antibiotic resistance mechanisms severely complicate achieving successful treatment outcomes.[3] Development and prioritization of promising drug candidates is essential to improve treatment success rates.

Determination of *in vitro* minimum inhibitory concentrations (MICs) is considered fundamental to antibiotic susceptibility testing, which can guide antibiotic treatment decisions. Yet, with MABC (and other non-tuberculous mycobacteria), the correlation between MICs and clinical treatment response is not clearly established.[4] As such, MICs alone are insufficient for identifying promising new drugs and evaluating their clinical potential. Additional *in vitro* drug activity assays are needed to complement the preclinical drug development pipeline, such as time-kill kinetics assays (TKKs) which add value to endpoint measurements like MICs by assessing a drug's inhibitory or killing activity over time.[5]

Apart from combining preclinical assays, including different isolates might be of additional interest when assessing the *in vitro* potential of novel drugs against *M. abscessus*. Currently, the type strain *M. abscessus* subsp. *abscessus* ATCC 19977 is most often used. However, being an environmental microorganism, MABC exhibits considerable genetic and phenotypic diversity, which potentially influences drug activity. Three genetically distinct MABC subspecies are distinguished (*abscessus*, *bolletii*, and *massiliense*) as well as two different colony morphotypes (smooth and rough). This morphotype difference has been gaining interest over recent years, as rough isolates have been associated with increased virulence and poorer clinical outcomes than smooth isolates.[6-8] Hence, the generalizability of *in vitro* preclinical drug activity testing based on ATCC 19977 alone could be questioned, and might benefit from utilizing a representative subset of clinical isolates. However, 'a representative subset' is not clearly defined, and the added value of including multiple isolates should first be investigated and balanced with practical feasibility.

Hence, this study assessed the variability in *in vitro* activity of amikacin, imipenem, and clofazimine (three guideline-recommended antibiotics with distinct mechanisms of action[9]) against ATCC 19977 and six clinical MABC isolates with similar MICs. This subset covers the three subspecies and two morphotypes that MABC organisms can adopt as representatives of the divers MABC family. TKKs were used to quantify concentration- and time-dependent activity of these cornerstone drugs across the different MABC clinical

isolates. Thereby, this study aimed to assess whether the relationship between MICs and the quantitative antimycobacterial activity differed between clinical isolates and ATCC 19977. This investigation offers insight into the importance of incorporating diverse isolates into an important component of the preclinical development pipeline for MABC.

Material and methods

Isolates, identification, and culture conditions

Experiments included *M. abscessus* subsp. *abscessus* ATCC 19977 and six clinical MABC isolates. The clinical isolates were selected from the Erasmus MC clinical microbiology isolate collection based on colony morphotype, subspecies and susceptibility profile on record to obtain a representative set of isolates with similar MIC values for the three drugs assessed. Isolates were passaged up to four times on Mueller Hinton agar (Becton, Dickinson, and Company [BD]) with 10% oleic acid, albumin, dextrose, catalase (OADC; BD), followed by stock solution preparation in 7H9 Middlebrook broth (BD) with 10% OADC, 0.05% Tween80, and 0.5% glycerol.
Stock solutions were stored at -80°C.

Subspecies identification was confirmed by internal transcribed spacer (ITS) and *hsp65* sequencing. Isolates were grown on Mueller Hinton agar plates (BD) supplemented with 10% OADC for 14 days prior to DNA isolation. After lysis in 250 µl MagNA Pure Bacteria Lysis Buffer (Roche) and heat shock inactivation (10 minutes, 95 °C), DNA was isolated on the MagNA Pure 96 platform using the Viral Nucleic Acid Small Volume kit (Roche) according to the manufacture's Pathogen Universal Protocol. Per isolate, 5 µl DNA was combined with 12.5 µl 1x FastStart PR Master Mix (Roche), and 3 µM primers (table 1). For the negative control, DNA was replaced by 5 µl dilution buffer. Cycling parameters involved pre-denaturation at 94°C for 5 minutes, denaturation at 94°C for 35 cycles of 30 seconds, annealing at 55°C for 30 seconds, and extension at 72°C for 1 minute. Gel electrophoresis using the E-gel Power Snap (Invitrogen) was used for PCR product confirmation. Amplicon sequences, obtained by BaseClear (Leiden, The Netherlands), were subjected to BLAST analysis using BioNumerics software (Applied Maths, Sint-Martens-Latem, Belgium). Subspecies were identified based on a ≥99% match with internal reference sequences.

In inconclusive cases, subsp. *massiliense* was differentiated from subsp. *abscessus/bolletii* based on *erm* (41) truncation. Thick solutions of each isolate were prepared in phosphate buffered saline, followed by centrifugation for 10 minutes at 21.000 *x g*. Supernatant was removed, and the pellet was suspended in 200 µl distilled water. After heat shock inactivation (10 minutes, 100°C), samples were stored at -20°C until further

Table 1. Primers used for ITS and *hsp65* sequencing

Region	Primer	Sequence
ITS	MycoITS-F	5'-ACCTCCTTTCTAAGGAGCACC-3'
ITS	MycoITS-R	5'-GATGCTCGCAACCACTATCCA-3'
hsp65	Tb11	5'-ACCAACGATGGTGTGTCCAT-5'
hsp65	Tb11	5'-CTTGTCGAACCGCATACCCT-3'

use. Per sample, a PCR mixture with a total volume of 25 µl was prepared, containing 2.5 µl bacterial suspension, 1x PCR taq buffer with $(NH_4)_2SO_4$ (ThermoFisher), 2.5 mM $MgCl_2$ (ThermoFisher), 0.1 mM dNTP's (ThermoFisher), 0.008 U/µl Fermentas Taq-polymerase (ThermoFisher), 0.5 pmol/µl forward primer (5'-TCGCTCAGGGGAGTTCGTTG-3'), 0.5 pmol/µl reverse primer (5'-ATCACCAGCACCGACGAATC-3'), and distilled water. Cycling parameters were as follows: pre-denaturation at 94°C for 2 minutes, denaturation at 94°C for 30 cycles of 30 seconds, annealing at 55°C for 30 seconds, extension at 72°C for 30 seconds, and lastly post-elongation at 72°C for 5 minutes. The PCR products, together with a GeneRuler 100 bp plus DNA-ladder (ThermoFisher) were loaded onto an 1%-agarose gel consisting of agarose (Sphaero) and 0.05% SYBR™ Safe DNA Gel Stain (Invitrogen) in 0.5X TBE electrophoresis buffer (ThermoFisher). The gel was run for 30 minutes in 0.5X TBE electrophoresis buffer at 110 mA, and imaged using the Gel Doc System and Proxima AQ4 software (Isogen Life Science B.V.).

Isolate morphology was categorized as rough or smooth by visual inspection.

Drug susceptibility testing

MICs for amikacin (Sigma-Aldrich), imipenem (Fresenius Kabi), and clofazimine (Sigma-Aldrich) were determined in duplicate according to the Clinical and Laboratory Standards Institute (CLSI) guidelines (M24, 3rd edition)[4] by broth microdilution in Cation Adjusted Mueller Hinton Broth (CAMHB, BD) at 30°C. Stock solutions of amikacin and imipenem were prepared in distilled water, and clofazimine in DMSO (Sigma-Aldrich).

Time-kill kinetics assays

Amikacin, imipenem, and clofazimine activity against the MABC isolates was assessed using TKKs as previously described[10], with modifications regarding medium composition (no OADC) and culture volume (2.5 mL instead of 25 mL). Each isolate was cultured in CAMHB (+/- 10^5 bacterial/mL) and exposed to four-fold increasing drug concentrations. Since drug MICs were similar, but not identical between the different isolates, concentrations were based on isolate-specific MICs: 1/4x, 1x, 4x, 16x, and additionally 64x MIC for amikacin. For imipenem and clofazimine, 64x MIC was excluded due to solubility issues. Cultures were incubated for seven days at 30°C without agitation. Prior to the TKKs,

drug stability of imipenem was assessed using the standard large-plate agar diffusion assay showing 40% daily decay, which was supplemented in 50 µL/day to restore the original concentration. Amikacin and clofazimine were previously demonstrated to be stable.[10] Cultures were sampled (100 µL) at days 0, 3, 5, and 7 for mycobacterial load determination After ten-fold serial dilution, 3x10 µl per dilution was spotted onto Mueller Hinton agar (BD) with 10% OADC, and 6x10 µl for undiluted samples, resulting in a lower limit of detection of 1.2 Log_{10} CFU/mL. CFUs were counted after 4-7 days incubation at 30°C.

Results and discussion

The MABC clinical isolate collection included one smooth subsp. *abscessus* (Cl18), one smooth subsp. *abscessus/bolletii* (Cl20), two smooth subsp. *massiliense* (Cl21 and Cl26), and two rough subsp. *abscessus/bolletii* (Cl23 and Cl24). The MICs and TKK results for amikacin, imipenem, and clofazimine per MABC isolate are displayed in figure 1, figure 2, and figure 3, respectively. Of note, reliable CFU counting of the rough morphotype isolates was hampered by mycobacterial aggregation at high mycobacterial loads, as indicated in the figures.

Similar to ATCC 19977, amikacin at 1/4x MIC was inactive against all clinical isolates. Activity of 1x MIC against ATCC 19977 was inhibitory up to day 3 followed by mycobacterial outgrowth, whereas against the clinical isolates activity varied between being inactive or inhibitory. At 4-64x MIC, amikacin demonstrated killing activity against all clinical isolates until at least day 5, with the amount of killing being comparable for ATCC19977, Cl21, Cl26, and Cl24, and for Cl18, Cl20, and Cl23.

As to imipenem, compared to ATCC 19977, 1/4x MIC demonstrated similar activity against Cl21, while little activity was observed against the other clinical isolates. Activity of 1x MIC was somewhat variable among the isolates, demonstrating either slight outgrowth, stabilization or continued reduction of the mycobacterial load after day 3, whereas killing activity similar to ATCC 19977 was observed for 4x and 16x MIC against the clinical isolates.

Amongst the clinical isolates, clofazimine activity at 1/4x-16x MIC was overall comparable. Yet, activity of these concentrations was mostly inhibitory, whereas 1x and 16x MIC demonstrated killing activity instead against ATCC 19977. Of note, against ATCC 19977, activity of clofazimine at 1x MIC lasted longer compared to 4x MIC which showed mycobacterial outgrowth from day 3 onwards, thus 1x MIC being more active than 4x MIC. This observation has previously been described for other antimycobacterial drugs and has been attributed to the so called Eagle effect: a paradoxical phenomenon where higher drug concentrations lead to less *in vitro* killing.[11, 12] The exact mechanisms responsible for this observation are unknown, although it has been speculated that high drug concentrations might inhibit RNA and protein synthesis necessary for killing.[13] The relevance of this finding in the present study is debatable, particularly since this effect was less pronounced for the clinical isolates.

Macroscopic aggregation of the rough isolates posed a technical challenge in the TKKs, and likely led to an underestimation of the true CFU count, especially for the non-drug-exposed controls. Nevertheless, assuming that aggregation is related to high loads and that non-drug-exposed rough isolates exhibit a similar increase in CFU count over time compared to smooth isolates, the impact of different antibiotic concentrations on the mycobacterial load could still be assessed, and suggested similar overall activities of the three drugs between smooth and rough morphotypes. MABC morphotype is thought to be of clinical relevance, as rough isolates have been associated with a worse clinical outcome.[7, 8, 14] It is hypothesized that reduced levels of cell wall glycopeptidolipids in rough isolates expose virulence factors that are covered in smooth isolates.[6] Such virulence factors likely facilitate increased cording capabilities of rough isolates,[15] which might contribute to the observed macroscopic aggregation in these experiments.

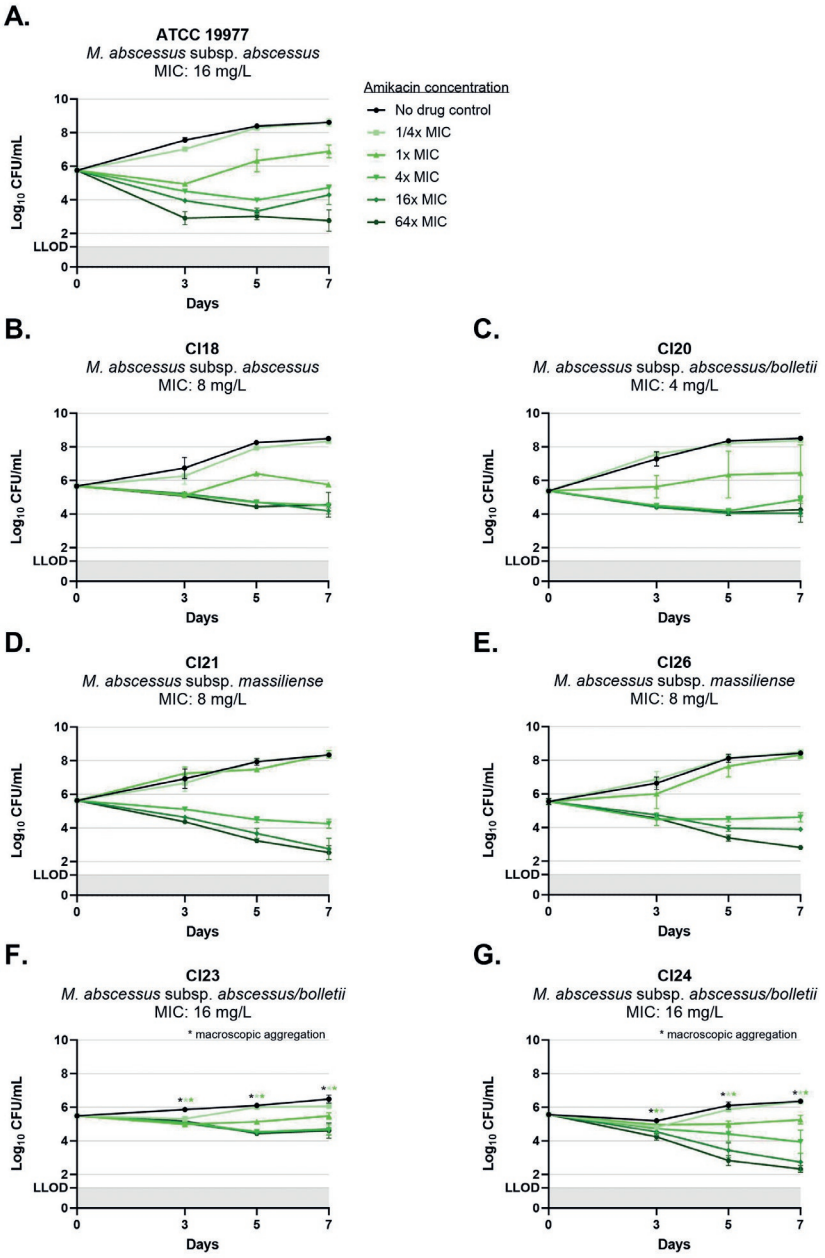

Figure 1. Time- and concentration dependent activity of amikacin against 7 *Mycobacterium abscessus* complex isolates: A) ATCC 19977 (type strain): smooth morphotype *M. abscessus* subsp. *abscessus*; B) CI18: smooth morphotype *M. abscessus* subsp. *abscessus*; C) CI20: smooth morphotype *M. abscessus* subsp. *abscessus/bolletii*; D) CI21: smooth morphotype *M. abscessus* subsp. *massiliense*; E) CI26: smooth morphotype *M. abscessus* subsp. *massiliense*; F) CI23: rough morphotype *M. abscessus* subsp. *abscessus/bolletii*; G) CI24: rough morphotype *M. abcessus* subsp. *abscessus/bolletii*. Mycobacterial cultures were exposed to 4-fold increasing drug concentrations starting at 1/4x the isolate-specific minimum inhibitory concentration. Experiments were performed in duplicate. Results are presented as mean Log_{10} colony forming units per mL (+/- the range). *Bacterial aggregation was visually present.

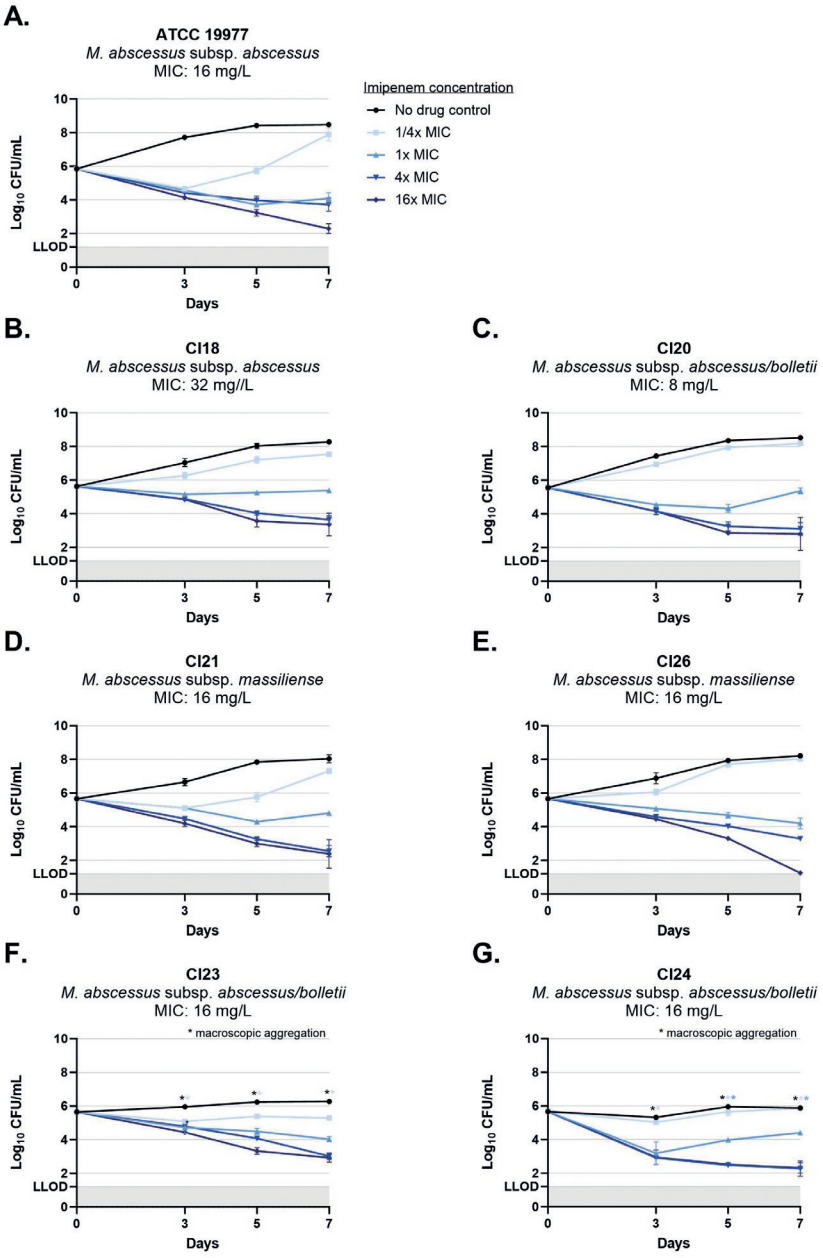

Figure 2. Time- and concentration dependent activity of imipenem against 7 *Mycobacterium abscessus* complex isolates: A) ATCC 19977 (type strain): smooth morphotype *M. abscessus* subsp. *abscessus*; B) CI18: smooth morphotype *M. abscessus* subsp. *abscessus*; C) CI20: smooth morphotype *M. abscessus* subsp. *abscessus/bolletii*; D) CI21: smooth morphotype *M. abscessus* subsp. *massiliense*; E) CI26: smooth morphotype *M. abscessus* subsp. *massiliense*; F) CI23: rough morphotype *M. abscessus* subsp. *abscessus/bolletii*; G) CI24: rough morphotype *M. abcessus* subsp. *abscessus/bolletii*. Mycobacterial cultures were exposed to 4-fold increasing drug concentrations starting at 1/4x the isolate-specific minimum inhibitory concentration. Experiments were performed in duplicate. Results are presented as mean Log_{10} colony forming units per mL (+/- the range). *Bacterial aggregation was visually present.

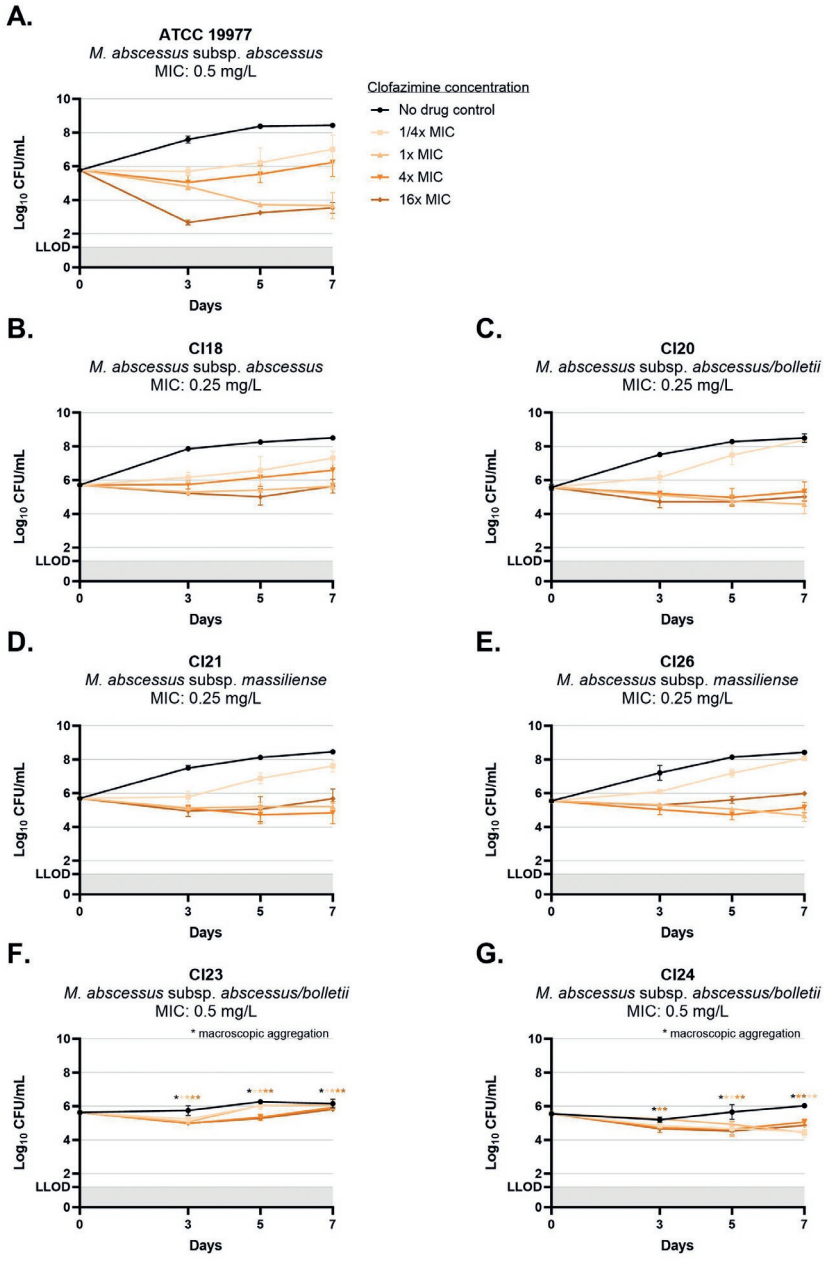

Figure 3. Time- and concentration dependent activity of clofazimine against 7 *Mycobacterium abscessus* complex isolates: A) ATCC 19977 (type strain): smooth morphotype *M. abscessus* subsp. *abscessus*; B) CI18: smooth morphotype *M. abscessus* subsp. *abscessus*; C) CI20: smooth morphotype *M. abscessus* subsp. *abscessus/bolletii*; D) CI21: smooth morphotype *M. abscessus* subsp. *massiliense*; E) CI26: smooth morphotype *M. abscessus* subsp. *massiliense*; F) CI23: rough morphotype *M. abscessus* subsp. *abscessus/bolletii*; G) CI24: rough morphotype *M. abcessus* subsp. *abscessus/bolletii*. Mycobacterial cultures were exposed to 4-fold increasing drug concentrations starting at 1/4x the isolate-specific minimum inhibitory concentration. Experiments were performed in duplicate. Results are presented as mean Log_{10} colony forming units per mL (+/- the range). *Bacterial aggregation was visually present.

In conclusion, across a collection of six clinical isolates with similar MICs for amikacin, imipenem, and clofazimine, and covering the different MABC subspecies and morphotypes, variability in concentration- and time-dependent activity was little. Only slight variations were observed between the smooth as well as rough clinical isolates and ATCC 19977. Altogether, these findings indicate that drug activity over time against ATCC 19977 is generally suggestive for *in vitro* drug behavior against other MABC isolates. Based on these results, including one smooth clinical isolate alongside ATCC 19977 may be sufficient for reliable interpretation of this particular *in vitro* drug activity assay as part of the preclinical drug development pipeline. Considering the technical challenges as well as minimal variations in drug activity observed, excluding rough MABC isolates seems appropriate.

References

1. Qvist T, Taylor-Robinson D, Waldmann E et al. Comparing the harmful effects of nontuberculous mycobacteria and Gram negative bacteria on lung function in patients with cystic fibrosis. *J Cyst Fibros* 2016; **15**: 380-5.
2. Esther CR, Jr., Esserman DA, Gilligan P et al. Chronic *Mycobacterium abscessus* infection and lung function decline in cystic fibrosis. *J Cyst Fibros* 2010; **9**: 117-23.
3. Johansen MD, Herrmann JL, Kremer L. Non-tuberculous mycobacteria and the rise of *Mycobacterium abscessus*. *Nat Rev Microbiol* 2020; **18**: 392-407.
4. CLSI. *Susceptibility Testing of Mycobacteria, Nocardia spp., and Other Aerobic Actinomycetes. 3rd ed. CLSI standard M24*. Clinical and Laboratory Standards Institute Wayne, PA, 2018.
5. Bax HI, Bakker-Woudenberg I, de Vogel CP et al. The role of the time-kill kinetics assay as part of a preclinical modeling framework for assessing the activity of anti-tuberculosis drugs. *Tuberculosis (Edinb)* 2017; **105**: 80-5.
6. Bernut A, Herrmann JL, Kissa K et al. *Mycobacterium abscessus* cording prevents phagocytosis and promotes abscess formation. *Proc Natl Acad Sci U S A* 2014; **111**: E943-52.
7. Hedin W, Fröberg G, Fredman K et al. A Rough Colony Morphology of *Mycobacterium abscessus* Is Associated With Cavitary Pulmonary Disease and Poor Clinical Outcome. *J Infect Dis* 2023; **227**: 820-7.
8. Li B, Ye M, Zhao L et al. Glycopeptidolipid Genotype Correlates With the Severity of *Mycobacterium abscessus* Lung Disease. *J Infect Dis* 2020; **221**: S257-S62.
9. Daley CL, Iaccarino JM, Lange C et al. Treatment of Nontuberculous Mycobacterial Pulmonary Disease: An Official ATS/ERS/ESCMID/IDSA Clinical Practice Guideline. *Clin Infect Dis* 2020; **71**: e1-e36.
10. Mudde SE, Schildkraut JA, Ammerman NC et al. Unraveling antibiotic resistance mechanisms in *Mycobacterium abscessus*: the potential role of efflux pumps. *J Glob Antimicrob Resist* 2022; **31**: 345-52.
11. Drlica K, Xu C, Wang JY et al. Fluoroquinolone action in mycobacteria: similarity with effects in *Escherichia coli* and detection by cell lysate viscosity. *Antimicrob Agents Chemother* 1996; **40**: 1594-9.
12. de Knegt GJ, van der Meijden A, de Vogel CP et al. Activity of moxifloxacin and linezolid against *Mycobacterium tuberculosis* in combination with potentiator drugs verapamil, timcodar, colistin and SQ109. *Int J Antimicrob Agents* 2017; **49**: 302-7.
13. Prasetyoputri A, Jarrad AM, Cooper MA et al. The Eagle Effect and Antibiotic-Induced Persistence: Two Sides of the Same Coin? *Trends Microbiol* 2019; **27**: 339-54.
14. Catherinot E, Roux AL, Macheras E et al. Acute respiratory failure involving an R variant of *Mycobacterium abscessus*. *J Clin Microbiol* 2009; **47**: 271-4.
15. Howard ST, Rhoades E, Recht J et al. Spontaneous reversion of *Mycobacterium abscessus* from a smooth to a rough morphotype is associated with reduced expression of glycopeptidolipid and reacquisition of an invasive phenotype. *Microbiology (Reading)* 2006; **152**: 1581-90.

CHAPTER 5

Summarizing discussion
and future perspectives

While TB and NTM infections may differ on many fronts, including predisposing conditions and clinical manifestations, they are similar in their intrinsic resistance to many antibiotics and the need for lengthy and burdensome treatment regimens.[1-3] The studies presented in this thesis were conducted with the overarching aim of contributing to better treatment options for mycobacterial disease. The variety of topics illustrate the considerable knowledge gaps and distance between bench and bedside that are still present in mycobacterial disease research. Our evaluation of new TB drug regimens and comparison of two newly approved TB drugs were discussed in the **chapters 2.1 and 2.2**, followed by an assessment of various repurposed drugs against *M. abscessus* and *M. avium* in the **chapters 3.1, 3.2, and 3.3**. Lastly, in the **chapters 4.1, 4.2, and 4.3** several ways were studied to improve both our *in vitro* and *in vivo* preclinical models for mycobacterial drug activity testing.

Improving treatment options for TB

To realize the End TB strategy goals of 90% reduction in TB cases and 95% reduction in TB deaths in 2035, effective, safe, and faster-acting treatment regimens are essential. The current standard of care, 2 months of isoniazid, rifampicin, pyrazinamide, and ethambutol followed by 4 months of isoniazid and rifampicin (2HRZE/4HR), was established via the iterative process of adding and replacing drugs by new drug candidates. In recent years, this approach has been accompanied by testing completely new drug backbones, thereby accelerating the process of introducing improved combination therapies into the clinic.[4] However, with the current well-filled drug pipeline, the number of potential drug combinations is overwhelming, and preclinical models are therefore vital for prioritizing the most promising drugs and drug combinations to advance to clinical trials.[4-6]

In that context, in **chapter 2.1**, we studied the treatment-shortening potential of two new regimens, with historical HRZE data as comparison, for which we used a combined mouse relapse and mathematical modelling approach. The two new regimens were BPaMZ and BPaL, which consist of multiple new and established drugs: bedaquiline (B), pretomanid (Pa), moxifloxacin (M), pyrazinamide (Z), and linezolid (L). BPaMZ required a treatment duration of only 1.6 months to reach 95% probability of cure in the mice, whereas this was 4.3 months for BPaL, and 7.9 months for HRZE, using mathematical modelling in our new model. Although the exact treatment durations cannot be directly extrapolated to clinical settings, this murine model has been shown to be a valuable tool for ranking drug regimens in terms of efficacy,[7] and the benefit of the mathematical modelling lies in the bundling of data from different studies as illustrated by the incorporation of HRZE. The BPaL regimen was recently endorsed by the WHO for the treatment of drug-resistant TB with a total duration of only 6 months, which is much shorter than the

duration of the until then available regimens for drug-resistant TB.[2] Our results imply that the BPaMZ combination might be a suitable alternative to both BPaL in the context of drug-resistant TB and possibly even to HRZE for drug-sensitive TB. Recently, the results of the clinical phase 2c SimpliciTB trial were published, which evaluated the efficacy and safety of 4 months BPaMZ for drug-sensitive TB, compared with the standard 6 months HRZE regimen. An additional study arm evaluated 6 months BPaMZ in participants with drug-resistant TB.[8] Sputum-culture conversion rates after 8 weeks of treatment were found to be higher for BPaMZ (84%) than for HRZE (47%), but long-term favorable clinical outcomes (determined at week 52) were actually lower for BPaMZ than for HRZE. This disappointing finding was attributable to unexpected hepatotoxicity-based withdrawals in the BPaMZ-group. When looking at the per-protocol analysis, however, 4 months of BPaMZ was actually non-inferior to 6 months HRZE, thereby providing a clinical validation of the treatment-shortening potential of BPaMZ relative to HRZE as was found in our study as well as other mouse TB relapse models.[9, 10] For drug-resistant TB, 6 months BPaMZ resulted in long-term favorable clinical outcomes in 86% of participants, which is similar to the performance of 6 months BPaL in earlier clinical trials.[11, 12] Our study results, however, imply that compared to BPaL shorter treatment durations of BPaMZ could potentially be sufficient. Coming back to BPaMZ as potential new TB regimen, despite promising preclinical and clinical *in vivo* efficacy, its clinical application might be hampered due to considerable hepatotoxicity as was observed in the SimpliciTB trial.[8] This was supposedly driven by the combination of pretomanid and pyrazinamide.[8, 13] Thus, preclinical mouse TB models are valuable for selecting promising regimens based on efficacy, but it is important to keep in mind that clinical application may be hindered by safety issues that may become apparent only in the clinical trial phase. The impact of safety concerns should not be underestimated, especially given that access to close patient monitoring might be limited in certain high-burden TB settings.

In **Chapter 2.2** a literature review was performed on the preclinical performance of delamanid and pretomanid and, more specifically, on the preclinical studies that led to the approval of these two new drugs for the treatment of TB. Pretomanid is currently recommended as part of the short-term BPaL(M) regimen for drug-resistant TB. Delamanid is recommended for treating drug-resistant TB as well, but only as a group C drug within long-term regimens, illustrating that based on limited available safety and efficacy data, other drugs are currently preferred over delamanid.[2] Because delamanid and pretomanid belong to the same class of drugs and were developed relatively in parallel, we were interested in their similarities and differences regarding drug discovery, modes of action, drug resistance mechanisms, *in vitro* and *in vivo* activity and efficacy, and *in vivo* pharmacokinetic profiles. Proper one-on-one comparison of the drugs was hampered by heterogeneity in preclinical experimental designs. Yet, when taken together, preclinical drug activity studies indicated that the mycobacterial killing

capacity of delamanid is higher at lower drug concentrations and doses than observed for pretomanid. However, concluding that delamanid is preferred over pretomanid in treating TB would be too simplistic, as such results are best interpreted in the light of clinical drug exposures. At preclinical doses resulting in exposures that are observed at current clinical dosing, the preclinical activity of delamanid and pretomanid was actually evenly matched. These results suggest that if higher exposures were to be reached safely in the clinic, higher efficacies might be expected, especially for delamanid. Although the risk of QT-prolongation, delamanid's major adverse event,[14] seems to be lower than initially anticipated,[15, 16] there are indications that QT-prolongation might be dose-dependent, which could hinder efforts to increase delamanid exposure.[17] Another interesting finding was that an increase in MIC for one of the two drugs does not necessarily coincide with an increase in MIC of the other drug, suggesting that cross-resistance between delamanid and pretomanid might not be a given. Reports of delamanid resistance in clinical *M. tuberculosis* isolates[18] highlight the importance of this finding, but more in-depth knowledge of the underlying resistance mechanisms would be helpful in determining under what circumstances delamanid and pretomanid might replace each other. In conclusion, our preclinical comparison indicates that delamanid and pretomanid are equipotent, which might be beneficial when one of the drugs is not available or needs replacement due to resistance, drug intolerance or drug-drug interactions. Clinical head-to-head comparison of the two drugs is scarce, however, at the moment, a clinical trial studying various drug combinations including delamanid or pretomanid is ongoing (PARADIGM4TB trial, ClinicalTrials.gov ID: NCT06114628), which might provide additional insight into the relative role of delamanid and pretomanid in clinical treatment of drug-sensitive and drug-resistant TB.

Improving treatment options for NTM infections

The currently available NTM treatment options are complex, lengthy, and often toxic and thus unsuccessful. Not only the number of available antibiotics for NTM treatment is scarce, but also the scientific evidence underlying their effectiveness. Expansion of the anti-NTM antibiotic arsenal is therefore urgently needed, to which we aimed to contribute in **chapter 3**.[3]

One approach to developing new therapeutic interventions is via deepening our understanding of the (intrinsic) drug resistance mechanisms of NTM that contribute to their difficulty to treat. Efflux pumps that can transport antibiotics out of bacterial cells are a well-known resistance mechanism in other bacteria. Although upregulation of multiple efflux pump-encoding genes have been described in antibiotic-resistant *M. abscessus* isolates,[19, 20] much is still unknown about their exact contribution to antibiotic

resistance in *M. abscessus*. Hence, in **chapter 3.1**, we investigated the impact of antibiotic stress on the transcription of efflux pump-encoding genes in *M. abscessus* by using transcriptomics. Subsequently, we studied whether the putative efflux inhibitors thioridazine and verapamil could enhance the *in vitro* activity of various guideline-recommended antibiotics for treating *M. abscessus* by using time-kill kinetics assays. We selected thioridazine (originally an antipsychotic drug)[21] and verapamil (used in the treatment of cardiovascular diseases)[22] based on their previously demonstrated efflux inhibition properties in mycobacteria[19, 23] and encouraging preclinical activity against *M. tuberculosis*.[24, 25] We found that antibiotic exposure resulted in a profound increase in transcription of transporter-encoding genes, with amikacin, clarithromycin and tigecycline upregulating substantially more genes than clofazimine and cefoxitin. Based on the transcriptomic data, we expected that thioridazine and verapamil would enhance the activity of amikacin, clarithromycin and tigecycline, but not, or to a much lesser extent, the activity of clofazimine and cefoxitin. However, synergy was observed for all drug combinations, and especially the activity of the cefoxitin-containing combinations did not lag behind the activity of the other combinations. As such, the time-kill kinetics results imply that there might be mechanisms other than efflux inhibition underlying the potent activity of thioridazine- and verapamil-containing drug combinations. Thioridazine, which was quite active against *M. abscessus* on its own (though at clinical unfeasible concentrations), has been described to target the aerobic respiratory chain via inhibition of the quinone reductases type II NADH dehydrogenase and succinate dehydrogenase, while verapamil acts by inhibition of calcium channels.[26-28] These modes of action might indirectly inhibit efflux pump activity, thereby boosting antibiotic activity, but it could be that these (or yet to be identified) mechanisms lead to synergistic activity in alternative ways. Such mechanisms deserve further attention as they might be interesting drug targets in NTM drug discovery. Although the concentrations of thioridazine and verapamil that showed promising activity in our *in vitro* study are not attainable in the human body,[29, 30] these encouraging proof-of-principle results make a case for the development and evaluation of safer derivatives[31] or alternative routes of administration including inhalation therapy[32, 33] or via nanocarriers.[34] Lastly, returning to the role of efflux pumps in *M. abscessus* antibiotic resistance, our findings show that the upregulation of transporter-encoding genes is antibiotic-specific, but with the proviso an increase in gene transcription does not necessarily lead to a corresponding increase in the number or activity of efflux pumps. Other techniques such as proteomics could be used to further elucidate the role of efflux pumps as functional resistance mechanisms.

Many of the currently used antibiotics against NTM are repurposed drugs that were originally developed for treating other bacterial infections. Benefits of this approach are that the pharmacokinetic and toxicity profiles of such drugs are often already well-understood, facilitating faster clinical introduction for NTM treatment. Building on

this concept, we evaluated the activity of omadacycline, a relatively new antibiotic that is already FDA-endorsed for the treatment of community-acquired bacterial pneumonia and acute bacterial skin and skin structure infections.[35] In the last years, omadacycline gained interest in the field of NTM infections as it showed potent preclinical activity against *M. abscessus*.[36-39] We expanded this growing body of evidence in **chapter 3.2** by investigating what antibiotics omadacycline could best be combined with to reach maximum potential, for which we used *in vitro* time-kill kinetics assays. We detected no additional activity of omadacycline combined with cefoxitin, amikacin or imipenem. Combining omadacycline with clofazimine, on the other hand, resulted in strong and enhanced killing activity. Importantly, the concentrations of omadacycline and clofazimine at which the boosted activity was observed are potentially achievable at the site of infection in humans.[40-42] Speculating on possible clinical implications of this finding, this drug combination might have the potential to improve the continuation phase of *M. abscessus* treatment, since oral formulations are available of both omadacycline and clofazimine. It should, however, be noted that other research groups, who used checkerboard assays to investigate *in vitro* synergy between omadacycline and other antibiotics detected synergy between omadacycline and clofazimine only in a subset of *M. abscessus* isolates.[37, 38] Also, the strong activity of this combination was not observed in a mouse model of *M. abscessus* pulmonary disease.[43, 44] The discrepancy in the results obtained by various preclinical drug activity models, both *in vitro* and *in vivo*, underline the need for refinement of the preclinical NTM drug development pipeline. Until we have a better understanding of the relative predictive value of the various preclinical NTM models used, we should not simply dismiss *in vitro* findings when they do not align with animal model outcomes. However, our study was exploratory in nature, investigating only drug activity against an actively replicating, planktonic culture. It would be interesting to study whether the observed synergy between omadacycline and clofazimine remains against even harder to treat nonreplicating populations or *M. abscessus* biofilms.

While the body of evidence supporting omadacycline's activity against *M. abscessus* is rapidly expanding, research on its activity against *M. avium* is sparse.[45-47] Based on high MICs, omadacycline was initially considered not to be a suitable candidate to improve *M. avium* treatment.[45] However, we actually found promising *in vitro* activity of omadacycline against *M. avium*, as described in **chapter 3.3**. Indeed, we measured high omadacycline MICs against *M. avium* in Mueller Hinton broth (128 mg/L), which is the guideline recommended broth.[48] MICs in Middlebrook 7H9 broth, however, were 8-fold lower (8 mg/L), showing the potential impact of medium type on drug activity testing. In this medium, omadacycline proved to be highly unstable, impacting drug activity as well, as the MIC was another 8-fold lower (1 mg/L) when drug decay was compensated. These findings not only underline the recently raised discussion whether or not Mueller Hinton is the most optimal broth for MAC drug susceptibility testing for all antibiotics,[49] but also

argues for incorporation of drug stability testing into the preclinical drug activity pipeline, which has been gaining interest lately as well.[50, 51] Omadacycline's activity pattern in time-kill kinetics assays generally matched that of clarithromycin and rifampicin, being mostly inhibitory in nature. In line with our *M. abscessus* work, we combined omadacycline with current guideline-recommended antibiotics to study whether anti-*M. avium* activity might be boosted. We additionally investigated whether co-exposure of *M. avium* to omadacycline and clarithromycin or amikacin prevented resistance to these drugs, as these are the only two drugs for which a link has been established between drug susceptibility results and clinical outcome.[3] Drug resistance was studied at the end of the time-kill kinetics assays by redetermining the MICs and Sanger sequencing of the *rrl* and *rrs* genes. Of all investigated drug combinations, omadacycline plus amikacin was most remarkable. Amikacin on its own was highly bactericidal in the early days of the experiment, but subsequent rapid outgrowth indicated selection of a resistant subpopulation, which was confirmed by high amikacin MICs and an A1408G mutation in the *rrs* gene, which is known to cause high-level amikacin resistance in clinical isolates.[52, 53] When combined with omadacycline, *M. avium* outgrowth was delayed or even completely prevented, MICs remained relatively low and *rrs* point mutations could not be detected, all in an omadacycline concentration-dependent manner. Interestingly, while exposure to a subinhibitory amikacin concentration led to *M. avium* outgrowth accompanied by high MICs, no *rrs* gene mutations were detected by Sanger sequencing. This prompted the question whether an alternative, yet to be discovered, amikacin resistance mechanism could be detected and whether this mechanism could be prevented by omadacycline as well. To answer this question, Whole Genome Sequencing was performed on these samples, but no specific genomic changes that were present in all samples exposed to amikacin, but not to the combination of omadacycline and amikacin could be detected. It is possible that the observed amikacin resistance is a consequence of non-mutational modifications, such as epigenetic changes. Nevertheless, the results imply that the combination of omadacycline plus amikacin might be of additive value in the clinic, not only because it might enhance bactericidal activity, but also because mutational amikacin resistance was previously shown to hamper culture conversion.[54] Although the boosted activity of omadacycline and clarithromycin was only minimal, omadacycline could prevent clarithromycin resistance-associated A2058G/C mutations in the *rrl*-gene. This finding might have promising clinical implications as well, since macrolides are the cornerstone of *M. avium* treatment and macrolide-resistance significantly compromises successful treatment outcomes.[55, 56]

In conclusion, our results further substantiate that omadacycline is an interesting new drug candidate in the field of NTM infections. In 2021, the FDA officially recognized omadacycline as orphan drug for the treatment of infections caused by NTM,[57] which was recently followed by the EMA.[58] Additionally, a clinical, placebo-controlled phase 2

trial is currently ongoing (NCT04922554), in which patients with *M. abscessus* complex pulmonary disease will be treated with oral omadacycline or placebo for 3 months. Outcomes parameters include improvement of clinical symptoms, safety and tolerability of the drug, patient perception, and microbiological efficacy measured by quantitative sputum culture, time-to-positivity of the liquid culture, and time until first negative culture. Expecting significant microbiological improvement after only 3 months of omadacycline unaccompanied by other drugs might be slightly optimistic. Still, it is exciting that omadacycline reached the clinical trial stage for treatment of NTM infections and hopefully future studies as well as reports on off-label application of the drug will collectively provide a better understanding on the potential role of omadacycline in treating NTM infections, thereby simultaneously providing valuable results that can be used to validate the various preclinical NTM models.

Improving the translational value of preclinical mycobacterial models

Parallel to preclinical drug activity testing, it is necessary to strive towards further refinement of the models to ensure they provide the highest translational value possible, which was the aim of the studies in **chapter 4**.

It is important to consider the potential impact that biological differences between humans and mice might have on study outcomes, thereby ensuring that the results are carefully and appropriately interpreted and placed in the correct context when extrapolating to the human situation. In that context, in **chapter 4.1** we focused on the metabolization of the new anti-TB diarylquinoline compound TBAJ-876 and determined the relative contribution of its main metabolite, TBAJ-876-M3 (M3), to TBAJ-876's overall bactericidal activity in our mouse TB model. The relevance of this question is highlighted by the previously demonstrated difference in bedaquiline metabolism between mice and humans.[59] To this aim, we first compared the *in vitro* bactericidal activity of TBAJ-876, M3, and bedaquiline against *M. tuberculosis* and found that TBAJ-876 and M3 performed similarly, while for bedaquiline higher concentrations were required to achieve comparable bactericidal activity. Subsequently, mice were treated for 4 weeks with increasing doses of TBAJ-876 or with M3 only. The contribution of M3 to TBAJ-876 activity was based on the exposure to M3 after TBAJ-876 treatment and the activity of M3 associated with this exposure level in the animals that were treated with M3. We found that treatment with TBAJ-876 and with M3 demonstrated profound bactericidal activity, and in line with our *in vitro* findings, this bactericidal activity was superior to that of bedaquiline, both dose- and exposure-based.[60, 61] When looking at plasma concentrations, exposures to M3 were 2.2-3.6x higher than exposure to TBAJ-876 after

treatment with TBAJ-876. Based on the relatively high M3-exposure upon treatment with TBAJ-876 and the potent activity of M3, we could conclude that the bactericidal activity of TBAJ-876 in our mouse model was predominantly driven by the M3-metabolite. Whether the parent compound-to-metabolite ratio observed in the mice indeed differs from the ratio in humans will become clear once the results of the currently ongoing phase I trials (NCT04493671 and NCT05526911) are published. Yet, we expect that potential interspecies variability in TBAJ-876 metabolism will probably not substantially affect the translation of our mouse model findings to humans, because the activity of TBAJ-876 and M3 was similar. In other words, if activity patterns of the parent compound and its major metabolite are comparable, species-specific differences in compound metabolism might be of less relevance. However, in the case of active metabolite formation and species-specific variability in drug metabolism, properties other than bactericidal activity could potentially be important as well, such as differential activity against *M. tuberculosis* in various metabolic states (which we approximated with our *in vitro* nutrient starvation model), activity against intracellular *M. tuberculosis*, or the ability of the compounds to penetrate into the different layers of the TB granuloma. This research area of active metabolites has been relatively understudied and deserves further investigation to improve the use of mouse models.

In chapter 3.1 and 3.2 we used *M. abscessus* subspecies *abscessus* ATCC 19977 in our time-kill kinetics assays. This is a reference strain that is often used in preclinical drug activity studies. Testing only this strain is generally considered as a study limitation, based on the argument that the results might not be generalizable to other *M. abscessus* complex isolates since the complex encompasses a genetically and phenotypically diverse group. Although drug susceptibility based on MICs might vary between isolates, it is not well-studied whether this translates into variability amongst isolates in time- and concentration-dependent drug activity patterns relative to their MIC. This was the rationale for the study described in **chapter 4.2**. We compared the activity patterns of 3 antibiotics against a panel of 7 *M. abscessus* complex isolates, including the ATCC reference strain, the 3 *M. abscessus* subspecies (*abscessus, bolletii*, and *massiliense*) and the 2 known morphotypes (smooth and rough). Amikacin, imipenem, and clofazimine were tested as guideline-recommended drugs for *M. abscessus* treatment with distinct mechanisms of action.[3] Interestingly, we found only minor differences in drug activity patterns against the ATCC strain versus the clinical isolates, and the patterns amongst the clinical isolates were highly similar, even for smooth versus rough morphotypes. While much is still unknown about the circumstances that give rise to rough morphotypes and their role in *M. abscessus* pathogenicity, infections with rough morphotype *M. abscessus* have been associated with more severe symptoms and worse outcomes.[62, 63] Based on our findings and those of others,[64] there seems to be no role for decreased drug activity against rough morphotype isolates. It is postulated that the markedly reduced

glycopeptidolipid content in the cell wall results in exposure of virulence factors that are normally covered.[65] Such virulence factors include cord factor, leading to clumping of the mycobacteria, which resulted in excessive aggregation in our rough morphotype cultures that were not drug exposed or exposed to sub-inhibitory concentrations. This probably resulted in an underestimation of the true mycobacterial load based on CFU counting in these conditions, but did not hamper the general interpretation of the drug activity patterns. Based on the low variability in drug activity patterns amongst the various (clinical) isolates, it would be more efficient to dedicate time and resources to testing more promising drug candidates with this assay rather than reproducing results in various isolates.

As environmental bacteria, NTM are well-equipped against harsh environmental circumstances. Previous studies showed that MAC can survive external stresses by adopting a nonreplicating state.[66-68] In the case of *M. tuberculosis*, nonreplicating, low metabolically active populations are believed to contribute to the need for long treatment durations, as they are less easily killed by antibiotics.[69, 70] Based on similar environmental stresses that are encountered by MAC in the human host and the hypothesis that the metabolic shutdown in reaction to such external stressors might be a common preserved response amongst mycobacteria, it is conceivable that nonreplicating populations play a role in MAC disease as well.[71, 72] Whereas *in vitro* nonreplicating models are widely used in the field of TB,[73] nonreplicating MAC studies are lacking. Therefore, in **chapter 4.3** we set-up and characterized a nutrient starvation model of nonreplicating *M. avium* and subsequently evaluated how this state affected the activity of currently used and new antibiotics. Strikingly, the current cornerstone drugs clarithromycin, ethambutol, rifampicin, and amikacin were practically inactive against nonreplicating *M. avium*, even at the highest concentration tested (64x MIC). Assuming that nonreplicating populations indeed play a role in MAC pathogenesis, inactivity of these antibiotics might contribute to the long treatment durations required to establish cure in patients. Clofazimine and bedaquiline, on the other hand, showed clear time- and concentration dependent killing activity. Under nutrient starved conditions, mycobacteria are thought to switch towards lipid metabolism, which relies on ATP-production via the electron transport chain. Clofazimine and bedaquiline being active against nonreplicating *M. avium* might be a consequence of these two drugs interfering with the electron transport chain.[74-76] Whether drug activity in our *in vitro* non-replication model indicates that these two drugs can potentially improve the sterilizing activity of drug regimens is uncertain for now. For bedaquiline, clinical studies are too limited to speculate on this topic,[77] while more information is available on the clinical performance of clofazimine as substitute for rifampicin in the current macrolide-ethambutol-rifampicin combination. Looking at our results, clofazimine was clearly more potent in killing nonreplicating *M. avium* than rifampicin, which would substantiate the idea that replacing rifampicin for clofazimine

has the potential to improve treatment success rates. Yet, a recent clinical trial demonstrated equal sputum culture conversion rates after 6 months of treatment with clofazimine- versus rifampicin-containing regimens.[78] There are, however, indications that the beneficial effect of clofazimine on microbiological cure might occur after 6 months of treatment duration,[79] possibly due to clofazimine requiring months to reach steady-state.[80] Thus, it remains to be seen if drug activity against nonreplicating *M. avium* indicates promising clinical sterilizing activity.

Future perspectives

Although the field of mycobacterial research has dedicated tremendous efforts towards improving treatment options, the alarming numbers of TB cases and deaths, low treatment success rates of NTM disease, and sluggishness of advancements underscore the substantial work that still remains.

For a long time, TB drugs and research models have been copy-pasted to the field of NTM. As the TB field is years or maybe even decades ahead of NTM, this seems like a logical approach.[6] However, the suboptimal performance of TB drugs against NTM and other differences between the two in terms of risk populations and clinical manifestations highlight that each face their own challenges in drug development. Integrating the lessons learned during my PhD trajectory while looking ahead, in the coming section, I would like to share my thoughts on the future of preclinical drug development for both TB and NTM.

Treatment

TB and NTM share an ambitious **wish list of ideal treatment features**. More regimens are required that: are effective against mycobacteria with both bactericidal and sterilizing activity, can shorten treatment duration, are available in oral formulation, have favorable pharmacokinetic profiles, come with high bioavailability also at the site(s) of infection, are not toxic, have no drug-drug interactions, have no cross-resistance to other used antibiotics, and are affordable and widely available. A daunting challenge. Therefore, it is essential that time and resources are dedicated as efficiently as possible.

Tuberculosis treatment

Collaborative efforts by academia, industry, and (non-)governmental organizations have ultimately led to the introduction of the new BPaL(M) regimen in the clinic for drug resistant TB. This regimen meets multiple of the abovementioned features of an ideal regimen: it is all-oral, highly effective, and greatly shortened treatment duration. However, with BPaL(M), the journey is not yet complete, as just one effective new

regimen is insufficient to achieve the End TB strategy goals. In the case of drug resistance, intolerability, drug-drug interactions or unavailability,[11, 81] we are back at square one and still rely on the much less effective long-term treatment regimens.[2] The field should strive towards **a palette of available regimens** to overcome this problem. Based on our mouse TB relapse model, the BPaMZ regimen would be an interesting recruit in this regard (**chapter 2.1**) although the hepatotoxicity in the SimpliciTB trial is a cautious reminder to consider the safety aspects of drug regimens in early stages when developing candidate regimens.[8] Furthermore, emerging bedaquiline resistance highlights the need for equally active regimens that are non-bedaquiline based.[81] The current drug pipeline is filled with promising compounds and hopefully, effective drug combinations will be identified in the coming years.[82]

Besides focusing on the development of new drug candidates or regimens, another approach is **to further optimize the dosing of old as well as new drugs** to maximize drug activity, while minimizing the risk of adverse events. Regarding maximizing activity, our literature study on delamanid and pretomanid (**chapter 2.2**) highlights that if higher clinical drug exposures would be feasible, the activity of especially delamanid might be enhanced. This strategy of dose optimization to maximize potential has shown encouraging results for rifampicin.[83] From a toxicity point of view, the dosing of newer drugs in the early clinical trials has led to unsatisfactory adverse events including myelosuppression and neuropathy for linezolid[11] and hepatotoxicity possibly due to the combination of pretomanid and pyrazinamide.[8] The challenge here lies in identifying dosing that minimizes the risk of adverse events while regimen effectivity is retained.[12] Lastly, instead of altering the dosing regimen, another interesting approach is the development of co-medication that enables lower doses while maintaining drug activity. An example is co-administration of ethionamide, an older TB drug that has relatively fallen out of favor due to high toxicity, and the new drug alpibectir (BVL-GSK098). Ethionamide requires biological activation, but its bioactivation pathway is rather inefficient, and high doses are required for sufficient drug activity. Alpibectir stimulates an alternative, more efficient bioactivation pathway, meaning that lower doses of ethionamide suffice.[84]

The extent of the current TB drug pipeline is unprecedented. Several of these compounds belong to the same class of drugs or share mechanisms of action. For example, where bedaquiline was the first of the diarylquinoline class of drugs to be officially approved for TB treatment, now multiple diarylquinolines are in development such as TBAJ-587, TBAJ-876 (studied in **chapter 4.1**), and sudapiridine. Another promising group of compounds are those targeting the cytochrome bc1 complex, including telacebec (Q203), BTZ-043, macozinone (PBTZ-169), quabodepisat (OPC-167832), and TBA-7371.[82] So, at the moment, there are many similar compounds from the same class of drugs under development. From a drug development perspective, it makes sense to build

on promising lead compounds to expand the arsenal of effective treatments. Having multiple similar therapeutic options available can be beneficial, for example when specific drugs are not accessible. However, the relative role within TB treatment of many of such similar compounds is unclear, as head-to-head comparisons are lacking, which is highlighted by our literature review on the nitroimidazoles delamanid and pretomanid (**chapter 2.2**). For delamanid and pretomanid, a currently ongoing clinical trial (PARADIGM4TB trial, ClinicalTrials.gov ID: NCT06114628) might shed light on this matter. However, the question remains whether such precise positioning of similar compounds in the treatment of TB is truly necessary, or if financial resources supporting such studies might be better dedicated to advancing other compounds further along the development pipeline.

NTM treatment

Since the important introduction of macrolides in the 1990s, the field of NTM drug development has stayed relatively quiet.[72] Apart from the macrolides, the NTM field is limited by the availability of effective antibiotics, and of most currently used antibiotics, the contribution to clinical outcome is unclear due to scarce scientific evidence.

Our *in vitro* studies with verapamil, thioridazine (**chapter 3.1**), and omadacycline (**chapter 3.2 and 3.3**) highlight that **repurposing drugs** can be a useful strategy for NTM, with the major advantage of omitting the lengthy process of early-stage drug discovery, which would accelerate introduction of the drugs into the clinic. However, like some of the abovementioned TB drugs, the use of verapamil and thioridazine is hampered by the toxicities associated with concentrations that are much lower than the effective concentrations in our study. Yet, this should not be a reason to abandon these drugs as potential NTM drug candidates. Instead, a potential ways forward could be to aim for **inhalation therapy** with high drug exposure at the site of infection and low systemic exposure.[33, 85] The promise of the latter strategy is underlined by the application of inhaled amikacin for MAC pulmonary disease,[86, 87] and the ongoing work on inhaled clofazimine[88] and tigecycline.[89]

With cure rates as low as 33%, *M. abscessus* subspecies *abscessus* is a true challenge to treat.[90] When a potent drug or drug combination is identified (*in vitro*), such as the verapamil- or thioridazine-containing antibiotic combinations (**chapter 3.1**) or omadacycline plus clofazimine (**chapter 3.2**), it is therefore worthwhile to **unravel the mechanisms underlying drug activity or drug synergy** by for example cytological, transcriptional, or metabolomic profiling.[91] Hopefully such methods can identify targets that may guide medicinal chemistry activities to develop new compounds with strong killing activity. This strategy would align with the growing ambition to **develop drugs specifically targeting NTM**, instead of solely repurposing drugs. An example is the

design of rifamycin-derivatives that overcome ADP-ribosylation-driven resistance in *M. abscessus*.[92, 93] Such strategies will hopefully effectively overcome the multitude of intrinsic resistance mechanisms that NTM are equipped with.

Furthermore, based on what is known about the pathogenesis of NTM infections, it would stand to reason that new drug candidates **should be active against NTM present within biofilms, macrophages, possibly epithelial cells, granulomas, and in non-replicating states**, where, with regard to the latter subject, our research showed that he activity of current guideline-recommended antibiotics for *M. avium* is suboptimal (**chapter 4.3**).

Improving the preclinical drug development pipeline

An adequate preclinical model is one that provides information on how a drug or regimen will behave in humans. Mycobacterial disease and treatment success in humans are the result of a complex interplay between the host environment, the pathogen, and the treatment. All preclinical models are, by nature, a simplification of this complex reality, and **results from various models should be integrated** to increase the translational value of their results.

For TB, discrepancies between preclinical models and clinical trial results, for example illustrated by the disappointing treatment-shortening potential of moxifloxacin,[94, 95] emphasize the room for improvement that is still left. One approach would be to better understand which and to what extent biological differences between mice and humans impact the interpretation and translation of findings to the clinic, a strategy that we explored in **chapter 4.1**. It would be highly valuable if predictive models could be used that bundle experimental data, while adjusting for relevant pathological, pharmacological, metabolic or other differences between mice and humans.[96] However, it is important to mention that the preclinical TB drug development pipeline is relatively well-structured when compared to the largely **untamed preclinical NTM landscape**. For NTM, there is a vast heterogeneity in models used, with difficulty to establish reproducible results, lacking standardization, and with uncertain translational value. Therefore, the following section will mainly focus on NTM.

Development preclinical models

The current unstructured preclinical NTM pipeline is probably a consequence of multiple factors. For example, compared to TB, NTM research is relatively accessible, since no biosafety level 3 laboratory is required, resulting in many different research groups working on their own NTM models. There seems to be less overarching coordination of research activities compared to TB. However, the primary reason for the plethora of

models with uncertain predictive value is the fundamental question of **how to model what we do not yet know?**

Several aspects of **NTM pathophysiology have yet to be comprehensively explored**. For instance, NTM are well-known to be able to produce biofilms *in vitro* or even on medical devices,[97] but clinical evidence substantiating the role of biofilms in the pathogenesis of NTM pulmonary disease is rather limited.[98, 99] It is unclear where NTM precisely reside during infection: within airway mucus, in the bronchioles or alveoli, extracellularly and/or intracellularly, and inside what cells specifically. Also, what external stresses are relevant in these niches: low oxygen levels, nutrient limitation, exposure to reactive oxygen species, nitric oxide, others? And what is the influence of these external stresses on the metabolic state of NTM? Answers to these questions would pave the way towards the design of meaningful *in vitro* models to assess how such conditions affect drug activity. Lung explants of people with NTM infections might form a valuable source of information regarding the pathogenesis of NTM infections.

The problem of reliable models specifically apply to current mouse models of *M. abscessus* pulmonary disease.[100] As such, from an ethical perspective, dedicating resources to the development of so-called New Approach Methods, or NAMs, while **moving away from mouse models** would be preferable. These include complex *in vitro* models that mimic the host situation. Potentially valuable models may include biofilm models, liquid-air-interface models, artificial sputum models, synthetic mucus media, organoids, organ-on-a-chip, or granuloma models.[72, 97] Since *in vitro* models can only partially reflect human infections, results obtained by these various models should be integrated to better approximate the complexity of *in vivo* infections. This approach should be explored for TB as well, since, if successful, such models might have the potential to phase out animal studies in that field too.

Apart from developing meaningful model systems, it is also worthwhile to invest in **alternative outcome parameters**. The classic outcome parameter in (myco)bacterial research is CFU counting. However, not all models might be fully compatible with this parameter, like our encountered issues with this method for the rough morphotype *M. abscessus* isolates in **chapter 4.2**. Alternative outcome parameters such as microcalorimetry or the RS-ratio, which provide information on the metabolic activity of the bacteria, might be of added value here.[101, 102] However, what exact model and outcome parameter(s) to choose, should always depend on the specific research question that is to be answered.

Validating preclinical models by clinical trial results

Well-conducted, prospective clinical trials in the field of NTM are needed, primarily to investigate interesting drugs and regimens in patient populations, but also for validation of preclinical models. Adaptive, multi-arm clinical trials, such as the FOR*Ma*T trial studying *M. abscessus* treatment, where multiple treatment arms are tested, discontinued or added based on ongoing analyses, hold promise in this regard. However, performing clinical NTM trials is not straightforward. On the host-level, the challenge lies in the variation of disease manifestations (ranging from fibro-cavitary to nodular-bronchiectatic disease) and predisposing conditions (including cystic fibrosis, COPD, and potential immune deficiencies). On the NTM-level, there is variety in species and subspecies causing disease, as well as in NTM morphology including the rough and smooth morphotype in *M. abscessus*, with potential impact on clinical outcome.[62, 63] There is also debate on what outcome parameters are most relevant for NTM infections. Classic outcome parameters used in TB clinical trials might not be optimal predictors for favorable treatment outcome in NTM infections. Especially the definition of cure is still up for debate due to the risk of re-infection,[103] which highlight the potential importance of outcomes other than microbiological cure, such as radiological or clinical improvement. However, such parameters are difficult to approximate in *in vitro* systems.

References

1. World Health Organization. WHO consolidated guidelines on tuberculosis. Module 4: treatment - drug-susceptible tuberculosis treatment. Licence: CC BY-NC-SA 3.0 IGO.: World Health Organization, 2022.
2. World Health Organization. WHO consolidated guidelines on tuberculosis. Module 4: treatment - drug-resistant tuberculosis treatment, 2022 update. Licence: CC BY-NC-SA 3.0 IGO. Geneva: World Health Organization, 2022.
3. Daley CL, Iaccarino JM, Lange C, Cambau E, Wallace RJ, Jr., Andrejak C, et al. Treatment of Nontuberculous Mycobacterial Pulmonary Disease: An Official ATS/ERS/ESCMID/IDSA Clinical Practice Guideline. *Clin Infect Dis*, 2020; e1-e36.
4. Larkins-Ford J and Aldridge BB. Advances in the design of combination therapies for the treatment of tuberculosis. *Expert Opin Drug Discov*, 2023; 83-97.
5. Alffenaar JC, de Steenwinkel JEM, Diacon AH, Simonsson USH, Srivastava S and Wicha SG. Pharmacokinetics and pharmacodynamics of anti-tuberculosis drugs: An evaluation of *in vitro, in vivo* methodologies and human studies. *Front Pharmacol*, 2022; 1063453.
6. Dartois VA and Rubin EJ. Anti-tuberculosis treatment strategies and drug development: challenges and priorities. *Nat Rev Microbiol*, 2022; 685-701.
7. Mourik BC, Svensson RJ, de Knegt GJ, Bax HI, Verbon A, Simonsson USH and de Steenwinkel JEM. Improving treatment outcome assessment in a mouse tuberculosis model. *Sci Rep*, 2018; 5714.
8. Cevik M, Thompson LC, Upton C, Rolla VC, Malahleha M, Mmbaga B, et al. Bedaquiline-pretomanid-moxifloxacin-pyrazinamide for drug-sensitive and drug-resistant pulmonary tuberculosis treatment: a phase 2c, open-label, multicentre, partially randomised controlled trial. *Lancet Infect Dis*, 2024; 1003-14.
9. Li SY, Tasneen R, Tyagi S, Soni H, Converse PJ, Mdluli K and Nuermberger EL. Bactericidal and Sterilizing Activity of a Novel Regimen with Bedaquiline, Pretomanid, Moxifloxacin, and Pyrazinamide in a Murine Model of Tuberculosis. *Antimicrob Agents Chemother*, 2017.
10. Xu J, Li SY, Almeida DV, Tasneen R, Barnes-Boyle K, Converse PJ, et al. Contribution of Pretomanid to Novel Regimens Containing Bedaquiline with either Linezolid or Moxifloxacin and Pyrazinamide in Murine Models of Tuberculosis. *Antimicrob Agents Chemother*, 2019.
11. Conradie F, Diacon AH, Ngubane N, Howell P, Everitt D, Crook AM, et al. Treatment of Highly Drug-Resistant Pulmonary Tuberculosis. *N Engl J Med*, 2020; 893-902.
12. Conradie F, Bagdasaryan TR, Borisov S, Howell P, Mikiashvili L, Ngubane N, et al. Bedaquiline-Pretomanid-Linezolid Regimens for Drug-Resistant Tuberculosis. *N Engl J Med*, 2022; 810-23.
13. Tweed CD, Dawson R, Burger DA, Conradie A, Crook AM, Mendel CM, et al. Bedaquiline, moxifloxacin, pretomanid, and pyrazinamide during the first 8 weeks of treatment of patients with drug-susceptible or drug-resistant pulmonary tuberculosis: a multicentre, open-label, partially randomised, phase 2b trial. *Lancet Respir Med*, 2019; 1048-58.
14. Gler MT, Skripconoka V, Sanchez-Garavito E, Xiao H, Cabrera-Rivero JL, Vargas-Vasquez DE, et al. Delamanid for multidrug-resistant pulmonary tuberculosis. *N Engl J Med*, 2012; 2151-60.
15. Huerga H, Khan U, Bastard M, Mitnick CD, Lachenal N, Khan PY, et al. Safety and Effectiveness Outcomes From a 14-Country Cohort of Patients With Multi-Drug Resistant Tuberculosis Treated Concomitantly With Bedaquiline, Delamanid, and Other Second-Line Drugs. *Clin Infect Dis*, 2022; 1307-14.

16. Dooley KE, Rosenkranz SL, Conradie F, Moran L, Hafner R, von Groote-Bidlingmaier F, et al. QT effects of bedaquiline, delamanid, or both in patients with rifampicin-resistant tuberculosis: a phase 2, open-label, randomised, controlled trial. *Lancet Infect Dis*, 2021; 975-83.
17. European Medicines Agency. Deltyba: EPAR - Annex I Summary of Product Characterisitics. 2014.
18. Battaglia S, Spitaleri A, Cabibbe AM, Meehan CJ, Utpatel C, Ismail N, et al. Characterization of Genomic Variants Associated with Resistance to Bedaquiline and Delamanid in Naive *Mycobacterium tuberculosis* Clinical Strains. *J Clin Microbiol*, 2020.
19. Vianna JS, Machado D, Ramis IB, Silva FP, Bierhals DV, Abril MA, et al. The Contribution of Efflux Pumps in *Mycobacterium abscessus* Complex Resistance to Clarithromycin. *Antibiotics (Basel)*, 2019.
20. Guo Q, Chen J, Zhang S, Zou Y, Zhang Y, Huang D, et al. Efflux Pumps Contribute to Intrinsic Clarithromycin Resistance in Clinical, *Mycobacterium abscessus* Isolates. *Infect Drug Resist*, 2020; 447-54.
21. National Center for Biotechnology Information. PubChem Compound Summary for CID 5452, Thioridazine. https://pubchem.ncbi.nlm.nih.gov/compound/Thioridazine.
22. National Center for Biotechnology Information. PubChem Compound Summary for CID 2520, Verapamil. https://pubchem.ncbi.nlm.nih.gov/compound/Verapamil.
23. Rodrigues L, Wagner D, Viveiros M, Sampaio D, Couto I, Vavra M, et al. Thioridazine and chlorpromazine inhibition of ethidium bromide efflux in *Mycobacterium avium* and *Mycobacterium smegmatis*. *J Antimicrob Chemother*, 2008; 1076-82.
24. Amaral L, Martins M and Viveiros M. Enhanced killing of intracellular multidrug-resistant *Mycobacterium tuberculosis* by compounds that affect the activity of efflux pumps. *J Antimicrob Chemother*, 2007; 1237-46.
25. Gupta S, Tyagi S, Almeida DV, Maiga MC, Ammerman NC and Bishai WR. Acceleration of tuberculosis treatment by adjunctive therapy with verapamil as an efflux inhibitor. *Am J Respir Crit Care Med*, 2013; 600-7.
26. Sohaskey CD. Nitrate enhances the survival of *Mycobacterium tuberculosis* during inhibition of respiration. *J Bacteriol*, 2008; 2981-6.
27. Boshoff HI, Myers TG, Copp BR, McNeil MR, Wilson MA and Barry CE, 3rd. The transcriptional responses of *Mycobacterium tuberculosis* to inhibitors of metabolism: novel insights into drug mechanisms of action. *J Biol Chem*, 2004; 40174-84.
28. Weinstein EA, Yano T, Li LS, Avarbock D, Avarbock A, Helm D, et al. Inhibitors of type II NADH:menaquinone oxidoreductase represent a class of antitubercular drugs. *Proc Natl Acad Sci U S A*, 2005; 4548-53.
29. Thanacoody HK. Thioridazine: resurrection as an antimicrobial agent? *Br J Clin Pharmacol*, 2007; 566-74.
30. Mandigers L, Bollen PD, Bijlstra PJ and Brands E. Severe verapamil intoxication despite correct use of low-dose verapamil. *Drug Metab Pers Ther*, 2016; 55-8.
31. Adams KN, Szumowski JD and Ramakrishnan L. Verapamil, and its metabolite norverapamil, inhibit macrophage-induced, bacterial efflux pump-mediated tolerance to multiple anti-tubercular drugs. *J Infect Dis*, 2014; 456-66.
32. Bozorgmehr R, Edalatifard M, Safavi E, Rahimi B, Ghorbani F, Abtahi H, et al. Therapeutic effects of nebulized verapamil on chronic obstructive pulmonary disease: A randomized and double-blind clinical trial. *Clin Respir J*, 2020; 370-81.
33. Parumasivam T, Chang RY, Abdelghany S, Ye TT, Britton WJ and Chan HK. Dry powder inhalable formulations for anti-tubercular therapy. *Adv Drug Deliv Rev*, 2016; 83-101.

34. Nehme H, Saulnier P, Ramadan AA, Cassisa V, Guillet C, Eveillard M and Umerska A. Antibacterial activity of antipsychotic agents, their association with lipid nanocapsules and its impact on the properties of the nanocarriers and on antibacterial activity. *PLoS One*, 2018; e0189950.
35. Food and Drug Administration. Highlights of prescribing information. NUZYRA (omadacycline) for injection, for intravenous use. NUZYRA (omadacycline) tablets, for oral use. https://www.accessdata.fda.gov/drugsatfda_docs/label/2018/209816_209817lbl.pdf.
36. Bax HI, de Vogel CP, Mouton JW and de Steenwinkel JEM. Omadacycline as a promising new agent for the treatment of infections with *Mycobacterium abscessus*. *J Antimicrob Chemother*, 2019; 2930-3.
37. Fujiwara K, Aono A, Asami T, Morimoto K, Kamada K, Morishige Y, et al. *In Vitro* Synergistic Effects of Omadacycline with Other Antimicrobial Agents against *Mycobacterium abscessus*. *Antimicrob Agents Chemother*, 2023; e0157922.
38. Nicklas DA, Maggioncalda EC, Story-Roller E, Eichelman B, Tabor C, Serio AW, et al. Potency of Omadacycline against *Mycobacteroides abscessus* Clinical Isolates *In Vitro* and in a Mouse Model of Pulmonary Infection. *Antimicrob Agents Chemother*, 2022; e0170421.
39. Kaushik A, Ammerman NC, Martins O, Parrish NM and Nuermberger EL. *In Vitro* Activity of New Tetracycline Analogs Omadacycline and Eravacycline against Drug-Resistant Clinical Isolates of *Mycobacterium abscessus*. *Antimicrob Agents Chemother*, 2019.
40. Bundrant LA, Tzanis E, Garrity-Ryan L, Bai S, Chitra S, Manley A and Villano S. Safety and Pharmacokinetics of the Aminomethylcycline Antibiotic Omadacycline Administered to Healthy Subjects in Oral Multiple-Dose Regimens. *Antimicrob Agents Chemother*, 2018.
41. Gotfried MH, Horn K, Garrity-Ryan L, Villano S, Tzanis E, Chitra S, et al. Comparison of Omadacycline and Tigecycline Pharmacokinetics in the Plasma, Epithelial Lining Fluid, and Alveolar Cells of Healthy Adult Subjects. *Antimicrob Agents Chemother*, 2017.
42. Abdelwahab MT, Wasserman S, Brust JCM, Gandhi NR, Meintjes G, Everitt D, et al. Clofazimine pharmacokinetics in patients with TB: dosing implications. *J Antimicrob Chemother*, 2020; 3269-77.
43. Rimal B, Nicklas DA, Panthi CM, Lippincott CK, Belz DC, Ignatius EH, et al. Efficacy of Omadacycline-Containing Regimen in a Mouse Model of Pulmonary *Mycobacteroides abscessus* Disease. *mSphere*, 2023; e0066522.
44. Rimal B, Panthi CM, Xie Y, Belz DC, Ignatius EH, Lippincott CK, et al. Efficacies of three drug regimens containing omadacycline to treat *Mycobacteroides abscessus* disease. *Tuberculosis (Edinb)*, 2024; 102482.
45. Li A, Tan Z, He S and Chu H. *In vitro* susceptibility testing of tetracycline-class antibiotics against slowly growing non-tuberculous mycobacteria. *Clin Exp Pharmacol Physiol*, 2023; 604-9.
46. Shankar P, Singh S, Boorgula GD, Gumbo T, Heysell SK and Srivastava S. Challenges and a potential solution to perform drug susceptibility testing of omadacycline against nontuberculous mycobacteria. *Tuberculosis (Edinb)*, 2022; 102269.
47. Brown-Elliott BA and Wallace RJ, Jr. *In Vitro* Susceptibility Testing of Omadacycline against Nontuberculous Mycobacteria. *Antimicrob Agents Chemother*, 2021.
48. CLSI. Susceptibility Testing of Mycobacteria, *Nocardia* spp., and Other Aerobic Actinomycetes. 3rd ed. CLSI standard M24. Wayne, PA: Clinical and Laboratory Standards Institute 2018.
49. Jaffré J, Aubry A, Maitre T, Morel F, Brossier F, Robert J, et al. Rational Choice of Antibiotics and Media for *Mycobacterium avium* Complex Drug Susceptibility Testing. *Front Microbiol*, 2020; 81.

50. Chapagain M, Pasipanodya JG, Athale S, Bernal C, Trammell R, Howe D and Gumbo T. Omadacycline efficacy in the hollow fibre system model of pulmonary *Mycobacterium avium* complex and potency at clinically attainable doses. *J Antimicrob Chemother*, 2022; 1694-705.
51. Schoutrop ELM, Brouwer MAE, Jenniskens JCA, Ferro BE, Mouton JW, Aarnoutse RE and van Ingen J. The stability of antimycobacterial drugs in media used for drug susceptibility testing. *Diagn Microbiol Infect Dis*, 2018; 305-8.
52. Brown-Elliott BA, Iakhiaeva E, Griffith DE, Woods GL, Stout JE, Wolfe CR, et al. *In vitro* activity of amikacin against isolates of *Mycobacterium avium* complex with proposed MIC breakpoints and finding of a 16S rRNA gene mutation in treated isolates. *J Clin Microbiol*, 2013; 3389-94.
53. Kim SY, Kim DH, Moon SM, Song JY, Huh HJ, Lee NY, et al. Association between 16S rRNA gene mutations and susceptibility to amikacin in *Mycobacterium avium* Complex and *Mycobacterium abscessus* clinical isolates. *Sci Rep*, 2021; 6108.
54. Olivier KN, Griffith DE, Eagle G, McGinnis JP, 2nd, Micioni L, Liu K, et al. Randomized Trial of Liposomal Amikacin for Inhalation in Nontuberculous Mycobacterial Lung Disease. *Am J Respir Crit Care Med*, 2017; 814-23.
55. Loewenstein D, van Balveren L, Lemson A, Hanemaaijer N, Hoefsloot W and van Ingen J. Monotherapy: Key cause of macrolide-resistant *Mycobacterium avium* complex disease. *Respir Med*, 2023; 107366.
56. Moon SM, Park HY, Kim SY, Jhun BW, Lee H, Jeon K, et al. Clinical Characteristics, Treatment Outcomes, and Resistance Mutations Associated with Macrolide-Resistant *Mycobacterium avium* Complex Lung Disease. *Antimicrob Agents Chemother*, 2016; 6758-65.
57. U.S. Food and Drug Administration. Orphan Drug Designations and Approvals - Omadacycline. https://www.accessdata.fda.gov/scripts/opdlisting/oopd/detailedIndex.cfm?cfgridkey=741020.
58. European Medicines Agency. EU/3/23/2804 - orphan designation for treatment of nontuberculous mycobacterial lung disease - Omadacycline. https://www.ema.europa.eu/en/medicines/human/orphan-designations/eu-3-23-2804.
59. Rouan MC, Lounis N, Gevers T, Dillen L, Gilissen R, Raoof A and Andries K. Pharmacokinetics and pharmacodynamics of TMC207 and its N-desmethyl metabolite in a murine model of tuberculosis. *Antimicrob Agents Chemother*, 2012; 1444-51.
60. Almeida D, Converse PJ, Li SY, Upton AM, Fotouhi N and Nuermberger EL. Comparative Efficacy of the Novel Diarylquinoline TBAJ-876 and Bedaquiline against a Resistant Rv0678 Mutant in a Mouse Model of Tuberculosis. *Antimicrob Agents Chemother*, 2021; e0141221.
61. Pieterman ED, Keutzer L, van der Meijden A, van den Berg S, Wang H, Zimmerman MD, et al. Superior efficacy of a bedaquiline, delamanid and linezolid combination regimen in a mouse-TB model. *J Infect Dis*, 2021.
62. Hedin W, Fröberg G, Fredman K, Chryssanthou E, Selmeryd I, Gillman A, et al. A Rough Colony Morphology of *Mycobacterium abscessus* Is Associated With Cavitary Pulmonary Disease and Poor Clinical Outcome. *J Infect Dis*, 2023; 820-7.
63. Li B, Ye M, Zhao L, Guo Q, Chen J, Xu B, et al. Glycopeptidolipid Genotype Correlates With the Severity of *Mycobacterium abscessus* Lung Disease. *J Infect Dis*, 2020; S257-S62.
64. Hershko Y, Adler A, Barkan D and Meir M. Glycopeptidolipid Defects Leading to Rough Morphotypes of *Mycobacterium abscessus* Do Not Confer Clinical Antibiotic Resistance. *Microbiol Spectr*, 2023; e0527022.
65. Johansen MD, Herrmann JL and Kremer L. Non-tuberculous mycobacteria and the rise of *Mycobacterium abscessus*. *Nat Rev Microbiol*, 2020; 392-407.

66. Rojony R, Martin M, Campeau A, Wozniak JM, Gonzalez DJ, Jaiswal P, et al. Quantitative analysis of *Mycobacterium avium* subsp. *hominissuis* proteome in response to antibiotics and during exposure to different environmental conditions. *Clin Proteomics*, 2019; 39.

67. Archuleta RJ, Yvonne Hoppes P and Primm TP. *Mycobacterium avium* enters a state of metabolic dormancy in response to starvation. *Tuberculosis (Edinb)*, 2005; 147-58.

68. Abukhalid N, Rojony R, Danelishvili L and Bermudez LE. Metabolic pathways that permit *Mycobacterium avium* subsp. *hominissuis* to transition to different environments encountered within the host during infection. *Front Cell Infect Microbiol*, 2023; 1092317.

69. Connolly LE, Edelstein PH and Ramakrishnan L. Why is long-term therapy required to cure tuberculosis? *PLoS Med*, 2007; e120.

70. Lenaerts A, Barry CE, 3rd and Dartois V. Heterogeneity in tuberculosis pathology, microenvironments and therapeutic responses. *Immunol Rev*, 2015; 288-307.

71. Parker H, Lorenc R, Ruelas Castillo J and Karakousis PC. Mechanisms of Antibiotic Tolerance in *Mycobacterium avium* Complex: Lessons From Related Mycobacteria. *Front Microbiol*, 2020; 573983.

72. Wu ML, Aziz DB, Dartois V and Dick T. NTM drug discovery: status, gaps and the way forward. *Drug Discov Today*, 2018; 1502-19.

73. Iacobino A, Piccaro G, Giannoni F, Mustazzolu A and Fattorini L. Fighting tuberculosis by drugs targeting nonreplicating *Mycobacterium tuberculosis* bacilli. *Int J Mycobacteriol*, 2017; 213-21.

74. Hards K, Robson JR, Berney M, Shaw L, Bald D, Koul A, et al. Bactericidal mode of action of bedaquiline. *J Antimicrob Chemother*, 2015; 2028-37.

75. Schildkraut JA, Coolen JPM, Burbaud S, Sangen JJN, Kwint MP, Floto RA, et al. RNA Sequencing Elucidates Drug-Specific Mechanisms of Antibiotic Tolerance and Resistance in *Mycobacterium abscessus*. *Antimicrob Agents Chemother*, 2022; e0150921.

76. Yano T, Kassovska-Bratinova S, Teh JS, Winkler J, Sullivan K, Isaacs A, et al. Reduction of clofazimine by mycobacterial type 2 NADH:quinone oxidoreductase: a pathway for the generation of bactericidal levels of reactive oxygen species. *J Biol Chem*, 2011; 10276-87.

77. Omar S, Whitfield MG, Nolan MB, Ngom JT, Ismail N, Warren RM and Klopper M. Bedaquiline for treatment of non-tuberculous mycobacteria (NTM): a systematic review and meta-analysis. *J Antimicrob Chemother*, 2024; 211-40.

78. Zweijpfenning SMH, Aarnoutse R, Boeree MJ, Magis-Escurra C, Stemkens R, Geurts B, et al. Safety and Efficacy of Clofazimine as an Alternative for Rifampicin in *Mycobacterium avium* Complex Pulmonary Disease Treatment: Outcomes of a Randomized Trial. *Chest*, 2024; 1082-92.

79. Lee I, Hwang EJ, Kim JY, Yim JJ and Kwak N. Treatment Outcomes of Clofazimine-Containing Regimens in Severe *Mycobacterium avium* Complex Pulmonary Disease. *Open Forum Infect Dis*, 2024; ofad682.

80. Watanabe F, Furuuchi K, Hanada K, Fujiwara K, Uesugi F, Hiramatsu M, et al. Pharmacokinetics and Adverse Effects of Clofazimine in the Treatment of Pulmonary Non-Tuberculous Mycobacterial Infection. *Antimicrob Agents Chemother*, 2022; e0044122.

81. Derendinger B, Dippenaar A, de Vos M, Huo S, Alberts R, Tadokera R, et al. Bedaquiline resistance in patients with drug-resistant tuberculosis in Cape Town, South Africa: a retrospective longitudinal cohort study. *Lancet Microbe*, 2023; e972-e82.

82. Hoelscher M, Barros-Aguirre D, Dara M, Heinrich N, Sun E, Lange C, et al. Candidate anti-tuberculosis medicines and regimens under clinical evaluation. *Clin Microbiol Infect*, 2024; 1131-8.

83. Seijger C, Hoefsloot W, Bergsma-de Guchteneire I, Te Brake L, van Ingen J, Kuipers S, et al. High-dose rifampicin in tuberculosis: Experiences from a Dutch tuberculosis centre. *PLoS One*, 2019; e0213718.

84. Pieren M, Abáigar Gutiérrez-Solana A, Antonijoan Arbós RM, Boyle GW, Davila M, Davy M, et al. First-in-human study of alpibectir (BVL-GSK098), a novel potent anti-TB drug. *J Antimicrob Chemother*, 2024; 1353-61.

85. Fahimi F, Pourdowlat G, Behzadnia N, Mostofi SS, Forough AS, Parto O and Esmaeili A. Clinical evaluation of nebulized verapamil in out-patients with pulmonary hypertension secondary to chronic obstructive pulmonary disease. *Clin Respir J*, 2022; 802-11.

86. Griffith DE, Eagle G, Thomson R, Aksamit TR, Hasegawa N, Morimoto K, et al. Amikacin Liposome Inhalation Suspension for Treatment-Refractory Lung Disease Caused by *Mycobacterium avium* Complex (CONVERT). A Prospective, Open-Label, Randomized Study. *Am J Respir Crit Care Med*, 2018; 1559-69.

87. Winthrop KL, Flume PA, Thomson R, Mange KC, Yuen DW, Ciesielska M, et al. Amikacin Liposome Inhalation Suspension for *Mycobacterium avium* Complex Lung Disease: A 12-Month Open-Label Extension Clinical Trial. *Ann Am Thorac Soc*, 2021; 1147-57.

88. Kunkel M, Doyle-Eisele M, Kuehl P, Rotermund K, Hittinger M, Ufer S, et al. Clofazimine Inhalation Suspension Demonstrates Promising Toxicokinetics in Canines for Treating Pulmonary Nontuberculous Mycobacteria Infection. *Antimicrob Agents Chemother*, 2023; e0114422.

89. Pearce C, Ruth MM, Pennings LJ, Wertheim HFL, Walz A, Hoefsloot W, et al. Inhaled tigecycline is effective against *Mycobacterium abscessus in vitro* and *in vivo*. *J Antimicrob Chemother*, 2020; 1889-94.

90. Kwak N, Dalcolmo MP, Daley CL, Eather G, Gayoso R, Hasegawa N, et al. *Mycobacterium abscessus* pulmonary disease: individual patient data meta-analysis. *Eur Respir J*, 2019.

91. Hudson MA and Lockless SW. Elucidating the Mechanisms of Action of Antimicrobial Agents. *mBio*, 2022; e0224021.

92. Lan T, Ganapathy US, Sharma S, Ahn YM, Zimmerman M, Molodtsov V, et al. Redesign of Rifamycin Antibiotics to Overcome ADP-Ribosylation-Mediated Resistance. *Angew Chem Int Ed Engl*, 2022; e202211498.

93. Paulowski L, Beckham KSH, Johansen MD, Berneking L, Van N, Degefu Y, et al. C25-modified rifamycin derivatives with improved activity against *Mycobacterium abscessus*. *PNAS Nexus*, 2022; pgac130.

94. Gillespie SH, Crook AM, McHugh TD, Mendel CM, Meredith SK, Murray SR, et al. Four-month moxifloxacin-based regimens for drug-sensitive tuberculosis. *N Engl J Med*, 2014; 1577-87.

95. Nuermberger EL, Yoshimatsu T, Tyagi S, Williams K, Rosenthal I, O'Brien RJ, et al. Moxifloxacin-containing regimens of reduced duration produce a stable cure in murine tuberculosis. *Am J Respir Crit Care Med*, 2004; 1131-4.

96. Ernest JP, Strydom N, Wang Q, Zhang N, Nuermberger E, Dartois V and Savic RM. Development of New Tuberculosis Drugs: Translation to Regimen Composition for Drug-Sensitive and Multidrug-Resistant Tuberculosis. *Annu Rev Pharmacol Toxicol*, 2021; 495-516.

97. Meliefste HM, Mudde SE, Ammerman NC, de Steenwinkel JEM and Bax HI. A laboratory perspective on *Mycobacterium abscessus* biofilm culture, characterization and drug activity testing. *Front Microbiol*, 2024; 1392606.

98. Fennelly KP, Ojano-Dirain C, Yang Q, Liu L, Lu L, Progulske-Fox A, et al. Biofilm Formation by *Mycobacterium abscessus* in a Lung Cavity. *Am J Respir Crit Care Med*, 2016; 692-3.
99. Qvist T, Eickhardt S, Kragh KN, Andersen CB, Iversen M, Høiby N and Bjarnsholt T. Chronic pulmonary disease with *Mycobacterium abscessus* complex is a biofilm infection. *Eur Respir J*, 2015; 1823-6.
100. Dartois V, Bonfield TL, Boyce JP, Daley CL, Dick T, Gonzalez-Juarrero M, et al. Preclinical murine models for the testing of antimicrobials against *Mycobacterium abscessus* pulmonary infections: Current practices and recommendations. *Tuberculosis (Edinb)*, 2024; 102503.
101. Braissant O, Wirz D, Göpfert B and Daniels AU. Use of isothermal microcalorimetry to monitor microbial activities. *FEMS Microbiol Lett*, 2010; 1-8.
102. Walter ND, Born SEM, Robertson GT, Reichlen M, Dide-Agossou C, Ektnitphong VA, et al. *Mycobacterium tuberculosis* precursor rRNA as a measure of treatment-shortening activity of drugs and regimens. *Nat Commun*, 2021; 2899.
103. van Ingen J, Aksamit T, Andrejak C, Böttger EC, Cambau E, Daley CL, et al. Treatment outcome definitions in nontuberculous mycobacterial pulmonary disease: an NTM-NET consensus statement. *Eur Respir J*, 2018.

CHAPTER 6

Nederlandse samenvatting

Ondanks aanzienlijk verschillen tussen tuberculose (TB) en infecties met nontuberculeuze mycobacteriën, geldt voor beiden dat de behandeling langdurig en complex is. De studies die zijn opgenomen in dit proefschrift zijn uitgevoerd met het uiteindelijke doel om bij te dragen aan verbeterde behandelopties voor mycobacteriële ziekten. De variëteit aan besproken onderwerpen illustreert dat er nog veel kennishiaten bestaan in het veld. In **hoofdstuk 2.1 en 2.2** worden twee nieuwe TB behandelregimes en twee nieuwe TB middelen met elkaar vergeleken. Vervolgens wordt in **hoofdstuk 3.1, 3.2 en 3.3** de overstap gemaakt naar NTM-behandeling, waarin verschillende middelen tegen *Mycobacterium abscessus* en *Mycobacterium avium* worden geëvalueerd. **Hoofstuk 4.1, 4.2, en 4.3** richten zich op het verbeteren van zowel *in vitro* als *in vivo* preklinische modellen waarin de antimycobacteriële activiteit van middelen wordt onderzocht.

Verbeteren van behandelopties voor TB

In **hoofdstuk 2.1** onderzoeken we in hoeverre twee nieuwe behandelregimes, BPaMZ en BPaL, de behandelduur van TB kunnen verkorten. Hiervoor gebruiken we een zogenaamd 'relapse muis TB model' waarbij langdurige genezing zonder terugval wordt onderzocht. Vervolgens zijn deze resultaten wiskundig gemodelleerd. BPaMZ en BPaL bevatten meerdere relatief nieuwe middelen tegen TB: bedaquiline (B), pretomanid (Pa), moxifloxacine (M) en linezolid (L). De studie laat zien dat in het geval van het BPaMZ-regime een behandelduur van slechts 1.6 maanden voldoende is om 95% kans op genezing te bereiken in de muizen. Dit is 4.3 maanden voor BPaL en 7.9 maanden voor HRZE. Hoewel de exacte behandelduur in een muismodel niet direct kan worden geëxtrapoleerd naar de kliniek, is dit model eerder waardevol gebleken in het rangschikken van regimes op basis van effectiviteit. Wiskundig modeleren stelt ons in staat om historische resultaten te betrekken in het onderzoek, zoals we in deze studie hebben gedaan voor het eerstelijns HRZE-regime, wat een efficiëntieslag betekent, omdat een dergelijke behandelgroep niet opnieuw geïncludeerd hoeft te worden in het muismodel. Onze studieresultaten suggereren dat BPaMZ mogelijk met een kortere behandelduur dan BPaL gewenste behandeluitkomsten kan bereiken. Dat BPaL en BPaMZ veelbelovende regimes zijn wordt inmiddels onderstreept doordat de WHO BPaL adviseert in de behandeling van resistente TB. Daarnaast is er toenemende aandacht voor BPaMZ, bijvoorbeeld in een recente klinische trial die laat zien dat BPaMZ de behandelduur van gevoelige TB kan verkorten ten opzichte van HRZE.

In **hoofdstuk 2.2** vergelijken we de preklinische activiteit van twee nieuwe middelen, delamanid en pretomanid, in een literatuurstudie. Beide vallen binnen de nitroimidazole-klasse en zijn relatief gelijktijdig ontwikkeld en goedgekeurd als anti-TB middelen, wat maakt dat we geïnteresseerd zijn in de overeenkomsten en verschillen wat betreft middelontwikkeling, werkingsmechanismen, resistentiemechanismen, *in vitro* en *in vivo* activiteit en effectiviteit en *in vivo* farmacokinetiek. Pretomanid wordt

momenteel aanbevolen voor de behandeling van TB binnen het korte BPaL(M)-regime voor resistente TB. Delamanid is een zogenaamd klasse C middel, wat betekent dat het ook wordt aanbevolen als middel tegen resistente TB, maar alleen binnen langdurige regimes, en dat op basis van beperkte data over veiligheid en effectiviteit momenteel andere middelen de voorkeur verdienen. Er bestaat grote heterogeniteit in de opzet van de gepubliceerde preklinische studies, wat één-op-één vergelijking bemoeilijkt. Toch concluderen we dat de preklinische studies impliceren dat delamanid beter in staat is om *Mycobacterium tuberculosis* af te doden dan pretomanid. Dit wil echter niet direct zeggen dat delamanid de voorkeur zou moeten hebben in de behandeling van patiënten met TB. Wanneer namelijk de potentie van de middelen wordt vergeleken bij concentraties die in patiënten worden bereikt, is de effectiviteit van de middelen zeer vergelijkbaar. Wel impliceren de resultaten dat, indien een hogere blootstelling aan delamanid in patiënten zou kunnen worden bereikt, het middel mogelijk effectiever zou kunnen zijn. Een tweede interessante bevinding is dat een stijging in MIC van het ene middel niet altijd gepaard gaat met een stijging in MIC van het andere middel. Dit betekent dat kruisresistentie geen gegeven is en dat meer kennis van mutaties nodig is om te kunnen bepalen of de middelen elkaar eventueel kunnen vervangen in geval van resistentie.

Verbeteren van behandelopties voor NTM-infecties

In **hoofdstuk 3** stappen we over naar het verbeteren van NTM-behandeling. In **hoofdstuk 3.1** richten we ons op de rol van effluxpompen in het beïnvloeden van de antibiotica-activiteit tegen *M. abscessus*. We onderzoeken middels RNA sequencing in hoeverre blootstelling aan verschillende antibiotica leidt tot een upregulatie van genen die coderen voor effluxpompen. Vervolgens onderzoeken we of de vermeende effluxpompremmers thioridazine en verapamil in staat zijn om de activiteit van de geteste antibiotica te versterken, waarbij gebruik wordt gemaakt van time-kill kinetics assays. Thioridazine is van origine een antipsychoticum en verapamil wordt gebruikt in de behandeling van cardiovasculaire aandoeningen. Van beide middelen is eerder aangetoond dat ze de werking van effluxpompen in mycobacteriën kunnen remmen. Met name amikacine, clarithromycine en tigecycline leiden tot een sterke upregulatie van effluxpomp-coderende genen. Dit effect is minder groot voor clofazimine en cefoxitine. Thioridazine en verapamil tonen echter niet alleen synergie met amikacine, clarithromycine en tigecycline, maar ook met clofazimine en cefoxitine, wat impliceert dat mechanismen anders dan remming van effluxpompen hieraan zouden kunnen bijdragen. Thioridazine grijpt in op de aerobe ademhalingsketen via inhibitie van type II NADH dehydrogenase en succinaat dehydrogenase, terwijl verapamil calciumkanalen blokkeert. Het is mogelijk dat effluxmpompen indirect via deze mechanismen worden geremd, maar het kan ook zijn dat alternatieve, nog onbekende werkingsmechanismen ten grondslag liggen aan de geobserveerde synergie. Dergelijke mechanismen zijn interessant om verder uit te zoeken, aangezien ze kunnen dienen als potentieel

aangrijpingspunt voor de ontwikkeling van nieuwe middelen. Het is belangrijk te vermelden dat de concentraties van thioridazine en verapamil waarbij synergie wordt gezien, niet haalbaar zijn in patiënten bij de gebruikelijke doseringen. Om deze middelen verder richting de klinische behandeling van NTM-infecties te brengen, zou geïnvesteerd kunnen worden in de ontwikkeling van veiligere derivaten of alternatieve toedieningswegen zoals inhalatietherapie.

Omadacycline is een interessant nieuw middel dat momenteel door de FDA is goedgekeurd voor de behandeling van community-acquired bacteriële pneumonie en huid- en weke delen infecties. In het mycobacteriële veld is er een toenemende interesse voor dit middel vanwege *in vitro* activiteit tegen met name *M. abscessus*. In **hoofdstuk 3.2** onderzoeken we met welke antibiotica omadacycline het beste gecombineerd kan worden om tot een maximale activiteit te komen tegen *M. abscessus*. Wanneer omadacycline wordt gecombineerd met cefoxitin, amikacin of imipenem wordt geen versterking van de activiteit geobserveerd. Gelijktijdige blootstelling van *M. abscessus* aan omadacycline en clofazimine leidt daarentegen wel tot een synergistische activiteit. Bovendien zijn de concentraties waarbij synergie wordt geobserveerd haalbaar in patiënten. Omdat zowel omadacycline als clofazimine beschikbaar zijn als orale middelen, heeft deze combinatie de potentie om de continuatiefase van *M. abscessus*-behandeling te verbeteren.

In **hoofdstuk 3.3** onderzoeken we of omadacycline ook werkzaam is tegen de langzaam groeiende NTM *M. avium*. Op basis van hoge MICs in eerdere studies werd aanvankelijk gedacht dat omadacycline geen rol zou spelen in het verbeteren van *M. avium*-therapie. Onze resultaten laten echter zien dat de MIC van omadacycline afhankelijk is van het medium waarin de MIC wordt bepaalt. Zo is de MIC in standaard Mueller Hinton medium hoog (128 mg/L), maar is deze een stuk lager in Middlebrook 7H9 medium (8 mg/L). Tevens is de MIC onderhevig aan de instabiliteit van omadacycline, aangezien het middel vervalt over de duur van de MIC-bepaling. Wanneer middels dagelijks toevoegen van vers omadacycline wordt gecompenseerd voor dit verval, wordt een nog lagere MIC gevonden (1 mg/L). Dit suggereert dat Mueller Hinton mogelijk niet voor alle middelen het optimale medium is om een MIC-bepaling in uit te voeren en dat voorafgaand aan evaluatie van de activiteit van een nieuw middel de stabiliteit dient te worden bepaald. In time-kill kinetics assays is de activiteit van omadacycline grofweg gelijk aan dat van claritromycine en rifampicine, met een overwegend remmende activiteit. Van alle combinaties van middelen die zijn getest, blijkt de combinatie van omadacycline met amikacine het meest effectief. Amikacine alleen leidt tot een snelle afdoding van mycobacteriën in de eerste dagen van blootstelling, maar dit wordt gevolgd door snelle mycobacteriële uitgroei, wat wijst op uitselectie van een resistente subpopulatie. In combinatie met omadacycline wordt deze uitgroei vertraagd of zelfs geheel geremd, afhankelijk van de geteste concentratie. De remming van het ontstaan van

amikacineresistentie door omadacycline wordt tevens onderstreept door fenotypische gevoeligheidsbepalingen en de afwezigheid van mutaties in het *rrs*-gen. Blootstelling aan een subinhiberende concentratie van amikacine leidt interessant genoeg wel tot fenotypische amikacineresistentie, maar dit gaat niet gepaard met mutaties in het *rrs*-gen. Aanvullende Whole Genome Sequencing laat geen sluitend bewijs voor alternatieve resistentiemechanismen zien. Het is mogelijk dat mechanismen zoals epigenetische veranderingen hier een rol spelen. Desalniettemin concluderen we dat de combinatie van omadacycline en amikacine van toegevoegde waarde zou kunnen zijn in de behandeling van *M. avium* infecties. In combinatie met claritromycine toont omadacycline amper versterkte activiteit, maar de combinatie voorkomt wel mutaties die zijn geassocieerd met claritromycineresistentie. Dit is mogelijk van klinisch belang, aangezien macroliden de hoeksteen van *M. avium*-behandeling zijn en macrolideresistentie is geassocieerd met slechtere behandeluitkomsten.

Verbeteren van de translationele waarde van preklinische mycobacteriële modellen

Het is belangrijk te realiseren dat biologische verschillen tussen muis en mens invloed kunnen hebben op studieresultaten en dat deze verschillen moeten worden meegewogen bij de interpretatie en extrapolatie van studieresultaten naar de mens. Om die reden focust **hoofdstuk 4.1** op de metabolisering van het nieuwe TB middel TBAJ-876, dat behoort tot de nieuwe generatie diarylquinolines. We onderzoeken wat de relatieve bijdrage is van de belangrijkste metaboliet, TBAJ-876-M3 (M3), aan de totale bactericide activiteit van TBAJ-876 in een muismodel van TB. Dit is relevant, aangezien eerder voor bedaquiline, wat ook tot de diarylquinolines behoort, een verschil is aangetoond in metabolisme tussen muis en mens. In het TB muismodel zijn de dieren 4 weken behandeld met oplopende doseringen van TBAJ-876 of M3. De bijdrage van M3 aan de totale activiteit van TBAJ-876 wordt bepaald aan de hand van de blootstelling aan M3 gemeten na behandeling met TBAJ-876 en de activiteit van M3 die is geassocieerd met dezelfde mate van blootstelling in de dieren die met M3 zijn behandeld. Zowel TBAJ-876 als M3 tonen sterke bactericide activiteit in dit model. Blootstelling aan M3 is 2.2 tot 3.6 keer hoger dan blootstelling aan TBAJ-876 na behandeling met TBAJ-876. Op basis van de relatieve hoge blootstelling aan M3, gecombineerd met de sterke activiteit van M3, kunnen we concluderen dat de bactericide activiteit van TBAJ-876 in ons muismodel voornamelijk toe te schrijven is aan de M3-metaboliet. Resultaten van klinische trials zullen uitwijzen of de ratio tussen middel en metaboliet inderdaad verschilt tussen muis en mens voor TBAJ-876. Echter, in dit geval zullen eventuele verschillen in metabolisme geen grote invloed hebben op de translatie van de resultaten van muis naar mens, omdat de activiteit van TBAJ-876 en M3 min of meer gelijk is. In andere woorden, wanneer de activiteit van middel en metaboliet vergelijkbaar is, zijn soort-specifieke verschillen in metabolisme mogelijk minder relevant.

In hoofdstuk 3.1 en 3.2 onderzoeken we de activiteit van antibiotica tegen de *M. abscessus* subspecies *abscessus* ATCC 19977 stam middels time-kill kinetics assays. Dit is een referentiestam die veelvuldig wordt gebruikt in preklinisch *M. abscessus* onderzoek. Het gebruik van alleen deze stam wordt vaak beschouwd als een limitatie, omdat de resultaten mogelijk niet te generaliseren zijn naar andere (klinische) isolaten, aangezien het *M. abscessus* complex een genetisch en fenotypisch gevarieerde groep omvat. Hoewel het bekend is dat de gevoeligheid op basis van MIC inderdaad per isolaat kan verschillen, is niet goed onderzocht of dit betekent dat er ook verschillen zijn in de tijds- en concentratie-afhankelijke activiteit van middelen tegen verschillende isolaten bij gelijke MIC. Dit is dan ook de rationale voor de studie die wordt beschreven in **hoofdstuk 4.2**. In deze studie vergelijken we de activiteit van 3 antibiotica tegen een panel van 7 *M. abscessus* complex isolaten, inclusief de ATCC-referentiestam, de 3 subspecies van het *M. abscessus* complex (te weten *abscessus*, *bolletii* en *massiliense*) en de twee morfotypen (glad en ruw). We kiezen voor amikacine, imipenem en clofazimine, omdat deze drie middelen worden aanbevolen in de behandelrichtlijn en omdat ze ieder een ander werkingsmechanisme hebben. Er bestaan slechts minimale verschillen in activiteitspatroon van de middelen tegen de ATCC-stam versus de klinische isolaten. Ook wanneer we de klinische isolaten onderling vergelijken vinden we amper verschil in activiteitspatroon, zelfs als we de gladde morfotypen vergelijken met de ruwe morfotypen. Gezien deze resultaten lijkt het nuttiger om tijd en geld in te zetten om meer veelbelovende middelen te testen dan om resultaten te blijven reproduceren met verschillende isolaten.

In **hoofdstuk 4.3** zetten we een nieuw *in vitro* model op met *M. avium*, het zogenoemde 'nutrient-starvation model'. Doordat NTM omgevingsbacteriën zijn, zijn ze in staat om extreme omstandigheden te overleven, onder andere door een niet-delende staat aan te nemen waarin de metabole activiteit wordt afgeschaald. In geval van *M. tuberculosis* wordt aangenomen dat subpopulaties in een dergelijke staat bijdragen aan de noodzaak tot langdurige behandeling, aangezien zij minder gemakkelijk door antibiotica worden afgedood. Mogelijk spelen dergelijke populaties ook een rol in de pathogenese en de noodzaak tot lange behandeling van *M. avium*-infecties. Om die reden beschrijven we in **hoofdstuk 4.3** de opzet van een nieuw *in vitro* nutrient-starvation model, waarin we *M. avium* incuberen in afwezigheid van voedingsmiddelen om zo een niet-delende, metabool laag actieve staat te induceren. Vervolgens onderzoeken we de werking van verschillende antibiotica tegen *M. avium* in deze niet-delende staat. Opvallend genoeg zijn claritromycine, ethambutol, rifampicine en amikacine, allen middelen die in de huidige behandelrichtlijn wordt aangeraden, nagenoeg inactief tegen *M. avium* in niet-delende staat. Wanneer we aannemen dat niet-delende mycobacteriën inderdaad

een rol spelen tijdens *M. avium*-infectie, kan dit mogelijk verklaren waarom de benodigde therapieduur zo lang is. Clofazimine en bedaquiline vertonen daarentegen wel tijd- en concentratie-afhankelijke activiteit in dit model. Dit kan mogelijk te maken hebben met de werking van clofazimine en bedaquiline op de elektronentransportketen en de verhoogde afhankelijkheid van de keten in niet-delende mycobacteriën.

APPENDICES

Curriculum vitae

Name	Saskia Emily Mudde
Date and place of birth	11th of January, 1994, Breda
2006-2012	Pre-university education (VWO), Sint-Oelbert Gymnasium, Oosterhout (cum laude)
2012-2016	BSc Medicine, Erasmus MC, Rotterdam Minor: Global Health, icddr,b health research institute, Dhaka, Bangladesh
2015-2016	Propedeutic year Psychology, Erasmus University, Rotterdam
2016-2021	MSc Research Master Infection and Immunity, Erasmus MC, Rotterdam (cum laude) Research projects: • Erythrocyte membrane fluidity in the pathogenesis of malaria (Prof.dr. J. van Hellemond, Prof.dr A.G.M. Thielens) • Correlation between schistomiasis prevalence in snails and humans (Prof.dr. J. van Hellemond, Prof.dr A.G.M. Thielens) • Improving tuberculosis treatment and diagnostics (Dr. J.E.M. de Steenwinkel, Dr. H.I. Bax)
2017-2020	MSc Medicine, Erasmus MC, Rotterdam Elective internship: Tropical medicine, Kumi hospital, Kumi, Uganda
2021-2024	PhD research, Dept of. Medical Microbiology and Infectious diseases, Erasmus MC, Rotterdam (Dr. J.E.M. de Steenwinkel, Dr. H.I. Bax)
2021 – present	Resident in Medical Microbiology, Erasmus MC, Rotterdam (Dr. L.G.M. Bode, Dr. J.E.M. de Steenwinkel)

List of publications

Mudde SE, Meliefste HM, Ammerman NC, de Steenwinkel JEM, Bax HI. Omadacycline enhances the *in vitro* activity of clofazimine against *Mycobacterium abscessus*. Int J Antimicrob Chemother. 2024;79(12):3169-3173. Doi: 10.1093/jac/dkae336.

Mudde SE, Meliefste HM, Ammerman NC, de Steenwinkel JEM, Bax HI. *Mycobacterium abscessus* strain variability in preclinical drug development, does it really matter? J Antimicrob Chemother. 2024. Doi: 10.1093/jac/dkae336.

Mudde SE, Ammerman NC, ten Kate MT, Fotouhi N, Lotlikar MU, Bax HI, de Steenwinkel JEM. Relative contributions of the novel diarylquinoline TBAJ-876 and its active metabolite to the bactericidal activity in a murine model of tuberculosis. J Infect Dis. 2024;230(6):e1366-e1374. Doi: 10.1093/infdis/jiae332.

Meliefste HM, **Mudde SE**, Ammerman NC, de Steenwinkel JEM, Bax HI. A laboratory perspective on *Mycobacterium abscessus* biofilm culture, characterization and drug activity testing. Front Microbiol. 2024;15:1392606. Doi: 10.3389/fmicb.2024.1392606.

Mudde SE, Schildkraut JA, Ammerman NC, de Vogel CP, de Steenwinkel JEM, van Ingen J, Bax HI. Unraveling antibiotic resistance mechanisms in *Mycobacterium abscessus*: the potential role of efflux pumps. J Glob Antimicrob Resist. 2022;31:345-352. Doi: 10.1016/j.jgar.2022.10.015.

Mudde SE, Upton AM, Lenaerts A, Bax HI, De Steenwinkel JEM. Delamanid or pretomanid? A Solomonic judgement! J Antimicrob Chemother. 2022;77(4):880-902. Doi: 10.1093/jac/dkab505.

Mudde SE, Ayoun Alsoud R, van der Meijden A, Upton AM, Lotlikar MU, Simonsson USH, Bax HI, de Steenwinkel JEM. Predictive modeling to study the treatment-shortening potential of novel tuberculosis drug regimens, towards bundling of preclinical data. J Infect Dis. 2022;225(11):1876-1885. Doi: 10.1093/infdis/jiab101.

Houkes KMG, **Mudde SE**, Constantinescu AA, Verkaik NJ, Yusuf E. Concomitant endocarditis and spondylodiscitis due to coagulase-negative Staphylococci and a review of the literature. ID Cases. 2021;24:e01100. Doi: 10.1016/j.idcr.2021.e01100.

Mudde SE, Slobbe L. Infectieziekten in beeld: Oost-Afrikaanse trypanosomiasis. Tijdschr Infect 2020;15(5):202-4.

PhD portfolio

Presentations

Omadacycline alone and in combination as a treatment option for *Mycobacterium avium* infections. Science days internal medicine, Zeist, oral pitch	2024
Looking beyond the parent drug: The contribution of TBAJ-876 and its TBAJ-876-M3-metabolite to the bactericidal activity in a tuberculosis mouse model, NVMM scientific spring meeting, Arnhem, oral presentation	2024
Omadacycline as a treatment option against *Mycobacterium avium*. ESCMID in Oranje, Barcelona, oral pitch	2024
Omadacycline alone and in combination as a treatment option for *Mycobacterium avium* infections. ESCMID, Barcelona, poster presentation	2024
Activity of TBAJ-876 and the TBAJ-876-M3 metabolite in a mouse model of tuberculosis infection, Tuberculosis drug discovery and development Gordon research seminar and conference, Barcelona, poster presentation	2023
Project presentation Erasmus MC, Kick-off meeting of the NACTAR programma "Targeting *Mycobacterium tuberculosis*, setting the stage for the type VII secretion inhibitors"	2021
Project presentation "DMN-trehalose, een nieuwe, fluorescente kleuring voor mycobacteriële infecties", Beatrixoord, Groningen	2021

Conferences

Science days internal medicine, Zeist	2024
Nederlandse Vereniging voor Medische Microbiology (NVMM) Scientific spring meeting, Arnhem	2024
Conference The 3Rs and New Approach Methods (NAMs): all inclusive?, online	2024
Nederlandstalige Tuberculose Diagnostiekdagen (NTDD), Berg en Dal	2024
European Society of Clinical Microbiology and Infectious Diseases (ESCMID), Barcelona	2024

Mycobacterium tuberculosis research and drug development, MycoTube conference, online	2024
Tuberculosis drug discovery and development, Gordon research seminar and conference, Barcelona	2023
Nederlandstalige Tuberculose Diagnstiekdagen (NTDD), Bilthoven	2022
Nederlandse Vereniging voor Medische Microbiology (NVMM) Scientific spring meeting, Arnhem	2022

Courses and training

Personal leadership and communication, Erasmus MC	2024
Fenotypische interpretatie van de antimicrobiële gevoeligheidsbepaling, Erasmus MC	2023
Course on Sustainable research, Erasmus MC	2023
Discipline Overstijgend Onderwijs (DOO), AIOS in sync	2022
Training Animal Biosafety Level-3 (ABSL) laboratory	2022
Course on Laboratory Animal Science (LAS, article 9), Erasmus MC	2021

Seminars and meetings

RODIN symposium "Vaccinatiebereidheid en vergeten kinderziekten"	2024
MINC-LINK symposium "niet-tuberculeuze mycobacteriën: typisch-atypische infectie"	2024
6e Harry Blom beraad "Voorkomen van ernstig ongerief"	2023
Webinar Clinical & Laboratory Standards Institute (CLSI) "What's new in susceptibility testing of mycobacteria"	2023
Working Group for New TB Drugs (WGND), Advancements in TB drug discovery annual meeting	2023
RODIN webinar "Pandemische en rampenparaatheid"	2022
The Union world conference on lung health, workshop "Tools to build TB IRP trials: the EU-PEARL approach"	2022
TB Alliance Stakeholders virtual meeting	2022

Amsterdam UMC infectie-avond "Kriebel en jeuk"	2022
NVAMM symposium "In de schaduw van de pandemie"	2022
NCOH webinar "Emerging zoonosis and how the contagious jump between animals and humans"	2021
4e Harry Blom beraad "De invloed van het microbioom op dierproeven"	2021
Global TB Clinical and Educational Summit	2021
GARDP webinar "Discovering and developing new treatments for tuberculosis"	2021
Weekly departmental research meetings	2021-2024
Weekly departmental journal club meetings	2021-2024

Teaching activities

Workshop "TBC diagnostiek en labuitslagen", Nascholingsdag voor medisch-technische medewerkers	2024
Practical courses, Bachelor medicine, Erasmus MC	2022-2024
Lecture "Animal models for tuberculosis infection", Research Master Infection and Immunity, Erasmus MC	2021-2023
Supervising Honours Student Medicine	2022
Supervising HLO student, research internship	2021

Other activities

Green Team member, Medical Microbiology and Infectious Diseases, Erasmus MC	2021-present
Peer review of research articles (Antimicrobial Agents and Chemotherapy, Nature Communications)	2022-2023
Werkgroep NVMM Richtlijn Mycobacteriële Laboratoriumdiagnostiek, hoofdstuk 'NTM kweek'	2021-present